# DELIVERY OF REGULATORY T-CELL THERAPY VIA EX-SITU MACHINE PERFUSION

**Dr Angus John Hann**

**BSc MBBS (Hons) MRCS**

**Institute of Immunology and Immunotherapy**

**College of Medical and Dental Sciences**

**University of Birmingham**

**Doctor of Philosophy (PhD)**

**October 2024**

# Supervisors

**Professor Ye Oo**

PhD FRCP

Consultant hepatologist and clinician scientist

Queen Elizabeth Hospital Birmingham

Centre for Liver and Gastrointestinal Research

Institute of Immunology and Immunotherapy

University of Birmingham

**Professor Thamara Perera**

MD FRCS

Liver and multivisceral transplant surgeon

Queen Elizabeth Hospital Birmingham

Centre for Liver and Gastrointestinal Research

Institute of Immunology and Immunotherapy

# Abstract

Pharmacological immunosuppression following liver transplantation has improved considerably over the last half century. Despite an improved understanding, both acute and chronic rejection are frequently encountered by liver transplant clinicians and the latter is a significant cause of graft loss. In addition, the modern-day immunosuppressive medications such as calcineurin inhibitors, antimetabolites, anti-IL2 receptor antibodies and corticosteroids remain to be associated with sequalae such as diabetes, renal failure and post-transplant lymphoproliferative disorder. Regulatory T-cells (Tregs) represent a possible alternate therapy that may induce tolerance of the liver graft, rather than systemically supress the entire immune system. This research aimed to investigate the potential for Treg cell therapy to be administer directly to the liver graft through ex-situ normothermic machine perfusion (NMP). In order to do this, we firstly investigated the effect NMP has on the immune profile of the graft and immunological outcomes. Subsequently, we developed a liver wedge perfusion model to assess therapeutic Treg cell localisation after infusion, and the effect ex-situ administration has on the Treg phenotype. This was also then applied using a whole liver perfusion model consistent with that used in clinical practice (Liver Assist®). All experiments were done using human Tregs and liver. Post infusion Treg phenotype was assessed by re-isolating the infused cells from the liver tissue and perfusate, then performing flow cytometry to assess the expression of functional markers CD39, TIGIT and CTLA4. Clinical investigation comparing NMP preservation with cold storage demonstrated that early acute rejection occurred at a similar incidence in those undergoing primary transplant but was more frequent in those undergoing retransplant with an NMP preserved graft. The time of onset and severity were similar. After optimisation of our wedge perfusion model, expansion of human Tregs, and labelling with a fluorescent dye (Cell tracker red), these cells were

infused via a portal vein branch. These cells were visible within the liver parenchyma and appeared to have migrated out of the hepatic sinusoids. This process appears to occur within 4 hours, as evidenced by the findings of the whole liver experiments using the Liver Assist®. The Treg suppressive phenotype, remained stable for the infused cells that were re-isolated from the liver, but was reduced in the cells within the perfusate. A proportion of Tregs administer via ex-situ machine perfusion engraft within the liver parenchyma, and therefore could exert a long lasting local immunosuppressive effect.

# Foreword

Conducting the research described in this thesis was one of the most challenging things I have done to date. Prior to commencing this Doctorate of Philosophy in Birmingham, I was a middle grade general surgical trainee with the Royal Australasian College of Surgeons with minimal clinical research experience and no basic science training. I commenced this period of research with the aim of learning a bit more about basic science, with the hope that it would make me a better surgeon. In the end, I feel I have achieved a whole lot more. I have managed to meet incredible colleagues, make great friendships, travel to amazing places, and significantly improve my knowledge in both liver transplantation and research.

The support, encouragement and mentorship provided by my two supervisors was better than I could have ever anticipated. Working alongside highly motivated and talented individuals taught me what can be achieved with determination and persistence. These two individuals pushed me to achieve my full potential in both clinical work and research. I am very grateful for the opportunity they provided by taking me on as a research fellow and hope our relationship can continue into the future.

This period of research was conducted during a time with significant societal disruption due to the COVID-19 pandemic. Shortly after moving to the UK in February 2020, coronavirus struck the West Midlands with its full force, and there were numerous university closures, secondments to work in COVID critical care areas, and scarce resources. Despite this, our team persisted and produced important liver transplant clinical research during a time in which we were faced with many unknowns. This period highlighted the value of good quality scientific research that can be rapidly translated to clinical practice.

There is no doubt that I could not have commenced and completed this project without the unwavering support of my parents, close family and friends. The words of encouragement that you provided during the challenging times was really appreciated and am very grateful.

This project explores liver transplantation, machine preservation, and regulatory T-cells therapy.

I hope that you enjoy reading this thesis.

Angus

# Acknowledgements

**Supervisors**
Prof Ye Oo & Prof Thamara Perera

**Oo lab group and CLGR team**
Dr Scott Davies
Dr Remi Fiancette
Ms Grace Wootton
Dr Naomi Richardson
Ms Amber Bozward
Dr Suzanne Warner
Dr Vince Ronca
Prof Simon Afford
Dr Chris Weston
Dr Geoge Clarke
Ms Jingwen Mao
Dr Kayani Kayani
Ms Kulvinder Gill
Ms Janine Fear
Dr Graham Caine

**Clinical immunology team**
Dr Sian Faustini
Dr Adrian Shields

**Phenome centre team**
Dr Andrew Southam

**Cancer genomics centre**
Professor Andrew Beggs
Dr Matthew Newbould

**University Hospitals Birmingham**
Professor Desley Neil
Dr Anisa Nutu
Dr James Halle-Smith
Dr Hans Lembach

**Funding**
Catherine Marie Enright Kelly
Research Scholarship
*Royal Australasian College of Surgeons*

# Table of Contents

## List of figures

# List of tables

# List of abbreviations

| | |
|---|---|
| **IL** | Interleukin |
| **AILD** | Autoimmune liver disease |
| **AMR** | Antibody mediated rejection |
| **APC** | Antigen presenting cells |
| **AST** | Aspartate transaminase |
| **aTregs** | Activated regulatory T-cells |
| **BPAR** | Biopsy proven rejection |
| **BSA** | Bovine serum albumin |
| **CMTPX** | Cell tracker red |
| **CS** | Cold storage |
| **CSF** | Colony stimulating factor |
| **CTLA 4** | Cytotoxic T-lymphocyte antigen 4 |
| **DAPI** | 4′,6-diamidino-2-phenylindole |
| **DMSO** | Dimethyl sulfoxide |
| **DSA** | Donor specific antibody |
| **EAD** | Early allograft dysfunction |
| **EDTA** | Ethylenediaminetetraacetic |
| **FACS** | Fluorescence activated cell sorting |
| **FDR** | False discovery rate |
| **FoxP3** | Forkhead box P3 |
| **FSC** | Forward scatter |
| **GMP** | Good Manufacturing Practice |
| **GSTT-1** | anti-glutathione S transferase |
| **HBV** | Hepatitis B Virus |
| **HCV** | Hepatitis C Virus |
| **HGF** | Hepatocyte growth factor |
| **HOPE** | Hypothermic oxygenated machine perfusion |
| **HTK** | Histidine-Tryptophan-Ketoglutorate |
| **IFN** | Interferon |
| **iTregs** | Induced Regulatory T-cells |
| **ITU** | Intensive Treatment Unit |
| **LAG-3** | Lymphocyte-activation gene 3 |
| **LB** | Liver biopsy |
| **LDL** | Liver derived lymphocyte |
| **LIF** | Leukeamia inhibitory factor |
| **LPS** | Lipopolysaccharide |
| **LSEC** | Liver sinusoidal endothelial cells |
| **LT** | Liver transplantation |
| **LysoPC** | Lysophosphocholine |
| **M1** | Macrophage type 1 |
| **M2** | Macrophage type 2 |
| **MACS** | magnetic activated cell sorter |
| **MEAF** | Model of Early Allograft Function |
| **MHC** | Major histocompatability complexes |
| **NIH** | National Institute of Health |
| **NMP** | Normothermic Machine Perfusion |
| **NRP** | Normothermic regional perfusion |
| **PBMC** | Peripheral blood mononuclear cell |
| **PBS** | Phosphate buffered saline |
| **PPI** | Public and patient involvement |
| **PRI** | Preservation reperfusion injury |
| **PRS** | Post reperfusion syndrome |
| **PTLD** | Post transplant lymphoproliferative disorder |
| **QEHB** | Queen Elizabeth Hospital Birmingham |
| **RAI** | Rejection activity index |
| **REC** | Research ethics committee |
| **ROS** | Reactive oxygen species |
| **RPMI** | Roswell Park Memorial Institute medium |
| **RT** | Room temperature |
| **rTregs** | Resting regulatory T-cells |
| **SICS** | Sorter induced cellular stress |
| **SSC** | Side scatter |
| **TBS** | Tris buffered saline |
| **TCMR** | T-cell mediated rejection |
| **TCR** | T-cell receptor |
| **TGF** | Transforming growth factor |
| **Th** | Helper T-cells |
| **TNF** | Tumour necrosis factor |
| **Tr1** | T regulatory type 1 cells |
| **TRAIL** | TNF related apoptosis inducing ligand |
| **Tregs** | Regulatory T-cell |
| **tTregs** | Thymus derived Regulatory T-cells |
| **UHB** | University Hospital Birmingham |
| **UoB** | University of Birmingham |
| **VEGF** | Vascular endothelial growth factor |

# Chapter 1 - Introduction

## 1.1 The evolution of liver transplantation

The founding father of liver transplantation (LT), Thomas Starzl, identified 5 interlocking themes that led to success in human LT, and its transition from an experimental procedure with a high perioperative mortality and poor long-term survival to the routine procedure of today [1]. These themes continue to be developed and contribute to the ongoing improvements and success of LT today (Table 1.1). It has now been 60 years since the first LT was attempted in a human, and this journey has included both successes and failures. However, both have led to accrued knowledge and subsequent refinements in practice (Table 1.2). LT is now available in approximately 1200 centres around the globe (Figure 1.1A), with over 40 000 procedures being undertaken annually (Figure 1.1B).

**Table 1.1 Themes of liver transplantation**

| Theme | Description |
|---|---|
| **I** | Began in 1958-59 with canine studies of then theoretical hepatotrophic molecules in portal venous blood. These studies identified that insulin was the main hepatotophic factor and identified the importance of the portal vein. |
| **II** | Development of liver and multivisceral transplant models which developed in parallel with Theme I. |
| **III** | Development of successful immunosuppression which included azathioprine, prednisone, and ALG |
| **IV** | The development of newer immunosuppressive agents and better understanding of the mechanisms of rejection and tolerance which allowed for which include cylosporine (1979), tacrolimus (1989) and more recently, mycophenolate and sirolimus/everolimus (1999). |
| **V** | The human aspects, including the ethical and legal issues surrounding both organ donors as well as recipients |

**Themes of liver transplantation:** 5 themes leading to the development of successful human liver transplants since the inception of the procedure (from Starzl TE, Fung JJ. Themes of liver transplantation. Hepatology. 2010 Jun;51(6):1869-84). Previously published Hann A and Neuberger J (2023) The evolution of the liver transplant candidate. *Frontiers of Transplantation* 2:1178452. doi: 10.3389/frtra.2023.1178452.

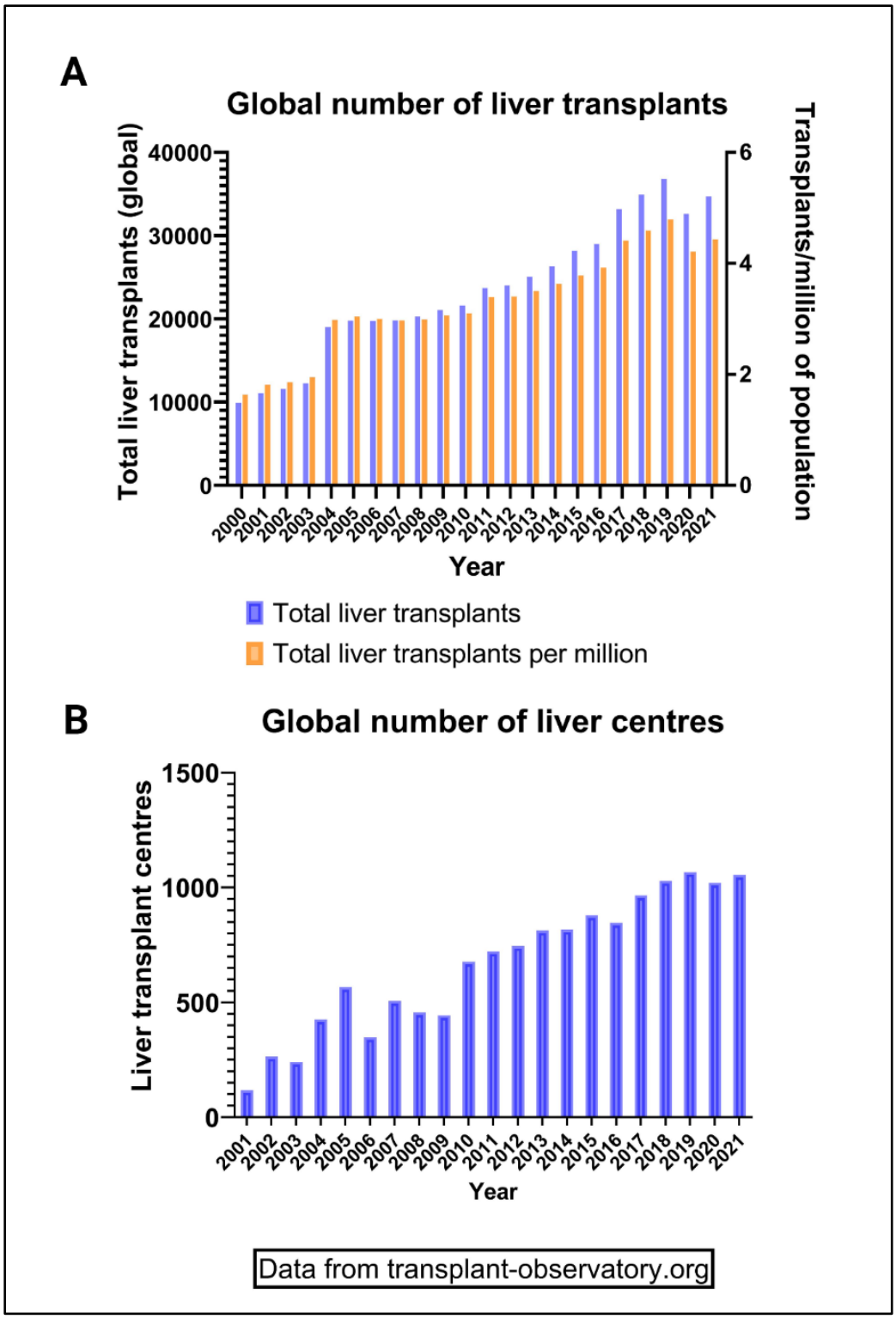


**Figure 1.1 Global transplant activity over the last 20 years**. (A) Demonstration of total liver transplants (left Y axis) and transplants in relation to the population size (right Y axis) since the year 2000. (B) Total number of active liver transplant centres around the world since 2000. Previously published Hann A and Neuberger J (2023) The evolution of the liver transplant candidate. *Frontiers of Transplantation* 2:1178452. doi: 10.3389/frtra.2023.1178452.

The initial attempts at human LT were characterised by very poor outcomes: out of the recipients transplanted between 1963 and 1964, none survived more than 23 days [2]. The youngest of this small group was a 3-year-old with biliary atresia, whom died on the day of surgery from uncontrollable bleeding [3]. The remaining seven, grafted in Denver, Boston and Paris, were transplanted for cancer (including two with colonic metastases) and the main causes of death were sepsis, bleeding and pulmonary emboli. These outcomes led to a 3-year moratorium until liver transplantation was re-started in 1967 by Starzl in Denver, and the following year a programme was started in Cambridge, UK, led by Sir Roy Calne.

The outcomes in the first years after the inception of this procedure, were very disappointing by today's standards. Thus, of the first 25 recipients in the Cambridge series, transplanted between 1968 and 1971, only 1 survived more than 1 year. This female patient was transplanted for primary liver cell cancer, and ironically would not meet current transplant criteria. Only 6 of these 25 recipients lived for more than 3 months. It is a great tribute to the courage, perspicacity, tenacity and dedication of these visionary transplant teams that the clinical and scientific teams continued to persevere. Furthermore, these pioneers managed to improve all aspects of the procedure, from selection of recipients and donors, to better retrieval, preservation, anaesthetic and surgical techniques. The understanding of the immunological, microbiological, haemostatic and physiological processes these individuals were able to achieve without the advanced technologies of modern day is remarkable. Since those early days, transplantation has expanded dramatically, as shown by the increase in both the number of patients transplanted and the number of transplant centres (Fig 1.1).

Based on a small number of pioneering transplant centres (and the relevant clinical and scientific personnel), the first National Institutes of Health (NIH) Consensus Conference was held in 1983 [4]. In this forum, Starzl and colleagues argued that LT had met the criteria necessary for it to be an accepted intervention. The rationale for this statement was based on

1) The procedure was within the capability of more than the 'occasional surgeon' 2) The indication for the procedure were clear, and 3) The results were good enough to justify the effort and expense[4]. The outcomes of 296 patients grafted between March 1963 and April 1983 were reviewed. Up to the end of 1979, 170 had been grafted; 56 (33%) of the recipients lived for at least one year; 26 survived 5 years and 6 survived 10 years. Death occurred mainly in the first three months and was attributed to the advanced stage of disease of recipients, technical surgical issues, the use of damaged liver grafts, the inability to control rejection, and a variety of infections. Most of the deaths in the first half of the second year were due to chronic rejection. During this period, immunosuppression was with azathioprine and prednisone, and induction with anti-lymphocyte globulin in most cases. In the subsequent period, between the years 1980 and 1982, of the 40 recipients with a follow-up extending to 38 months at the time of publication, the 1-year survival was 70%. Causes of death after 1 year included recurrent cholangiocarcinoma, recurrent Budd-Chiari syndrome, and chronic rejection. Improved outcomes were attributed to the use of cyclosporin and corticosteroids.

During these early years, it had also become clear that the clinical state of the recipient had a major association with outcome. The 6-week survival rate was 42% for the 26 patients taken to transplant from the intensive therapy unit (ITU) in comparison with 68% for the 63 patients who were managed as outpatients. On the basis of this limited data, the Conference concluded that LT could be considered for most patients who are near death with liver disease and should be considered as a service provision rather than an experimental procedure.

The gains that have been made likely reflect improved donor selection and management, preservation technology, anaesthesia and surgical technique. However, a significant proportion of the improvement likely results from the modern immunosuppressive

medications which are more efficacious and less toxic than their historic equivalents[5]. Figure 1.2 demonstrates stepwise improvements from the original antimetabolite (azathioprine) to the first calcineurin inhibitor (cyclosporine). The subsequent introduction of the more effective calcineurin inhibitor, tacrolimus, resulted in even better outcomes. These changes in immunosuppressive regimen occurred in parallel with the other aforementioned advances such as improved donor and recipient selection, operative technique and post operative care.

**Table 1. 2**

| Date | Event | Pioneers |
|---|---|---|
| 1955 | First article in literature about auxiliary liver transplant | Welch |
| 1959 | Models of canine total hepatectomy and replacement | Staudacher, Welch, Starzl, Cannon |
| 1963 | Introduction of corticosteroids/azathioprine | Starzl |
| 1963 | First attempt of human liver transplant (survival up to 3 weeks) | Starzl |
| 1967 | 1 year survival of human liver transplant recipients | Starzl |
| 1979 | Introduction of cyclosporine | Calne, White |
| 1981 | Reduced size liver graft | Bismuth, Houssin |
| 1983 | Combined liver kidney transplant | Margreiter |
| 1984 | Combined heart and liver transplant | Starzl |
| 1987 | Combined heart-lung liver transplant | Calne, Wallwork |
| 1989 | Combined liver intestine transplant | Starzl |
| 1989 | Introduction of tacrolimus | Starzl |
| 1989 | First split liver transplant | Pichlmayr |
| 1990 | Living donor transplant | Raia, Strong |
| 1993 | Baboon to human liver transplant | Starzl |
| 1995 | Domino liver transplant | Furtado |

**Key milestones in the early development of liver transplantation:** Some of key dates over the initial 40 years of liver transplantation (Source: Starzl TE and Fung JJ. Hepatology. 2010;51:1869-84, Zarrinpar A and Busuttil R. Nat Rev Gastroenterol Hepatol 2013; 10, 434–440). Previously published Hann A and Neuberger J (2023) The evolution of the liver transplant candidate. *Frontiers of Transplantation* 2:1178452. doi: 10.3389/frtra.2023.1178452.

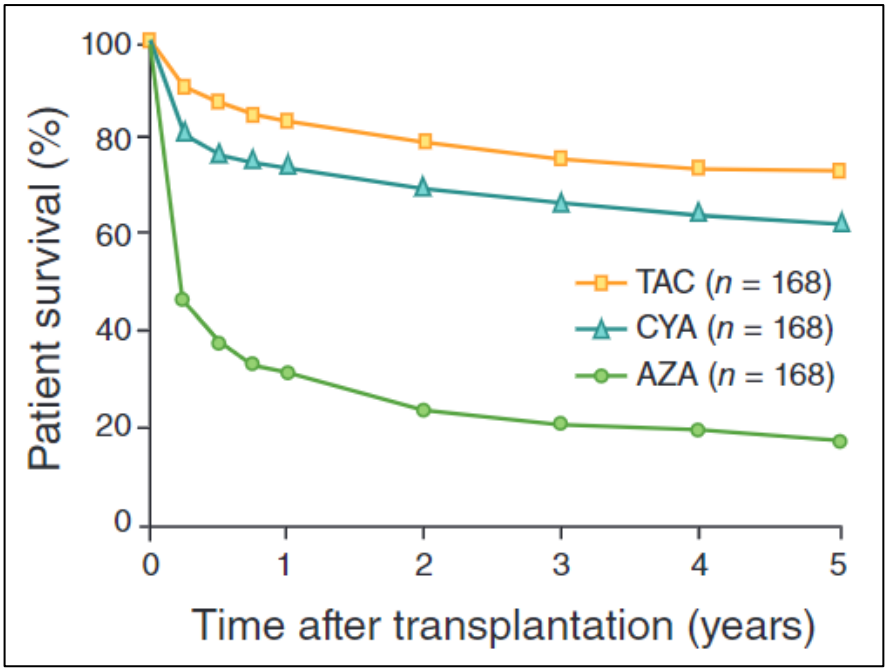


**Figure 1.2 Improvements with each generation of pharmacological immunosuppression**. Graph depicting the improvement in liver transplant survival with each successive generation of immunosuppressants. Source: Starzl TE. The long reach of liver transplantation. *Nat Med.* 2012 Oct;18(10):1489-92.

### 1.2 The immune response to liver transplantation

The transplantation of solid organs represents an event in which a huge number of foreign antigens (within the donors graft) are transferred to the recipient. This elicits a strong immune response, that changed over the post-transplant period. The evolution of events during the transplant period is displayed in Figure 1.3. The early innate response occurs as a result of the preservation-reperfusion injury (PRI) and manifests as early graft dysfunction, followed by the adaptive immune system which can cause acute and/or chronic rejection.

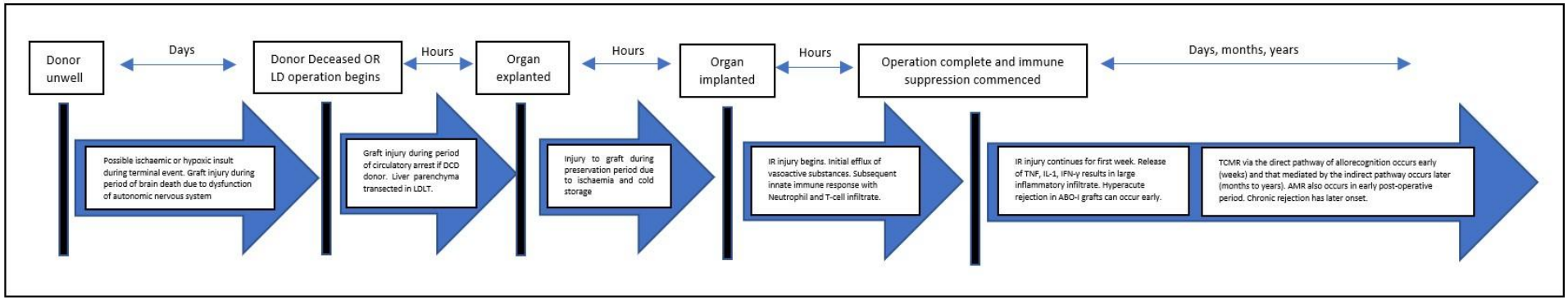


**Figure 1.3 Timeline of injury and immunological events during the liver transplantation.** The above timeline shows the journey of a liver allograft from donor to recipient, with the corresponding immunological events and complications LDLT: Living donor liver transplantation, IR: Ischaemia reperfusion, TCMR: T-cell mediated rejection, AMR: Antibody mediated rejection. Previously published in Hann A, Osei-Bordom DC, Neil DAH et al. Frontiers in Immunology. 2020 Jun 22;11:1227

### 1.2.1 The innate response

An intense inflammatory response occurs immediately post LT due to multiple factors including surgical stress, tissue trauma, alloantigen recognition, blood loss and the PRI. Standard cold storage (CS) preservation (Ice box at 4°C) conditions minimise oxidative phosphorylation and reduce metabolic activity to approximately 10% of the normal rate, the energy of which is mainly derived by anaerobic metabolism [6]. In addition to the ischaemia, hypothermic preservation conditions have a deleterious effects on the cell organelles, cytoskeletons and membranes [7]. Re-establishment of blood flow results in the release of reactive oxygen species (ROS) from the mitochondria which in turn cause the release of proinflammatory cytokines from Kupffer cells [8,9]. This PRI process is predominantly an innate immune response and characterised by liver sinusoidal endothelial cell (LSEC) dysfunction [9]. Intraoperative cardiovascular instability can occur immediately following re-establishment of blood flow due to a large efflux of metabolic substrates from the damaged liver, this entity is known as postreperfusion syndrome (PRS) [10]. Release of cytokines (Tumour necrosis factor-α, IL-1, Interferon-γ, tumour necrosis factor-β) results in the accumulation of neutrophils [9]. Previous literature has suggested that the immunogenicity of the graft is increased with PRI due to interactions between the innate and adaptive immune system [11]. Enhanced T-cell priming is thought to result from this interaction and contribute to both acute and chronic rejection [11]. Advanced donor age, graft steatosis and prolonged cold ischaemic time are associated with more severe PRI manifestations [12]. The more severe form may result in primary-nonfunction[13]. Strategies implemented in clinical practice to minimise the PRI are displayed in figure 1.4. Administration of anti-inflammatory type medications (such as corticosteroids) to the donor prior to retrieval has been shown to have no significant effect[14].

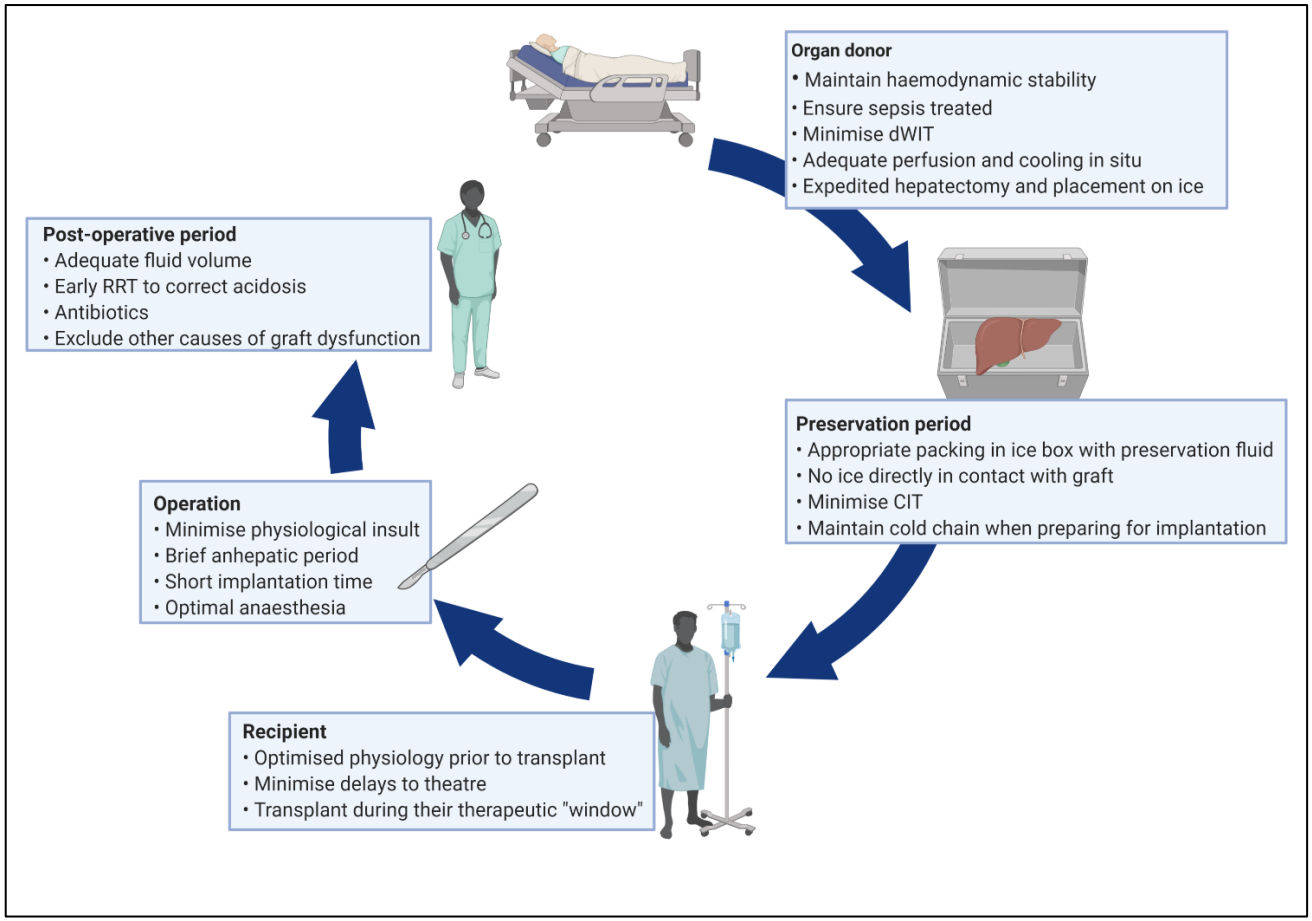


**Figure 1.4 Strategies to prevent severe preservation-reperfusion injury.** A variety of measures can be implemented to minimise severe preservation-reperfusion injury and graft dysfunction. These commence before organ donation and continue through to the post-operative period. DCD: Deceased circulatory death donor, dWIT: Donor warm ischaemic time, RRT: Renal replacement therapy CIT: Cold ischaemic time . Original figure by author (A.Hann). Published as Hartog H, Hann A, Perera MTPR. Primary Nonfunction of the Liver Allograft. *Transplantation*. 2022 Jan 1;106(1):117-128.

### 1.2.2 The adaptive response and acute rejection

The liver allograft represents a large amount of alloantigens and the adaptive arm of the recipient's immune system recognises these as such. However, in comparison to other transplanted solid organs the liver is less immunogenic. Acute T-cell mediated rejection (TCMR) is the most common immune mediated complication following liver transplantation [15]. Less frequent immune complications are recurrence of an AILD, plasma cell rich rejection, antibody mediated rejection (AMR) and unresolved TCMR/AMR progressing to chronic rejection. Allorecognition of transplanted tissue is known to occur via three pathways: direct, indirect and semi-direct (Figure 1.5) [16]. The direct pathway involves the recipients T-cells recognising the donor major histocompatibility complexes (MHC) molecules on donor antigen presenting cells (APCs). The indirect pathway occurs when the donor antigen is processed by recipient APCs and recipient MHC molecules expressed. The semi direct pathway involves cell exchange either via exosomes or the process of trogocytosis, which is the active transfer of plasma membrane fragments from an antigen presenting cell to a lymphocyte via cell conjugation [16,17]. The semi-direct pathway is yet to be completely understood but it is believed to involve the transfer of complete MHC-peptide complexes from donor APCs to recipient APCs. This results in a recipient APC displaying both a self and donor MHC molecule, both with an attached donor antigen. This brings both the direct and indirect pathway together onto a single APC and allows additional interaction between the two CD-4 or CD-8 T-cells that bind with each MHC:peptide complex, therefore forming a 3 cell model [16]. All pathways lead to increased secretion of IL-2 and other inflammatory cytokines which induce T-cell proliferation. The initial alloreactive T cell response is driven by the direct pathway with the indirect pathway assuming the main role as time progresses [18] [16].

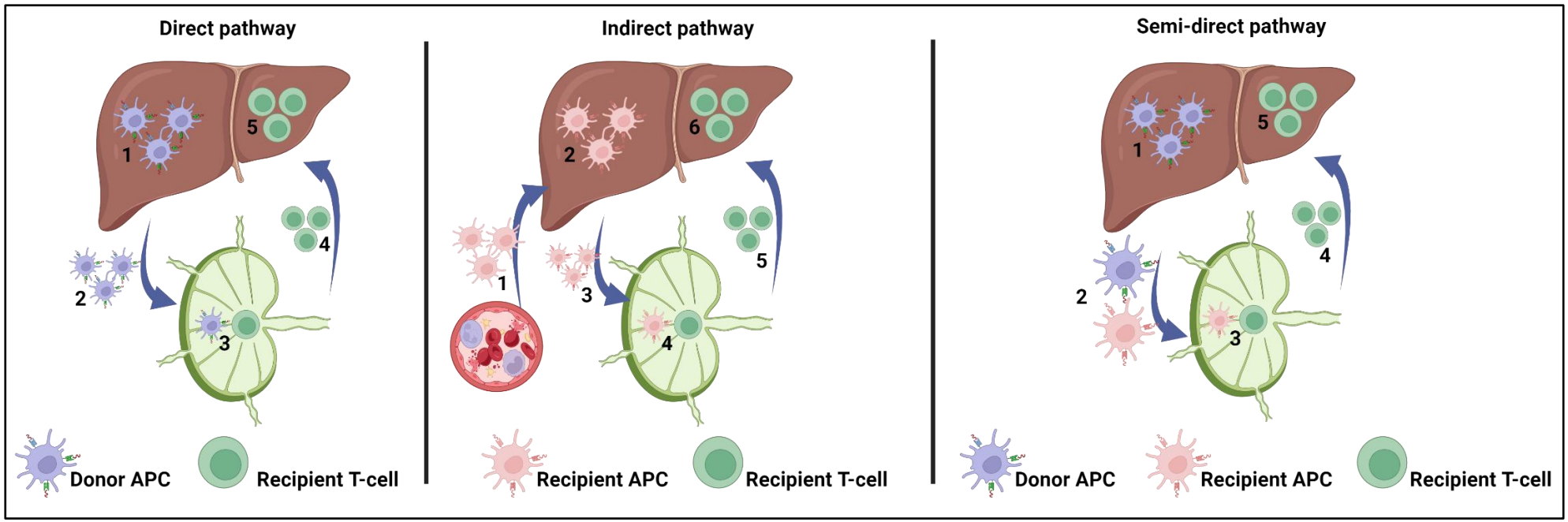


**Figure 1.5 T-cell mediated rejection pathways.** Graphical depiction of the three pathways; Direct, indirect and semidirect. In the direct pathway, donor antigen presenting cells (APC) with donor antigens travel to lymphatic tissue and present to recipient lymphocytes, which infitrate the graft and cause rejection. This is thought to cause early acute rejection (<6 weeks). The indirect pathway involves the recipient APCs infiltrating the liver, collecting donor antigens, which are then presented to recipient lymphocytes. This is thought to cause late rejection (≥6 weeks). The semi-direct pathway involves a transfer of antigen from donor APCs to recipient APCs.

The diagnosis of graft rejection is made via liver biopsy and graded in severity via the Banff criteria [19,20]. In addition to criteria for typical TCMR and chronic rejection, the 2016 update of the Banff working group recognised what had previously been termed de novo autoimmune hepatitis as a form of plasma cell rich rejection and added criteria for the diagnosis acute and chronic AMR [20]. Modern immunosuppressive agents have resulted in a reduction of early acute rejection from 60% to 33.5% [21,22] . This finding concurs with other authors that reported TCMR to occur most commonly in the early post-transplant period [19]. Early TCMR is a result of the direct alloantigen presentation pathway and is characterised by pleomorphic portal inflammation, bile duct injury and the lack of necro-inflammatory interface activity [20]. The indirect alloantigen presentation pathway is thought to result in the late TCMR and has predominantly mononuclear portal inflammatory change, less subendothelial inflammation than early TCMR but more interface and necro-inflammatory perivenular activity [20,23]. Chronic rejection is defined as 50% bile duct loss and/or a foam cell arteriopathy, it typically occurs early following non-responsive acute rejection, and is increasingly recognised to have an antibody mediated component [20,24].

Acute AMR causes graft dysfunction due to donor specific antibody (DSA) interaction to antigens on the graft. DSAs may be pre-existing (preformed) or develop post-transplant in response to foreign antigen (de novo antibodies). DSAs may be against human leukocyte antigens HLA antigens, which are the most readily detected by current assays, or non-HLA antigens such as anti-glutathione S transferase (GSTT-1) and anti-angiotensin 2 receptor[25,26]. The development of anti GSTT-1 antibodies has been demonstrated to occur in recipients who are negative for the GSTT-1 gene but receive a graft from a GSTT-1 positive donor [26]. These anti-GSTT1 antibodies have been shown to be pathogenic and are implicated in periportal

inflammation, fibrosis and the loss of bile ducts [26]. The understanding of AMR is evolving, it is also believed to often occur concurrently with TCMR. The liver exhibits ABO and MHC I antigen expression on all liver cells in normal circumstances, however the MHC I expression on hepatocytes is weaker [27]. Liver allografts in comparison to kidneys are highly resistant to HLA alloantibodies and numerous mechanisms are proposed to explain this phenomenon [28]. Secretion of soluble HLA class 1 molecules which form immune complexes with alloantibodies and then subsequently undergo clearance by Kupffer cells is one such mechanism [28]. Davies et al demonstrated that the liver graft also continues to deliver HLA class I antigens into the recipients serum for the lifetime of the graft, thus generating DSAs [29]. Resistance to AMR is also enhanced by the fenestrated endothelium of the sinusoidal network as occlusion by activated immune complexes does not result in the same degree of ischaemia as other transplanted organs [30]. The main clinical manifestations are graft dysfunction, transaminitis and thrombocytopenia [20]. The histological changes that occur are oedema, endothelial cell swelling, leukocyte sludging or margination and vascular deposition of tissue complement component 4d (C4d) [20]. The catastrophic vasculitis and intravascular thrombosis associated with hyperacute rejection of renal allografts is exceedingly rare following liver transplant [15,31]. Approximately 13% of liver transplant recipients have persisting DSA positivity and the most commonly found is the anti-HLA class II DSAs [32,33]. Del bello et al (2014) found in a cohort type study that 5 of out the 21 subjects with de novo DSA formation experienced acute AMR and the average liver fibrosis score was higher in these subjects with DSAs [32]. This latter finding is similar to previous authors who have associated DSA positivity with progressive fibrosis, graft loss and patient survival [20,33]. Anastomotic biliary strictures have also been associated with the presence of anti-HLA class II DSAs in patients who have undergone ABO compatible transplantation [34]. Rationale for this observation is that biliary structures receive their entire blood supply from the peri-biliary capillary plexus and therefore

is not protected from occlusion by immune complexes in the same manner as the hepatic sinusoids [30]. Establishing the histopathological evidence for the entity of chronic AMR is frequently challenging due to confounding factors [20]. The Banff working group has established criteria for probable and possible chronic AMR. The histology findings associated with chronic AMR are low levels of portal, periportal, perivenular lymphoplasmacytic inflammation and interface necro-inflammatory activity with noninflammatory fibrosis [20].

### 1.2.3 Clinical implications of graft rejection

Since the improved understanding of ABO compatibility, the incidence of hyperacute graft rejection that leads to very early graft failure is exceedingly rare following ABO compatible liver transplant. Institutions that are currently performing ABO incompatible transplants following living donation apply aggressive antibody and B cell depleting therapies, such as plasma exchange and Rituximab, to the recipient prior to transplantation. Despite improved pharmacology, understanding of T-cell activation pathways and DSAs, acute and chronic graft rejection are encountered commonly.

In the vast majority of instances, acute rejection is TCMR and generally responds to treatment and graft loss as a result is reported to be less than 1% [35]. If the aforementioned evidence of AMR is present, it is usually in combination with TCMR (so called mixed rejection). As demonstrated in figure 1.6, the incidence of early rejection was 30% between 2019 and 2021 at QEHB, with rates varying between indication. Although graft loss is infrequent with early acute rejection, it does have significant morbidity, lead to acute graft failure and can augment other more serious complications. Figure 1.7 shows the pH, lactate and glucose of two patients that experienced early severe mixed rejection at QEHB (The histology can be viewed at https://pubmed.ncbi.nlm.nih.gov/34018668/). Both these patients required admission to the intensive care unit. Inflammation within the graft can lead to

increased vascular resistance to both arterial and portal venous flow, which can potentiate hepatic arterial thrombosis and portal venous steal through the opening of spontaneous portosystemic shunts. The additional morbidity experienced by the patient also leads to increased consumption of healthcare resources, and preventing its occurrence would be hugely beneficial.

Late TCMR is less responsive and a preceding episode of moderate-severe early TCMR has been identified as a risk factor, however Jadloweic et al (2019) reported more than half of the patients who experience late TCMR had no history of early TCMR [21]. At this timepoint, the transplant recipient is usually out of hospital, and therefore subtherapeutic immunosuppression or non-compliance (either inadvertent or intentional) must be considered. The implications of late TCMR are more sinister with a higher rate of graft loss due to the progression to chronic rejection [21]. Chronic rejection occurs at a reported rate of 3-5% following liver transplant[24]. Between 2007 and 2021, 30/153 (20%) of late retransplants were performed for chronic rejection as the indication. In addition to those that made it to retransplant, many more with this complication would have never been relisted due to age or co-morbidities. Therefore, strategies that can avoid chronic rejection will improve survival, save healthcare resources, and allow grafts to be given to other patients with life limiting illnesses.

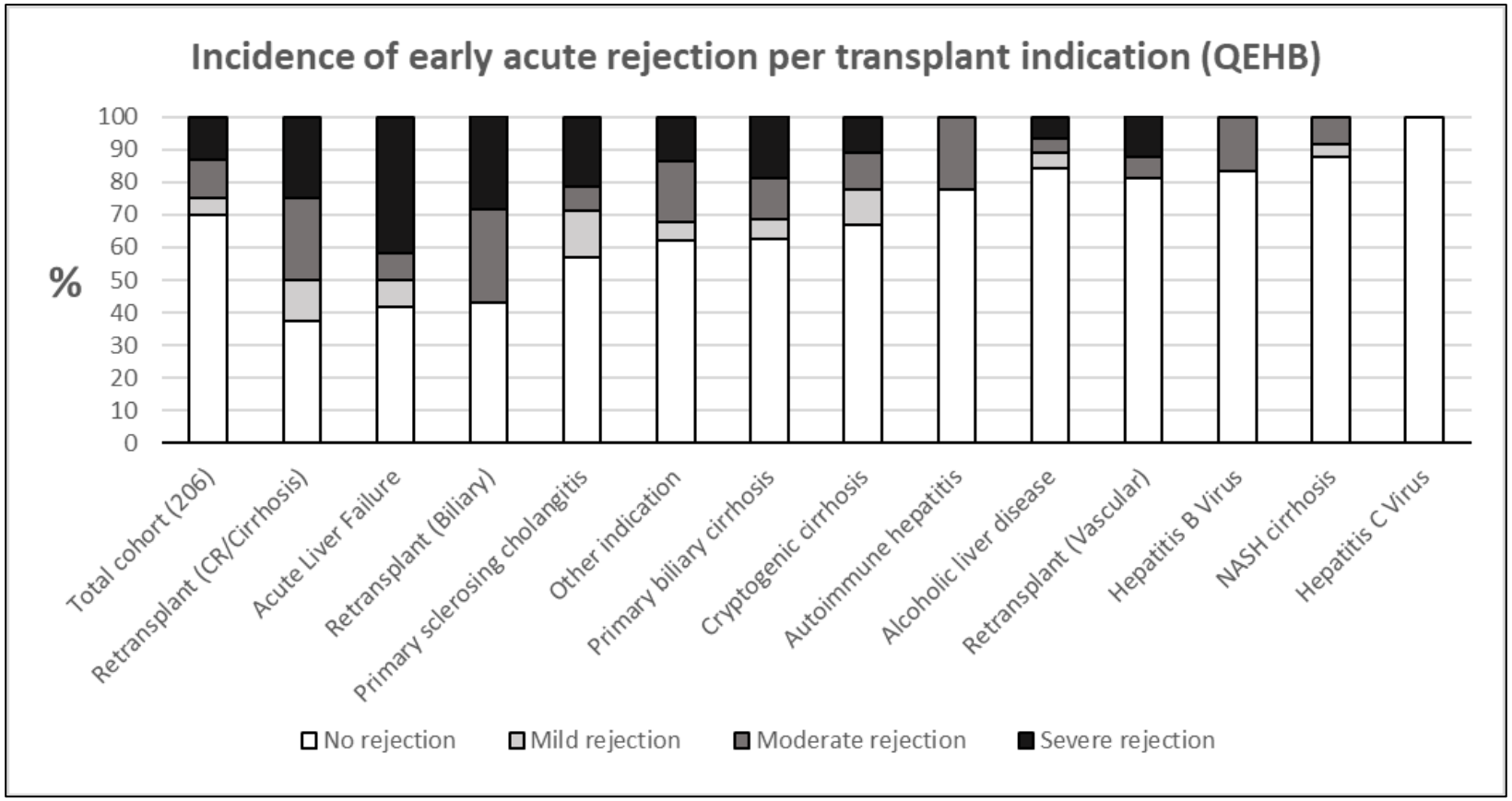


**Figure 1.6**: **Incidence of early acute graft rejection at QEHB (2019-2021).** Bar graph demonstrating the proportion of patients with each disease state that developed early acute rejection. Retransplant (CR/Cirrhosis) represents those transplanted for chronic rejection (CR) or unexplained graft cirrhosis. Retransplant (Biliary) represents those transplanted for biliary strictures with a patent hepatic artery. Retransplant (vascular) represents those with hepatic artery thrombosis.

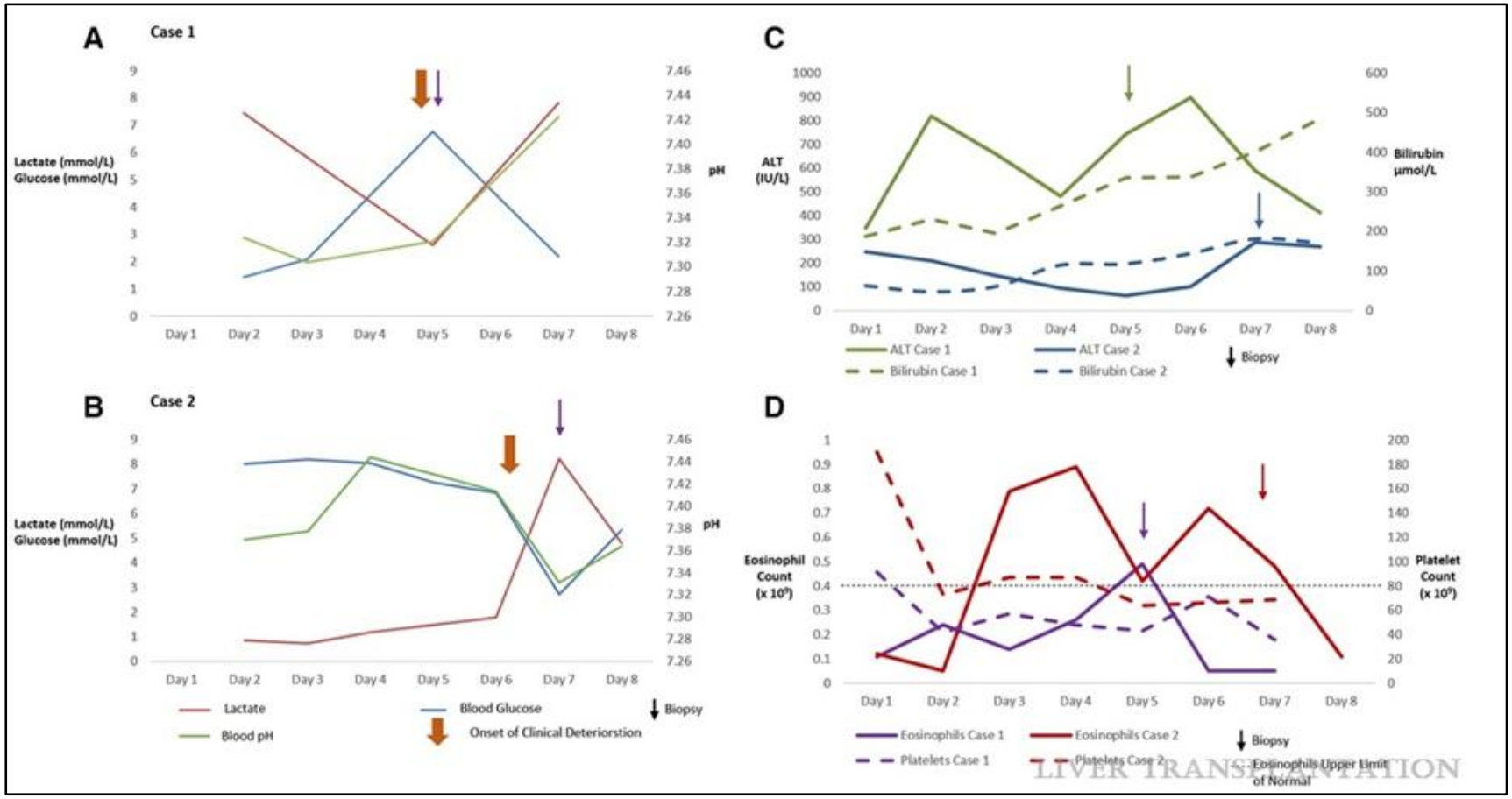


**Figure 1.7. Two examples of early severe acute rejection.** (A) Graph demonstrates the lactate, blood glucose, and pH trend for a 23-year-old female patient and (B) the 48-year-old female patient during the initial postoperative period. (C) Postoperative ALT and bilirubin levels are shown for both cases as well as the (D) postoperative eosinophilia and thrombocytopenia in both cases. Source: Halle-Smith JM**,** Hann A, Cain OL, Perera MTPR, Neil DAH. Lactic Acidosis, Hypoglycemia, and Eosinophilia: Novel Markers of Antibody-Mediated Rejection Causing Graft Ischemia. *Liver Transpl*. 2021 Dec;27(12):1857-1860. https://pubmed ncbi.nlm.nih.gov/34018668/

### 1.3 Operational tolerance

Tolerance in the transplant setting refers to the ability to endure continued exposure to foreign allograft antigens without an adverse reaction. A therapy that can induce tolerance of the allograft without immunosuppression has been referred to as a 'holy grail' of transplantation by many [36-38]. The term "operational tolerance" implies a state of stable graft function following cessation of immunosuppressive medications and without evidence of rejection or graft injury [39]. Operational tolerance is known to occur spontaneously following LT more frequently than any other solid organ transplant [18]. This observation became apparent from situations of non-compliance or intentional cessation due to post transplant lymphoproliferative disorder (PTLD). Therefore, the options to get patients off immunosuppression can be separated into two approaches 1) Accurate identification of those that will become spontaneously tolerant, or 2) Applying therapies that induce tolerance, with subsequent withdrawal.

Immunosuppression withdrawal trials suggest that the rate of spontaneous operational tolerance may be as high as 40% in adults and 60% in paediatric patients post OLT [40,41]. However, these studies included a highly selected sample of transplant recipients and lifelong immunosuppression remains the norm. In a more recent multicentre trial of immunosuppression withdrawal in paediatric recipients, the investigators only enrolled children transplanted at ≤6 years of age and more than 4 years since transplant[42]. Children transplanted for an AILD, Hepatitis B (HBV) or C (HCV) were excluded, along with those who had more than 1 organ transplant[42]. In this study, 35% of children were operationally tolerant with minimal pathological change on graft biopsy at 12 months from ceasing immunosuppression[42].

Research focused on detecting biomarkers that identify patients who have a higher probability of developing operational tolerance and therefore allow an expedited withdrawal of immunosuppression are ongoing [43]. Biomarkers from transplant recipients' peripheral blood that have previously been investigated include the monocytoid dendritic cells (DC) to plasmacytoid DC ratio, the ratio of Vdelta1 to Vdelta2 gammadelta T cells, hepcidin and ferritin. The phytohemagglutinin stimulation index and lymphocyte subpopulations in tolerant and non tolerant recipients have also been compared, with no significant difference being found in the lymphocyte populations but a lower Phytohemagglutinin stimulation index in tolerant patients[44]. Furthermore, transcriptional analysis of graft biopsies has also been analysed as part of prospective trials[42]. However, the gene expression at trial entry failed to show a difference between the subjects that demonstrated tolerance, and those that did not. A recent meta-analysis showed that as time from transplant lengthens, the likelihood of attaining operational tolerance increases[45]. These authors demonstrated that for every additional year of pre-withdrawal time from transplant, the likelihood of successfully attaining operational tolerance increased by 7%[45]. This suggests that integration of graft antigens into the recipients immune profile occurs, but slowly. Other predictors of operational tolerance have been investigated as part of the aforementioned immunosuppression withdrawal trial in children[42], and no clinical or serological biomarker predicted the successful withdrawal of immunosuppression. The only parameter that showed significance in predicting successful withdrawal was pre-withdrawal histology showing no portal or lobular inflammation, lower leukocytes and MHC class II cells. Given the inability to accurately predict those that will become tolerant via biomarkers, a major aim in the field of transplantation is the development of tolerance inducing strategies.

One approach put forward to induce tolerance following liver transplantation are T-cell depleting strategies. This has previously been applied in clinical practice in the form of anti-thymocyte globulin (ATG), which are IgG antibodies raised in rabbits against human thymocytes[46]. Starzl et al administered ATG immediately pretransplant to 17 liver transplant recipients, and demonstrated near total depletion of T-cell subsets[47]. In this small trial, these authors were able to get the majority of patients (12/17) onto monotherapy with tacrolimus only. A subsequent randomised trial of ATG as an induction therapy, followed by immunosuppression withdrawal, was terminated early due to a significantly higher rate of acute rejection in the ATG/weaning group[48]. Another drug tried as a depleting type therapy is Alemtuzamab, which is an antibody against CD54 which is expressed on mononuclear cells in the peripheral circulation[49]. However, both ATG and Alemtuzamab have not become common place in liver transplantation due to concerns regarding greater susceptibility to infection post operatively as a result of the lymphocyte depletion[49].

Another option put forward to induce tolerance following liver transplantation is via the administration of different immune cell populations. The cell populations postulated (and investigated) as tolerance inducing cellular strategies include dendritic cells (DCs), mesenchymal stem cells (MSCs) and regulatory T-cells (Tregs). DCs that have immunosuppressive properties are known as regulatory DCs and exert their tolerance inducing effect by inducing apoptosis of self-reactive T-cells, and liberation of cytokines that promote other tolerance inducing cell subsets (such as Tregs)[50]. The administration of regulatory DCs has been trialled in the living donor liver transplant setting and a major finding from this study was that it increased the proportion of circulating Tregs [51]. MSCs have been suggested to promote IL-10 secreting macrophages, and the secretion of HLA-G5 which promotes Treg development[50]. MSCs have been used in clinical practice post-

transplant but failed to demonstrate the ability to induce operational tolerance[52]. Tregs are described in greater detail in the next section but have shown the greatest promise as a tolerance inducing strategy.

### 1.4 Regulatory T-cells (Tregs)

A subset of $CD4^+$ T-cells proposed to have suppressive abilities was first identified by Nizuzhuka and Sakakura in 1969, subsequently Ghershon and Kondo (1971) demonstrated that thymus derived lymphocytes are required for tolerance induction [53-55]. Many decades of further research defined this tolerance inducing T-cell lineage as $CD4^+$ $CD25^+$ with the transcription factor FoxP3 and known as regulatory T-Cells (Treg) [55,56]. Tregs comprise between 5-10% of $CD4^+$ lymphocytes in the systemic circulation and their suppressive effects on effector T-cells comes from several different mechanisms (Figure 1.8) [57-60]. Enhancement of Treg function may be beneficial in autoimmune disease, chronic inflammation and transplant tolerance. In contrast, due to an individual's immune response having a pivotal role in removing tumour cells, Treg inhibition may have anti-oncogenic effects [61].

The process of Treg generation occurs in both the thymus and periphery, resulting in thymus derived Tregs (tTregs) and induced Tregs (iTregs) respectively [62]. T cell receptor (TCR) signalling in the thymus appears to mediate the generation of tTregs whereas the generation of iTregs can be mediated by numerous mechanisms including exposure to foreign antigens or the type 1 interferon family [62,63]. The process of tTreg generation from thymocytes is enhanced by CD28 co-stimulation as it increases the intensity and duration of T-cell receptor signalling (TCR) [64]. The *de-novo* generation of $FoxP3^+CD4^+CD25^+$ iTregs from naïve $CD4^+CD25^+$ T cells in the periphery has been demonstrated to occur with persistent exposure to a low dose of a foreign peptides [65] in the presence of TGF-β. A proportion of iTregs are known as T regulatory type 1 cells (Tr1) which are characterised by the co-expression of

CD49b and lymphocyte-activation gene 3 (LAG-3), with the ability to secrete high levels of IL-10 and TGF-β [62,66,67]. In contrast to other types of Tregs which constantly express FoxP3, Tr1 type cells only express FoxP3 temporarily upon activation [66].

As described above, the Treg cell population can be split based on the site of origin, but the subpopulations can also be based on phenotype and function as described by Miyara et al (2009)[68]. These authors described three functionally different subpopulation based on FoxP3 and CD45 staining; $CD45RA^{+}FoxP3^{lo}$ (resting or naive, rTregs), $CD45RA^{-}FoxP3^{hi}$ (activated, aTregs) and cytokine-secreting $CD45RA^{-}FoxP3^{lo}$ (cytokine-secreting non-Treg cells)[68]. The majority of the aTregs originate from rTregs. Once stimulated the rTregs increase their expression of proliferation marker Ki-67 and FoxP3[68]. The aTregs are terminally differentiated and are short-lived whereas the rTregs have a long lifespan in their resting state. The cytokine-secreting non-Treg cells secrete the largest amount of IL-17 and have the greatest potential to transform into Th-17 cells [68].

In the peripheral blood of healthy humans, Wang et al demonstrated $CD45RA^{+}$ and $CD45RO^{+}$ comprised 23.9% and 63.6% of $CD4^{+}$ $CD25^{+}$ $FoxP3^{+}$ Tregs [69]. These two markers ($CD45RA^{+}$ and $CD45RO^{+}$) have been reported to be mutually exclusive [70]. In LT recipients on calcineurin inhibitor (Tacrolimus) therapy, the frequency of $CD45RA^{+}FoxP3^{lo}$ and $CD45RA^{-}FoxP3^{hi}$ was decreased in comparison to healthy controls, but $CD45^{-}FoxP3^{lo}$ were similar [71]. These authors concluded that a limited availability of IL-2 was responsible for Treg cell death. Furthermore, $CD45RA^{+}$ Tregs have been demonstrated to be present in the peripheral circulation at a higher frequency in paediatric liver transplant recipients that have developed graft tolerance in comparison to recipients that have not developed tolerance [72]. Data on the frequency of each subset within the liver is more limited. In a study by Zhang et al that reported the cell subsets within the explanted livers of patients with biliary atresia,

these authors found $CD45RA^+$ Tregs to comprise approximately 50% Tregs within the parencyma [60].

To effectively maintain peripheral tissue immune homeostasis, Tregs are required to maintain a stable, anergic and immunosuppressive phenotype[73]. The anti-inflammatory and immunosuppressive effects of Tregs have been attributed to both direct and indirect mechanisms (Figure 1.8) [62]. Mechanisms include CTLA-4 on Treg leading to trans-endocytosis of CD80/86 molecules on antigen presenting cells, depriving effector T-cells of IL-2 by competitive consumption, depletion of extracellular adenosine triphosphate (ATP) via the release of adenosine through the CD39 molecule on Tregs, secretion of immunosuppressive cytokines (IL-10, IL-35 and TGFβ) and cytotoxic enzymes Granzyme and Perforin to kill T effector cells [62,74]. These functional mechanisms of Tregs can vary depending on given immune scenario, the stimulus and corresponding microenvironment[62,75,76]. For example, in a murine model of acute liver injury an alleviation of inflammation occurred with adoptive transfer of Tregs and this was associated with increased IL-10 levels within the liver [77,78].

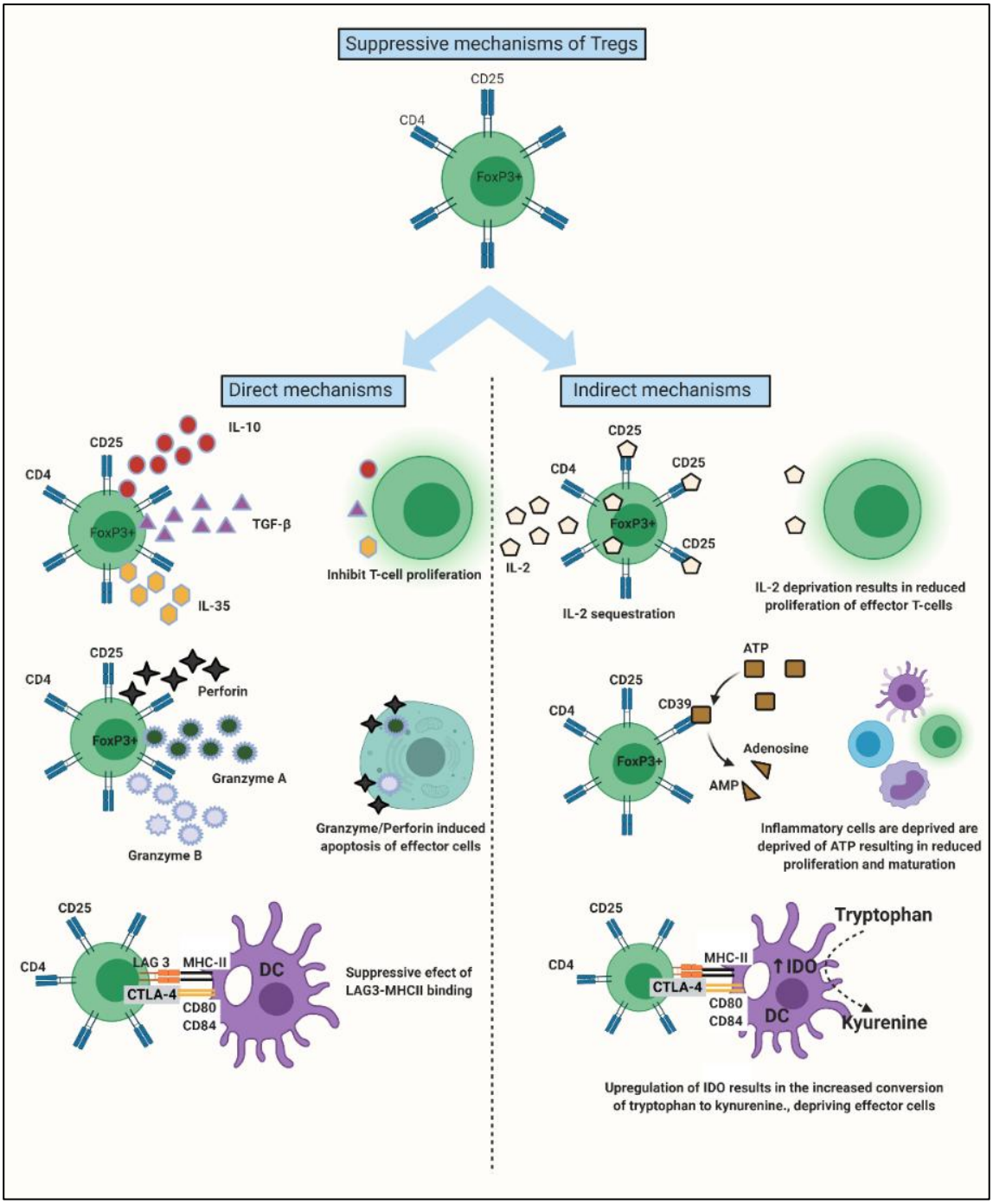


**Figure 1.8. Direct and indirect mechanisms of Regulatory T-cells immunosuppressive effects.** DC=Dendritic cell IDO= Indolamine-2,3-dioxygenase. Source: Hann A, Oo YH, Perera MTPR, Front Immunol. 2021 Oct 14;12:719954

### 1.4.1 Tregs and liver transplantation

Pharmacological immunosuppression to prevent rejection in the recipient has progressed significantly over the last five decades, however both graft rejection and medication side effects are significant causes of morbidity [21,79]. Therefore, a therapy that can induce tolerance of the graft without immunosuppression has been referred to as a 'holy grail' of transplantation by many [36-38]. Tregs have shown the ability to induce graft tolerance in animal models and have been demonstrated to be present at a higher frequency within liver grafts of spontaneously tolerant humans [80-82].

Several different recognised pathways for graft rejection exist (direct, indirect and semidirect), with the main difference being the origin of the APC [83]. Primed $CD8^+$ T-cells are the main effector cells that respond and induce the damage to the graft [84]. An inflammatory microenvironment, such as that which occurs with preservation-reperfusion injury, has been associated with an increased incidence of rejection [85]. The induction of MHC II expression on hepatocytes, LSEC and cholangiocytes by inflammation may provide the mechanistic explanation of this phenomenon [84]. The proposed immunosuppressive mechanism of Tregs in the setting of transplantation does not differ to that proposed in other disease states with IL-2 deprivation, chemokine secretion and direct inhibition of APCs reported [86].

Human trials of Treg therapy in the organ transplantation arena have yielded mixed results [36,87-89]. The greatest promise was shown by Todo et al (2016) in which early operational tolerance was achieved in 7 out of 10 subjects following the administration of a Treg-containing cell product that comprised ex-vivo expanded recipient Tregs, that had been co-cultured with irradiated donor lymphocytes [87]. This trial was terminated early due to rejection occurring in three subjects that were transplanted for autoimmune liver diseases, however the high rate of operational tolerance achieved at such a short time interval from transplant was

viewed as a step forward. The participants in this study had undergone living donor liver transplantation (LDLT) and therefore access to donor tissue antigens was possible ahead of the transplant operation, an option not possible in many countries with predominantly deceased liver transplant programs. During long term follow up of the seven patients with Treg induced tolerance, Todo et al (2018) demonstrated a variation in peripheral Treg frequency and responsiveness to donor antigens [90]. Despite all seven subjects having grafts without evidence of rejection on biopsy, three demonstrated a significant immune response to donor cells on mixed lymphocyte response analysis several years post-transplant [90]. Treg frequency in the peripheral blood increased gradually in three, increased then decreased in three, and remained static in one [90]. This suggests the changes in the peripheral blood compartment may not accurately reflect cell interactions within the liver graft.

In the ThRIL trial, Sanchez-Fueyo et al (2020) assessed the donor specific alloimmune response in liver transplant recipients that received an autologous polyclonal Treg infusion post liver transplant[88]. This trial was different that by Todo et al in that it was in the context of deceased donor liver transplantation, as opposed to living donation. Nine liver transplant recipients received polyclonal autologous Treg between 83 to 481 days post-transplant. These authors showed that in the participants that received the higher dose of Tregs (4.5 million/kg), the T-cell response against donor cells was diminished. This effect was not seen to third party cells and therefore suggests tolerance induction specifically to donor antigens. The details and results of subsequent Treg trials in liver transplantation have been extensively compared and contrasted in reviews by others [36,86].

Maintaining an immunosuppressive phenotype and function is one of the challenges when expanding Tregs for cellular therapy[91]. In a murine experimental model, Li et al demonstrated

that Tregs can be converted into IL-17 producing cells and that IL-1β was required for this to occur both *in-vitro* and *in vivo* [92]. This conversion has also been demonstrated with human Tregs but IL-2 and IL-15 were thought to be the key to this process [93]. However, both rapamycin and cyclosporin A have been shown to inhibit the generation of IL-17 producing cells in a murine model [94]. These authors also demonstrated an additional benefit of rapamycin over cyclosporin A was its ability to promote the generation of $FoxP3^+$ cells [94]. Therefore, Tregs expanded in the presence of Rapamycin and IL-2 has been shown to optimise the suppressive abilities of the final cell population [91].

Increasing Treg frequency or function within the liver is essential for the tolerance inducing benefits, given the aforementioned mechanisms. In an animal model, Fujiki et al (2010) demonstrated that $CD4^+$ $CD25^+$ $FoxP3^+$ cells had an increased frequency in the liver and spleen of tolerant liver transplant recipients, in comparison to the non-tolerant animals[80]. Extraction of these cells showed in-vitro suppression of T-cell proliferation, and transfer to another animal prolonged the survival of an additional heart graft [80]. Intravenous administration of Tregs to achieve tolerance following liver transplantation relies on these cells travelling through the peripheral circulation to reside within the liver. Tracking of intravenously administered Tregs via indium labelling was performed by Oo et al (2019) and these authors demonstrated that only 22-30% of the administered cells are present in the liver at 24 hours post administration in those individuals with a functioning spleen [95]. Subsequent assessment at 72 hours demonstrated the proportion of cells within the liver had fallen [95]. Functional asplenism resulted in a higher proportion of cells (44.8%) residing in the liver at 24 hours [95]. Once Tregs have migrated out from the hepatic sinusoids, chemokine gradients influence their position and they can reside around the portal tracts or parenchyma depending on the microenvironment [96,97]. Therapeutic efficacy of Tregs in liver transplantation may be

enhanced if homing mechanisms can be optimised, enabling these immune modulating cells to exert their direct effect within the graft. Administration of cell therapy directly into the graft prior to implantation may be a novel and worthwhile approach, as the utilisation of ex-situ machine preservation devices are becoming more common. Utilisation of these devices as a platform to deliver Tregs or modulating therapies would avoid the issues of cell homing and minimise the potential for undesirable systemic effects.

### 1.4.2 Tregs in acute graft rejection

The assessment of Treg frequency and function post-transplant is confounded by the additional introduction of pharmacological immunosuppression. In addition to suppressing effector cell activity, non-specific immunosuppressant therapies also affect the Treg population [98]. Treg frequency in the peripheral blood has been demonstrated to be higher in patients with liver disease awaiting transplantation than healthy controls [99]. A reduction in peripheral blood Treg frequency has been observed immediately post-transplant, with a subsequent increase over the first postoperative year but never returning the pre-transplant level[98,99]. The Treg frequency at 12 months post-transplant was reduced in patients that had experienced acute rejection [99]. Han et al (2020) demonstrated that the activated Treg frequency on day 7 was significantly lower in those that developed biopsy proven TCMR [98]. A Treg/CD4 frequency of less than 4.7% on post-transplant day 7 was shown to predict biopsy proven TCMR with a sensitivity and specificity of 100% and 91.4% respectively. Furthermore, these authors demonstrated that the expression of the anti-apoptotic molecule Bcl-2 was reduced on Tregs collected on day 7 post-transplant from patients that experienced rejection, in comparison to non rejectors [98]. Therefore, apoptotic Treg death may explain the reduced frequency of Tregs in acute rejection. In a study of paediatric liver transplant recipients, the frequency of Tregs was significantly lower and the frequency of Th17 cells

significantly higher in blood samples taken in patients experiencing rejection in comparison to non-rejectors and healthy controls [100]. The frequency of both Th17 and Tregs was reduced by the initiation of immunosuppression[100]. Treg cell-based therapy administered at the onset of acute rejection or in treatment resistant cases have not been trialled in humans but represents an interesting concept.

### 1.4.2 Tregs in chronic graft rejection

As time progresses from transplant, acute TCMR becomes less frequent as this most commonly occurs in the first 6 weeks post-transplant[21]. However, a chronic form of rejection can substantially contribute to graft dysfunction and loss [101,102]. Chronic rejection is characterised by ≥50% loss of bile ducts and ≥25% loss of arteriole within the portal tracts, perivenular bridging fibrosis and fibro-intimal hyperplasia of the large perihilar arteries [103]. The indirect pathway is proposed to be responsible for chronic rejection [102,103]. Wan et al (2012) demonstrated the dominance of Th2 cytokines, particularly IL-10, in an animal model of chronic rejection. These authors proposed that the Th2 response accelerates the production of alloreactive antibodies [102]. Minimal literature exists describing Treg frequency, localisation and function in human liver graft recipients with chronic rejection. In recipients of renal grafts, patients with chronic rejection have a significantly lower peripheral blood frequency of $CD25^{high}CD4$ Tregs than healthy controls and tolerant patients [104]. At present, there is no specific therapy for chronic rejection of a liver graft that will reverse the pathological changes. If organ function is significantly compromised, re-transplantation is the only option. The effect of augmenting Treg frequency and function in the setting of chronic rejection remains unknown at present.

### 1.5 Machine preservation technology

The concept of perfusing a liver ex-vivo as a preservation strategy is far from a new concept [105,106]. These early experiments in the 1960's and 1970's utilised a cold oxygenated perfusate [105]. Widespread uptake and further development of this approach was halted for several decades, potentially due to the introduction of more efficacious preservation solutions [105]. During the last decade, there has been a renewed interest in this technology due to a recognised need to transplant more deceased donor organs. In current clinical practice, both in-situ perfusion utilising a technique called normothermic regional perfusion (NRP) and ex-situ perfusion utilising NMP or hypothermic machine perfusion (HOPE) are common place.

The published literature is demonstrating that each perfusion technique has a different role, for example HOPE has evidence for the prevention of ischaemic type biliary lesions[107] (ITBL) in DCD grafts, and NMP has evidence that it improves graft utilisation[108].

HOPE is performed after the donor organ has been retrieved, and immediately prior to implantation at the recipient centre. The graft is perfused with a organ preservation solution (University of Wisconsion, UW) that is supplemented with glutathione, at approximately 10°C. The solution is oxygen enriched with a patial pressure of >750mmHg (>100Kpa)[107]. Two different perfusion strategies are currently being used by transplant centres: (1) Single HOPE which involves perfusion through the portal vein only; and (2) dual or 'D-HOPE' consisting of perfusion through the portal vein and the hepatic artery. The benefit of the former is that it is simple to perform and does not risk injury to the artery with the cannulation. Proponents of D-HOPE emphasize that the blood supply to the biliary epithelium is only from the artery and therefore delivering oxygen to these cells relies on this route[109]. The time of perfusion is generally shorter than that of NMP, with the duration of HOPE being as short as 2 hours[107]. Barriers to using HOPE as a delivery platform for cellular therapeutics are the non-

physiological electrolyte composition (intracellular concentrations of electrolytes) and the fact that normal cellular physiology of the graft does not take place at the hypothermic temperatures. Furthermore, the short period the graft is perfused with this modality may impact the proportion of cells engrafted.

Abdominal NRP is a perfusion technique that delivers oxygenated blood at physiological temperature whilst the abdominal organs are *in situ* in DCD donors[109]. This is performed by rapidly cannulating the femoral artery or aorta and perfusing using a circuit similar to that used in extracorporeal membranous oxygenation, straight after the donor is declared dead via circulatory criteria. This provides a period of resuscitation immediately after the cellular injury that resulted from the warm ischaemic period[110]. The provision of this machine-driven circulation with oxygenated blood is proposed to resuscitate the graft (both hepatocytes and cholangiocytes) and improving its energy stores, allowing greater tolerance of the cold ischaemic period[110]. The period of NRP is approximately 2 hours[111], and is followed by standard cold perfusion and storage, however further ex-situ machine perfusion of the graft is also possible. Although the abdominal NRP period does provide an opportunity for the administration of cellular intervention, it would be delivered to all abdominal viscera and not the liver graft specifically. Furthermore, bleeding often occurs during the abdominal NRP period and therefore there is potential that cellular medicinal products could be lost.

NMP of the liver involves the perfusion of oxygenated third-party donor blood at physiological temperatures via both the hepatic artery and portal vein whilst the liver is ex-vivo. This facilitates cellular processes to continue during the period of NMP, prevents depletion of adenosine triphosphate and restores hepatocyte glycogen [112]. Both hepatocyte and cholangiocyte viability can be assessed via several surrogate markers in the perfusate and bile

respectively. Several NMP devices are being used in clinical practice and these are adequately described by Ceresa et al [112]. The main differences in these devices are in the arterial inflow (pulsatile vs continuous), venous outflow (closed vs open system) and oxygenator characteristics (inbuilt vs external). The most utilised device in the UK is the Organox metra.

The clinical application of NMP has progressed rapidly over the last 10 years. An initial pilot study by Ravikumar et al demonstrated the safety of NMP in comparison to CS in a UK based study [113]. These results were replicated in two separate trials in Canada, however Bral et al found the length of intensive care and overall hospital admission was significantly longer in the patients that received an NMP preserved liver [114,115]. A subsequent randomized clinical trial by Nasralla et al that compared NMP preserved livers with SCS demonstrated greater graft utilisation and significantly lower aspartate transaminase (AST) for NMP preserved livers [108]. All NMP trials up until this point applied NMP at the donor hospital ("at source") to standard criteria grafts that were otherwise transplantable with CS preservation. In order to use this technology in the most efficacious and pragmatic manner, several centres have more recently focused on applying it at the recipient hospital ("back to base") to grafts that would otherwise be discarded [116-120]. The benefit derived from this approach is that the donor pool is expanded, facilitating more transplants and preventing waitlist mortality. The objective viability assessment provided by this technology has given clinicians the confidence to transplant sub-optimal organs with less concern of primary non-function [119]. The rationale for using NMP in different clinical scenarios, and the associated evidence is displayed in figure 1.9.

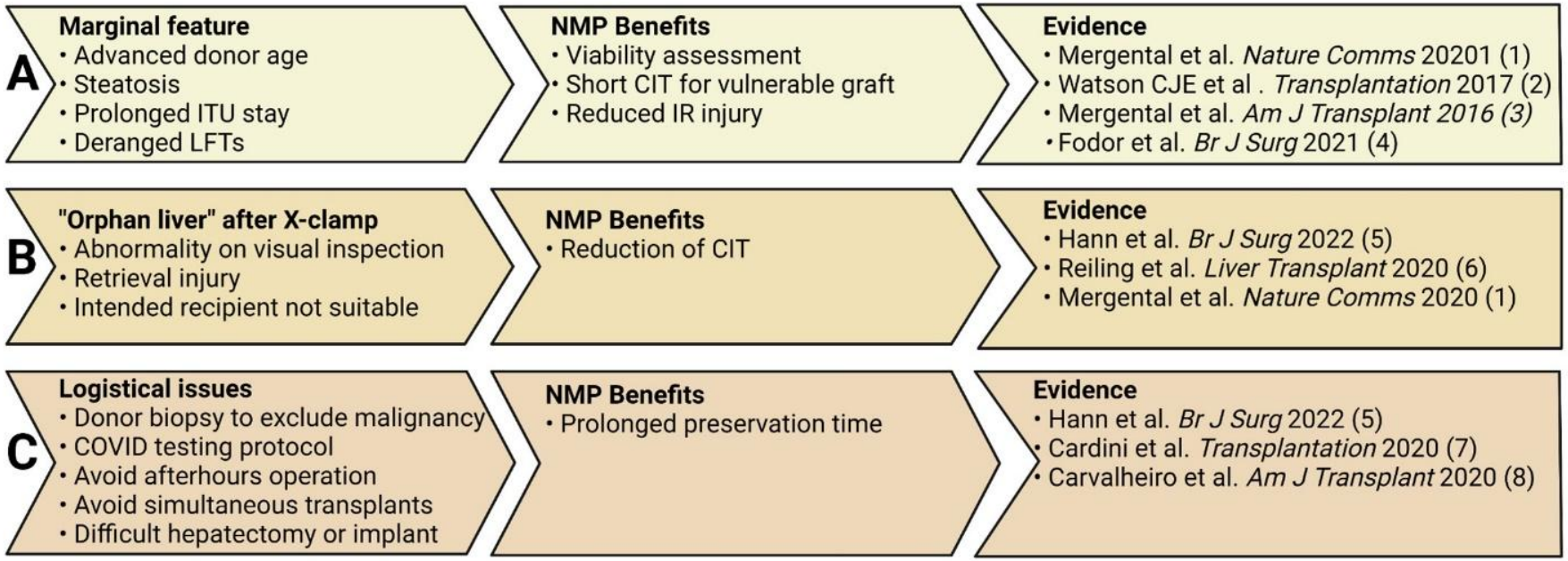


**Figure 1.9. The rationale, benefits and evidence for NMP for different indications.** Diagram demonstrates the benefits for A) Donors or grafts with suboptimal features B) Livers declined after removal from donor C) Logistical issues with transplanting the organ within an acceptable time period. CIT= Cold ischaemic time. IR= Ischaemia-reperfusion. Figure published as Hann A, Nutu A, Clarke G, Patel I, Sneiders D, Oo YH, Hartog H, Perera MTPR. Normothermic Machine Perfusion-Improving the Supply of Transplantable Livers for High-Risk Recipients. *Transpl Int*. 2022 May 31;35:10460. doi: 10.3389/ti.2022.10460.

### 1.6 NMP as a Treg therapy delivery platform

The ability to preserve an organ via an isolated circuit, outside the human body, provides the opportunity for numerous different types of assessment and therapies. These conditions are ideal as they prevent any undesirable or unknown 'off-target effects'[121]. In contrast to hypothermic ex-situ perfusion methods, during NMP the grafts cells metabolic pathways are active and therapeutic intervention can target these. Interventions being investigated include ribonucleic acid (RNA) silencing technology, biliary organoids and defatting therapies[121-123]. A benefit of NMP over abdominal NRP is that the therapeutic intervention can be organ specific, and is retained within the perfusion circuit for the entire duration of perfusion.

Utilising this time period, and the perfusion circuit, to administer therapeutic agents directly to the liver graft is now a realistic prospect[124,125]. A multicentre randomised control trial (DEFAT), recently commenced in the UK and is currently in its recruitment phase. It is comparing conventional NMP (control arm) with NMP combined with defatting drugs (Forskolin and L-carnitine)[126]. Liver specific therapies administered directly to the graft may have greater efficacy and reduce the off target effects of the pharmacological or cellular therapies. The administration of Tregs via the NMP circuit, and therefore direct delivery to the liver, may achieve a greater density of Tregs within the organ. Previous research by Oo et al has demonstrated that intravenous administration of expanded therapeutic Tregs only results in 20%-40% reaching the liver[95]. Therefore, direct administration of Tregs to the liver ex-situ may have greater efficacy for the induction of immune tolerance as many of the Treg mediated immunosuppressive mechanisms are local rather than systemic. The effectiveness of such an approach has not as yet been investigated in the laboratory or clinical practice. Little is known about ex-situ administered cell therapy and data on whether the cells are

retained within the graft and their functionality is lacking. This topic is the focus of research thesis and will be further described in the subsequent chapters.

### 1.7 Project hypothesis and aims

The overall hypothesis of this project is that the direct infusion of human expanded Tregs into the liver, via a NMP model, will result in them being engrafted into the hepatic parenchyma and induce a more tolerogenic profile of the tissue.

**Aim 1**: Delineate the immunological changes that occur within the liver during ex-vivo normothermic machine perfusion, as indicated by cytokine profile, proteomics and RNA sequencing. **(Chapter 3)**

**Aim 2**: Isolate human Tregs from peripheral blood, and expand them whilst also maintaining FoxP3 expression. **(Chapter 4)**

**Aim 3**: Determine the location and survival of Tregs that are directly infused into the human liver ex-vivo via a normothermic machine perfusion model. **(Chapter 5)**

## 1.8 Impact of the COVID-19 pandemic on the project

This research project commenced in February 2020, and within 8 weeks the SARS-CoV-2 virus was causing significant societal disruption. The United Kingdom was affected relatively early in the pandemic and had significant implications for health care and academic research. In April 2020, policies designed to avoid mass gatherings of people were implemented and therefore the University of Birmingham and the Institute of Biomedical Research was closed to post graduate researchers. In addition, all trained health care workers within the UHB trust were redeployed to assist in the clinical management of the large influx of patients with COVID-19. Both these factors meant that there was limited access to learn laboratory skills and complete experiments. The university closures, strict social distancing rules, and redeployment continued throughout 2020 and for the majority of 2021. Another COVID-19 related factor that affected the progress of this research was the lack of research funding for non-COVID-19 research. This likely reflected both a change in research priority to focus on this new disease, and global economic downturn with many institutions conserving funds. During my first year I was unsuccessful in obtaining the adequate funds to cover any major laboratory consumables, so focus was on research planning, background research and literature review.

# Chapter 2 – General methods

## 2.1 Cell isolation buffer

Isolation buffers are important to keep cells in optimal health, and prevent undesired antibody binding. Flouresence activated cell sorting (FACS) buffer aims to achieve both of these objectives. This buffer is used in numerous situations to suspend and store cell samples. It is also used during the antibody staining step for FACS, suspending cells for running on the flow cytometer or FACS analyser. The predominant fluid component of this buffer is Phosphate buffered saline (PBS) which provides an isotonic solution. The addition of some protein (Bovine serum albumin, BSA) prevents non-specific antibody binding. The addition of Ethylenediaminetetraacetic (EDTA) inactivates the platelets and prevents clumping. This buffer was used for my cell isolation experiments.

FACS Buffer: 500ml bottles of FACS buffer made by combining 473 mls of phosphate buffered saline (PBS), 25 mls of 10% Bovine serum albumin (BSA), and 2mls of Ethylenediaminetetraacetic acid (EDTA)

## 2.2 Peripheral blood mononuclear cell isolation

Peripheral blood mononuclear cell (PBMC) isolation from whole blood aims to obtain the lymphocytes and monocytes (mononuclear cell fraction). The principal applied is density gradient centrifugation, which utilises the fact that different cell and liquid components of whole blood have different densities. This type of PBMC isolation is common place in immune cell experiments, as it gives a relatively pure lymphocyte population for downstream applications. The cell population obtained has a high proportion of lymphocytes and monocytes, but a small number of granulocytes remain as indicated by flow cytometry plots. PBMC isolation is required prior to further T-cell subset isolation experiments.

During this research, PBMC isolation was performed on:

- Human blood from healthy volunteers who were able to donate up to 70mls each month (Ethics: 18-WA-0214 )
- Human blood from patients undergoing venesection for haemachromatosis who provided approximately 300mls of blood (Ethics: 04/Q2708/41)

PBMC isolation using venesection blood from humans with haemachromotosis was used for the majority of the cell isolation and flow cytometry optimisation experiments, this was because the volume available was larger and allowed numerous concurrent samples. However healthy volunteer blood was used for the final experiments.

Blood volumes were obtained based on the average that 1ml of whole human blood provides approximately 1 million PBMC. However, large variation in yield of lymphocytes does exist between individuals, and even for the same individual at different time points.

Peripheral blood mononuclear cell isolation was performed on the day of blood collection, or within 24 hours.

1. Lympholyte® cell separation media (CedarLane) taken out of storage and left to be at room temperature.
2. Using 50ml falcon tubes, add 15ml of Lympholyte® cell separation media to the bottom of falcon tube and then slowly layer 30ml of whole blood using electronic pipette on top of the Lympholyte®. The blood should not mix with the lympholyte®.
3. Centrifuge the falcon tube at 1800rpm with max acceleration (9) and minimum deceleration (0) speeds. This is to ensure that after the blood has been separated, it does not remix during deceleration.

4. After centrifugation, a thin band of lymphocytes will be evident between the serum and lympholyte®. This needs to be removed carefully using a pasteur pipette until a glassy interace between the two layers is remaining.
5. The removed lymphocytes should be removed and placed into a 15ml falcon tube. After removing all lymphocytes, top this tube up to at least 10ml using complete RPMI (RPMI with 100U/ml penicillin and 0.2ug/ml stretomycin, 5mM of glutamine)
6. Centrifuge the lymphocyte cell solution at 1800rpm for 10 minutes at maximum acceleration and deceleration. This should provide a clear cell pellet.
7. Resuspend cell pellet in complete RPMI and repeat centrifugation at 1800rpm for 10 minutes at maximum acceleration and deceleration. This should provide a clear cell pellet.
8. Resuspend cell pellet in appropriate volume of complete RPMI with 10% fetal bovine serum (FBS).
9. Perform manual cell count using trypan blue and microscope

**2.3 Liver derived lymphocyte isolation**

This process aimed to obtain the mononuclear cell fraction from whole liver tissue. Due to the fact that liver tissue is in solid form, this first requires mechanical dissociation of the so that the cellular fraction (hepatocytes, leukocytes and erythrocytes, cholangiocytes) and in liquid suspension. The combination of mechanical dissociation and washes with PBS remove the connective tissue stroma component. Once this has occurred, the principal of density gradient centrifugation is applied in a manner similar to PBMC isolation.

During this research, this process was performed on human liver tissue deemed not suitable for clinical transplantation. The donor families had provided consent for utilisation of the

liver for research purposes (Ethics: 18-WA-0214). After organ retrieval, the livers were transported to the University of Birmingham using ice storage (Temperature 1-4°C) and stored in Histidine-Tryptophan-Ketoglutorate (HTK) organ preservation solution. The liver tissue was used in experiments on the day of arrival, or the next morning if arrived during the night. Liver derived lymphocyte (LDL) isolation was performed at the end of cell infusion experiments (Methods 2.15 & 2.16) so that the labelled cell fraction could undergo post infusion phenotyping.

A limitation of LDL isolation is that it is influenced by the quality of the liver tissue. Steatotic liver often provides a very low yield of lymphocytes as a large amount of debri (intracellular fat) is released during the mechanical dissociation. Multiple washes of the cell population with discard of debri is required, however a fraction of lymphocytes is lost with each of these. Therefore, cautious selection of livers to use for this process was applied.

1. Before starting isolation, weigh the liver specimen and place on a large petri dish
2. Score the slices with a scalpel, dicing the liver into small pieces. Transfer into a plastic beaker.
3. Wash the tissue pieces with PBS in a sterile beaker until the effluent is clear.
4. Transfer the liver pieces intto a stomacher bag and add enough RPMI to cover. Heat seal the top of bag in 3 places, minimising the air trapped in the bag. Place in a second bag and heat seal again in 3 places.
5. Place in the stomacher machine for 6 minutes, at a speed of 260rpm.
6. Empty the bags through a fine mesh attached to the top of a large beaker and pour additional PBS until the fluid runs clear. Discard the liver tissue remaining that does not pass through the fine mesh.
7. Divide the cell solution in the beaker that has passed through the fine mesh into 50mL tubes.

8. Allow debris to start to separate out from supernatant by leaving 50ml tubes to stand for 15mins at room temperature.
9. Perform a slow spin to remove the large debri for 5 minutes, at 100g and maximum acceleration and deceleration. At the end of this centrifugation period, the leukocytes will be in the supernatant and the pellet is liver debri.
10. Repeat slow spin if the supernatant is still very cloudy.
11. Filter the supernatant (contains leukocytes), into clean 50mL tubes using 40uM filters.
12. Centrifuge for 10mins at 1800rpm, maximum acceleration and deceleration. The cell pellet now contains the leukocytes.
13. Remove supernatant and resuspend the pellets in PBS – combine pellets and make up the volume to 50mL with PBS.
14. Repeat the centrifugation for 10mins at 1800rpm, maximum acceleration and deceleration. The cell pellet contains the leukocytes.
15. Resuspend the cell pellet in PBS
16. Pipette 20mL Lympholyte® into 50mL tubes (the number of tubes depends on volume of cells) and gently layer 25ml cell suspension on top of Lympholyte® using an electronic pipette.
17. Centrifuge for 25 minutes, at 1800rpm with maximum acceleration (9) and minimum deceleration (9)
18. Remove lymphocyte layer using a Pasteur pipette. This layer sits between the lympholyte® and the PBS. Avoid removing solution below.
19. Pipette into a clean 50mL tube and top up with PBS, and centrifuge for 10 minutes at 1800rpm with maximum acceleration (9) and deceleration (9).
20. Remove supernatant. Resuspend pellet in complete RPMI and centrifuge for 10 minutes at 1800rpm with max acceleration (9) and deceleration (9)

21. Discard the supernatant and resuspend cell pellet in an appropriate volume of RPMI with 10% FBS.
22. Perform cell count using Perform manual cell count using trypan blue and microscope
23. Cells are now ready for staining.

### 2.4 Flow cytometry staining for cell surface and intracellular markers

Flow cytometry allows the assessment of properties of single cells or particles. It uses a laser light source to assess light scatter and fluorescence[127]. In order to utilise the assessment of fluorescence, the cell samples require staining with fluorescently conjugated antibodies. In the study of immunology, these antibodies are directed towards markers on the cell surface or within the cell (intracellular) and can provide information about the cell type and its functional state (phenotype).

During this research, flow cytometry was performed on cell populations isolated from human blood, and human liver tissue. It is a useful method to assess the purity of cell populations during the isolation process. However, a limitation is that different combinations of fluorescent markers can interact with each other and influence the results. Therefore, optimisation experiments are required to ensure all fluorescent markers within the panel are compatible, and that compensation for any interactions can be achieved. The different fluorescently conjugated antibodies used during this research are demonstrated in Table 2.1.

Staining for intracellular markers requires cell death, and a special fixation process. After the cell is killed during the fixation process, a special permeability buffer is required so that the fluorescently conjugated antibody can get within the cell and bind to the intracellular marker. Additional reagents used for the flow cytometry experiments are displayed in Table 2.2.

All flow cytometry experiments were performed on BD LSRFortessa$^{TM}$ flow cytometer.

1. Add 1 and 3x$10^6$ cells into a 5ml FACS tube. Add additional FACS buffer to make a minimum of 1ml
2. Centrifuge FACS tubes for 5mins at 1500 revolutions per minute (rpm), then discard supernatant
3. Suspend cells in 100ul FACS buffer and add 1ul of Fc blocking antibody
4. Incubate for 10minutes at 4°C
5. Add an additional 1mL of FACS buffer and centrifuge FACS tubes for 5mins at 1500rpm, then discard supernatant
6. In a separate epindorph tube, add 100ul of buffer per tube and make up the master mix with the required antibodies. Concentrations of antibodies used in experiments displayed below.
7. Incubate for 25mins at 4°C
8. Add an additional 1mL of FACS buffer and centrifuge FACS tubes for 5mins at 1500rpm, then discard supernatant
9. Repeat wash in step 8 using 1mL FACS buffer, then discard supernatant
10. **If cell surface staining only, add 100ul of cytofix cell fixative and incubate at room temperature for 30 minutes in the dark**.

    If performing additional stains for intracellular markers, add 100ul of FoxP3 fixative (diluted 1:4 with diluent provided in kit) per tube and incubate for 40mins at room temperature (RT) in the dark
11. Add an additional 1mL of FACS buffer and centrifuge FACS tubes for 5mins at 1500rpm, then discard supernatant.
12. **If performing cell surface staining only, resuspend in 350ul of FACS buffer and keep in dark until processed on flow cytometer.**

If performing intracellular staining, add 100ul of permealisation buffer (diluted 1:10 with $H_2O$) and incubate in dark for 30 minutes

13. Add an additional 1mL of perm buffer and centrifuge FACS tubes for 5mins at 1500rpm, then discard supernatant
14. In a separate epindorph tube, add 100ul of perm buffer per tube and make up the master mix with the required antibodies (concentrations as per Table 2.1). Incubate overnight (at least 6-8 hours).
15. Add an additional 1mL of perm buffer and centrifuge FACS tubes for 5mins at 1500rpm, then discard supernatant
16. Add an additional 1mL of perm buffer and centrifuge FACS tubes for 5mins at 1500rpm, then discard supernatant
17. Add 1mL Perm buffer. Centrifuge tube for 5mins at 1500rpm, discard supernatant
18. Add 1mL FACS bufferAdd an additional 1ml of FACS buffer and Centrifuge tube for 5mins at 1500rpm, discard supernatant
19. Resuspend in 350ul FACS buffer for acquisition on flow cytometer

**Table 2.1.** Flow cytometry antibodies and dilutions

| Cell marker | Fluorochrome | Clone | Manufacturer | Catalogue # | Dilution |
|---|---|---|---|---|---|
| Live-Dead* | eFlour780 | - | Invitrogen | 65-0865-14 | 1/100 |
| CD3 | BV510 | OKT3 | Biolegend | 317332 | 1/100 |
| CD4 | FITC | RPA-T4 | Biolegend | 300538 | 1/100 |
| CD4 | PerCP | OKT4 | Biolegend | 317432 | 1/200 |
| CD8 | BV605 | SK1 | Biolegend | 344742 | 1/400 |
| CD25 | BV421 | 2A3 | BD biosciences | 564033 | 1/75 |
| CD127 | BV711 | A019D5 | Biolegend | 351328 | 1/100 |
| TIGIT | BV421 | A15153G | Biolegend | 372710 | 1/100 |
| TIGIT | PE | A15153G | Biolegend | 372704 | 1/50 |
| CTLA4 | BV785 | CD152 | Biolegend | 369624 | 1/200 |
| FoxP3 | APC | PCH101 | Invitrogen | 17477642 | 1/50 |
| CD39 | BV650 | TU66 | BD Bioscience | 563681 | 1/100 |

*Fixable viability dye

Table 2.2. Additional components for flow cytometry

| Component | Product | Method |
|---|---|---|
| Compensation beads | Ultracomp ebeads (Invitrogen™) | 1 drop of in 100ml FACS buffer |
| Permeability buffer | Foxp3 Transcription Factor Staining Buffer Set (Invitrogen™) | Diluted 1:10 with distilled water |
| Standard Fixative (Cytofix) | BD Cytofix™ | Added directly to cell pellet |
| FoxP3 Fixative | Foxp3 Transcription Factor Staining Buffer Set (Invitrogen™) | Diluted 1:4 with diluent provided in kit. |

## 2.6. Cell labelling with cell tracker red (CMTPX)

This method was required so that the Treg cell population infused in experiments described in 2.15 and 2.16 could be identified using confocal microscopy, and re-identified with flow cytometry after liver derived lymphocyte isolation.

This process involved labelling the cell population of interest with a fluorescent dye (Cell tracker red™ CMTPX, Thermofisher C34552). This dye emits fluorescence which allows it to be detected with the lasers used in both confocal microscopy and flow cytometry. The dye contains fluorescent probes that are able to move through membranes and become intracellular, however once they have moved into the cell cytoplasm they are converted into a cell impermeant form. CMTPX has an absorption and emission spectrum wavelength of 577nm and 602nm respectively. The fluorochrome most comparable to this is PE-Texas Red and this was used in the settings of the flow cytometer.

Flow cytometry using fluorescent dyes adds complexity as they are very bright and interact with many other flourochromes. An extensive period of optimisation to ensure all markers in the panel are compatible was required.

1. Prepare cell tracker red by diluting the powder concentrate in each vial with 14.6 ul of dimethyl sulfoxide (DMSO).
2. Wash cell for CMTPX labelling with FACS buffer in a 5 minute spin at 1500 rpm and discard supernatant.
3. Resuspend cell pellet in a suitable volume of FACS buffer for manual cell counting.
4. After cells counted, centrifuge at 1500 rpm for 5 minutes to obtain cell pellet
5. Resuspend cell pellet in serum free media (RPMI) so that the final cell concentration is $5x10^6$ cells per 1ml.
6. Add the prepared CMTPX solution at a dose of 1ul per 1ml of cell solution (1ul of CMTPX per 5 million cells). Gently manipulate tube so that CMTPX distributes throughout solution.
7. Ensure that all cells suspended (no cell clumping) in media mixed with CMTPX
8. Incubate at 37°C for 1 hour, intermittently gently shake tube so that cells not settling at bottom
9. Centrifuge at 1500rpm to reobtain labelled cell pellet.
10. Wash once by adding 1mL of FACS buffer and centrifuge for 5mins at 1500rpm, then discard supernatant
11. Cells labelled and ready to use.

**2.7 Immunomagnetic isolation**

This technique utilises antibody complexes and magnetic beads that bind to a specific cell type of interest. The cell solution (containing antibody complexes and magnetic beads) is subsequently exposed to a strong magnetic field which draws (and holds) the cells, which have been labelled with antibody complexes and magnetic beads, to the edge of the tube. This cell population can then either be removed or progress to the next stage of isolation, depending on whether *negative* or *positive* selection is being applied. To isolate a specific cell

population for down stream experiments (ie Tregs), several rounds of selection may be required.

Human blood from either healthy volunteers or patients undergoing venesection for hemochromatosis was used for cell isolation experiments. The whole blood was first subject to PBMC isolation, and this served as the starting cell population.

Immunomagnetic cell isolation was performed using two different magnetic systems.

1. EasySep™ Human CD4+CD127low CD25+ Regulatory T Cell Isolation Kit (StemCell)
2. CD4+ CD25+CD127dim/-Regulatory T Cell Isolation Kit II, human (Miltenyi biotec)

These isolations were performed on freshly isolated PBMCs.

### 2.7.1 Stemcell Treg isolation

This kit uses a two-step process in order to obtain $CD4^+$, $CD25^+$, CD127low Tregs. The sequence of steps are depicted in figure 5. The cell solution remains static within the Easysep$^{TM}$ magnet. This kit employs positive selection of $CD4^+$ and $CD25^+$ cells, then negative selection of the CD127low population

The starting cell population for these isolation experiments was PBMCs, and the easysep$^{TM}$ magnet utilised. Due to the size of the magnet, the maximum recommended cell concentration for this method was $5 \times 10^7$ per ml to a maximum of 2mls. Therefore only 100 000 000 PBMCs could be put through the isolation process per experiment. This limitation is one drawbacks of this immunomagnetic approach.

This was performed on freshly isolated PBMCs. The process has both a positive negative selection steps (Figure 2.1)

1. Prepare cell sample at the following concentration5 x 10^7 cells/mL 0.25 - 2 mL in a 5ml polystyrene 5ml FACS tube
2. Add CD25 Positive Selection Cocktail to sample at 50 µL/mL of sample
3. Mix and incubate at room temprature for 5 minutes
4. Vortex Releasable RapidSpheres™ for 30 seconds. Add Releasable RapidSpheres™ to sample and mix at 30 µL/mL of sample
5. Add CD4+ T Cell Enrichment Cocktail to sample at 50 µL/mL of sample. Mix and incubate at room temprature for 5 minutes
6. Add recommended medium to top up the sample to the indicated volume. Mix by gently pipetting up and down 2  3 times. Top up to 2.5 mL.
7. Place the tube (without lid) into the magnet and incubate (Figure 2.3A). RT for 10 minutes
8. Pick up the magnet, and in one continuous motion invert the magnet and tube pouring the supernatant into a new tube.
9. Remove the tube from the magnet and add recommended medium to top up the sample to the indicated volume. Mix by gently pipetting up and down 2  3 times. Top up to 2.5 mL.
10. Place the tube (without lid) into the magnet and incubate at room temprature for 5 minutes.
11. Pick up the magnet, and in one continuous motion invert the magnet and tube pouring off the supernatant. Discard supernatant

12. Repeat steps  so that a total of 1 x 10-minute and 3 x 5-minute separations in the magnet are performed

13. Remove the tube from the magnet and add recommended medium to top up the sample to the indicated volume. Mix by gently pipetting up and down 2  3 times. Be sure to collect cells off the sides of the tube. Add the same volume as the original starting sample volume (i.e. same volume used in step 1)

14. Add Release Buffer to sample at 100 µL/mL of sample. Mix by Vigorously pipetting up and down more than 5 times.

15. Add CD127high Depletion Cocktail to sample at 50 µL/mL of sample. Mix and incubate. RT for 5 minutes

16. Vortex Dextran RapidSpheres™ for 30 seconds. Add Dextran RapidSpheres™ to sample at 10 µL/mL of sample. Mix and incubate at room temprature for 5 minutes

17. Add recommended medium to top up the sample to the indicated volume. Mix by gently pipetting up and down 2  3 times. Top up to 2.5 mL

18. Place the tube (without lid) into the magnet and incubate at room temperature for 5 minutes

19. Pick up the magnet, and in one continuous motion invert the magnet and tube pouring the enriched cell suspension into a new tube. Isolated cells in the new tube are ready for use

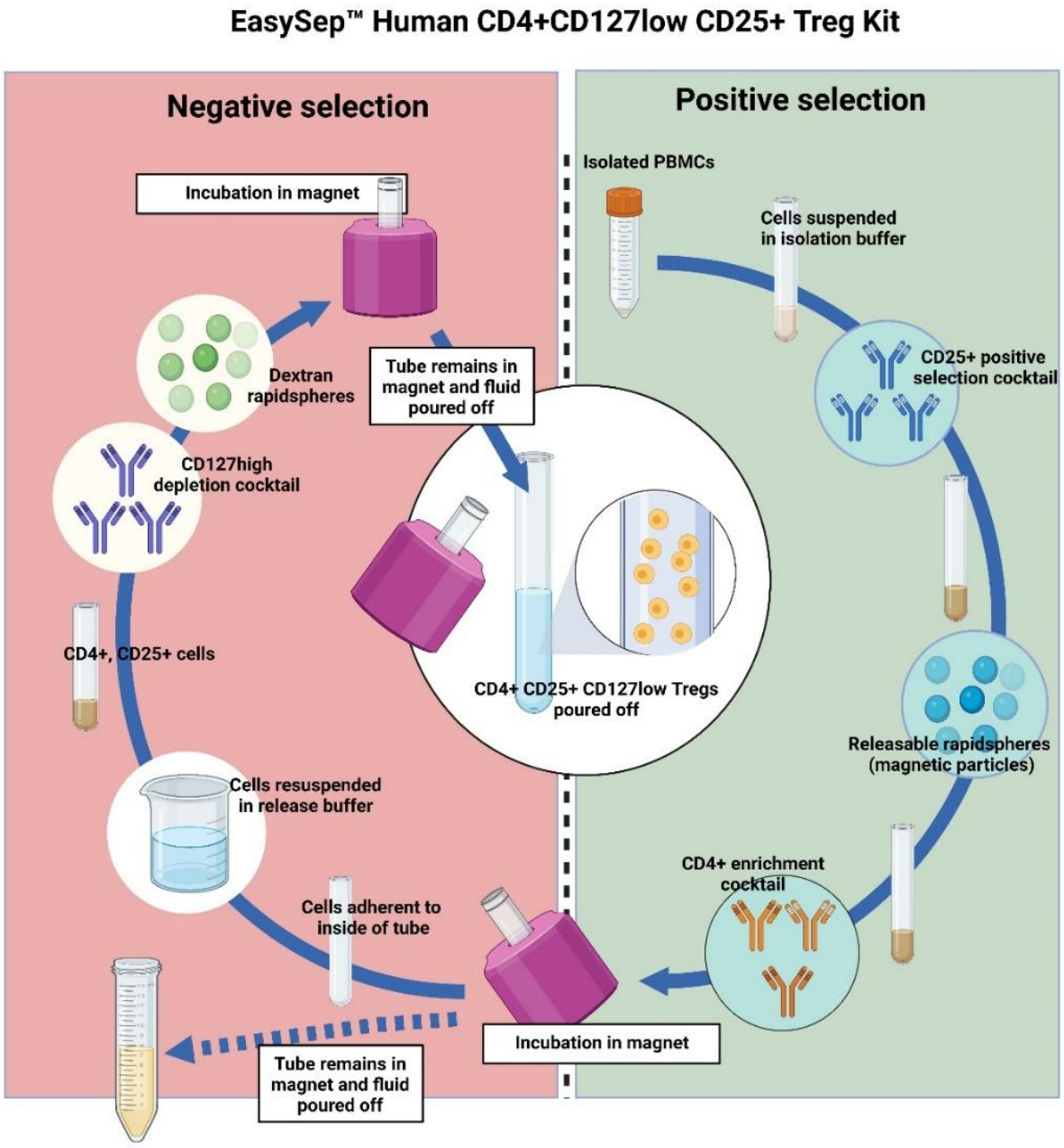


**Figure 2.1. Treg isolation process using kit from StemCell**. Two step isolation process to obtain Tregs. Initial step is positive selection, followed by negative selection. The non-magnetically bound cell fraction is tipped of as tube remains within magnet holder, and fluid poured into separate tube. In the positive selection step, the cells that progress to the second step remain adherent to the tube. In the negative selection step, the cells that need to be removed are adherent to the tube.

### 2.7.2 Miltenyi MACS Treg isolation

This technique utilises the MACS® separation columns and magnet. Two types of columns are used and these include MS and LD. The MS columns are designed for positively selecting cells and the LD for negative selection (Figure 2.2). The maximum total number of starting PBMCs for the Miltenyi $CD4^{+}CD25^{+}CD127^{low}$ Regulatory T cell isolation kit II (human) is $5x10^{8}$ as this is the maximum number of cells for the LD column.

1. Ensure cell numbers have been accurately counted. PBMC cell sample suspended in 5ml of FACS buffer and centrifuged for 5 minutes at 1500 rpm with maximum acceleration and deceleration.

2. Cell pellet resuspend in FACS buffer at a volume of 40uL per $10^{7}$ cells and put through a 40uM mesh filter to obtain a single cell suspension

3. Add 10 µL of CD4+ CD25+ CD127dim/– T Cell Biotin-Antibody Cocktail II per $10^{7}$ total cells. Mix well and incubate for 5 minutes in the refrigerator (2−8 °C).

4.. Add 30 µL of buffer and 20 µL of Anti-Biotin MicroBeads per $10^{7}$ total cells. 7. Mix well and incubate for 10 minutes in the refrigerator (2−8 °C).

5. Adjust the volume to a minimum of 500 µL of buffer

6. Place LD Column in the magnetic field of a suitable magnetic activated cell sorter (MACS) Separator.

7. Prepare column by rinsing with 2 mL of buffer.

8. Apply cell suspension onto the column and collect unlabeled cells that pass through and wash column with 2×1 mL of buffer. Collect total effluent; this is the unlabeled pre-enriched CD4+ cell fraction. Perform washing steps by adding buffer two times. Only add new buffer when the column reservoir is empty.

9. Centrifuge cell suspension at 300×g for 10 minutes. Aspirate supernatant completely.*

10. Resuspend cell pellet in 90 µL of buffer per $10^7$ total cells.

11. Add 10 µL of CD25 MicroBeads II per $10^7$ total cells.

12. Mix well and incubate for 15 minutes in the refrigerator (2−8 °C).

13. Wash cells by adding 1−2 mL of buffer and centrifuge at 300×g for 10 minutes. Aspirate supernatant completely.

14. Resuspend up to $10^8$ cells in 500 µL of buffer.

15. Place MS Column in the magnetic field of a suitable MACS Separator (Figure 2.3B&C).

16. Prepare column by rinsing with 500 µL of buffer.

17. Apply cell suspension onto the column. Collect flow-through containing unlabeled cells.

18. Wash column with 3×500 µL of buffer. Perform washing steps by adding buffer aliquots only when the column reservoir is empty.

19. Remove column from the separator and place it on a suitable collection tube. Pipette 1 mL of buffer onto the column. Immediately flush out the magnetically labeled cells by firmly pushing the plunger into the column (Figure 2.3D).**

20. Prepare a second MS colum as per step 16. Repeat steps 17-19 to improve purity.

21. Centrifuge eluted fraction to obtain cell pellet, resuspend in appropriate volume of FACS buffer and perform manual count with trypan blue and microscope.

* The eluted fraction of this step can also be collected, and sample obtained. This will allow you to assess the effectiveness of step 1 of the isolation (negative selection).** The flow through fraction of step 2 can also be collected and a sample obtained, this will allow assessment of the effectiveness of step 2 (positive selection).

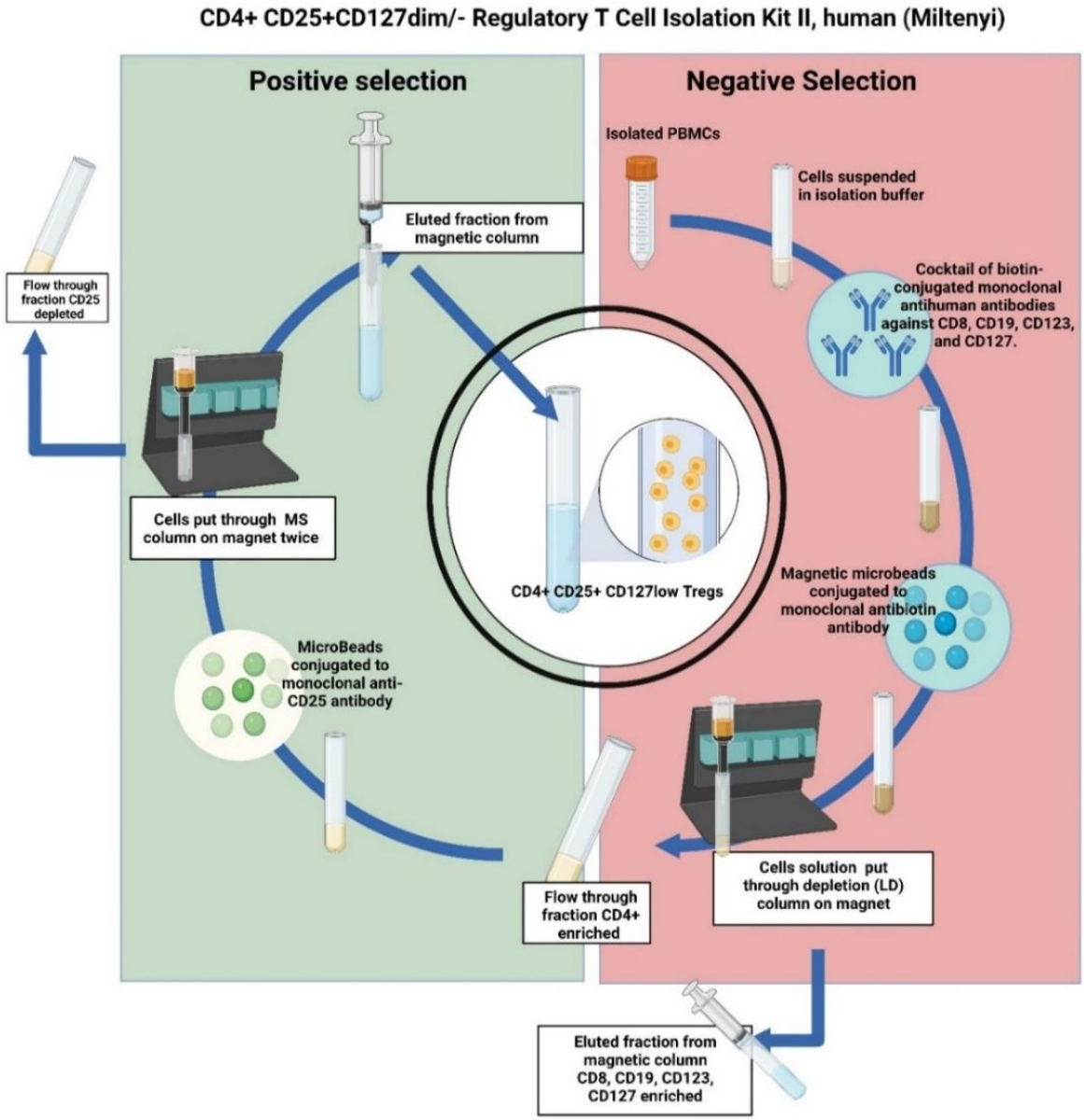


**Figure 2.2**. **Isolation sequence for the kit provided by Miltenyi.** This Treg isolation kit has a two step sequence to obtain the final isolate of Tregs. Step 1 is negative selection and step 2 is positive selection. In step 1, $CD4^-$ cells and $CD127^{high}$ are depleted from the PBMC sample and adhere to the magnetic column. Therefore the flow through fraction is $CD4^+$ enriched and proceeds to the next step. The depleted fraction ($CD4^-$) can be obtained be eluting the column. In step 2, the $CD25^+$ cells are positively selected from the remaining $CD4^+$, $CD127^{low}$ enriched sample. The final isolate of Tregs is then obtained by eluting the magnetically bound cells remaining in the column.

.

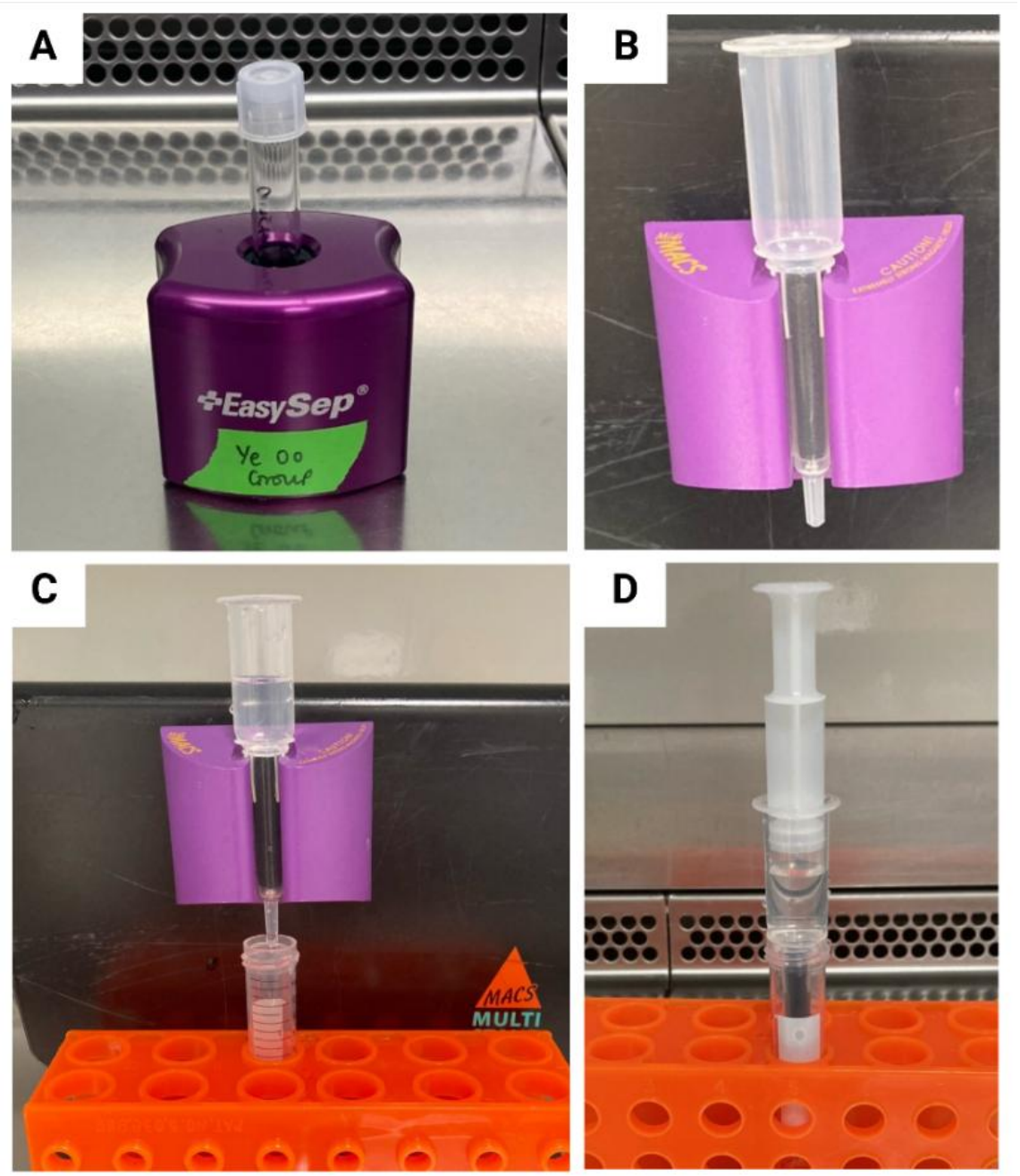


**Figure 2.3. Different magnets used for immunomagnetic cell isolation.** A) static magnet used in the StemCell isolation kit. Tube incubated within the magnet. To obtain the non-magnetically bound cell fraction the tube remains within magnet and both are tipped and fluid poured off. B and C) Miltenyi magnet with column attached. Cell solution runs downward through column and drips out the bottom (flow through fraction). The Magnetically bound fraction adheres to side of column due to magnetic force. D) To obtain the magnetically bound fraction, column taken out of magnet and buffer flushed through column with plunger (eluted fraction)

### 2.7.3 $CD4^+$ T-cell pre-enrichment

Although FACS can be performed with any appropriately antibody-stained starting cell population, the process is very slow if the subpopulation to be isolated via FACS has a low frequency. Therefore, a preceding step of pre-enrichment is often applied which reduces the time required on the cell sorter. In regards to FACS isolation of Tregs, this pre-enrichment can be based on $CD4^+$ or $CD25^+$ and is best to be performed via negative selection (ie depleting the non $CD4^+$) to prevent cell activation. In the ideal situation, this pre-enrichment step has a high purity of the intended marker (ie $CD4^+$) and yield (ie minimal $CD4^+$ are in the depleted fraction)

This technique utilises the MACS® separation columns and magnet technology. This was performed on freshly isolated PBMCs. The maximum total number of starting PBMCs for the Miltenyi $CD4^+$ T cell isolation kit (human) is $2x10^9$ as this is the maximum number of cells for the LS column.

1. Resuspend cell pellet in 40 µL of buffer per $10^7$ total cells and pass through a 40uM filter to obtain a single cell suspension
2. Add 10 µL of $CD4^+$ T Cell Biotin-Antibody Cocktail per $10^7$ total cells.
3. Mix well and incubate for 5 minutes in the refrigerator (2−8 °C).
4. Add 30 µL of buffer per $10^7$ total cells.
5. Add 20 µL of $CD4^+$ T Cell MicroBead Cocktail per $10^7$ total cells.
6. Mix well and incubate for 10 minutes in the refrigerator (2−8 °C).
7. Place LS Column in the magnetic field of a suitable MACS Separator.
8. Prepare column by rinsing with 3 mL of buffer.

9. Apply cell suspension onto the column. Collect flow-through containing unlabeled cells, representing the enriched CD4+ T cells. Wash column with 3 mL of buffer.

10. Remove column from the separator and place it on a suitable collection tube. Pipette 5 mL of buffer onto the column. Immediately flush out the magnetically labeled non CD4+ T cells by firmly pushing the plunger into the column.

11. The flow through fraction represents the $CD4^+$ enriched sample

12. The eluted fraction represents the CD4 deplete fraction*

** The eluted fraction of this step can also be collected and sample obtained. This will allow you to assess the effectiveness of the isolation (negative selection).

**2.8 Fluorescence activated cell sorting for Tregs after CD4 pre-enrichment**

This approach uses fluorophore coupled antibodies which bind to different cell populations, then these cells are subject to hydrodynamic focusing and pass in single file across the path of a laser. If a cell meets the criteria set (ie $CD4^+$, $CD25^+$ and $CD127^{low}$), it becomes charged and makes its way into the collection tube[128]. The capability of the different machines vary, but some are able to sort based based on up to 18 different flourochromes[129]. Isolation of cells via FACS is commonly performed for experiments that require cell subpopulations and the purity is generally considered to be superior to magnetic isolation. An additional benefit of FACS is that multiple different cell subpopulations can be sorted simultaneously[129]. However, FACS requires complex and costly machinery, and can inflict stress on the cells due to the high pressure and the forced passage through a nozzle with a small diameter. This can have functional implications for downstram application of the cells and is referred to as sorter induced cellular stress (SICS)[128].

Prior to running the pre-enriched cell samples through the cell sorter, fluorochrome compensation was carried out.

The flow cytometer used in these experiments was the FACSaria Fusion®The FACS was performed by appropriately trained post-doctoral scientists.

### 2.8.1 Compensation beads for flow cytometry

Flow cytometry and FACS are highly dependent on the recognition of positive (stained with the fluorochrome) and negative (not stained for the fluorochrome) populations. Therefore, prior to each analysis with the flow cytometer or sorter, accurate compensation must be performed. Due to each fluorophore being able to emit photons at different wavelengths and energy, the possibility that of spectral overlap exists when more than one fluorophore is in the panel. The flow cytometer aims to improve its precision of measurement by measuring via different coloured lasers.

Compensation beads are prepared for each fluorochrome, and run as part of the compensation process. This allows the machine to determine the relative contribution of each fluorophores detection signal when they are combined. This is determined via mathematical modelling.

Compensation beads prepared prior to flow cytometry. Kept for repeated usage for 10 days.

1. Label the FACS tubes with the separate  fluorochromes that require compensation
2. Add 100ul of FACS buffer to each tube, then add 1 drop OneComp (Invitrogen, 01-1111-42) beads to each tube alongside
3. Add 1ul of appropriate antibody labelled with the fluorochrome that requires compensation.
4. Incubate at 4°C for 10 minutes.
5. Add 1mL FACS buffer per tube and wash at 1500rpm for 5 minutes with maximum acceleration and deceleration (9)
6. Tip off supernatant and resuspend the beads in 300-500ul of FACS buffer

7. Store covered in foil in the fridge. Beads can be used for up to 2 weeks.

### 2.9 Treg cell culture media and expansion protocol

To obtain Treg cell volumes large enough for effective cell-based therapy, expansion post isolation is required. Numerous protocols for expansion are reported in the literature, however the overall goal is to maintain the immunosuppressive phenotype of the expanded Treg population. This process is made challenging by the fact that Tregs are known to have significant plasticity and can develop a IL-17 secreting phenotype during the expansion period[91]. This pro-inflammatory cytokine could then prevent the Tregs from having the desired immunosuppressive effects. However, previous researchers have demonstrated that this is preventable with the addition of Rapamycin to the media[91]. Rapamycin is a substance produced by Streptomyces hydroscopicus that binds to a protein Kinase called 'mammalian target of rapamycin', the result this has is the inhibition of cell proliferation and growth in response to IL-2 in the majority of T cell subtypes[94,130]. However for Tregs, the IL-2 effects are mediated by a certain pathway (Janus kinase/STAT) that does not appear to be disturbed by rapamycin[94]. In order to expand the Tregs in culture, activation of the T-cell receptor (TCR) with CD3 antibodies along with co-stimulation via CD28 is required. complex is required. This is commonly performed at the commencement and at subsequent intervals during the culture period using stimulation beads conjugated with CD3 and CD28 antibodies.

Treg culture media was included;

- TexMACS® media (Miltenyi, 130-097-196)
- Recombinant Interleukin-2 (500IU/ml) (Peprotech, 200-02)
- Human AB serum (5%) (Sigma Aldrich, H4522)
- Rapamycin (100nmol) (Miltenyi, 170-076-308)

The Human AB serum and rapamycin were added to TexMACS® and stored for 14 days. The IL-2 was prepared and aliquoted out so that 1uL contained 125 IU, and 1uL added directly to each well of the 96 well plate (250ul volume of each well.

After cell isolation (either via magnetic or fluorescent activated cell sorting), the cells were washed in cell media and then placed in either one or two wells of a 96 well plate. The maximum numbers of cells per well at the initiation of cell culture was 300 000.

The cells were stimulated on the next day (day 1) with CD3/28 stimulation beads (Miltenyi Biotec) at a ratio of 4 beads to 1 cell. Prior to placing the stimulation beads in the well, they were washed with FACS buffer (5 minutes at 1500rpm). The beads were then suspended in 100ul of warmed media. This was then placed into the well, after 100ul of media was aspirated from the top of the well to ensure the well did not over flow. The protocol is demonstrated in figure 2.4 and 2.5.

Stimulation at the same ratio was performed on day 14 of the cell culture.

The media was changed every 48-72 hours, or sooner if a colour change (orang changed to yellow) was evident.

The wells were split if the media was changing colour within 72 hours, or if the cell pellet had approximately doubled in size.

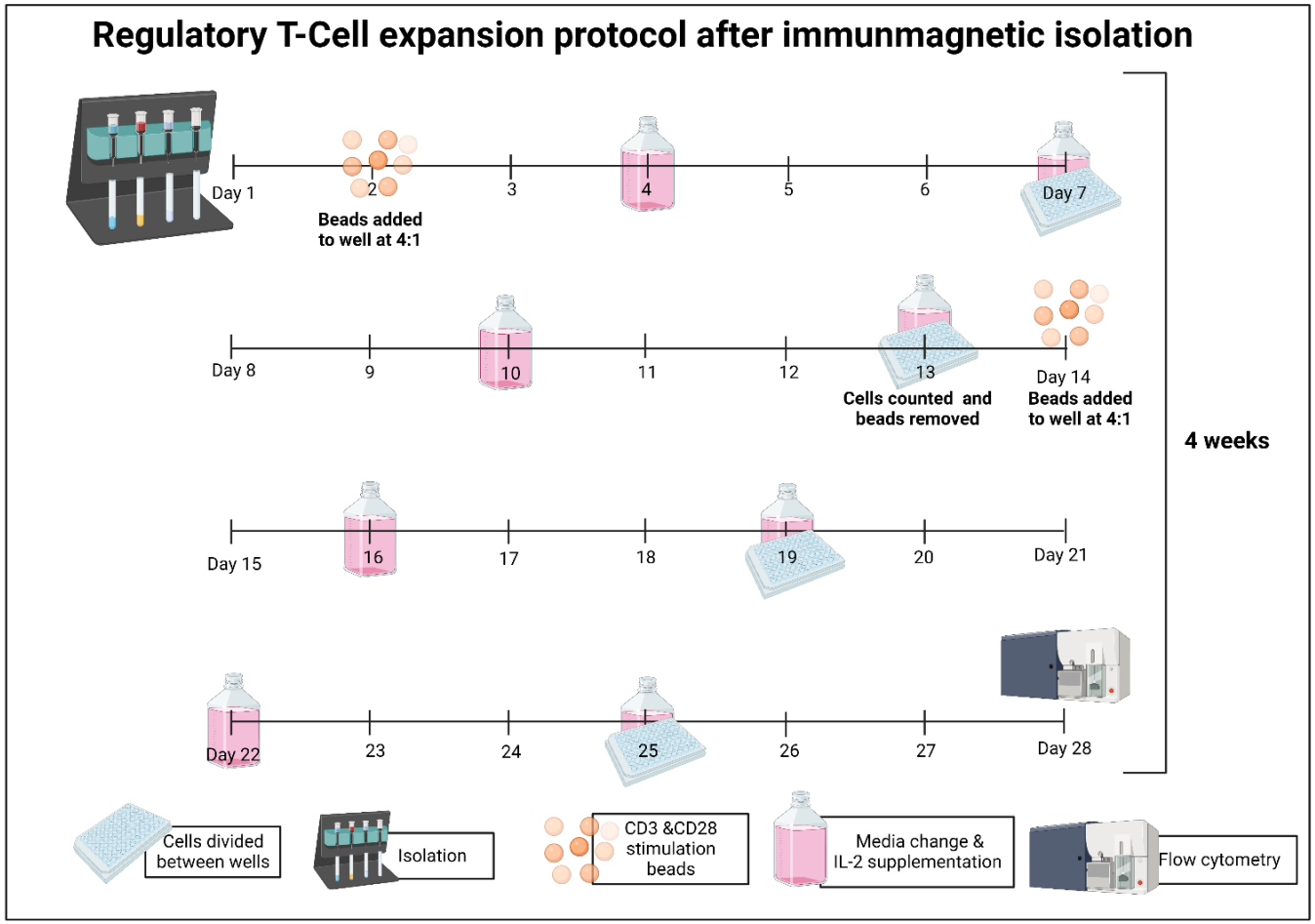


**Figure 2.4. Expansion protocol used after isolation with CD4+ CD25+CD127dim/-Regulatory T Cell Isolation Kit II, human (Miltenyi).** CD3/CD28 activation beads added on second day and day 14. Media changed every 2-3 days and additional IL-2 supplementation. Magnetic removal of beads prior to stimulation at day 14

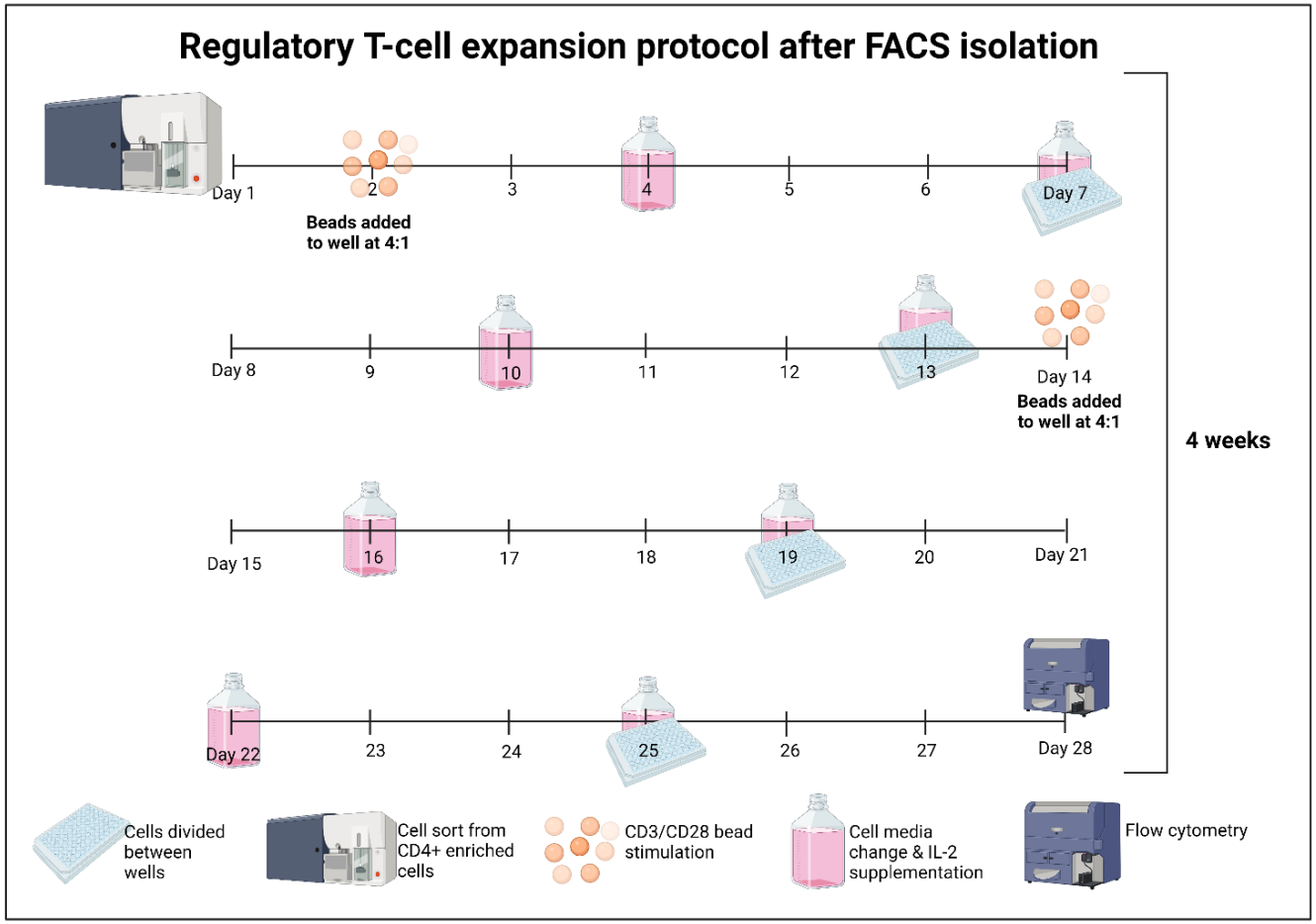


**Figure 2.5.** Expansion protocol used after Treg sorting via flouresence activated cell sorting (FACS). CD3/CD28 activation beads added on second day and day 14. Media changed every 2-3 days and additional IL-2 supplementation. Restimulation performed on day 14 and initial beads left in-situ.

## 2.10 Immunofluorescence tissue staining

This process was used to identify the CMTPX labelled cells that were infused into the liver tissue. The CMTPX labelled cells display flouresence, and this can be detected using laser based microscopes. In addition to recognising CMTPX positive cells, the liver was stained with other fluorescently conjugated antibodies so that relevant structures could be identified. These included E-cadherin (membranes of hepatocytes and cholangiocytes), CD31 (vascular endothelium), FoxP3 (intracellular marker for Tregs) and DAPI (stains nuclear material in cell nucleus).

The process of immunoflouresence tissue staining involves both a primary and Flourescently conjugated secondary antibody (Table 2.3). The primary antibody binds to the tissue antigen of interest and the fluorescently conjugated secondary then binds to the primary antibody. The confocal microscope allows images to be taken at different depths of the tissue block, and compilation of these images is called a Z-stack. This allows 3-dimensional reconstruction using a computer software called Imaris®.

All confocal microscopy was performed on the Zeis 880®.

Liver tissue specimens underwent formalin fixation for at least 24 hours, and were then placed in cassettes for and embedding as per standard procedure

Sections of these tissue blocks were sliced at 4uM thickness to facilitate multicolor confocal microscopy and the acquisition of Z-stack images.

1. Slides were rehydrated by submerging in the following sequence:
    a. Clearine 1 (C1) – 3 minutes
    b. Clearine 2 (C2) – 3 minutes
    c. Clearine 3 (C3) – 3 minutes

d. Alcohol 1 (A1) – 3 minutes
e. Alcohol 2 (A2) – 3 minutes
f. Alcohol 3 (A3) – 3 minutes
g. Water 1 (W1) – 3 minutes
h. Water 2 (W2) – 3 minutes

2 Assemble a wet box by covering a shallow plastic tray in damp paper towels. Place shortened stripettes tubes inside to serve as a rack for the slides. This is to prevent the slides from drying out. **Ensure the box is covered in foil as the UV light can affect the antibodies.**

3 Prepare the Tris based antigen unmasking solution buffer unmasking solution in a microwavable bucket. Add 10ml of Antigen unmasking solution, Tris based (Vector®) to 1 litre of distilled water and microwave for 10 minutes to warm up

4 Transfer slides to new plastic rack that is submerged in water. Place slides in warm unmasking solution in a non-metal slide rack and microwave for 30 mins and allow 10 minutes for cooling. Add cold water to the bucket to bring up to room temperature before removing the slides.

5 Remove slides from unmasking mix and use a wax pen to draw a ring around the tissue specimen. Ensure the ring is complete as it needs to hold all the subsequent fluid over the tissue, and prevent run off. Cover the tissue in TBS immediately.

6 Place slides on rocker for 5 minutes. Prepare a 2x casein based solution by diluting the 10x casein 1:4 with TBS (ie make 20 mls using 4mls of 10x casein with 16ml of TBS)

7 Add 100-150µl 2x casein to each slide and rest on rocker for 10 mins.

8 Dilute primary antibody in the casein solution at a predetermined concentration, allowing at least 150µl of solution per slides for liver. You may need more for larger slides. The concentration of primary and secondary antibodies shown in table 2.3 below

9 Tap off the Casein solution and add primary antibody. Cover with lid to protect from light and leave for on rocker at 5°C leave overnight.

10 Prepare secondary antibodies in casein also. Secondary antibodies have the fluorophore tag and are directed against your primary antibody. Ensure diluted in master mix at appropriate concentration (Table 2.3)

11 Perform two washes of slides with TBS, each for 5 minutes on the rocker

12 Add secondary antibody and leave on the rocker for 1 hour.

13 After the incubation with the secondary antibody, wash with TBS for 5 minutes.

14 Prepare TruView (Vector, SP-8400) with DAPI reagent (equal parts from bottle A+B+C into a small container ( allowing 150ul per slide).

15 Incubate on the rocker with TruView for 5 mins.

16 Wash twice with TBS, for 5 mins. Between washes, use a Pasteur pippete to try and wash away any TruView aggregations that have formed.

17 Place a very small amount of the Vectashield vibrance antifade mounting medium with DAPI (Vector, H-1800) – use a Pasteur to dab a small amount on to the cover slip.

18 Allow slides to dry for 5-10 minutes

19 Keep cold and covered until you image.

**Table 2.3. Liver tissue immunoflourescence antibodies and dilutions**

| | Species | Clone | Binds | Flouro | Catalogue | Brand | Dilution |
|---|---|---|---|---|---|---|---|
| Primary | | | | | | | |
| | Mouse | IgG1 (JC70A) | CD31 | NA | M0823 | Dako | 1/100 |
| | Rabbit | IgG (SP97) | FoxP3 | NA | MA5-16365 | Invitrogen | 1/50 |
| | Mouse | IgG2a (36/E-cadherin) | E-Cadherin | NA | 610182 | BD Biosciences | 1/100 |
| Secondary | | | | | | | |
| | Goat | | Mouse IgG1 | AF647 | A21121 | Invitrogen | 1/1000 |
| | Horse | | Rabbit IgG | Dylight 488 | D1-1088 | Vector | 1/500 |
| | Goat | | Mouse IgG2a | AF546 | A21133 | Invitrogen | 1/1000 |

### 2.11 Cytokine analysis of machine perfusate

In order to investigate the effect NMP has on the immune profile of the donor liver graft, we measured the cytokine concentrations at various time points. Cytokine manufacture and release is influenced by upstream changes in the gene activity of the cell. These livers were transplanted at the Queen Elizabeth Hospital Birmingham and had satisfied the institutions viability testing. The cytokine concentration was used as a surrogate for immune cell activity within the liver graft. Following transplant, the grafts were grouped on the basis of whether they experienced early rejection or not. This was in an effort to see if early pro-rejection changes became evident during the perfusion period. Comparisons of absolute values and rate of increase were performed.

Cytokine analysis was performed on the perfusate from NMP preserved livers at QEHB. These samples were collected at QEHB, prepared at the Institute of Biomedical Research (UoB) and analysed by the clinical immunology service. They were obtained under the research project RRK7086/IRAS 281445 that was approved by the Human Research Ethics Committee of Wales (Approval number 21/WA/0300). The sampling protocol is further outlined in section 2.17.

1. Aspirate 10ml of blood from inferior vena cava tubing on organox device
2. Using blunt fill syringe, transfer to a large purple top EDTA tube
3. At first opportunity, transfer to laboratory at University of Birmingham and centrifuge at 1800 RPM for 5 minutes (Acceleration 9 and deceleration (9) in 15ml falcon tube.
4. Remove the remaining supernatant and fill as many cryovials as possible with 1000microlitres. Place these in -80 freezer, they do not need to be snap frozen or put in Mr Frosty.

These samples were then transferred to the clinical immunology service for cytokine analysis by a specialist using the Bio-Plex Pro Human Cytokine Screening Panel, 48-Plex (#12007283) on the Bio-Plex Luminex 200 machine (Biorad, UK) machine.

This technique uses capture antibodies raised against the biomarker of interests (cytokine) that are covalently bound to magnetic beads. These bind with the cytokine of interest, then a biotinylated antibody is added which also binds with the biomarker and creates a sandwich complex. A streptavidin-phycoerythin conjugate is then added to form the final detection complex. In the Bioplex machine, a green laser (532nm) excites the phycoerythrin and this is detected by a photomultiplier tube.

**2.12 Metabolomic analysis of machine perfusate**

Metabolomic analysis was performed on the perfusate from NMP preserved livers at UHB. These samples were collected at QEHB, prepared (and stored) at the Institute of Biomedical Research (UoB) and analysed by the Phenome centre (UoB). They were obtained under the research project RRK7086/IRAS 281445 that was approved by the Human Research Ethics Committee of Wales (Approval number 21/WA/0300). The sampling protocol is further outlined in section 2.17.

1. Aspirate 10ml of blood from inferior vena cava tubing on organox device
2. Using blunt fill syringe, transfer to a large purple top EDTA tube
3. At first opportunity, transfer to laboratory at University of Birmingham and centrifuge at 1800 RPM for 5 minutes (Acceleration 9 and deceleration (9) in 15ml falcon tube.
4. Using P1000 pippete, remove 2 x 500 microlitres of supernatant and place in separate 1ml cryo vials, Snap freeze these specimens using liquid nitrogen.

To prepare samples for analysis on the liquid chromatography mass spectrometer (LC-MS), extraction of proteins is required as they interfere with the analysis. To extract proteins and ensure the metabolites remain in solution, the sample needs to be mixed with a solvent. The solvent required depends on the metabolites of interest. Due to the fact this was a non-tageted analysis, a broad approach was required and two different solvents were used to assess for 1) Polar metabolites and 2) Lipidomics;

**Polar metabolites:** 30uL of sample added to 90 uL of 50/50 methanol/acetonitrile, then sample vortexed (15 seconds), then centrifuged (20,000-g, 10 mins 4degC). Sample then loaded loaded into a vial for LC-MS analysis.

**Lipidomics:** 30uL of sample added to 90 uL of 100% isopropanol, then sample vortexed (15 seconds), then centrifuged (20,000-g, 10 mins 4degC). Sample then loaded loaded into a vial for LC-MS analysis.

Metabolomics samples were kept frozen throughout until extraction and at 4°C during the extraction process to minimise metabolic changes. The ThermoFisher Dionex U3000 liquid chromatography system was used.

### 2.13 Liver biopsy collection and storage

To investigate the effect NMP has on the immune profile of the graft, analysis of the liver tissue was imperative. Serial biopsies were collected on patients enrolled in a clinical study (RRK7086/IRAS 281445), with 10 undergoing either NMP or cold storage preservation. Biopsies were collected at different time points of the preservation process (Figure 2.8).

The liver biopsies were collected for RNA sequencing at the University of Birmingham, and standard histology as per clinical practice at QEHB. RNA sequencing requires a different storage process and this had to be implemented from the time of biopsy.

The same technique was used at each time point, however the size of specimen did vary.

1. Take biopsy using menghini needle from left lobe in direction away from hepatic hilum. Aim to get biopsy of 4cm in length.
2. Close needle hole with 5.0 prolene suture
3. Spread tissue specimen out on card on backtable in operating theatre
4. Using scalpel, divide a 1.5cm length and put in formalin for histopathology. If doing frozen section, place in wet gauze. Send this piece to University Hospital Birmingham histopathology.
5. Remainder of biopsy to be placed in 1.5ml epindorph tube containing 1.5ml RNA later. Sample to be frozen in -20 freezer at first opportunity.

**2.14 RNA extraction and sequencing**

Although microscopic analysis of liver tissue during preservation is commonplace, this provides limited information about subtle changes in cell activity. In order to determine the changes in gene activity, liver biopsy specimens from patients enrolled in (RRK7086/IRAS 281445) were subject to 3' RNA sequencing analysis. This was in effort to determine if the gene activity signal differed between NMP and cold preserved livers, and those that experience early acute rejection. This type of RNA sequencing measures nuclear material from all sources in the tissue such as hepatocytes, leukocytes and cholangiocytes. The solid liver tissue needs to be converted to liquid RNA, so that it can be run through the analyser. The quality of results is highly influenced by the quality or RNA extraction.

RNA extraction of liver tissue was performed using the RNAeasy Mini Kit (Qiagen, 74104) with on column DNA digestion using the RNAase free DNAse set (Qiagen 79254)

Liver tissue specimens were stored in RNAlater at -20°C. They were placed in RNAlater as soon as they were collected.

Prior to starting, the following buffers need preparing;

RLT Buffer: Add β-Mercaptoethanol (β-ME) must be added to Buffer RLT supplied in kit. Add 10 µl β-ME per 1 ml Buffer RLT. Dispense in a fume hood and wear appropriate protective clothing. Buffer RLT containing β-ME can be stored for up to 1 month.

RPE Buffer: RPE is supplied as a concentrate. Before using for the first time, add 4 volumes of ethanol (96–100%) as indicated on the bottle to obtain a working solution.

DNase I solution: Before using the RNAse-Free DNase Set for the first time, dissolve the lyophilized DNase I (1500 Kunitz units) in 550 µl of the RNAse-free water provided. To avoid loss of DNase I, do not open the vial. Inject RNAse-free water into the vial using an RNAse-free needle and syringe. Mix gently by inverting the vial. Do not vortex.

RW1 Buffer: Provided ready to use in RNAeasy mini Kit

1. Remove RNAlater stabilized tissues from the reagent using forceps.

2. Liver biopsies were weighed, and reduced in size if more than 30mg as this is the maximum accommodated by the RNA extraction spin columns. Liver specimen placed in 2ml epindorph tube with 600ul of RLT buffer. This volume of RLT buffer used due to size of tissue specimen and the fact it was preserved in RNA later.

3. Disruption and homogenization of the liver specimen was performed using the TissueLyser device. Add a 5ml stainless steel bead (Qiagen 69989) to the epidorph tube. Place the tubes in the TissueLyser

4. Run the TissueLyser for 2 min at 20–30 Hz. Disassemble the adapter set, rotate the rack of tubes so that the tubes nearest to the TissueLyser are now outermost, and reassemble the adapter set. Operate the TissueLyser for another 2 min at 20–30 Hz. Check that the tissue specimen has been disrupted and there are minimal visible pieces of solid tissue left in epindorph.

5. Centrifuge the lysate for 3 min at full speed (>10 000rpm) on a mini-centrifuge. Carefully remove the supernatant by pipetting and transfer it to a new microcentrifuge tube (not supplied). Use only this supernatant (lysate) in subsequent steps

6. Add 1 volume of 50% ethanol* to the cleared lysate, and mix immediately by pipetting. Do not centrifuge.

6. Transfer up to 700 µl of the sample, including any precipitate that may have formed, to an RNeasy spin column placed in a 2 ml collection tube. Close the lid gently, and centrifuge for 15 s at ≥10,000 rpm. Discard the flow-through fluid. If the sample volume exceeds 700 µl, centrifuge successive aliquots in the same RNeasy spin column. Discard the flow-through after each centrifugation

7. On column DNAse digestion: Add 350 µl Buffer RW1 to the RNeasy spin column. Close the lid gently, and centrifuge for 15 s at ≥10,000 rpm to wash the spin column membrane. Discard the flow-through.Reuse the collection tube in step.

8. Add 10 µl DNase I stock solution to 70 µl Buffer RDD. Mix by gently inverting the tube. Centrifuge briefly to collect residual liquid from the sides of the tube. Buffer RDD is supplied with the RNAse-Free DNase Set.

9. Add the DNase I incubation mix (80 µl) directly to the RNeasy spin column membrane, and place on the benchtop (20–30°C) for 15 minutes. Be sure to add the DNase I incubation mix directly to the RNeasy spin column membrane..

10. Add 350 µl Buffer RW1 to the RNeasy spin column. Close the lid gently, and centrifuge for 15 seconds at ≥10,000 rpm. Discard the flow-through.

11. Add 500 µl Buffer RPE to the RNeasy spin column.  Centrifuge for 15 s at ≥10,000 rpm to wash the spin column membrane. Discard the flow-through.

12. Add 500 µl Buffer RPE to the RNeasy spin column. Close the lid gently, and centrifuge for 2 min at ≥10,000 rpm to wash the spin column membrane. The long centrifugation dries the spin column membrane, ensuring that no ethanol is carried over during RNA elution. Residual ethanol may interfere with downstream reactions.

13. Place the RNeasy spin column in a new 1.5 ml collection tube. Add 30ul of RNAse-free water directly to the spin column membrane. Close the lid gently, and centrifuge for 1 min at ≥10,000 rpm to elute the RNA.

14. Pipette 5ul into a separate epindorph tube for Quality control (QC) analysis. Freeze both epindorph tubes at -80°C as soon as possible.

Samples were then stored at -80 until processed by post-doctoral scientist in genomics

Overview of the sample processing

- RNA samples were quality-assessed with the 4200 TapeStation System (Agilent Technologies), and quantified with the Qubit 4 Fluorometer (Thermo Fisher Scientific).
- Samples were normalised to 55ng input mass, and sequencing libraries were prepared with the QuantSeq 3' mRNA-Seq Library Prep Kit FWD for Illumina (Lexogen GmbH), according to the manufacturer's protocol (standard input).
- Sequencing libraries were quality-assessed with the 4200 TapeStation System (Agilent Technologies), and quantified with the Qubit 4 Fluorometer (Thermo Fisher Scientific).
- Sequencing libraries were then pooled together, and the pool was quality-assessed with the 4200 TapeStation System (Agilent Technologies), and quantified with the Qubit 4 Fluorometer (Thermo Fisher Scientific).

- The sequencing pool was loaded onto the NextSeq 2000 (Illumina) with the P3 50 cycles sequencing kit. Single-read single-index sequencing was performed with read lengths of 75, 6, for read1, index1, respectively.
- The raw sequencing output (BCL files) was coverted to fastq files and demultiplexed using bcl-convert version 4.1.23 software.

**2.15 Liver wedge perfusion experiments**

In order to investigate the localisation and phenotypic change of infused Tregs, a model that was cost effective, able to run without constant supervision, and could efficiently deliver a low number of human Tregs was required. The incorporation of both a control and experimental lobe was also desirable so that any observations relating to the infused CMTPX positive cells in the experimental lobe could be compared to the control lobe. This perfusion model was modified during experiments described in chapter 5 and the final setup and protocol is described below. Images of the circuit are shown in figure 2.6, and a schematic in figure 2.7.

1. Obtain required wedge from donor liver. Optimal results obtained when Glissonian capsule covering large amount of surface as it will prevent perfusion fluid leaking out of numerous surfaces. Using left lateral segment ideal.

2. Ensure bead bath warmed to 37°C, leave TexMACS in the bead bath so that it is warmed to 37°C.

2. Place on petri dish and weigh. Optimal wedge size between 25-50 grams

3. Identify vascular inflow on cut surface. This will be surrounded by white tissue (Glissonian sheath). The largest structure within the glissonian sheath is the portal

vein branch and needs to be cannulated. The vessels with thin wall and no Glissonian sheath are hepatic veins (outflow).

` 4. Insert Venflon intravenous cannulae (Blue, 22 gauge) into the portal vein branch on two separate sites. Ideally these should be on opposing sides of the cut surface to maximise delivery of perfusion fluid (and cells). In the periphery of the liver there is minimal overlap in vascular territory and therefore perfusion via two places ideal. Cannula can be shortened in length to suit depth of portal vein branch.

5. Secure cannula in place using 5.0 Prolene sutures

6. Secure male-male leur lock adaptor to blue cannulas in liver tissue.

7. Cut adequate lengths of Masterflex® silicon tubing (1/8" internal diameter, Avantor MFLX95802-05). Four lengths are needed if perfusing two wedges.

8. Secure tubing into Watson Marlow® 505S peristaltic pump and prime using warmed TexMACs. Note which direction the fluid is flowing in each of the tubes.

9. Connect the tubing with TexMACS flowing away from the peristaltic pump to the male adaptor on the blue cannulas. Ensure that fluid is flowing in the correct direction and that the tubing is not being displaced into the peristaltic pump.

10. Set the peristaltic pump at 50 rpm, which provides a flow of 27ml/min with the Masterflex® tubing.

11 Fill two 500ml beakers with 200mls of TexMACS. Carefully slide a liver wedge into each beaker so that it is submerged in TexMACS. If required, add further TexMACS into beaker so that the liver tissue is not exposed to air.

12. Place beakers into the bead bath, ensuring the fluid within the beaker is surrounded by beads.

12. To administer cells, ensure correct tubing to experimental lobe identified. Suspend cells in 25ml of TexMACS in 50ml tube. Temporarily pause the peristaltic pump. Transfer both of tubing ends that are providing the return from the experimental lobe (flowing from beaker to peristaltic pump) into the test tube with the cells. Restart the peristaltic pump so that the suspend cells are drawn into the tubing. Refill the 50ml tube with another 25mls of TexMACS and allow this to also be drawn into tubing. Pause the peristaltic pump and return the tubing to the beaker.

13. Cover the beakers with aluminium fouil overnight to retain heat and prevent evaporative loss.

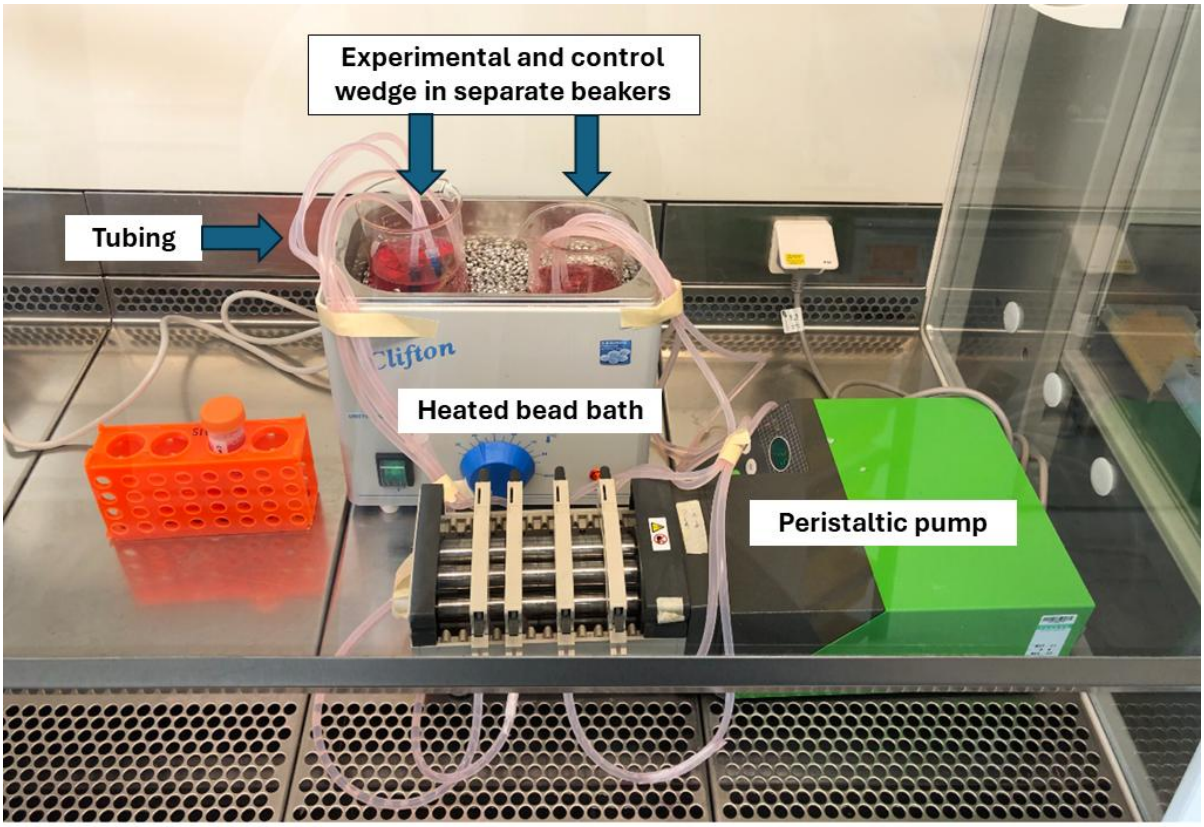


**Figure 2.6. Set up of wedge perfusion circuit.** Photograph of the final liver wedge perfusion model that incorporated both an experimental and control lobe. The whole experimental model can be contained within a hooded cabinet.

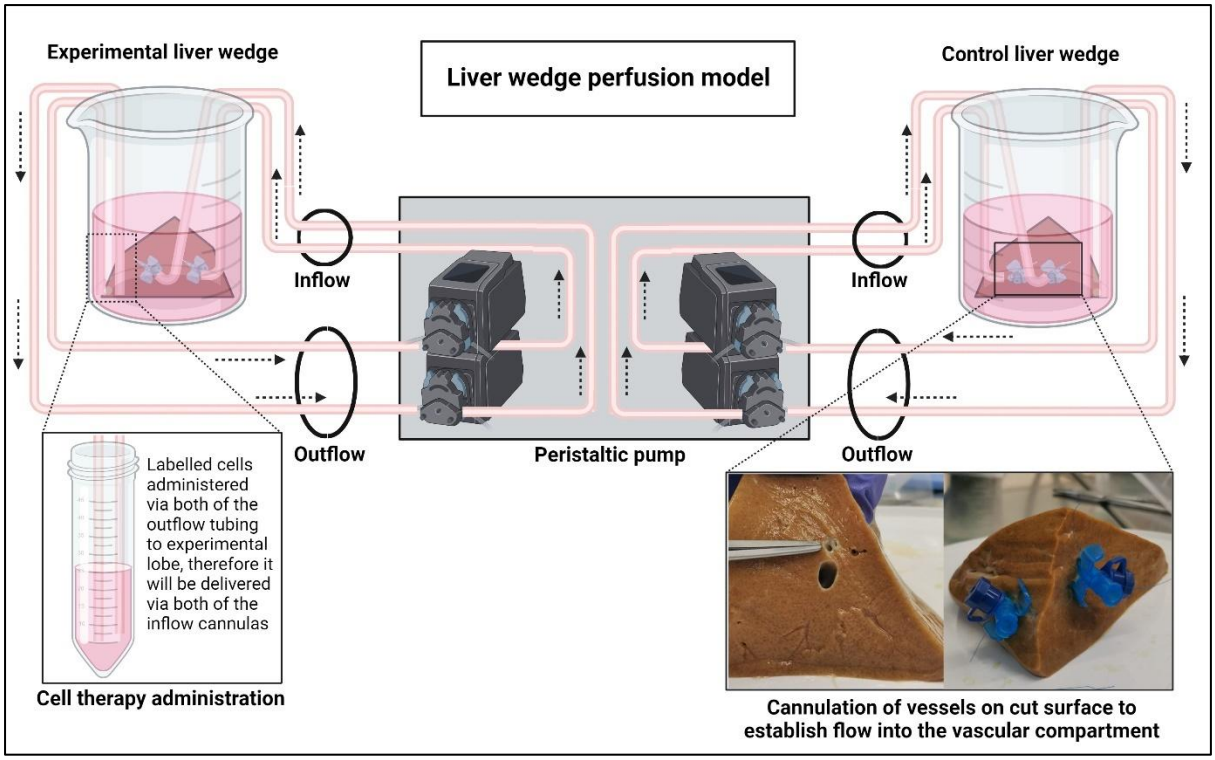


**Figure 2.7. Schematic of wedge perfusion circuit.** Liver wedge cannulated in portal vein at two sites on cut surface to provide inflow. Portal vein branch identified on cut surface by surrounding glissonian sheath (indicated by surgical instrument in inset image) which sorrounds the portal tracts but not hepatic vein branches. Experimental inflow tubes transferred to tube containing labelled cells. This model was used for the wedge perfusion experiments.

## 2.16 Whole liver perfusion experiments

These experiments were performed using a commercially available machine perfusion device (LiverAssist, XVIVO). The organs used were human livers declined for clinical transplantation. These were also utilised in an ongoing research project investigating defatting therapy. The Treg infusion experiment was performed after the livers had been perfused for 72 hours and received defatting.

1. Excessive tissue removed from graft to expose the inferior vena cava, portal vein and hepatic artery. Hepatic artery and portal vein cannulated as per manufacturer's instructions.

2. Menghini biopsies from liver at the following locations prior to infusion of cells; Right lobe, left lobe, segment 4.

3. Cells suspended in media and injected through the arterial cannula tubing. Tubing flushed with additional 10mls of media.

4. Menghini biopsies from liver at the following locations 2-hours after infusion of cells; Right lobe, left lobe, segment 4.

5. Menghini biopsies from liver at the following locations 4-hours after the infusion of cells; Right lobe, left lobe, segment 4.

6. Perfusion stopped 4-hours after the infusion of cells. Slice of left lobe and right

**2.17 Sampling protocol for study RRK7086/IRAS 281445**

During this research, clinical samples were taken from patients receiving a liver transplant at Queen Elizabeth Hospital Birmingham and this was apptoved by the Human Research and Ethics Committee (21/WA/0300). This involved collecting samples from patients that were undergoing transplantation followimg cld preservation or normothermic machine perfusion. This is further described in chapter 3. Figure 2.8 demonstrates the sampling protocol for each group.

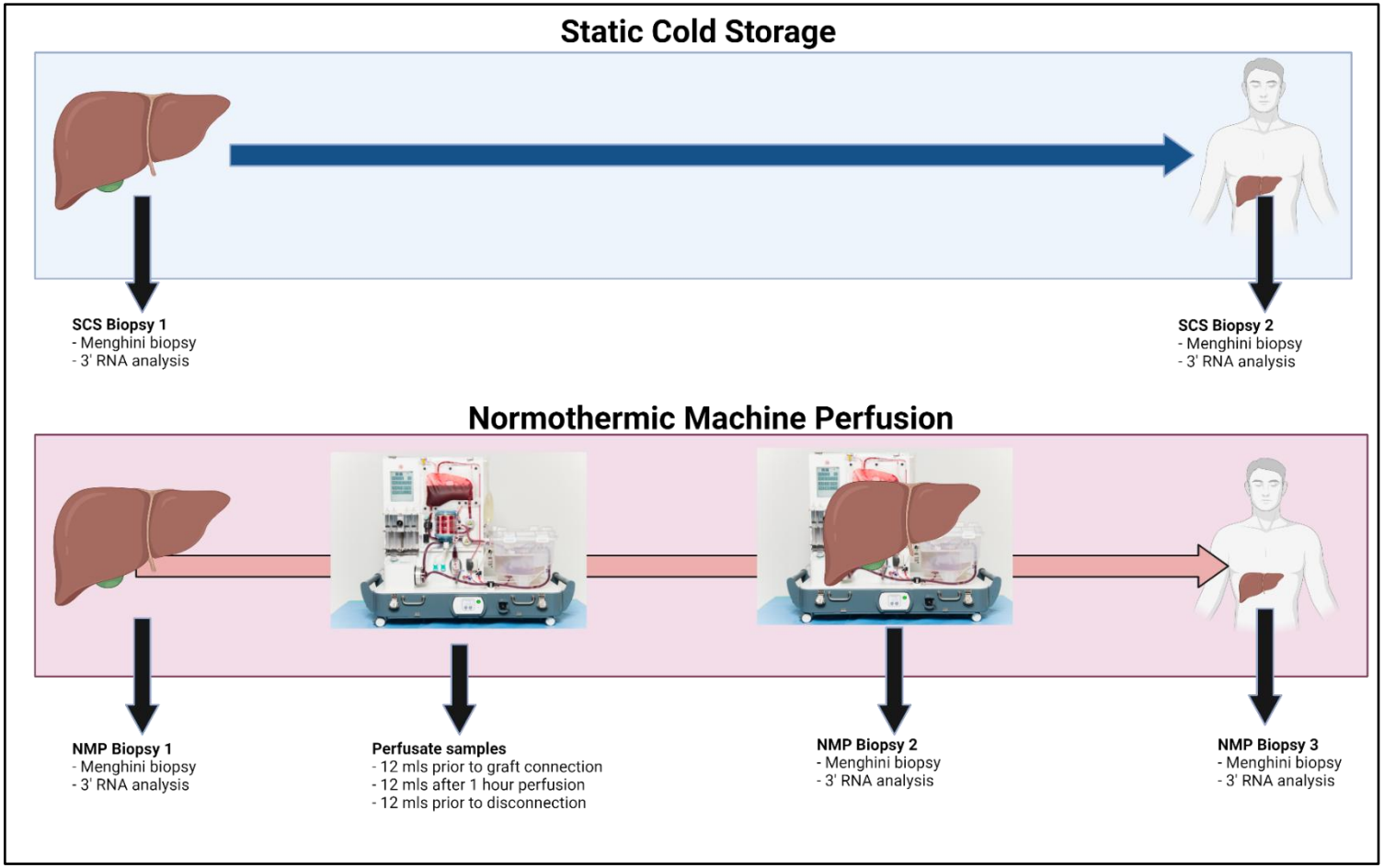


**Figure 2.8.** Sampling protocol for clinical study. Schematic demonstrating the sampling protocol of the 10 patients enrolled in each of the cold storage and NMP groups. Liver biopsies were taken from both groups after arrival at the recipient centre, after perfusion in the NMP group (bottom row), and after implantation in both groups. Perfusate samples were taken prior to graft connection, after one hour and at the end of perfusion.

## 2.18 Statistical analysis

Statistical analysis was performed via SPSS (Version 25.0. Armonk, NY: IBM Corp) or GraphPad Prism (GraphPad Prism version 10.0.0 for Windows, GraphPad Software, Boston, Massachusetts USA, www.graphpad.com). Variables were reported as medians with IQR range if they did not follow a normal distribution. The Mann-Whitney U test was used to compare continuous variables. Categorical variables were compared with the Pearson chi-square test for independence. Continuous variables that did not follow the normal distribution were compared with the Kruskal-Wallis test. A repeated measures ANOVA test was used to assess for statistical significance when multiple continuous variables were compared at different timepoints . P-values <0.050 was considered statistically significant.

# Chapter 3 – Immunological impact of NMP

### 3.1 NMP in clinical practice

The utilisation of NMP as a liver graft preservation strategy has increased around the world following several seminal publications[108,113]. To date there have been three multicentre, randomised controlled trials comparing livers preserved with NMP to cold storage (Table 3.1)[108,131,132].

**Table 3.1. Randomised controlled trials of Normothermic machine perfusion**

| | | Number of livers in NMP arm | | |
|---|---|---|---|---|
| **First author** | **Year** | **DBDs** | **DCDs** | **Primary outcome** |
| Nasralla D | 2018 | 87 | 34 | Day 1-7 Peak AST |
| Markman JF | 2022 | 123 | 28 | EAD |
| Chapman WC | 2023 | 114 | 22 | EAD |

The Study by Nasralla D was completed in the UK, and the other two were completed in the USA. EAD= Early allograft dysfunction as measured by the Olthoff criteria.

These three randomised trials all used biochemical markers of early graft function as their primary outcome measure, will all three demonstrating a significant reduction in early graft dysfunction in the NMP arm. This has provided overwhelming evidence that NMP preservation results in a lesser amount of hepatocellular injury in comparison to cold storage. Despite this benefit, graft and patient survival did not differ between the NMP and cold storage arms in any of these trials.

A benefit that has been consistently demonstrated is that NMP increases graft utilisation. This has been demonstrated in both standard risk and marginal grafts[108,119]. This is of paramount importance given the high demand for donor livers, but a shortage in supply. This is one of the main benefits of NMP in current practice, and a dedicated trial investigating whether NMP can increase utilisation within an entire allocation system is in its final stages of follow up (PLUS trial). Since 2018, the Queen Elizabeth Hospital Birmingham has been using NMP regularly outside of registered clinical trials, with the main purpose of increasing graft

utilisation. Figure 3.1 demonstrates the number of liver transplants following NMP preservation in comparison to overall transplants.

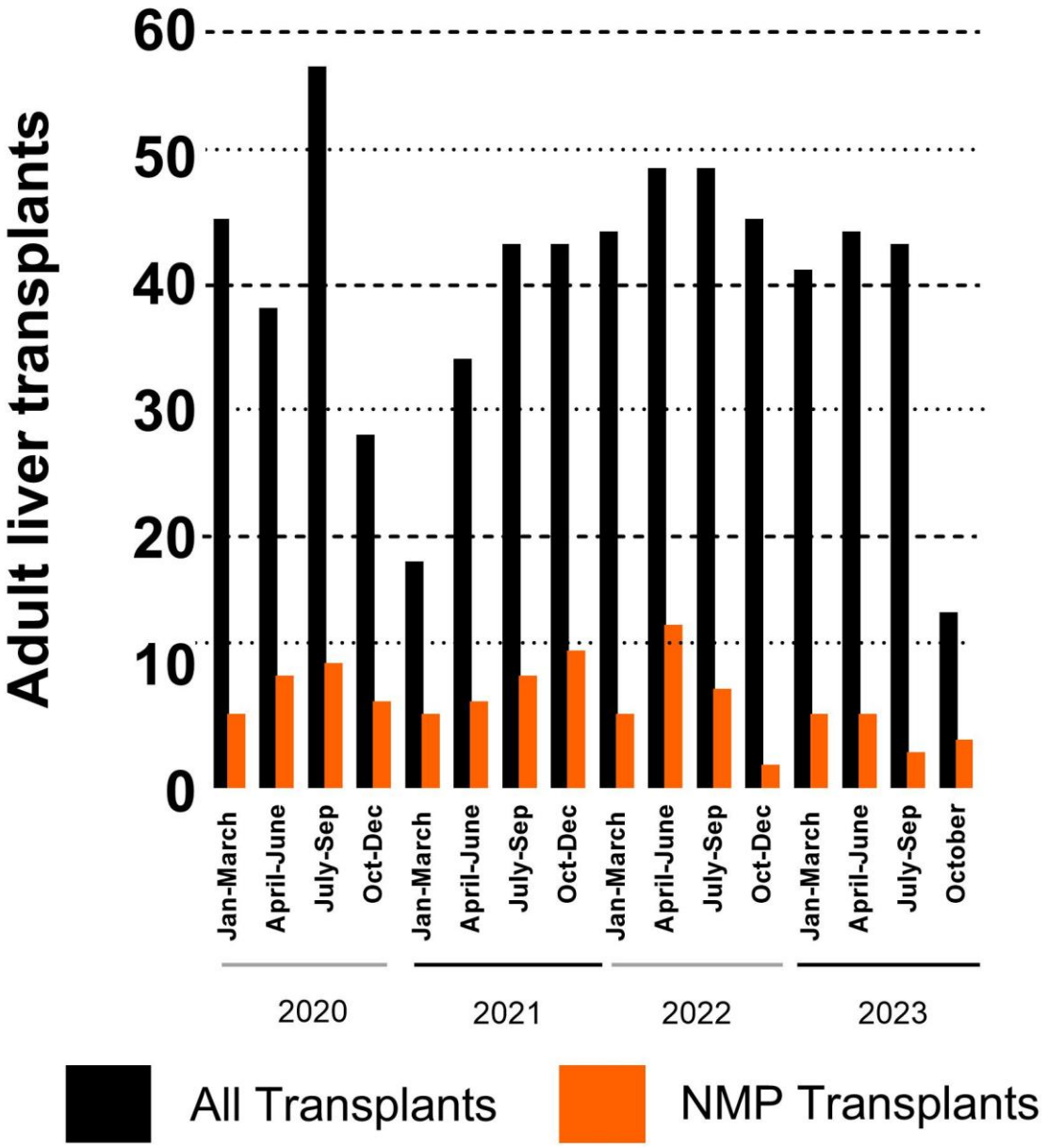


**Figure 3.1. NMP activity at Queen Elizabeth Hospital Birmingham.** NMP activity from 2020 until late 2023. There was a noticeable fall in all transplant activity during the second COVID-19 pandemic wave.

The majority of grafts preserved with NMP were from DBD donors (Figure 3.2), due to the ongoing concern for ischaemic type biliary lesions developing in the DCD grafts. The evidence that NMP preservation of DCD grafts at the recipient hospital prevents ITBL is not

strong[109], and therefore not the routine approach. Following viability testing, between January 2018 and October 2023, the discard rate was 19/155 (12%) (Figure 3.2) and the reasons for discard are shown in table 3.2. The viability criteria applied at QEHB have evolved over time and consist of both major and minor criteria[133]. Lactate clearance to <2.5mmol/L is the major criterion[133].

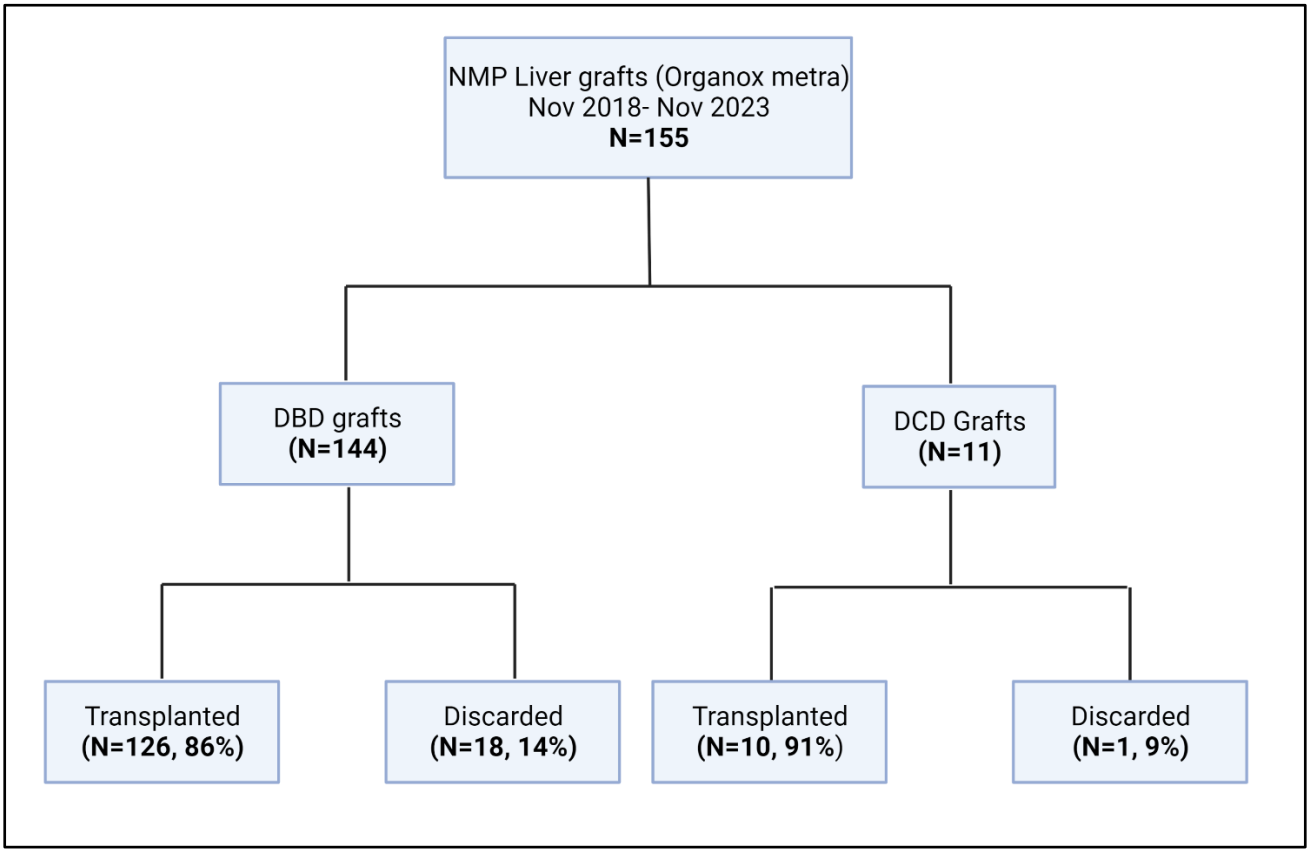


**Figure 3.2**. **Flow chart of livers preserved with NMP**. DBD= Deceased brain death DCD= Deceased circulatory death

**Table 3.2. Reasons for discard following NMP preservation**

| Reason not transplanted | DBD (N=18) | DCD (N=1) |
|---|---|---|
| Inadequate lactate clearance | 11 | |
| Persistent acidosis & no glucose metabolism | 3 | |
| Graft portal vein thrombosis (VITT donor) | 1 | |
| No hospital capacity | 1 | |
| Machine malfunction | 1 | |
| Recipient had peritoneal metastases | 1 | |
| No bile production | | 1 |

VITT=Vaccine induced thrombosis and thrombocytopenia

### 3.1 Effect of NMP on graft rejection

In both the scientific and clinical literature, there is a large amount of evidence that NMP reduces the amount of preservation reperfusion injury and the associated surrogate markers such as peak transaminases. However, there was very little reported in the literature regarding the immune consequences of NMP such as biopsy proven acute rejection (BPAR). In the three randomised controlled trials listed in Table 3.1, only Nasralla et al reported the rejection rate [NMP=12/128 (9.3), SCS=13/164 (7.9%)]. Our clinical observations at QEHB were that graft rejection appeared more frequent and severe following NMP preservation.

In a clinical study conducted at the QEHB that investigated the outcomes of patients undergoing late liver retransplant using NMP preserved livers, we found that the rate of BPAR was significantly higher in comparison to cold storage. This was despite similar rates of underlying autoimmune liver disease (Table 3.3). Given these findings in a small sample of NMP retransplant patient (N=26). We investigated the incidence of biopsy proven rejection (BPAR) in a larger cohort of primary (Figure 3.3) and repeat liver transplant recipients (Figure 3.4).

**Table 3.3** Immune mediated disease, immunosuppression and rejection details of each group

| Characteristic | SCS 1 (N=31) | SCS 2 (N=25) | NMP (N=26) | *P* |
|---|---|---|---|---|
| Autoimmune disease in native liver | 13/31 | 15/25 | 17/26 | 0.384 |
| *Autoimmune hepatitis* | 1/13 | 4/25 | 2/17 | |
| *Primary sclerosing cholangitis* | 8/13 | 9/25 | 9/17 | |
| *Primary biliary cirrhosis* | 2/13 | 2/25 | 0 | |
| *Overlap syndrome* | 2/13 | 0/25 | 1/17 | |
| Chronic rejection in previous graft | 2/31 | 4/25 | 6/26 | 0.204 |
| Post-operative immunosuppression† | | | | **0.007** |
| *Tacrolimus and Azathioprine* | 22 | 7 | 9 | **0.002** |
| *Tacrolimus and MMF* | 6 | 16 | 15 | **0.001** |
| *Basiliximab, Tacrolimus and MMF‡* | *3* | 2 | 2 | 0.959 |
| **Acute T cell mediated rejection** | **SCS 1 (N=9)** | **SCS 2 (N=6)** | **NMP (N=16)** | |
| Post-op day rejection diagnosed (IQR) | 6 (6-7) | 15.5 (5.8-34.2) | 7 (7-11) | 0.228 |
| Trough Tacrolimus Level (IQR) | | | | |
| *Day 3* | 4.4 (2-9.8) | 4.2 (2.5-15.1) | 9.2 (6.7-12.2) | 0.171 |
| *Day 7* | 6.3 (4.0-9.3) | 5.5 (4.6-10.2) | 6.7 (4.7-8.8) | 0.912 |
| *Last level prior to BPAR* | 5.0 (3.7-7.1) | 6.9 (3.7-10.6) | 7.4 (5.9-8.9) | 0.140 |
| Severity of rejection | | | | 0.231 |
| *Mild* | 0 | 0 | 2/16 | |
| *Moderate* | 6/9 | 6/9 | 12/16 | |
| *Severe* | 3/9 | 0 | 2/16 | |
| Required >1 high dose steroid pulse | 0 | 0 | 2/16 | 0.504 |

† All patient also received corticosteroids ‡This regime consisted of basiliximab at time of operation and on post-operative day 4, with either low dose or no tacrolimus on post-operative days 1-4.

**Immune mediated disease, immunosuppression and rejection details of each group.** Categorical variables compared with Chi-Square test. One-way analysis of variance (ANOVA) was used to compare continuous variables that followed the normal distribution. The Kruskal-Wallis test was used to compare continuous variables that did not follow the normal distribution. SCS= Static cold storage MMF=Mycophenolate Mofetil, BPAR=Biopsy proven acute rejection. Source: Hann A, Lembach H, Nutu A et al Br J Surg. 2022 Mar 15;109(4):372-380.

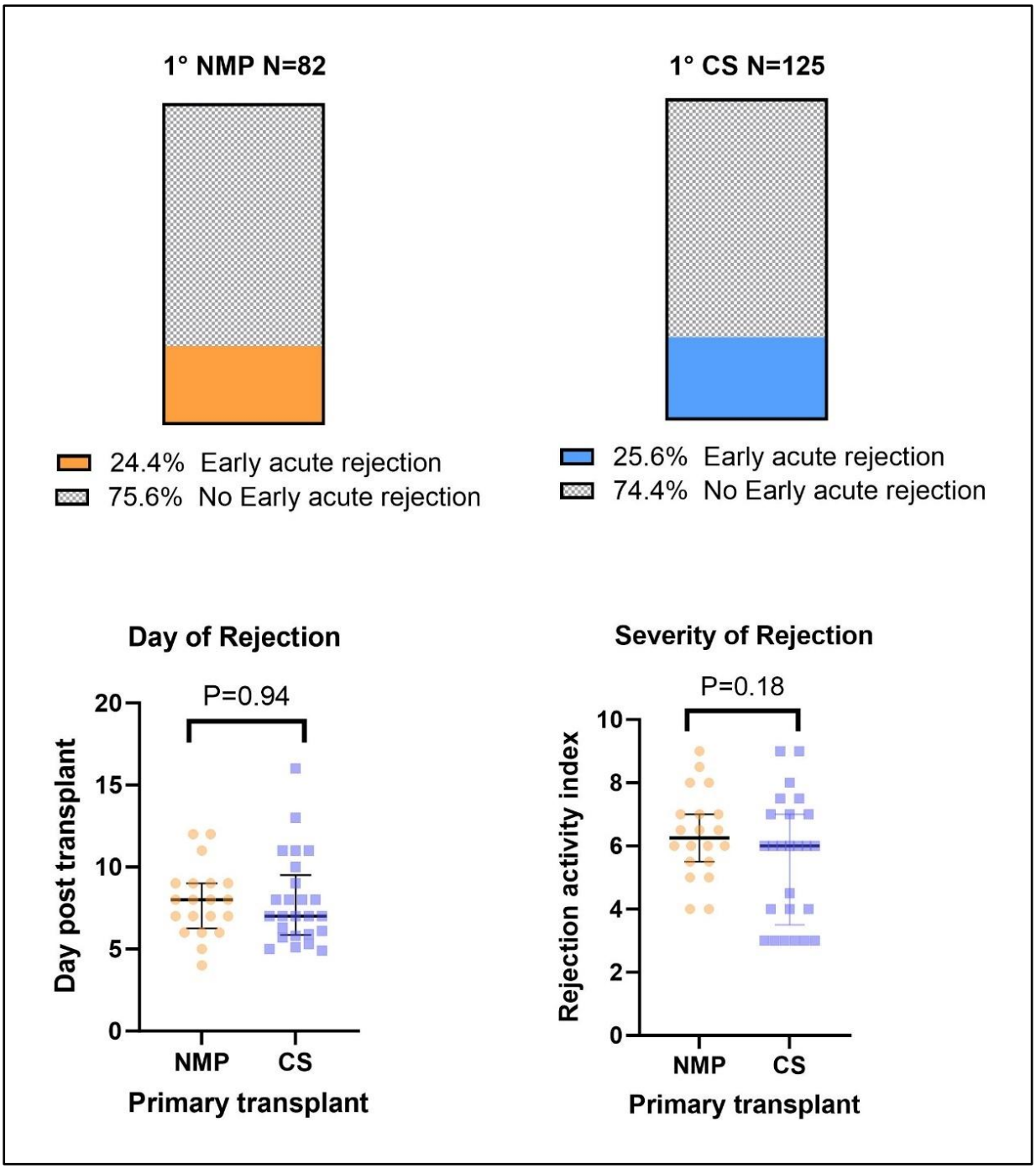


**Figure 3.3. Incidence, severity and day of acute rejection following primary transplant.** The graphs demonstrate the similar incidence, day of onset and severity of rejection following NMP and cold storage (CS) primary liver transplant. Rejection activity index is a scale of grading severity of rejection from 0-9 (9 being severe).

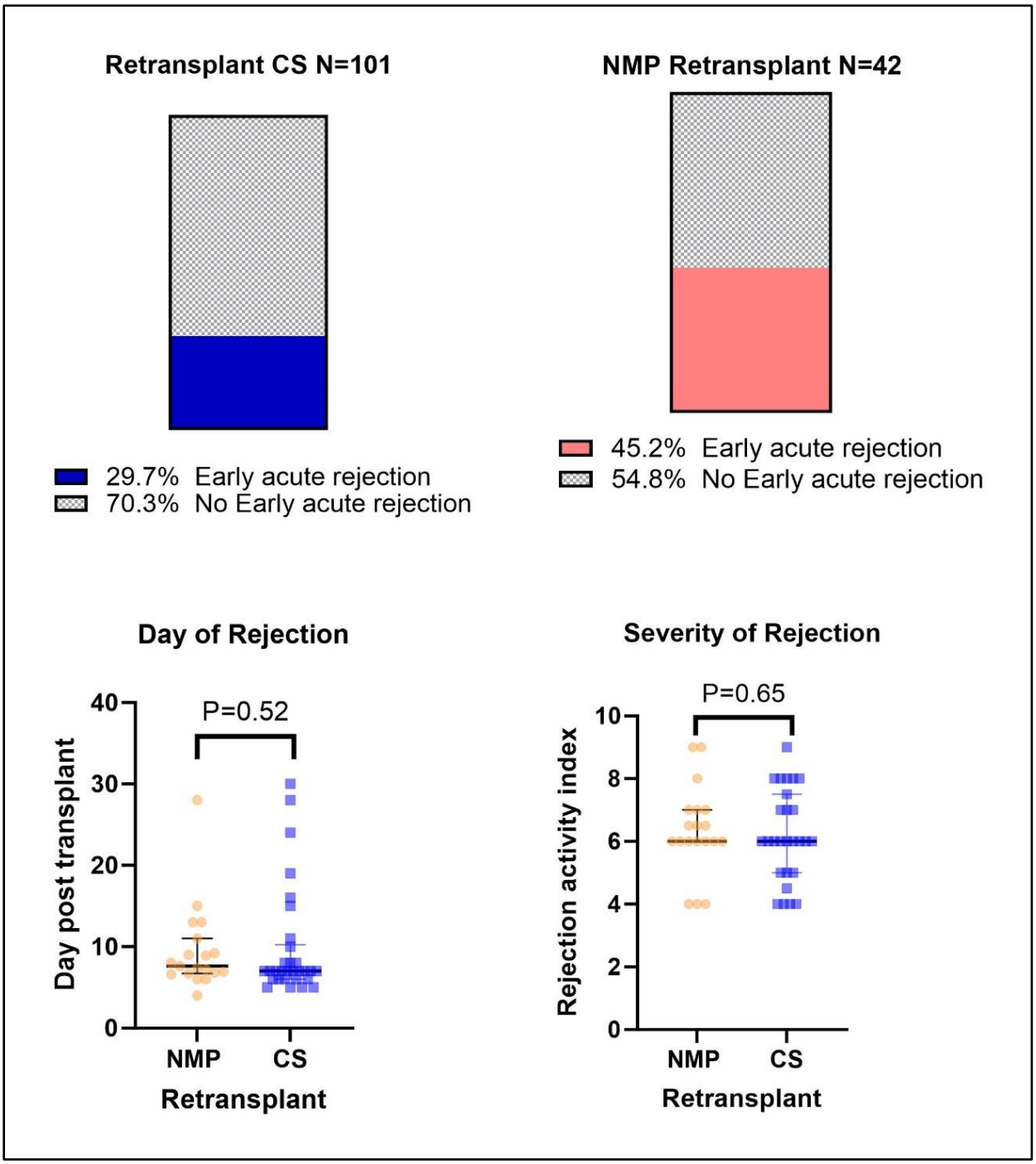


**Figure 3.4. Incidence, severity and day of acute rejection following retransplant.** The graphs demonstrate a significantly higher incidence of acute rejection, but similar day of onset and severity following NMP and cold storage (CS) retransplant. Rejection activity index is a scale of grading severity of rejection from 0-9 (9 being severe).

The time on onset and histological severity of BPAR according the Rejection Activity Index (RAI) was shown to be similar for both primary transplants and retransplants ( Figure 3.3 & 3.4). The incidence of BPAR was similar between NMP and cold storage preserved primary transplants (24.4% V 25.6%), however the incidence of BPAR was significantly higher for NMP in the retransplant group (29.7% V 45.2 %P=<0.05). This observation indicates that the mechanism is likely complex, involving both graft and recipient factors.

If NMP is to be used as a platform for delivery immunotherapy, the changes that occur within the grafts immune cells during NMP need to be further investigated and understood. Our hypothesis was that there is activation of the grafts antigen presenting cells (APCs) during NMP and these then present antigens to the recipients T-cells after graft implantation. This process then results in BPAR via the direct pathway, and retransplant recipients are more susceptible due to previous foreign allograft exposure.

### 3.2 Scientific investigation of immunological mechanisms

To investigate the above hypothesis, analysis of human liver samples from patients undergoing transplantation was required. Other large animal models would not have provided the most accurate representation. In order to determine the unique changes that occurred during the NMP preservation process, samples of the cold stored livers was also required to serve as a control.

#### 3.2.1 Ethical approval process

To complete the planned project, specific Human Research Ethics Committee (REC) approval would be required. The research team formulated the study protocol, giving consideration to the resources and expertise available. The hospitals department of Patient and Public Involvement (PPI) was contacted and this projects patient information sheet and consent form appraised by members of the public and patients. These service users assessed this research as acceptable and provided suggested amendments for the consent and patient information sheet. These amendments were incorporated to ensure perspective participants in the study clearly understand the nature of this research. The Research & Development department at UHB foundation trust agreed to act as the study sponsor. Both REC (21/WA/0300) and trust approval (RRK7086) was obtained pior to commencement.

#### 3.2.2 Study methods

The study design was that of a non-randomised observational cohort study at the Queen Elizabeth Hospital Birmingham, with both an experimental (NMP) and control group (Cold storage). This hospital has a large deceased donor liver transplant program. The tissue samples were collected in the operating theatre in this institution and the laboratory assessment of these samples occurred at the University of Birmingham.

The study involves an experimental and follow-up phase.

**Experimental Phase:**

The study included both an experimental (NMP) and control group (Cold storage) and the assignment to groups was non-randomised. The experimental group included the participants that received a graft that was preserved via NMP, and the control group will be participants receiving a graft that has been preserved with cold storage. The determination of the type of preservation strategy was determined by the patients treating clinicians. Each participant in the experimental group provided consent to the collection of perfusate fluid and 3 biopsies from the donor liver at the time of their operation; one pre-NMP, one post-NMP, and one post-implantation (at time of surgery). Participants in the control group consented to the collection of two biopsies, one pre-implantation and one post implantation. The liver tissue samples were preserved in RNAlater solution and stored at -20°C. The perfusate was centrifuged to obtain the supernatant and stored at -80°C. Table 3.4 and 3.5 outline the sampling protocol for both the experimental and control groups

Following back table preparation of the donor graft at QEHB, a liver biopsy was taken using a Menghini (11520–19, 17swg (1.4mm) x 70mm; Dixons Surgical Instruments Ltd, Wickford, Essex, UK) biopsy needle. In the case of the experimental group, the graft was then connected to the NMP circuit and perfusion commenced. The NMP procedure did not deviate from standard clinical practice. The biopsy specimens will be divided into two portions. One portion will go into formalin for routine histopathological analysis. The other will be suspended in RNAlater solution for 3' RNA sequencing analysis.

Three blood samples (12ml each) were collected from the specifically designed hub on the circuit. The first sample will be taken prior to connection of the liver to the perfusion circuit. The second will be two hours after the perfusion has commenced, the third just prior to

disconnection of the graft. The blood samples were put into Ethylenediaminetetraacetic acid (EDTA) tubes.

A second liver biopsy will be performed immediately prior to disconnecting the liver from the NMP circuit. A third liver biopsy will be taken after the portal vein has been anastomosed and opened to re-perfuse the graft in the recipient. This biopsy will occur in both the experimental and control group. The RNA was extracted from the liver tissue as outlined in chapter 2

**Table 3.4. Samples collected from NMP group**

| Tissue Sample | Number | Timepoint of collection | Test |
|---|---|---|---|
| Perfusate (NMP group) | Perfusate 1 | Sample drawn from NMP circuit prior to graft connection | Flow cytometry & metabolomics |
| | Perfusate 2 | Sample drawn after graft perfused for 1 hour | Flow cytometry & metabolomics |
| | Perfusate 3 | Sample drawn immediately prior to graft disconnection | Flow cytometry & metabolomics |
| Liver biopsy (NMP group) | Liver biopsy 1 ( LB1) | Biopsy performed after liver prepared for NMP connection | 3'RNA |
| | Liver biopsy 2 (LB2) | Biopsy performed prior to graft disconnection and flush | 3'RNA |
| | Liver biopsy 3 (LB 3) | Biopsy performed after reperfusion in recipient | 3'RNA |

**Table 3.5. Samples collected from cold storage group**

| Tissue Sample | Number | Timepoint of collection | Test |
|---|---|---|---|
| Liver biops (CS group) | Liver biopsy 1 (LB1) | Biopsy performed after back table preparation of graft | 3'RNA |
| | Liver biopsy 2 (LB2) | Biopsy performed after reperfusion in recipient | 3'RNA |

**Follow up phase:**

Following transplantation, follow up data will be obtained for 12 months. This was collected by a member of the clinical team from routinely collected patient data. The patient's electronic medical chart was reviewed at 1-monthly intervals during the follow up period. Clinical data including the following variables will be collected; Liver function test results, rejection episodes and severity, complications, graft loss, mortality. These variables were collected from the Patient Information and Communication (PICS) system at our institution. The participants were not contacted by the research team and did not have to attend the hospital for any additional research related visits.

### 3.2.3 Donor and recipient combinations

During the study recruitment period (January 2021 – September 2021), 20 recipients were enrolled in the study. All received whole DBD grafts, and 10 each were preserved with cold storage and NMP. The characteristics of the donors are shown in table 3.6. The individual donor-graft-recipient combinations shown in figure 3.5.

**Table 3.6. Donor and preservation characteristics**

| | NMP Group (N=10) | Cold storage Group (N=10) | P Value |
|---|---|---|---|
| Donor age | 61 (51-65) | 60 (26-69) | 0.806 |
| Donor BMI | 26 (23-27) | 24 (23-33) | 0.934 |
| Donor COD | | | 0.259 |
| *HBI* | 1/10(10%) | 5/10 (50%) | |
| *CVA* | 1/10 (10%) | 1/10 (10%) | |
| *ICH* | 7/10 (70%) | 4/10 (40%) | |
| *Trauma* | 1/10 (10%) | 0/10 (0%) | |
| Cold ischaemic time (IQR) | 420 minutes (329-524) | 364 (283-471) | 0.327 |
| NMP time (IQR) | 967 minutes (627-1346) | NA | |
| dWIT time (IQR) | 28 minutes (20-32) | 25minutes (19-29) | 0.413 |
| Recipient age | 42 (28-54) | 49 (44-58) | 0.278 |
| Recipient disease | | | 0.876 |
| *AILD* | 4/10 (40%) | 3/10 (30%) | |
| *No AILD* | 6/10 (60%) | 7/10 (70%) | |

Baseline demographic and disease characteristics of the donors and recipients in each group. Categorical variables compared with the Chi Square test, and continuous variables with the Mann-Whitney U test. BMI= Body mass index, COD= Cause of death, HBI=Hypoxic brain injury, CVA=Cerebrovascular accident, ICH= Intracranial haemorrhage, NMP= Normothermic machine perfusion, dWIT=Donor warm ischaemic time (implant time), AILD=Autoimmune liver disease

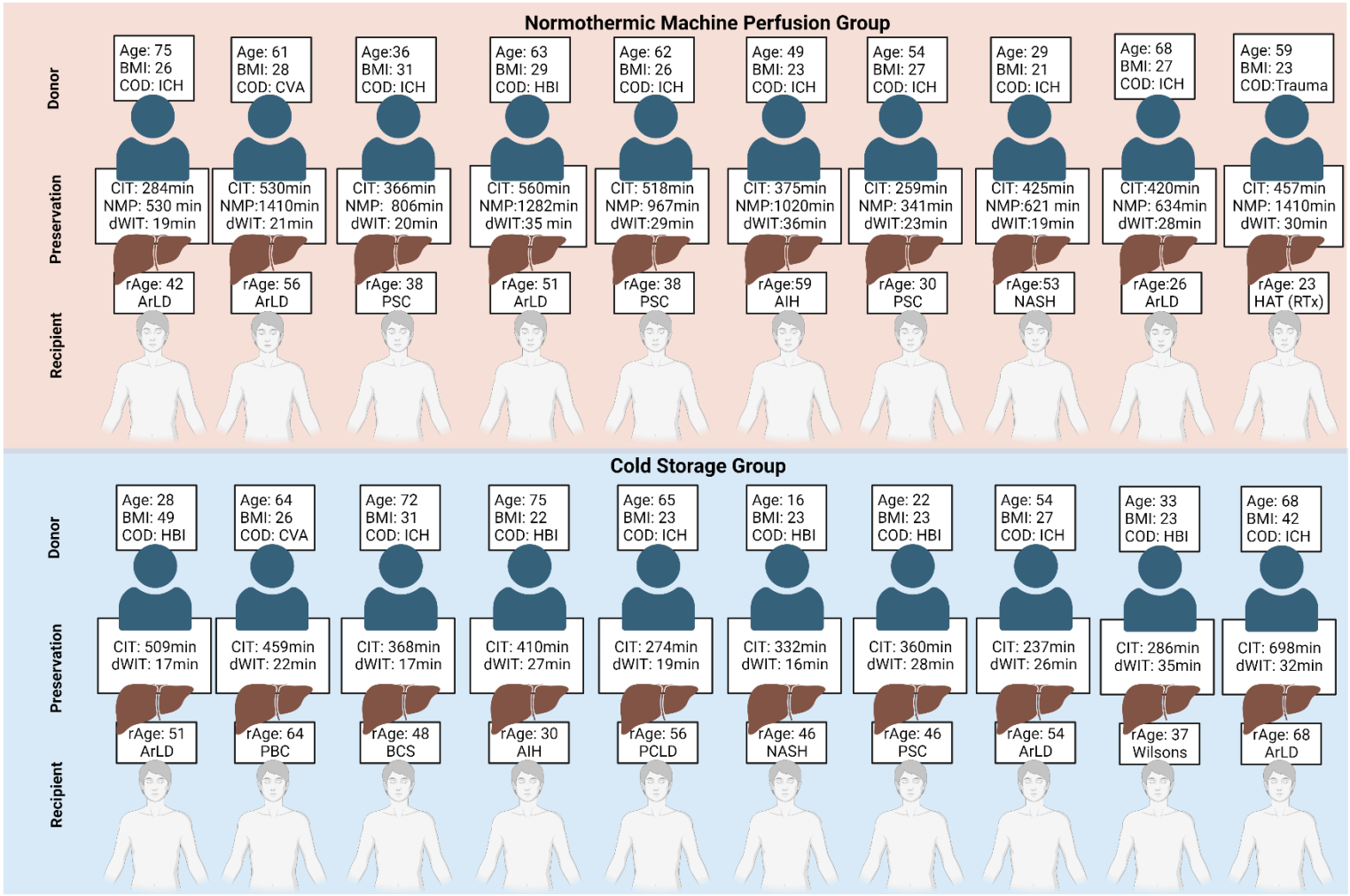


**Figure 3.5. Donor, graft and recipient characteristics. The NMP group is represented in the top panel and the cold storage group in the bottom panel.** BMI= Body mass index, COD= Cause of death, CIT= Cold ischaemic time, NMP= Normothermic machine perfusion, dWIT= donor warm ischaemic time, ArLD= Alcohol related liver disease, PSC= Primary sclerosing cholangitis, AIH= Autoimmune hepatitis, HAT=Hepatic artery thrombosis, PBC= Primay biliary cholangitis, BCS= Budd chiari syndrome, PCLD= Polycystic liver disease

### 3.2.4 Clinical outcomes

The subjects have been followed up for a median of 19 (IQR: 18-22) months. The early graft function as indicated by bilirubin and ALT is indicated in figure 3.6. There was no significant difference in ITU length of stay (3.0 [2.8-5.0] v 2.0 [1.7-3.2], P=0.01), however the modified early allograft function (MEAF) score was significantly higher in the NMP group (4.9 [3.8-5.5] v 3.3 [2.2-4.9], P=0.05) (Figure 3.7). According to the Olthoff criteria[134], 2/10 and 0/10 patients in the NMP group and SCS group developed early allograft dysfunction respectively. In total, 5 patients experienced early BPAR between day 5 and 11 post transplant (Figure 3.8). The rate of early BPAR was higher in the NMP group (4/10 vs 1/10). There was no cases of primary non-function, hepatic artery thrombosis, ischaemic type biliary or biopsy proven chronic rejection in either group. All patients were alive with a functioning graft at 12-months post transplant.

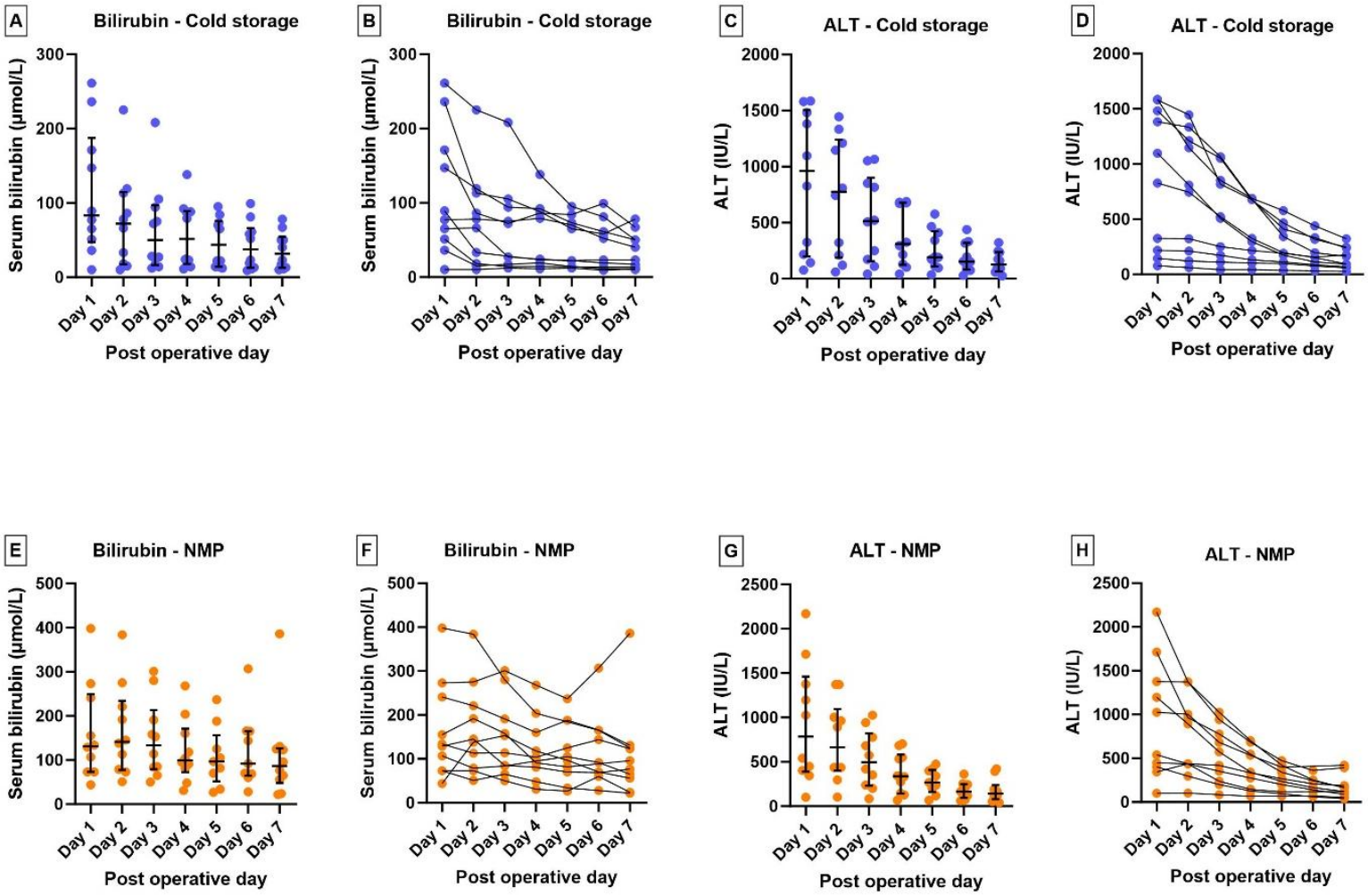


**Figure 3.6.** Early graft function in NMP and cold storage groups. Day 1-7 biochemical parameters for the cold storage group indicated in top row and NMP group in bottom row. Graft function as indicated by post transplant day 1-7 bilirubin and alanine transaminase (ALT). Median bilirubin demonstrated in A & E, and trend demonstrated in B & F. Median ALT demonstrated in C & G, and trend demonstrated in D & H.

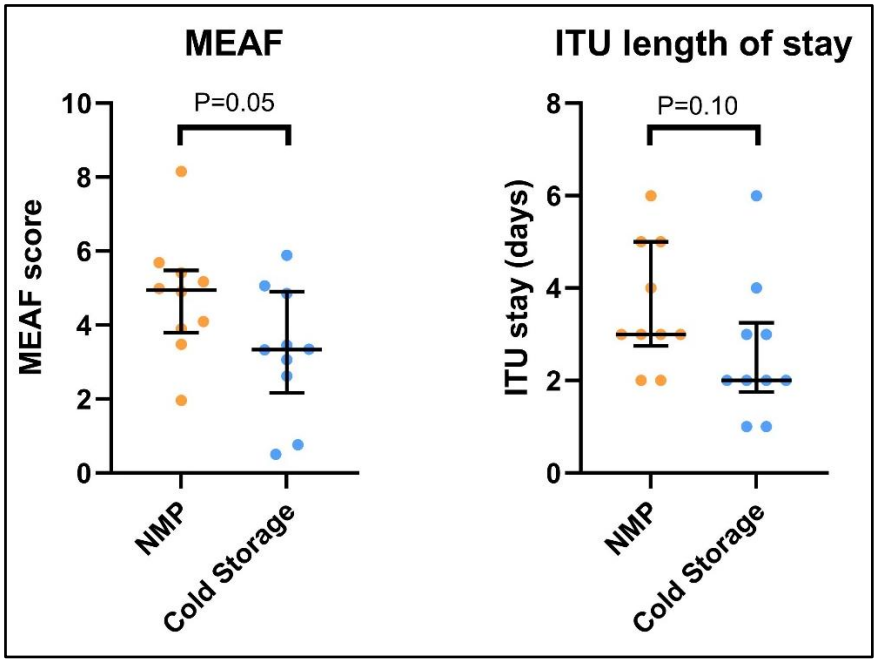


**Figure 3.7.** Model for early allograft function (MEAF) score and duration of intensive treatment unit stay. The post operative MEAF score and ITU length of stay of the NMP and cold storage group are demonstrated on the left and right respectively. The MEAF score was significantly higher in the NMP group, but there was no difference in the duration of ITU length of stay.

The characteristics, time of onset, and severity of early BPAR is demonstrated in figure 3.8 & 3.9. All patients with BPAR required high dose corticosteroid treatment. The trend of bilirubin and ALT at the time of biopsy for each of the patients that experienced BPAR is shown in figure 3.9. All patients received a calcineurin inhibitor, antimetabolite and corticosteroids from day 0, except one patient in the cold storage group who had Basiliximab induction and delayed commencement of tacrolimus (day 5). The patients tacrolimus levels during the early post operative period are shown and compared in figure 3.10. There was no statistically significant difference between the levels on day 3,6,9, and 12. On day 15, the NMP group had higher serum tacrolimus level (7.1 [6.4-7.8] v 4.2 [1.7-5.2], P=0.01).

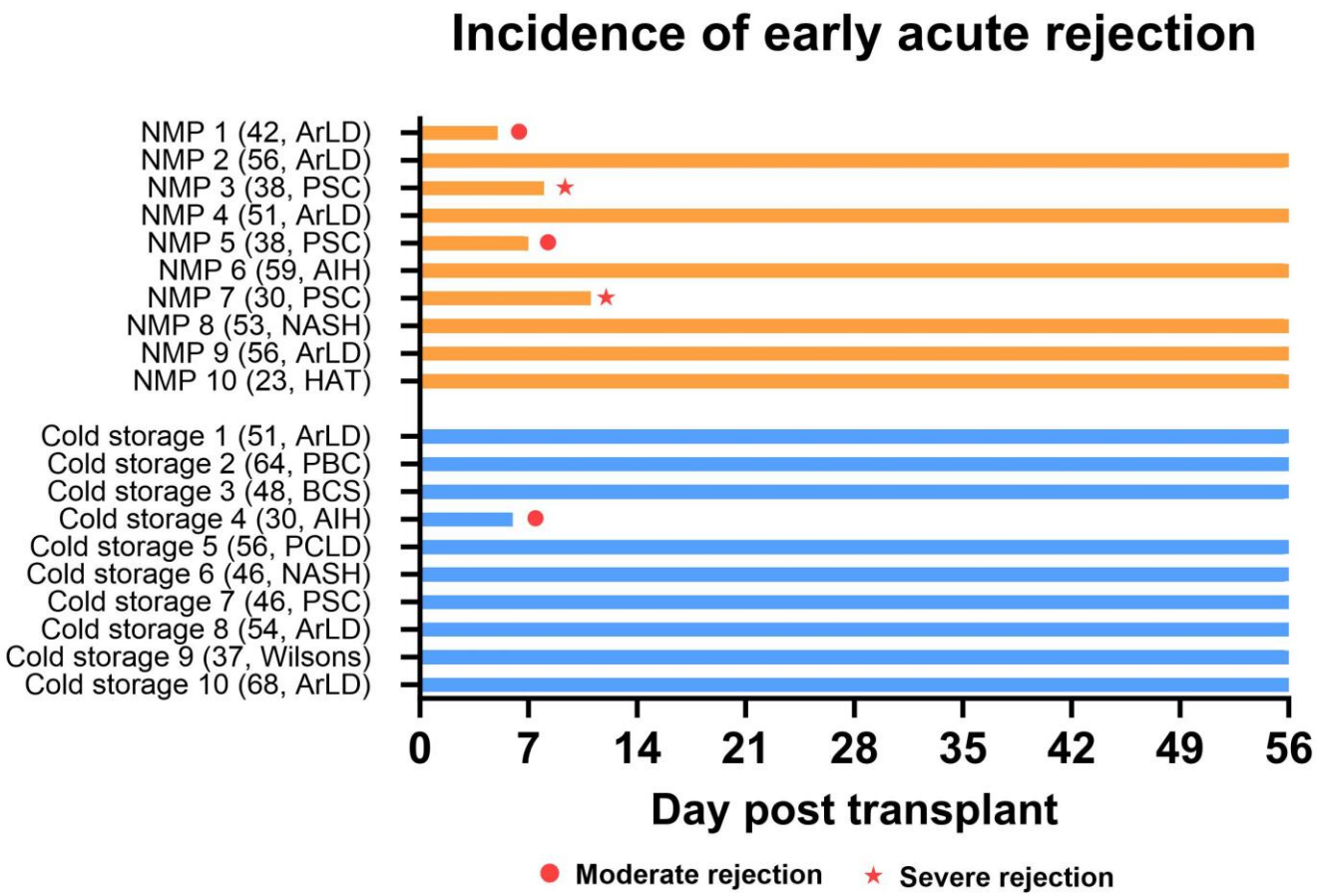


**Figure 3.8. Early acute rejection in NMP and cold storage group. In the NMP group (Upper panel) there was 4 cases of acute early acute rejection, and in the cold storage group (lower panel) there was 1 case.** ArLD= Alcohol related liver disease, PSC= Primary sclerosing cholangitis, AIH=Autoimmune hepatitis, NASH= Non-alcoholic fatty liver disease. HAT=Hepatic artery thrombosis. PBC= Primary biliary cholangitis. BCS=Budd chiari syndrome PCLD= Polycystic liver disease

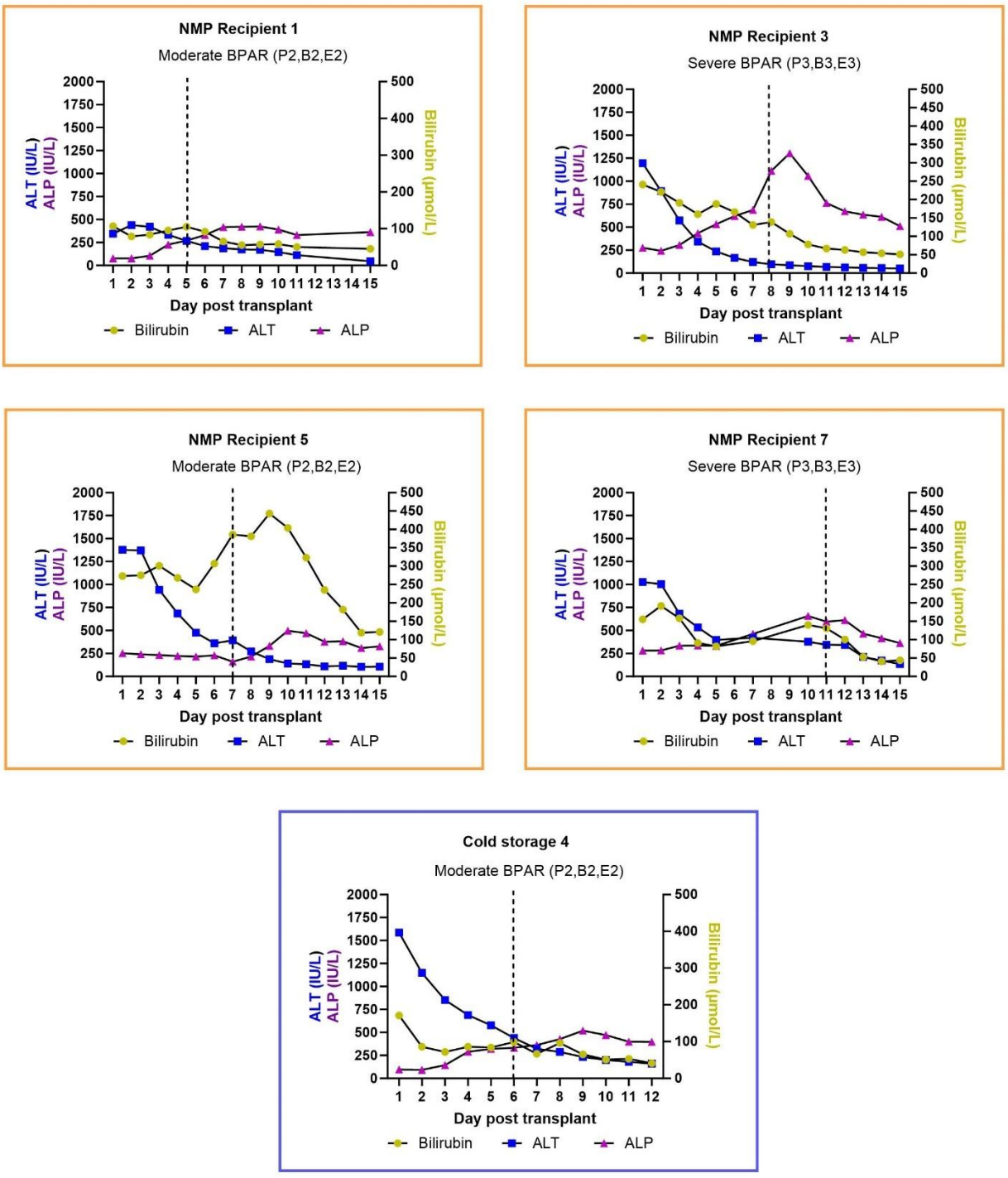


**Figure 3.9**. Participants who developed early biopsy proven acute rejection (BPAR). Each square represents a separate patient. There was 4 cases in the NMP group (orange box) and 1 in the cold storage group (blue box). Dashed line represents day rejection was diagnosed.

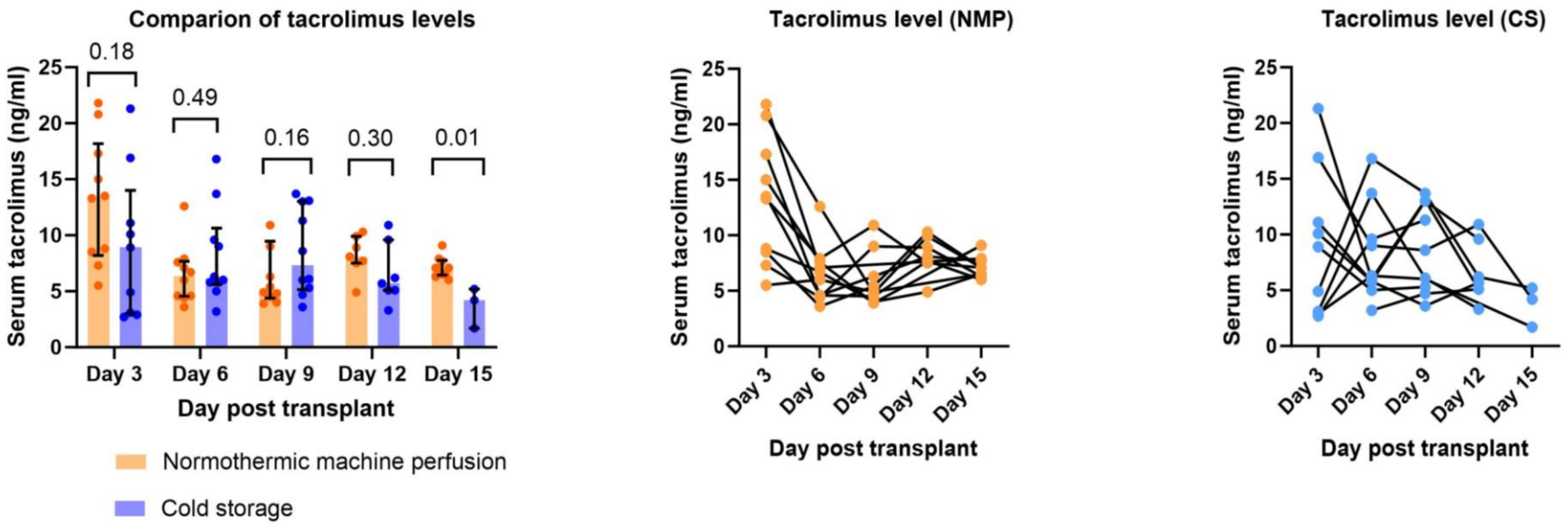


**Figure 3.10**. **Tacrolimus levels in NMP and cold storage group. Graph on left compares serum levels with the only significant difference being on day 15.**

### 3.2.4 Perfusate cytokine assessment – Whole group

Cytokine measurements were performed on NMP perfusate samples drawn prior to liver connection (pre), after 60 minutes of liver NMP (1 hour), and at the end of NMP (end). These samples were processed as per methods section 2.11. After removing significant outliers, 8 patients results were included in the analysis. The levels of the interleukin 1 family in all NMP subjects are demonstrated in figure 28. Similar to previous authors, we found a constant increase in IL-1beta and IL-18 (Figure 3.11 B&D) throughout the duration of NMP[135,136]. In addition, the levels of IL-1alpha and IL-1RA increased throught the period of NMP (Figure 3.11 A&C). These cytokines are secreted by numerous cell types including neutrophils, monocytes/macrophages, endothelial cells and dendritic cells[137].

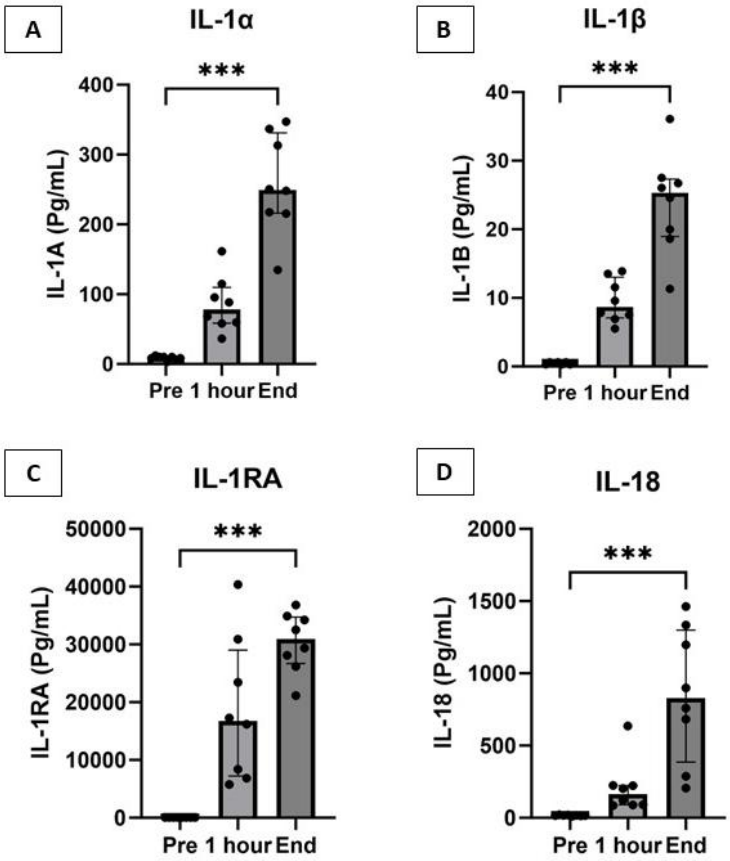


**Figure 3.11. Interleukin 1 (IL-1) Family.** A-D demonstrate the absolute values of the IL1 family for the 8 grafts included in the analysis. There was a consistent increase in these cytokines during the perfusion. Statistical comparison with Mann-Whitney U test. *** P = <0.001.

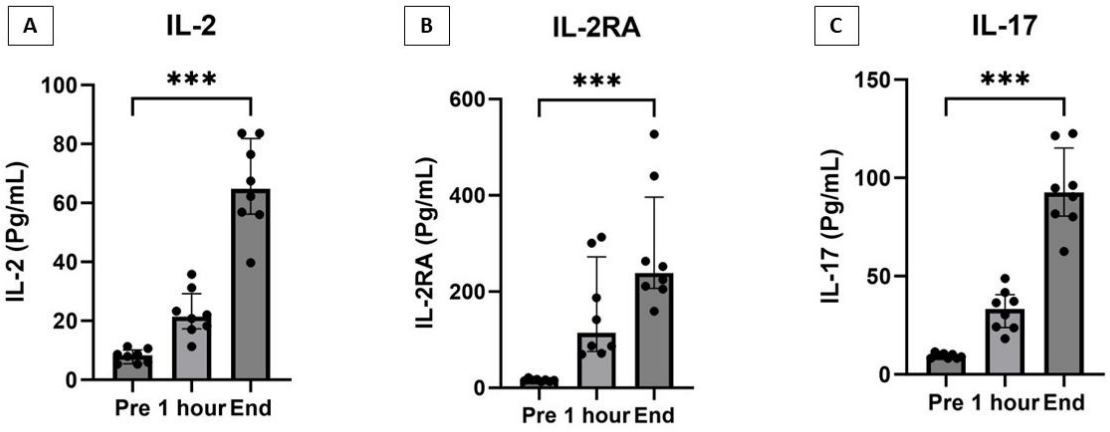


**Figure 3.12. Interleukin-2 (IL-2) family and interleukin-17 (IL-17) levels during NMP.** There was an increase in IL-2, IL-2RA and IL-17 across the perfusion in the 8 grafts included in the analysis. Statistical comparison with Mann-Whitney U test.*** P=0.001

The levels of IL-2, IL2RA and IL17 in the machine perfusate increased significantly throughout the period of machine perfusion (Figure 3.12). The cell type that secretes IL-2 are $CD4^+$ T-cells, following T-cell receptor (TCR) activation[138]. A subset of $CD4^+$ T cells, T helper 17 (Th17), are the primary source of IL-17 secretion[139]. Other types of immune cells, including cells of the innate system have been shown to also have the capability of secreting IL-17[139]. This cytokine is regarded as proinflammatory and has been implicated in several autoimmune pathologies. Lee et al 2022 also demonstrated an increase in IL-17 throughout NMP[135].

The trend of interferon (IFN) α2 and γ are demonstrated in Figure 3.13. IFN-γ is secreted by T-helper 1 (Th1) cells, cytotoxic T lymphocytes and NK cells. It is known to have a role in the innate, adaptive and antitumour immune responses[140]. IFN-α is most well known for its role in the innate immune response against intracellular infections, mainly viruses, and is secreted by numerous cell types[141]. The concentration of both of these cytokines increased significantly throughout NMP (Figure 3.13). The cell type that secretes TNF-α is activated macrophages, however Th1, neutrophils, NK cells, Tregs are also capable of secreting this

cytokine. TNF-β (also known as Lymphotoxin-α, LTα) has a role in modulating DC and $CD4^+$ T-cell activity[142].

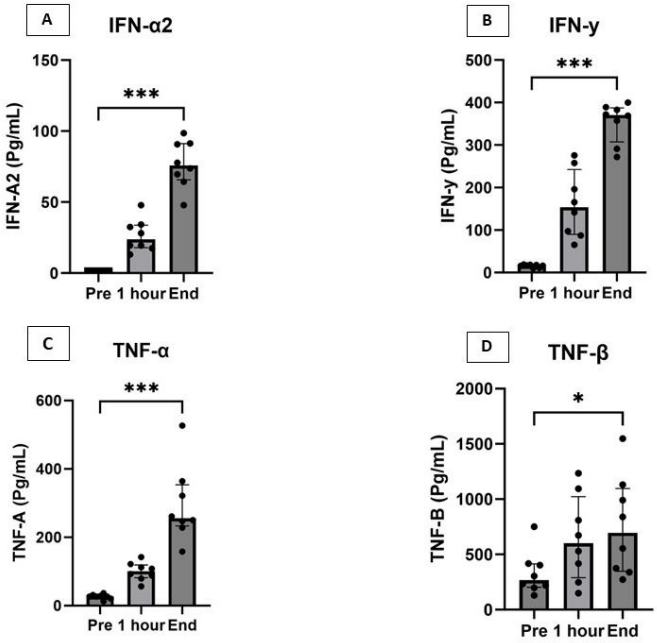


**Figure 3.13. Interferon (IFN) and Tumour necrosis factor (TNF) levels during NMP.** All increase significantly throughout perfusion. Statistical comparison with Mann-Whitney U test. *P=<0.05, ***P=<0.001.

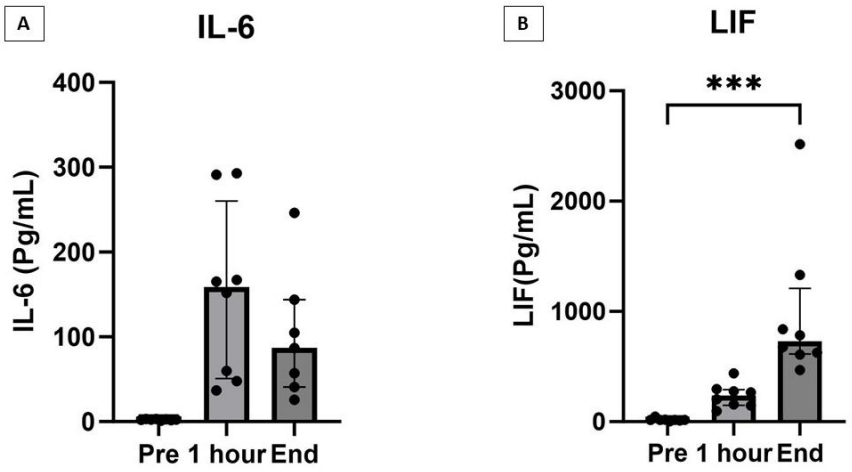


**Figure 3.14. Interleukin-6 and Leukaemia inhibitory factor (LIF) levels during NMP.** IL-6 levels increased initially, then fell throughout the perfusion. LIF (Leukemia Inhibitory Factor) increased throughout.Statistical comparison with Mann-Whitney U test. *****P=<0.001**

Interleukin-6 (IL-6) is a pleiotropic cytokine that can be produced by almost all immune and non-immune cells in the body, with TNF-α and IL-1β being a major stimulus for its synthesis and release[143]. IL-6 levels during NMP have previously been investigated in one of the only other studies to date that has correlated NMP cytokine levels with clinical outcomes[144]. These authors demonstrated that higher IL-6 levels during NMP correlated with worsening post-reperfusion syndrome, which suggests it may reflect the severity of the preservation-reperfusion injury. Similar to Mathis et al, the levels of IL-6 initially increased, then decreased (Figure 3.14). IL-6 may be released rapidly by cells within the graft during the early phase of NMP in response to the warm perfusion with oxygenated blood. Leukaemia inhibitory factor (LIF) is a cytokine that belongs to the IL-6 family and is also pleiotropic cytokine[145]. This cytokine also contributes to autoimmunity and inflammation[146]. In contrast to IL-6, the levels of LIF show a progressive increase throughout NMP.

The results of the colony stimulating factor family are demonstrated in Figure 32. Granulocyte/macrophage (GM-CSF), granulocyte (G-CSF) and macrophage (M-CSF) colony stimulating factor derived their names from the early observations that in-vitro they caused differentiation of immature bone marrow precursors into their respective lineages. It was subsequently identified that they were also pro-inflammatory[147]. Both GM-CSF and M-CSF have been shown to activate mature macrophage populations with the former promoting antigen presenting capabilities and the former promoting phagocytic functions. The concentrations of all the CSF cytokines increased throughout perfusion (Figure 3.15). Hepatocyte growth facor (HGF) is a mitogenic cytokine secreted by stellate and endothelial cells within the liver and promotes DNA synthesis and hepatocyte proliferation[148]. In contrast to the other cytokines measured, VEGF did not increase significantly throughout the duration of perfusion (Figure 3.15E). TNF related apoptosis inducing ligand (TRAIL) increased most

rapidly during the first hour of NMP, then remained a steady level throughout the duration of NMP (Figure 3.15F).

Figure 3.16 demonstrates the trend of the chemotactic chemokines (CC) during NMP. All increased significantly from beginning to end with the exception of RANTES/CCL5 and Eotaxin/CCL11. Elevation of MCP-1/CCL2, MIP-1A/CCL3, MIP-1B/CCL4 were also demonstrated by Hautz et al during NMP[136]. The trend of IL-3, IL-4, IL-5, IL-7, IL-8, IL-9, IL-10 and IL-12 are demonstrated in figure 3.17. IL-10 is secreted by a wide variety of both innate and adaptive immune cells and is generally considered to be anti-inflammatory. It has previously been shown to act on DCs and macrophages to inhibit the Th1 type responses. In contrast to the other interleukins, IL10 showed an initial increase over the first hour of NMP but then the concentration fell in the majority of perfusion (Figure 3.17, G).

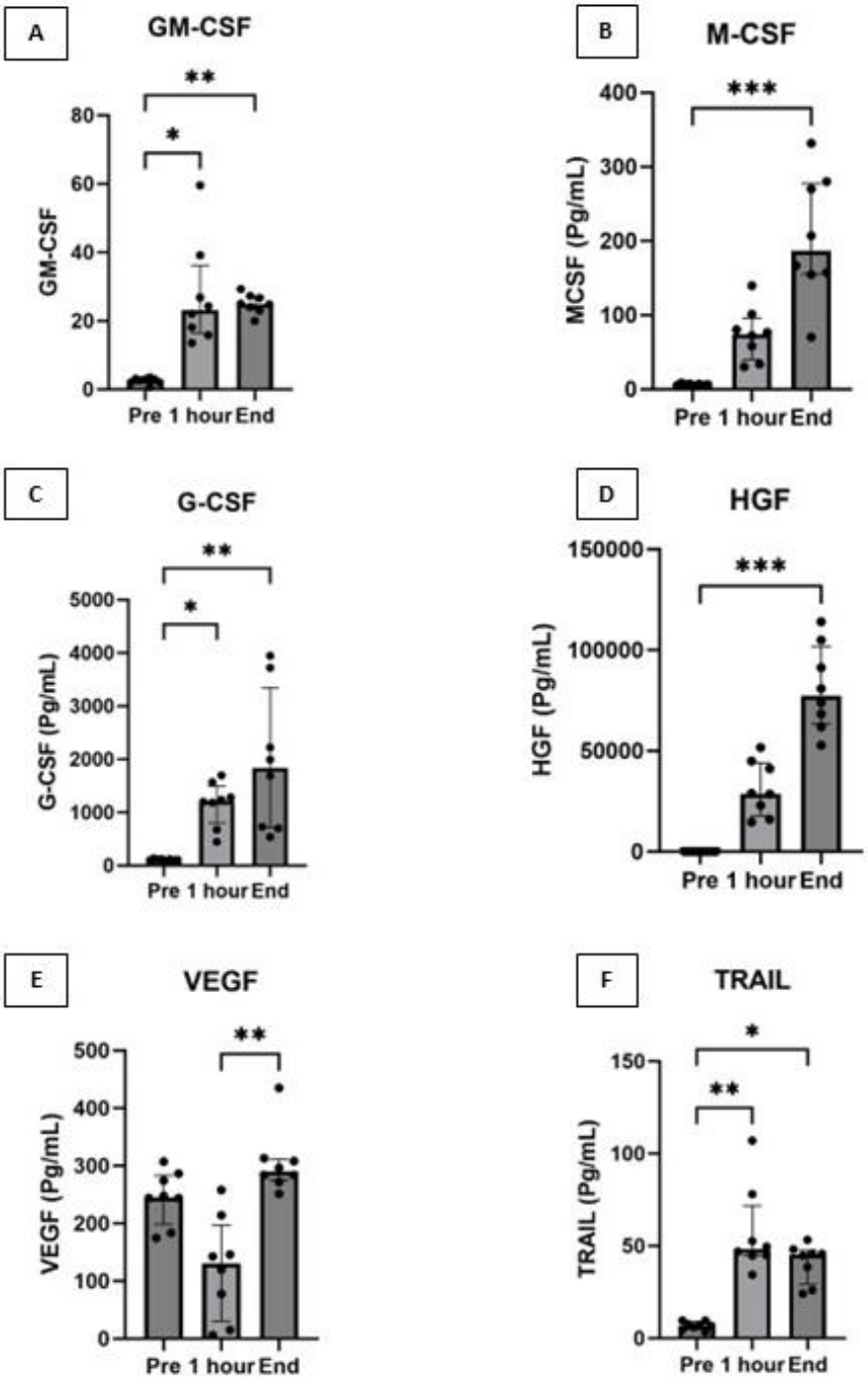


**Figure 3.15. Colony stimulating factor family, HGF, VEGF and TRAIL levels during NMP. All increase significantly from pre graft connection until the end, with the exception of VEGF.** Statistical comparison with Mann-Whitney U test.***P=<0.05, **P=<0.01, ***P=<0.001**

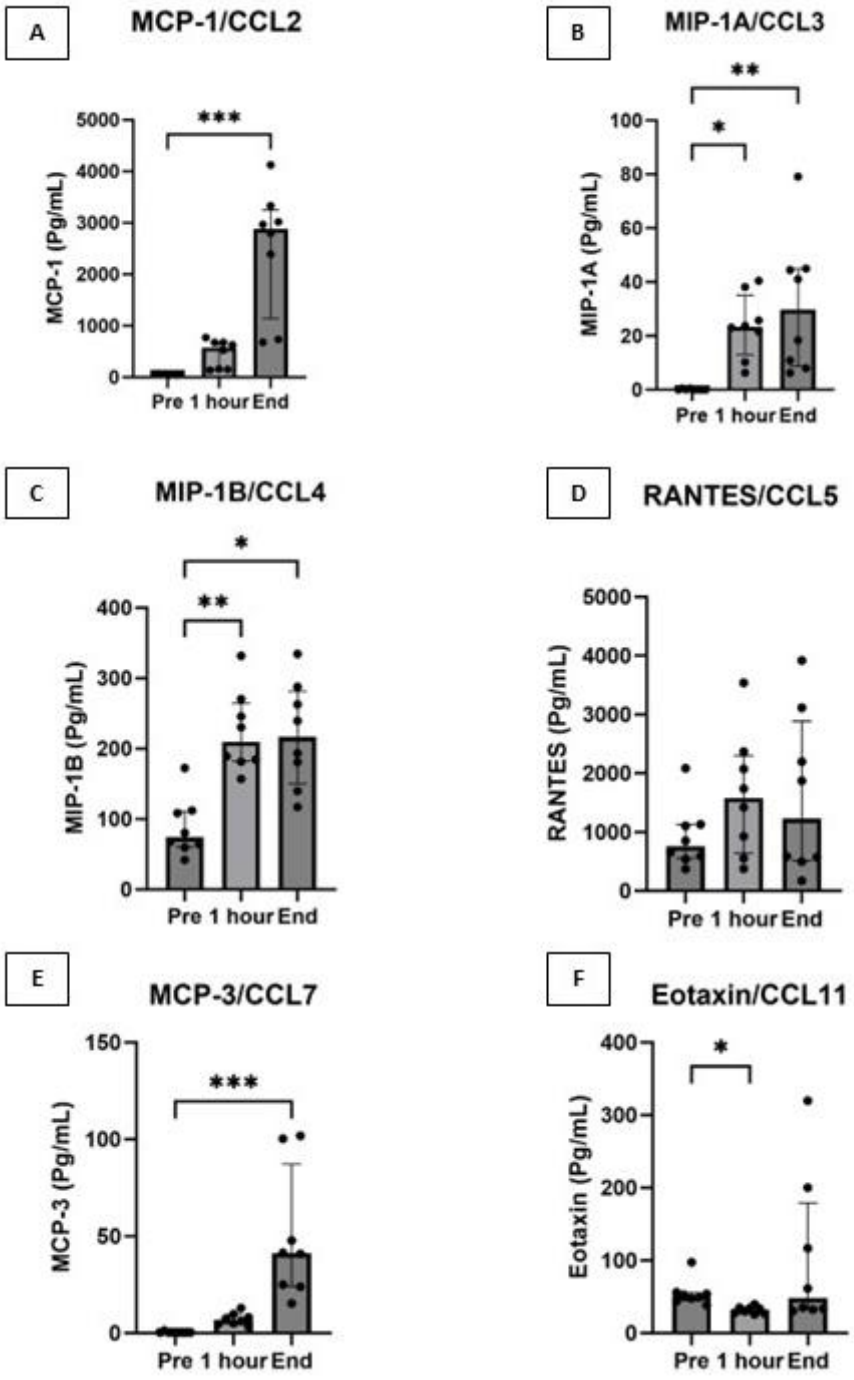


**Figure 3.16. Levels of CCL2-5, CCL7 and CCL11 during NMP.** All increase significantly with the exception of RANTES/CCL5. Statistical comparison with Mann-Whitney U test**. *P=<0.05, **P=<0.01, ***P=<0.001**

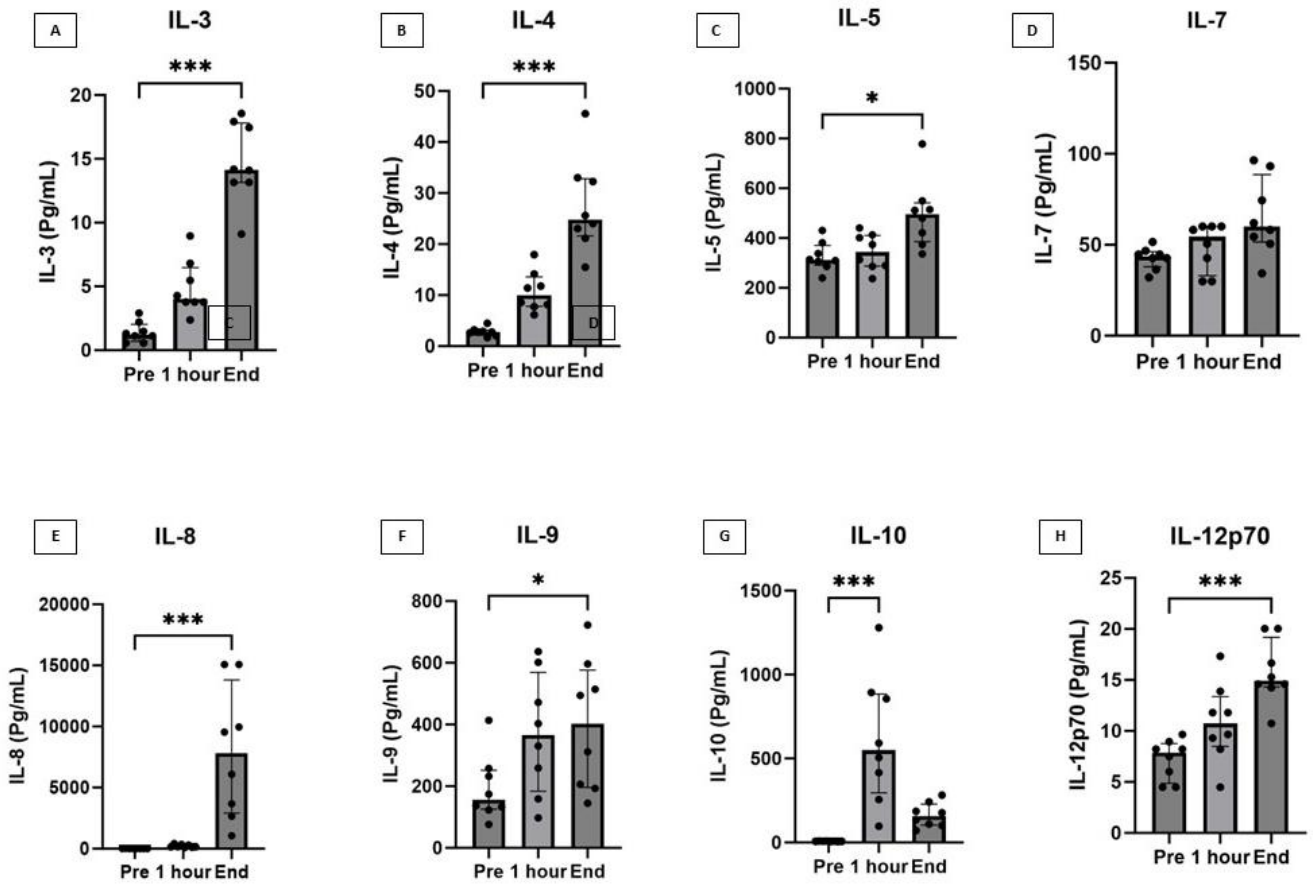


**Figure 3.17. Levels of interleukins during NMP. All continue to increase throughout perfusion with the exception of IL-7.** Statistical comparison with Mann-Whitney U test. ***P=<0.05, **P=<0.01, ***P=<0.001**

### 3.2.5 Perfusate cytokine assessment – Rejection vs No rejection

In order to identify the cytokine profile associated with early acute rejection, the 8 subjects included in the analysis were separated into those that experienced early rejection (n=3) and those that did not (n=5). Due to a large variation in time spent on the machine, the end values were re-corrected for time [(*End value-1hr value)/time (hours))* and graphs re-plotted. The overall rate of cytokine increase (delta [Δ]) was determined by the following formula (*End value-1hr value)/time (hours*). The 1 hour value was used as a the start point for determining the cytokine rate of increase due to the high likelihood that preformed cytokines would be washed out of the graft at the time of commencing NMP. The cytokines have been grouped according to $CD4^+$ helper T-cell subsets and macrophage polarizing effects:

- Th1 cytokines
- Th2 cytokines
- Th17 cytokines
- Macrophage type 1 (M1) polarizing cytokines
- Macrophage type 2 (M2) polarizing cytokines

**Th1 cytokines:** The cytokines IL-1β, IL-2, TNF-α and IFN-γ are considered to be Th1 cytokines and elicit an inflammatory response[140,149,150]. The rate of change for each cytokine, according to group, is displayed in figure 3.18. The only statistically significant difference was for IFN-γ, which showed a higher rate of increase in the group that experienced rejection.

**Th2 cytokines:** In contrast, the Th2 response is thought to be more anti-inflammatory (via IL-10) and promotes atopy/eosinophilic reactions (Via IL-4, IL-5 and IL-13). The group that experienced rejection had a higher rate of IL-4, IL-5 and Il-13 production than the group that did not experience rejection (Figure 3.19). In addition, IL-10 declined at a higher rate in those that experienced rejection.

**Th17 cytokines:** The predominant cytokine secreted by Th17 cells is IL-17. As described earlier this is proinflammatory cytokine and has been associated with autoimmunity. There was no significant difference in the rate of production of IL-17 between the groups with and without rejection (Figure 3.20).

**M1 type polarizing cytokines: A** M1 type macrophage response is activated via the 'classical' pathway that involves proinflammatory cytokines (IFN-γ, TNF-α), GM-CSF or microbial products such as lipopolysaccharide (LPS)[151]. A Th1 response results in secretion of cytokines that promote a M1 type response. The rate of IFN-γ and TNF-α was shown previously in figure 3.18 along with the other Th1 type cytokines, with IFN-γ production being significantly higher in the group that experienced rejection. The levels of GM-CSF is shown in figure 3.15.

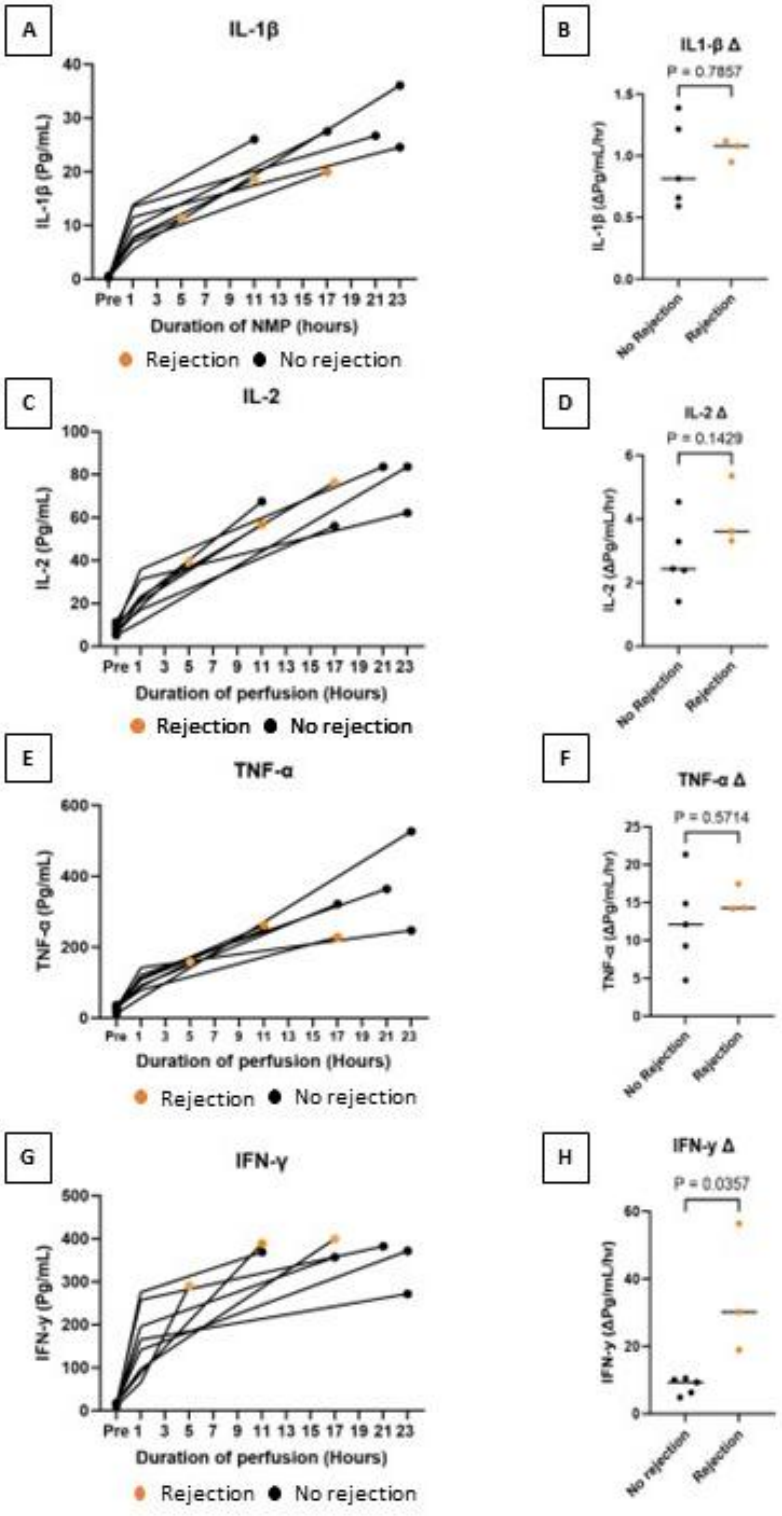


**Figure 3.18. T-Helper type 1 (Th1) cytokines during NMP.** A,C,E, G demonstrate the trend of cytokines with those grafts experiencing early rejection as orange and those that did not as black. B,D,F,G show the rate of increase adjusted for duration of perfusion from 1 hour until the end of the perfusion. IFN-γ increased significantly in those that experienced rejection, in comparison to those that did not.

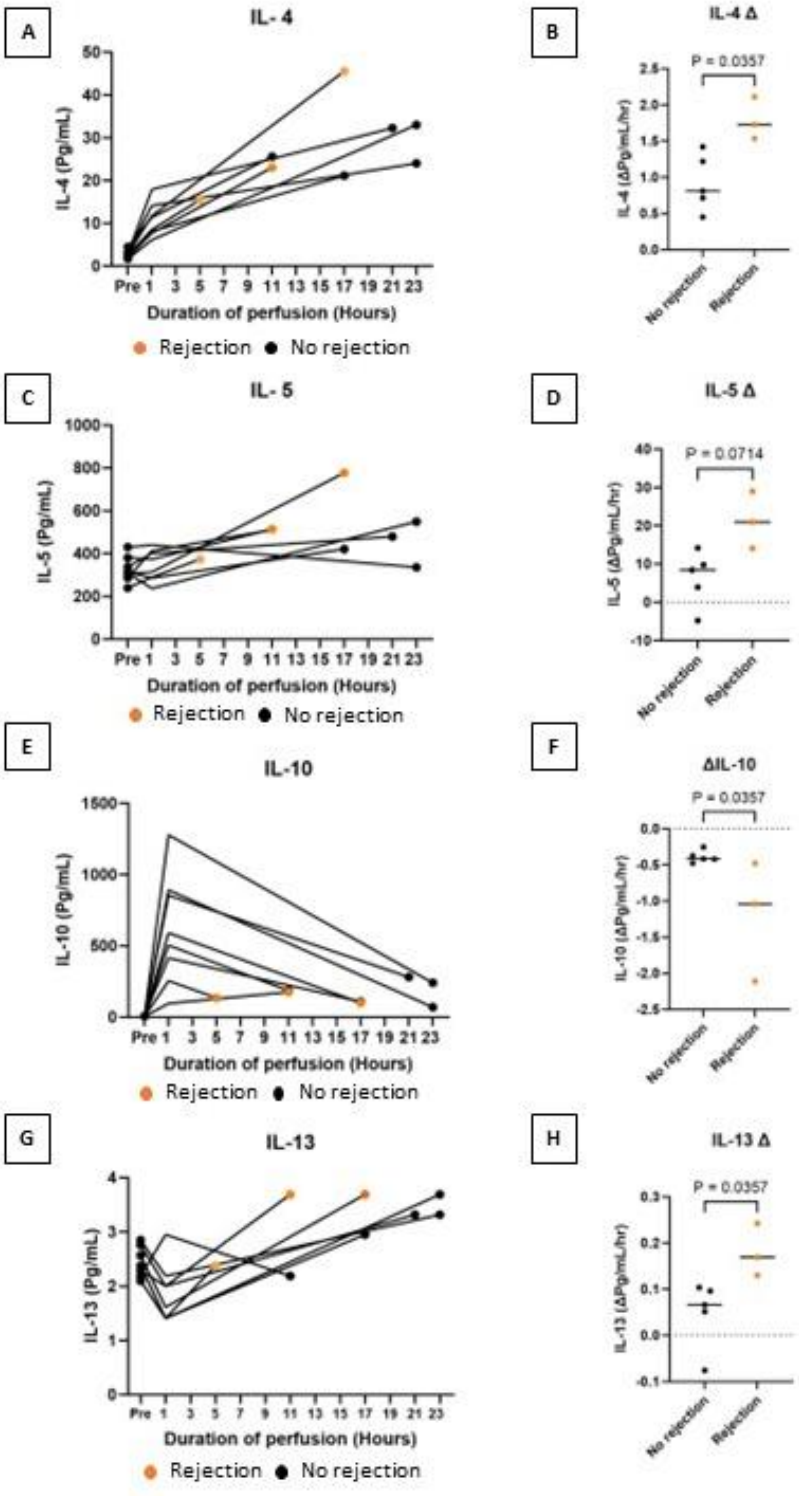


**Figure 3.19**. **T-Helper type 2 (Th2) cytokines during NMP**. A,C,E,G demonstrate the trend of cytokines with those grafts experiencing early rejection as orange and those that did not as black. B,D,F,G show the rate of increase adjusted for duration of perfusion for 1 hour until the end of perfusion. IL-4 and IL-13 increased significantly, whilst IL-10 decreased significantly.

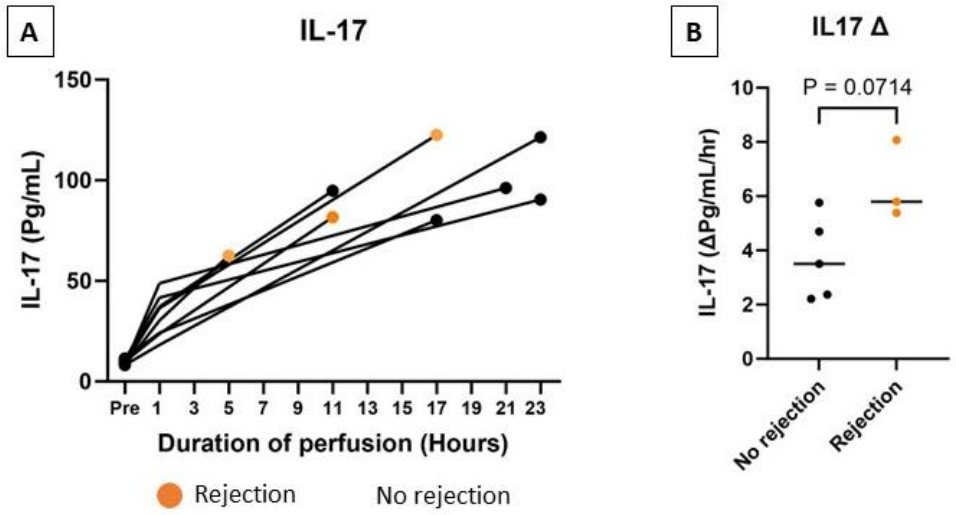


**Figure 3.20**. **T-Helper type 17 (Th17) cytokine production during NMP. A)** Demonstrates the trend of cytokines with those grafts experiencing early rejection as orange and those that did not as black. B) Shows the rate of increase adjusted for duration of perfusion for 1 hour until the end of perfusion. IL-17 did not increase significantly.

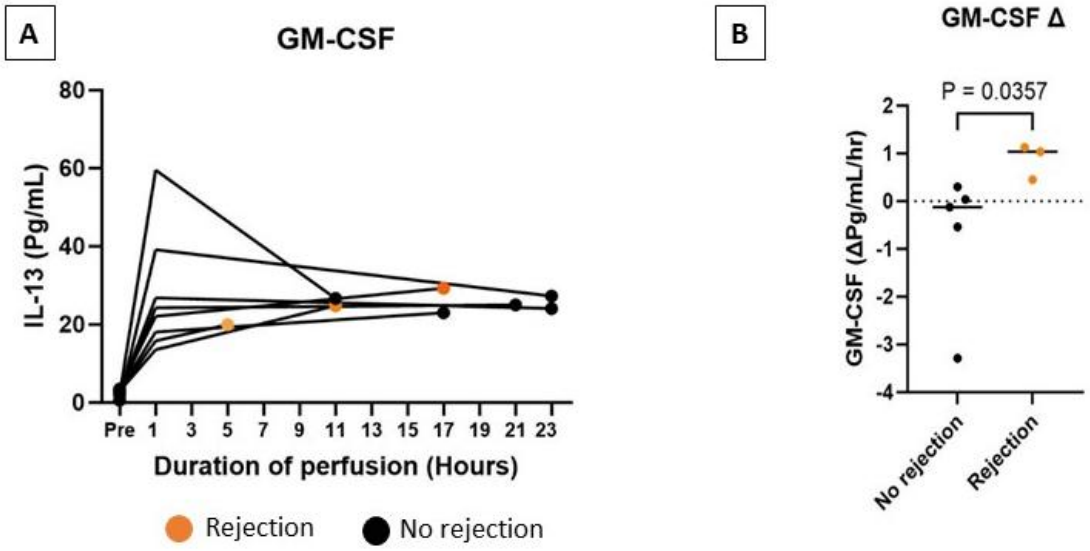


**Figure 3.21**. **GM-CSF cytokine levels. A)** Demonstrates the trend with those grafts experiencing early rejection as orange and those that did not as black. B) Shows the rate of increase adjusted for duration of perfusion for 1 hour until the end of perfusion. GM-CSF production increased at a significantly higher rate.

**M2 type polarizing cytokines:** A M2 type macrophage response is initiated via an alternate pathway that involves IL-4, IL-13, TGF-β, M-CSF and LIF. The cytokine results of IL-4 and IL-5 are demonstrated along with other Th2 cytokines in figure 3.19. The levels of LIF and M-CSF in each group are demonstrated in figure 3.22.

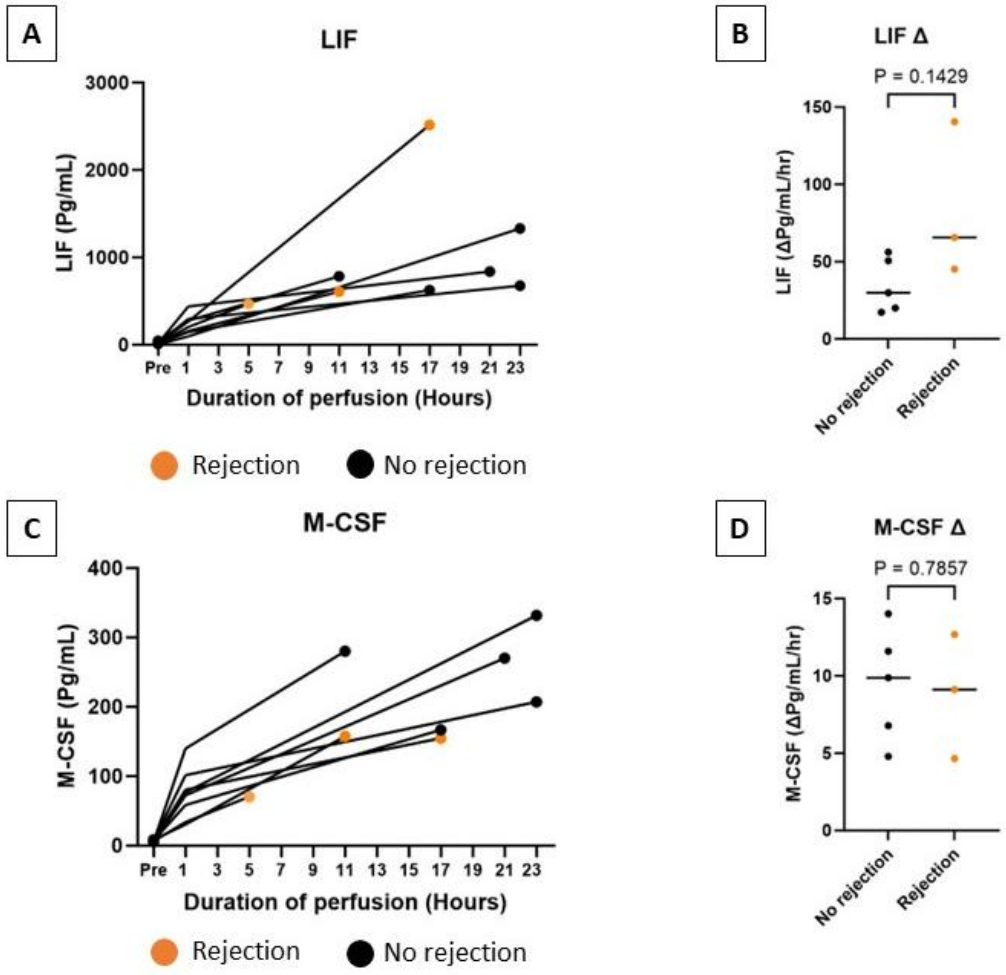


**Figure 3.22**. **M-CSF and LIF cytokine levels**. Demonstrates the trend with those grafts experiencing early rejection as orange and those that did not as black. B) Shows the rate of increase adjusted for duration of perfusion for 1 hour until the end of perfusion. The rate of production of LIF and M-CSF was similar between those that experienced rejection and those that did not.

### 3.2.6 Metabolomic analysis of perfusate

NMP aims to preserve the human liver ex-situ, under physiological conditions that closely mimic that when it is inside a living human body. Given the incredibly complex state of the human body and the cellular processes that take place, it is unlikely that this will ever be achieved entirely.. Metabolomics involves the measurement of the small metabolic products of cellular metabolism[152]. This can provide information about individual cellular processes, many of which have complex interactions with others. Although lactate clearance is commonly measured during NMP and used a surrogate for hepatocyte function, this is the end result of numerous metabolic pathways and substrates which all interact. Measuring the 'metabolome' or a sample can provide further delineation of its physiological status[153]. The small molecular signals of <1000 Daltons (Da) are very sensitive indicators of cellular function[154]. Despite significant research interest around the globe in biomarkers that predict organ function during NMP, there is little published data on the metabolomic profile. Furthermore, much of what is reported comes from human livers in the laboratory that were not transplanted into a human[155-158], therefore the relationship with post-transplant graft function is purely speculative.

Previous researchers have focused on measuring metabolites from both the liver tissue and machine perfusion fluid that indicate grafts that will function well. Zhang et al demonstrated that livers undergoing NMP display a greater amount of tryptophan metabolism via the kynurenine pathway than liver perfused at sub-normothermic temperatures[156]. Interestingly, changes in this pathway were also detected by Hrydziuszko et al when they compared metabolites of DBD and DCD grafts[154]. In a study that assessed metabolites in the circulation of paediatric transplant recipients experiencing acute rejection, tryptophan metabolites were also shown to be significantly different, and suggested that tryptophan metabolism also linked with T cell metabolism[159].

During this study, samples of perfusate were collected at several time points as specified in methods section 2.17. This perfusate fluid was then subjected to high throughput mass spectrometry, and metabolites measured. The 10 patients that underwent machine perfusion were then grouped based on the following outcomes, and differences between groups assessed.

1. Early biopsy proven acute rejection
2. Early allograft dysfunction as per Olthoff criteria[134]
3. Early allograft dysfunction as by the model of early allograft function (MEAF) score ≥5[160]

In the 10 livers transplanted during this project, 4 experienced early BPAR, 3 and 4 met Olthoff criteria and MEAF ≥5 for early allograft dysfunction respective

**Early biopsy proven rejection**

The perfusate was subject to mass spectrometry and the metabolite molecules within the fluid assessed. The levels of these metabolites were compared between those that experienced early rejection and those that did not. The metabolites that had a significant difference on univariate analysis (P value of <0.05) are displayed in table 3.7. However, no metabolite was significantly different between groups when the P value was corrected for the false discovery rate (FDR).

**Table 3.7. Metabolites and early biopsy proven rejection**

| Compound | Ion | Metabolite Database ID | P-Value | FDR corrected P-Value |
|---|---|---|---|---|
| 2-Aminobenzoic acid | [M+Na]+1 | HMDB0001123 | 0.064044556 | 0.991406148 |
| 4-Acetamidobutanoic acid | [M+H]+1 | HMDB0003681 | 0.006989244 | 0.466386269 |
| 4-Acetamidobutanoic acid | [M+Na]+1 | HMDB0003681 | 0.007307952 | 0.466386269 |
| 4-Pyridoxic_acid | [M+H]+1 | HMDB0000017 | 0.018695182 | 0.701717741 |
| Biotin | [M+Na]+1 | HMDB0000030 | 0.087498516 | 0.991406148 |
| Cer(d18:1_24:1) | [M+formate]- | | 0.056313683 | 0.980979203 |
| D-Glucose (or hexose sugar) | [M+NH4]+1 | HMDB0000122 | 0.02807543 | 0.82551614 |
| Leucine / Isoleucine | [M-H]-1 | HMDB0003640 | 0.0391831 | 0.703177798 |
| Leucine / Isoleucine | [M+H]+1 | HMDB0000172 | 0.053717929 | 0.965497179 |
| L-Tryptophan | [M-H]-1 | HMDB0000929 | 0.056305668 | 0.802189769 |
| L-Valine | [M-H]-1 | HMDB0000883 | 0.029221865 | 0.69753951 |
| LysoPC(18:0) | [M+Cl]-1 | HMDB0010384 | 0.028055616 | 0.69753951 |
| LysoPE(16:0/0:0) | [M-H]-1 | HMDB0011503 | 0.06375133 | 0.980979203 |
| Methylguanidine | [M+H]+1 | HMDB0001522 | 0.080630996 | 0.991406148 |
| N-Acetyl-L-aspartic acid | [M-H]-1 | HMDB0000812 | 0.05852008 | 0.802189769 |
| Palmitoyl sphingomyelin [aka SM(d18:1/16:0)] | [M+H]+1 | | 0.0209343 | 0.701717741 |
| PC(16:0/20:4) | [M+Cl]-1 | HMDB0008048 | 0.05571822 | 0.802189769 |
| PC(16:0/22:6) | [M+Na]+1 | HMDB0008057 | 0.069072842 | 0.9997815 |
| PC(18:1_18:2) | [M+formate]- | | 0.098062902 | 0.980979203 |
| TG(17:0_18:1_18:1) | [M+NH4]+0 | | 0.043549492 | 0.9997815 |
| TG(18:0_18:1_20:4) | [M+NH4]+1 | HMDB05406 | 0.03875062 | 0.9997815 |
| trans-3-Indoleacrylic acid | [M+H]+1 | HMDB0000734 | 0.090495131 | 0.991406148 |
| Trigonelline | [M+Na]+1 | HMDB0000875 | 0.064044556 | 0.991406148 |
| Xanthine | [M-H]-1 | HMDB0000292 | 0.036943799 | 0.703177798 |

Differences in metabolites between the NMP recipients that experienced rejection and those that did not experience rejection. A repeated measures ANOVA test was used to assess for statistical significance. Due to the comparison of a large number of metabolites the P value was corrected for false discovery rate (FDR).

**Early allograft dysfunction (Olthoff)**

The metabolites that differed between the grafts that demonstrated early allograft dysfunction (as per Olthoff criteria), and those that did not are listed, based on univariate comparison (P=<0.05) are listed in Table 3.8. No metabolite was significantly different when the P-value was corrected for FDR.

**Table 3.8. Metabolites and Early allograft dysfunction (Olthoff)**

| Compound | Ion | Metabolite Database ID | P value | FDR corrected P-value |
|---|---|---|---|---|
| 3-Methylxanthine | [M-H]-1 | HMDB0001886 | 0.00236445 | 0.607663723 |
| 7-Methylguanosine | [M+H]+1 | | 0.039399156 | 0.999783379 |
| Acetylspermidine (N8 = CD, N1 = Mtox) | [M+H]+1 | HMDB0002189 | 0.038101417 | 0.999783379 |
| Acetyl-β-methylcholine | [M+H]+1 | HMDB0015654 | 0.030079324 | 0.999783379 |
| Creatine | [M+H]+1 | HMDB0000064 | 0.012591581 | 0.999783379 |
| dimethylarginine (symmetric / asymmetric) | [M+H]+1 | HMDB0003334 | 0.016486362 | 0.999783379 |
| Inositol (several isomers possible) | [M-H]-1 | HMDB0006088 | 0.035837806 | 0.988782905 |
| LPE(18:2) | [M-H]-1 | HMDB0011507 | 0.064159139 | 0.998997588 |
| LysoPC(18:0) | [M+Na]+1 | HMDB0010384 | 0.096535689 | 0.999271728 |
| N-(6-[3-(trifluoromethyl)phenoxy]-3-pyridinyl)-2,3-dihydro-1-benzofuran-5-carboxamide | [M-H]-1 | | 0.057885695 | 0.988782905 |
| PC(14:0_18:2) | [M+formate]- | HMDB0008130 | 0.025558144 | 0.998997588 |
| PC(16:0/20:4(5Z_8Z_11Z_14Z)) | [M+H]+1 | HMDB0008048 | 0.059084327 | 0.999271728 |
| PC(16:0/22:6(4Z_7Z_10Z_13Z_16Z_19Z)) | [M+H]+1 | HMDB0007991 | 0.086997511 | 0.999271728 |
| PC(16:1e_20:4) | [M+formate]- | | 0.058553764 | 0.998997588 |
| PE(18:1_18:2) | [M-H]-1 | HMDB0009092 | 0.06997041 | 0.998997588 |
| Pseudouridine | [M+Na]+1 | HMDB0000767 | 0.095835054 | 0.999783379 |
| Ribothymidine | [M-H]-1 | HMDB0000884 | 0.007209703 | 0.988782905 |
| TG(15:0_16:0_18:1) | [M+NH4]+0 | | 0.014274144 | 0.999271728 |
| TG(15:0_16:0_18:1) | [M+Na]+1 | | 0.014755987 | 0.999271728 |
| Uric_acid | [M-H]-1 | HMDB0000289 | 0.061348087 | 0.988782905 |

Differences in metabolites between the NMP recipients that experienced early graft dysfunction (Olthoff criteria) and those that did not experience early graft dysfunction. A repeated measures ANOVA test was used to assess for statistical significance. Due to the comparison of a large number of metabolites the P value was corrected for false discovery rate (FDR).

**Early allograft function (MEAF score ≥5)**

The levels of metabolites were compared between those grafts that had a MEAF score ≤5 and >5. After correction for FDR, the only metabolite that differed significantly was the level of the Lysophosphatidylcholine (LysoPC) (18:0) species (Table 3.9). The level of LysoPC (18:0) fell at a greater rate in those with MEAF ≥5 (early graft dysfunction). As demonstrated in Figure 41, the starting level of LysoPC (18:0) was higher in those that had MEAF ≥5. This molecule is a lysophospholipid with a phosphorylcholine occupies a glycerol position. LysoPC (18:0), has a stearic acid chain at the C-1 position. The Lysophosphatidylcholine molecule family make up approximately 1% of low density lipoproteins in the circulation[161]. Lower levels of LysoPC have been demonstrated as a result of liver disease[161]. Conversely, the serum level has been demonstrated to increase in diabetes, cardiovascular disease and cancer[162]. The effect LysoPCs have in the liver is to upregulate genes that cause cholesterol synthesis but downregulate those involved in hepatic fatty acid oxidation[162]. The effect LysoPCs have on the lymphocytes is generally that of activation of B cells, macrophages, polarisation of macrophages towards the M1 phenotype, secretion of IFN-γ and TNF-α.

Figure 3.23 is a scatter plot of a pathway analysis of all metabolites that had a FDR corrected P value of <0.20 (Methionine, Phenyalanine, LysoPC, Aconitic acid, Hydroxyphenyllactic acid). The trend of these metabolites is demonstrated in figure 3.24. In the situation of both Lyso PC (18:0) and Aconitic acid, the starting level of these metabolites was different before connecting the liver to the circuit (blue boxes, Figure 3.24). All pathways identified using this analysis method were non-significant and had had a low impact (0.05-0.5). Although insignificant, the ether lipid pathway and tyrosine - tryptophan biosynthesis pathways are demonstrated in figure 3.25. It is likely that there is several confounding factors that lead to variations in the metabolite levels. These may include the

duration of human blood storage (used as perfusate) before usage, the duration of cold preservation, degree of organ steatosis.

**Table 3.9. Early allograft dysfunction (MEAF)**

| Compound | Ion | Metabolite database ID | P value | FDR corrected P value |
|---|---|---|---|---|
| 4-Acetamidobutanoic acid | [M+Na]+1 | HMDB0003681 | 0.015481651 | 0.335606235 |
| 4-Acetamidobutanoic acid | [M+H]+1 | HMDB0003681 | 0.037709395 | 0.380096594 |
| 6-Methylnicotinamide | [M+H]+1 | HMDB0013704 | 0.08378893 | 0.455861373 |
| AcCa(14:1) | | | 0.097783575 | 0.662861054 |
| AcCa(16:1) | | | 0.09816918 | 0.662861054 |
| Acetyl-β-methylcholine | [M+H]+1 | HMDB0015654 | 0.071702114 | 0.439479651 |
| Aconitic acid (trans or cis) | [M-H]-1 | HMDB0000958 | 0.007146942 | 0.200795662 |
| alpha-Ketoisovaleric acid | [M-H]-1 | HMDB0000019 | 0.051085142 | 0.341845574 |
| Betaine | [M+Na]+1 | | 0.009034242 | 0.335606235 |
| Betaine | [M-e]+1 | | 0.014032296 | 0.335606235 |
| Betaine | [M+Na]+1 | | 0.038861647 | 0.380096594 |
| Betaine | [M+K]+1 | | 0.055033872 | 0.417657795 |
| Biliverdin | [M+H]+1 | HMDB0001008 | 0.019437807 | 0.542389372 |
| Biotin | [M+Na]+1 | HMDB0000030 | 0.085428591 | 0.457549743 |
| DL-Lysine | [M+H-NH3]+1 | HMDB0142894 | 0.010636336 | 0.335606235 |
| gamma-Aminobutyric acid / Dimethylglycine / 3-Aminoisobutanoic acid | [M+H]+1 | HMDB0000112 | 0.023299691 | 0.344051505 |
| Glycerol 3-phosphate | [M+H]+1 | HMDB0000126 | 0.033876903 | 0.380096594 |
| Glycerophosphocholine | [M+H]+1 | HMDB0000086 | 0.021169593 | 0.335606235 |
| Glycine | [M+H]+1 | HMDB0000123 | 0.077271333 | 0.451970402 |
| Glycoursodeoxycholic acid | [M-H]-1 | HMDB0000708 | 0.020378116 | 0.296132761 |
| Glycoursodeoxycholic_acid (or similar) | [M-H]-1 | HMDB0000708 | 0.015246136 | 0.433561495 |
| Guanidinosuccinic acid | [M+H]+1 | HMDB0003157 | 0.056821704 | 0.421494329 |
| Homocysteine | [M-H]-1 | HMDB0000742 | 0.064478369 | 0.376754074 |
| Hydroxyglutaric acid | [M-H]-1 | HMDB0000606 | 0.081035625 | 0.399055113 |
| Hydroxyphenyllactic_acid | [M-H]-1 | HMDB0000755 | 0.003854935 | 0.183660138 |
| Hypoxanthine | [M+K]+1 | HMDB0000157 | 0.031756705 | 0.380096594 |
| Hypoxanthine | [M-H]-1 | HMDB0000157 | 0.065265644 | 0.376754074 |
| Hypoxanthine | [M+H]+1 | HMDB0000157 | 0.083567135 | 0.455861373 |
| L-Asparagine | [M-H]-1 | HMDB0000168 | 0.038738232 | 0.323552082 |
| L-Ergothioneine | [M+K]+1 | | 0.022469078 | 0.335606235 |
| L-Histidine | [M+H]+1 | HMDB0000177 | 0.001305039 | 0.237176329 |
| L-Lysine | [M-H]-1 | HMDB0000182 | 0.008242341 | 0.200795662 |
| L-Methionine | [M-H]-1 | HMDB0000696 | 0.007400811 | 0.200795662 |
| L-Methionine | [M+H]+1 | HMDB0000696 | 0.01491262 | 0.335606235 |

| | | | | |
|---|---|---|---|---|
| L-Palmitoylcarnitine | [M+H]+1 | HMDB0000222 | 0.003818253 | 0.46519043 |
| L-Phenylalanine | [M-H]-1 | HMDB0000159 | 0.011652963 | 0.22860372 |
| L-Phenylalanine | [M+H]+1 | HMDB0000159 | 0.05996743 | 0.426717136 |
| LPI(20:4) | | | 0.057358028 | 0.618648754 |
| LysoPC(16:0) | [M+Cl]-1 | HMDB0010382 | 0.00593562 | 0.200795662 |
| LysoPC(16:0) | [M+H]+1 | HMDB0010382 | 0.042107654 | 0.386488939 |
| LysoPC(16:0) | [M-H+HAc]-1 | HMDB0010382 | 0.069981833 | 0.387885807 |
| LysoPC (18:0) | [M+Cl]-1 | HMDB0010384 | 8.18376E-06 | 0.005458565 |
| LysoPC(18:0) | [M-H+CHO2]-1 | HMDB0010384 | 0.000356883 | 0.23946873 |
| LysoPC(18:0) | [M+H]+1 | HMDB0010384 | 0.000596232 | 0.237176329 |
| LysoPC(18:1(9Z)) | [M+Cl]-1 | HMDB0002815 | 0.063683549 | 0.376432372 |
| Methylguanidine | [M+H]+1 | HMDB0001522 | 0.059540653 | 0.426717136 |
| N-Acetylneuraminic acid | [M+Na]+1 | HMDB0000230 | 0.09589019 | 0.47945095 |
| Nervonic acid | [M-H+HAc]-1 | HMDB0002368 | 0.015490713 | 0.26148295 |
| Ornithine | [M-H]-1 | HMDB0000214 | 0.03661822 | 0.323552082 |
| Ornithine | [M+H-H2O]+1 | | 0.048847845 | 0.402510955 |
| Ornithine | [M+H-NH3]+1 | | 0.048912724 | 0.402510955 |
| Ornithine | [M+H]+1 | | 0.055426101 | 0.417657795 |
| Palmitoylcarnitine [aka AcCa(16:0)] | [M+H]+1 | | 0.06782375 | 0.431186511 |
| Pantothenic acid | [M+Na]+1 | HMDB0000210 | 0.068498617 | 0.431186511 |
| Pantothenic_acid | [M+H]+1 | HMDB0000210 | 0.082299739 | 0.455861373 |
| PC(16:0/20:4(5Z_8Z_11Z_14Z)) | [M+Cl]-1 | HMDB0008048 | 0.041590926 | 0.328403548 |
| PC(17:0_18:2) | | | 0.019474658 | 0.433561495 |
| PE(16:0_20:4) | | HMDB0009385 | 0.085293412 | 0.634739365 |
| PE(16:0p_20:4) | | | 0.087265809 | 0.634739365 |
| PE(18:0_20:3) | | HMDB0009002 | 0.08082921 | 0.630656186 |
| PE(18:0p_20:4) | | | 0.043828779 | 0.5933118 |
| Phosphoenolpyruvic acid | [M-H]-1 | HMDB0000263 | 0.029937802 | 0.323552082 |
| PS(18:0_20:4) | | HMDB0012383 | 0.060350824 | 0.607054171 |
| Pseudouridine | [M-H]-1 | HMDB0000767 | 0.0637734 | 0.376432372 |
| SM(d18:1/16:0) | [M+Cl]-1 | HMDB0010169 | 0.081885515 | 0.399055113 |
| SM(d18:1/24:0) | [M+H]+1 | HMDB0012105 | 0.040878547 | 0.593289686 |
| SM(d18:1/24:0) | [M+Na]+1 | HMDB0012105 | 0.055383163 | 0.606887319 |
| Sphingosine 1-phosphate | [M+H]+1 | HMDB0000277 | 0.066260567 | 0.429395717 |
| Tetradecanoylcarnitine [aka AcCa(14:0)] | [M+H]+1 | HMDB0005066 | 0.053434393 | 0.606887319 |
| TG(15:0_16:1_18:1) | | | 0.08060566 | 0.634739365 |
| TG(15:0_18:1_18:2) | | | 0.055759335 | 0.606887319 |
| TG(15:0_18:2_20:4) | | | 0.093061635 | 0.656768581 |
| TG(16:0_18:1_22:6) | | | 0.029502487 | 0.591404811 |

| | | | | |
|---|---|---|---|---|
| TG(17:0_18:1_18:1) | | | 0.014567093 | 0.542389372 |
| TG(17:0_18:1_18:2) | | | 0.005972234 | 0.542389372 |
| TG(17:0_18:1_20:4) | | | 0.093780216 | 0.656768581 |
| TG(18:1_17:1_20:4) | | | 0.093318828 | 0.656768581 |
| TG(18:2_18:2_20:4) | | HMDB05475 | 0.066310958 | 0.62252017 |
| Thyroxine | [M+Na]+1 | HMDB0000248 | 0.01778732 | 0.542389372 |
| Valerylcarnitine | [M+H]+1 | HMDB0013128 | 0.069299825 | 0.434498902 |
| Xanthine | [M-H]-1 | HMDB0000292 | 0.087750411 | 0.409297373 |

Differences in metabolites between the NMP recipients that experienced early graft dysfunction based on MEAF score and those that did not. A repeated measures ANOVA test was used to assess for statistical significance. Due to the comparison of a large number of metabolites the P value was corrected for false discovery rate (FDR).

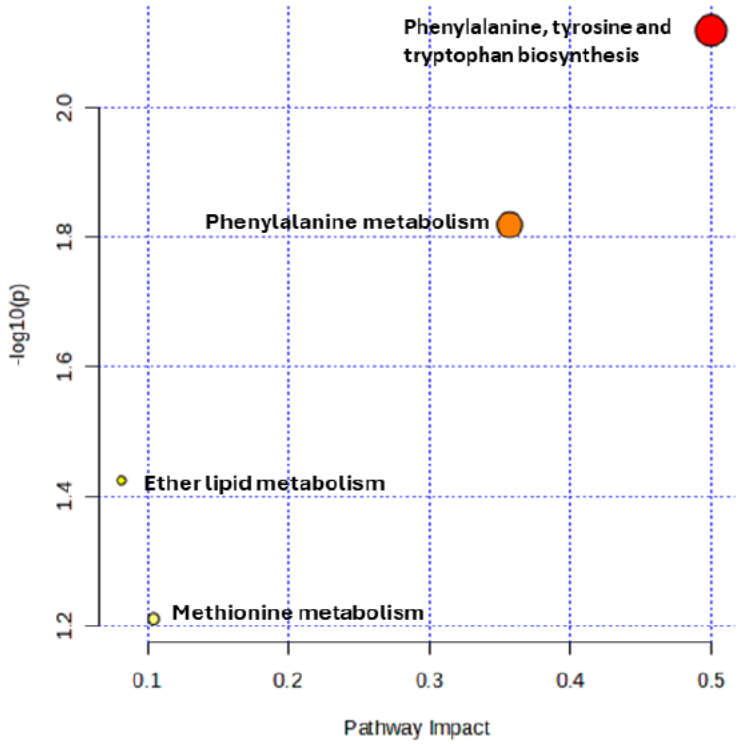


**Figure 3.23. Scatter plot of a pathway analysis.** The pathway impact of phenyalanine, tyrosine and tryptophan biosynthesis pathway had the highest impact on pathway analysis but was not statistically significant.

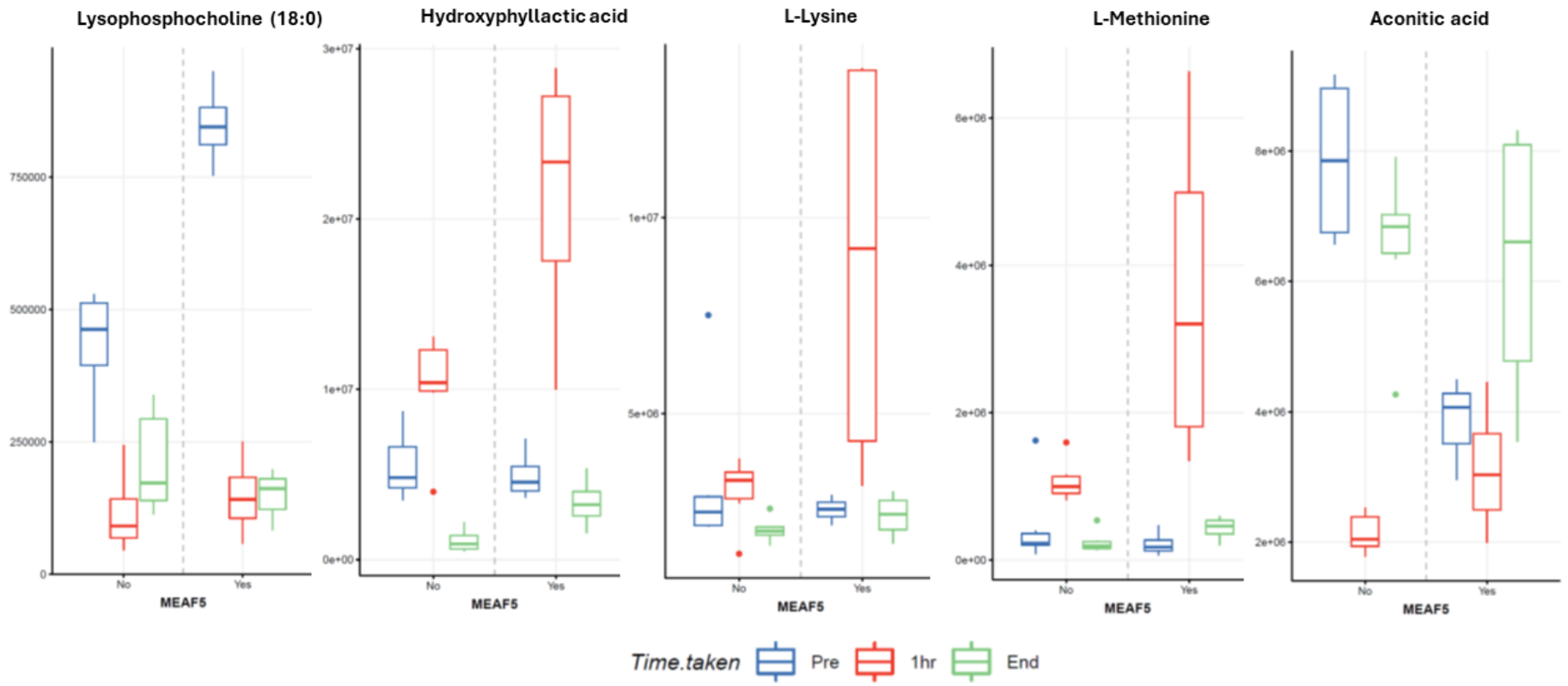


**Figure 3.24. Trend of five metabolites across three time points grouped on wether they demonstrated early graft dysfunction as per MEAF criteria**. Lysophosphocholine had a FDR corrected P value of <0.05, all others had a FDR corrected P value of ≈0.20.

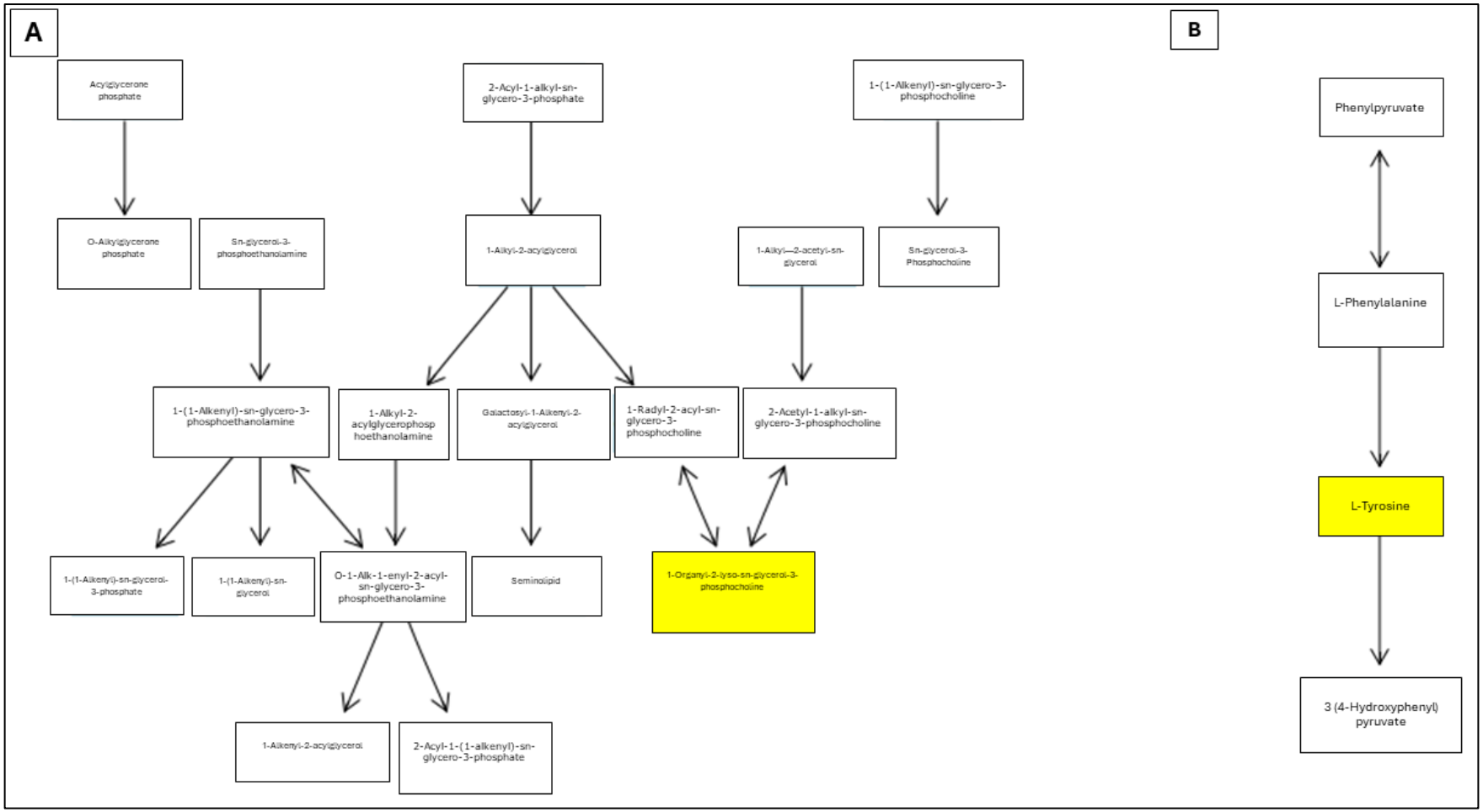


**Figure 3.25.** The complex metabolic pathways that involve phosphocholine metabolism and Ether lipid metabolism (A) and Tyrosine in phenyalanine, tyrosine and tryptophan metabolism (B). Source -Metaboanalyst.

### 3.3 Chapter summary

The results described in this chapter demonstrate that the immune cell compartment of the graft is active during NMP, as evidenced by the production of multiple cytokines. Furthermore, the clinical results also indicate that early BPAR is more common following NMP preservation. The retrospective data from the QEHB indicated the rate of BPAR following primary transplant was similar between preservation modalities, but in patients undergoing retransplant it was significantly higher following NMP. The time of onset and severity of rejection appeared to be similar. In the 20 patients recruited in the prospective study, 4/10 in the NMP group experienced early BPAR compared with 1/10 in the CS group.

The cytokine analysis showed that numerous cytokines are produced by cells within the graft during NMP. This suggests that the normothermic conditions restores immune cell activity. A comparison of the cytokine profiles for the grafts that demonstrated early BPAR suggested a bias towards Th1 (increased IFN-γ and reduced IL-10) and M1 polarising cytokines, however acknowledging that both IL-4 and IL-13 were also increased, and these are recognised as Th2 type. IL-4 and IL-13, along with other Th2 cytokines, are thought to have a role in allergic reactions[164] Given that cell mediated graft rejection is considered a type IV hypersensitivy reaction, the mechanistic role these cytokines may have in subsequent graft rejection cannot be excluded. High throughput mass spectrometry did not demonstrate any significant differences in metabolites for those that experienced early BPAR. A minor metabolite signal was identified for early allograft dysfunction only, however this is difficult to interpret given the actual change in Phosphocholine was a greater fall from baseline.

A limitation to the data presented in this chapter is the small sample size, and several variables that are difficult to accurately control for in the analysis. These include the perimortem circumstances of the donor, the graft size, and parenchymal quality (especially

steatosis). All of the 20 donors included had experienced neurological brain death, but from different causes and had differing levels of haemodynamic stability prior to donation. The process of brain death is known to be associated with numerous physiological changes, including cytokine release and organ injury. In addition, a liver graft varies considerably in size and it would be expected that livers with larger cellular mass would elaborate a greater amount of cytokines, into a circuit with a fixed volume. Therefore, this has the potential to greatly influence the concentration of cytokines, and metabolites measured.

The fact that it is the retransplant recipients that experience a higher rate of early BPAR suggests that there is both graft and recipient factors contributing. Individuals who have previously received liver transplants are known to have donor leukocytes incorporated into their immune cell repetoire[165], a concept known as chimerism. This likely results in a more complex immune response and cellular interactions on receiving exposure to a third set of antigens. Despite NMP providing oxygenated blood at physiological temperature ex-vivo, it should not be expected to exactly replicate the in-vivo normal immune physiology of the human liver and the interaction with the recipient is complex. It would be overly simplistic to assume early BPAR following NMP is only caused by elevated levels of inflammatory cytokines. Further research, which includes molecular analysis, may be beneficial as it is likely the gene expression that will demonstrate the earliest changes during the preservation period.

# Chapter 4 – Regulatory T-cell isolation and expansion

### 4.1 Treg isolation

Regulatory T-cells (Tregs) are present in within the circulating blood, lymphoid and non-lymphoid tissue. In the vascular circulation, Tregs ($CD25^+$, CD127low, $FoxP3^+$) comprise 5-10% of $CD4^+$ lymphocytes and this $CD4^+$ population is reported to comprise up to 65% of T-cells (CD3+) in healthy controls[57,166]. Therefore, Tregs are a very small proportion of circulating cells and ex-vitro expansion is required to achieve the quantities required for a therapeutic infusion. Although Tregs are present within lymphoid and non-lymphoid tissues, the density of this cell population is low and isolating a sufficient quantity to expand is not practical in the majority of circumstances. However, recent work published by Romano et al has shown successful isolation and Good Manafacturing Practice (GMP)- compatible expansion of Tregs from human thymus tissue obtained at the time of heart transplantation[167]. Blood obtained from patients peripheral circulation, represent the dominant source of cells for therapeutic Treg isolation and expansion.

Give the low absolute number of Tregs circulating within the vascular compartment, large volumes of whole blood are required to obtain a cell number that can be expanded to therapeutic quantities. Rather than collecting whole blood from an individual, leukopharesis can be performed in which only the patients leukocytes are extracted. However, this is a lengthy and expensive procedure that can only be performed under strictly controlled conditions. The technique applied, quantity of cells isolated, and expanded Treg number achieved in recent clinical trials is demonstrated in table 4.1.

**Table 4.1 . Tregs isolated in clinical studies**

| Study | Technique | Blood volume | Cells isolated | Expansion period | Expanded number |
|---|---|---|---|---|---|
| Todo et al 2016 | Lymphopharesis | NA | $>5x10^9$ (lymphocytes) | 14 days | $3.39\pm2.12 \times 10^6$/kg |
| Sanchez-Fueyo A et al 2020 | Leukopharesis or WB | 250 ml - WB 180ml -leukopharesis | $1.5\text{-}5.5 \times 10^6$ | 36 days | $680\text{-}2680 \times 10^6$ |
| Harden et al 2021 | WB | 380 ml | Not reported | 36 days | Not reported |
| Trzonkowski et al 2009 | WB | 500ml | $3 \times 10^5$ | 21 day | $3 \times 10^6$ |

**WB= Whole blood**

This project used peripherally collected whole blood from either healthy volunteers or patients undergoing venesection at QEHB due to hereditary haemochromatosis. Existing ethical approvals are in place for the acquisition of this human tissue. Up to 75mls of blood could be collected via venepuncture from healthy volunteers, whereas 300-400ml of venesection blood was obtained from patients with haemochromotosis. Isolating Tregs from human whole blood can be performed via an immunomagnetic approach, or via machine operated cell sorting (with or without immunomagnetic pre-enrichment). The merits and effectiveness of both strategies have been investigated during this project, and are subsequently described.

## 4.2 Immunomagnetic Treg isolation

In this project, two different immunomagnetic isolation kits were tested. These were;

3. EasySep™ Human CD4+CD127low CD25+ Regulatory T Cell Isolation Kit (StemCell)
4. CD4+ CD25+CD127dim/-Regulatory T Cell Isolation Kit II, human (Miltenyi biotec)

The yield and purity of the above isolation kits are described below. As per the manufacturer recommendation, the isolation process was commenced from peripheral blood mononuclear cells (PBMCs) that were obtained via the process of density gradient centrifugation (described in section 2. 7).

### 3.2.1 EasySep™ Hu CD4+CD127low CD25+ Regulatory T Cell Kit (StemCell)

The yield of Tregs from five isolation experiments are demonstrated in figure 4.1. As is evident, the yield of Tregs using this isolation kit was low.

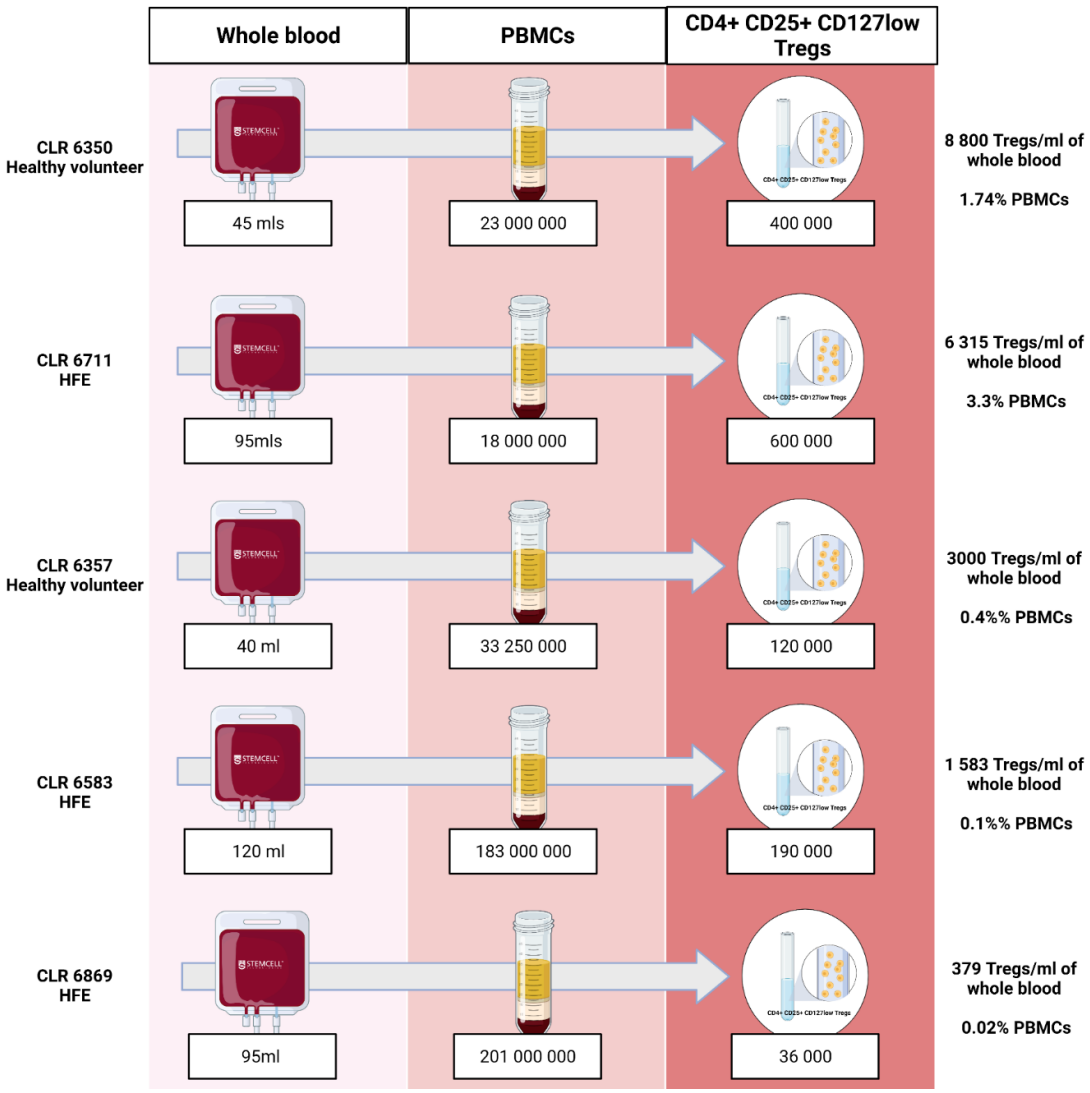


**Figure 4.1. Yield of Treg isolation experiments using StemCell isolation kit.** This diagram demonstrates the volume of whole blood, the subsequent yield of PBMCs after density gradient centrifugation, and then Treg absoluter number and percentage. The final two experiments (CLR 6583 and 6869) had a larger number of PBMCs but these were subject to isolation in two separate batches so that the 100 000 000 cell limit was not exceeded.

Flow cytometry was performed after the positive selection step but before the negative selection step, and at the end of isolation to assess the purity during the process. The flow cytometry results are depicted in figure 4.2.

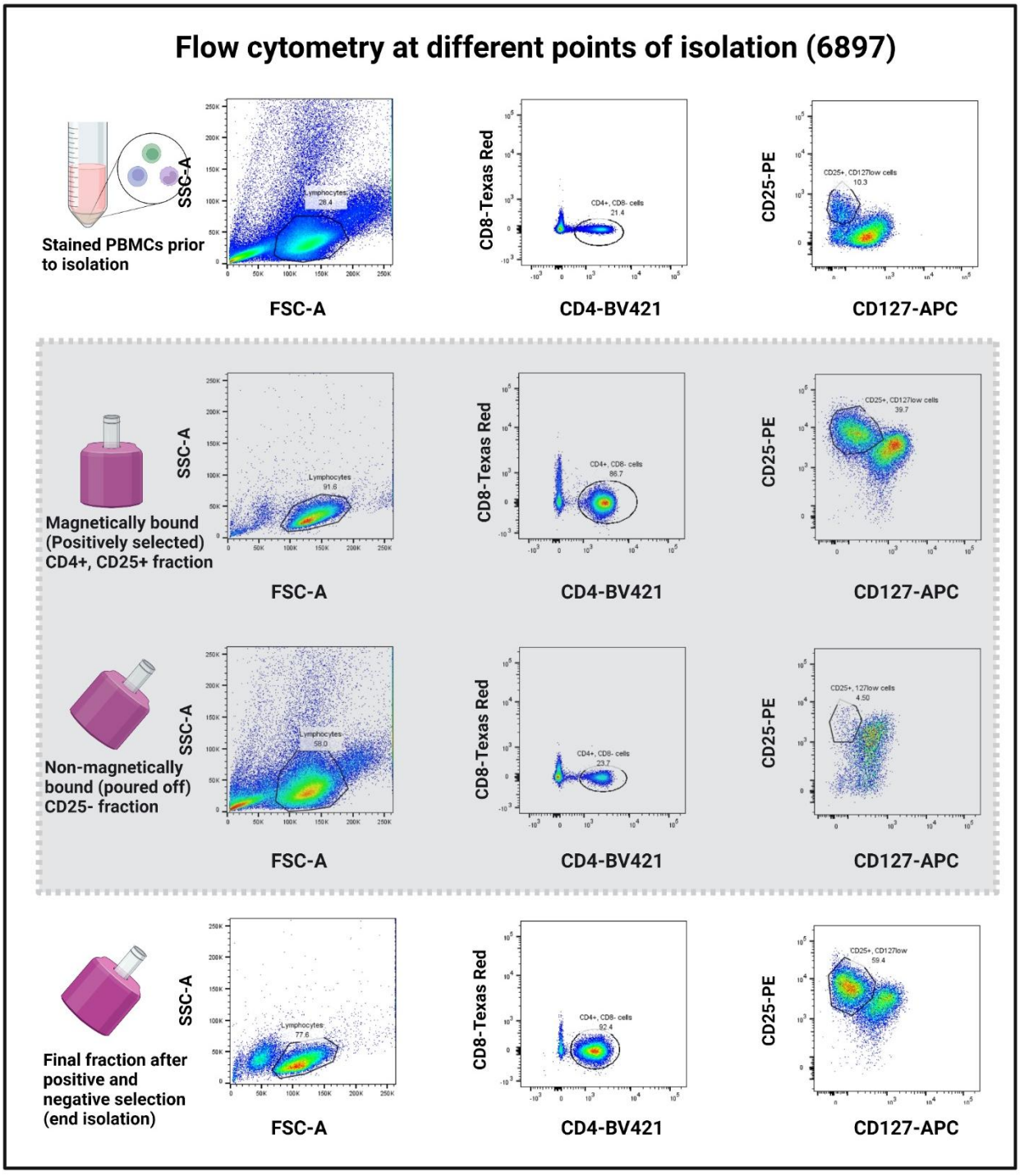


**Figure 4.2.** Flow cytometry results of EasySep Stem cell isolation kit. Flow cytometry scatter plots demonstrating gating strategy and proportion of cells that were $CD25^+$ and CD127low. The uppermost panel depicts the stained PBMCs, the percentage of $CD25^+CD127^{low}$ Tregs was 10% of $CD4^+$ cells, consistent with what is expected. Grey panel in the middle demonstrates the positively selected $CD25^+$ cell fraction that proceeded to the negative selection (superior) and the discarded $CD25^-$ fraction that remained unbound during the positive selection step. Approximately 84% of the positively selected fraction of lymphocytes consisted of $CD4^+$cells, as opposed to 23% of those not positively selected (unbound, discarded fraction row 3). The final sample (row 4) consisted of 92% $CD4^+$ cells with approximately 60% being $CD25^+$CD127 low cells.

The yield of the isolations using this kit was low, ranging from 0.02% - 3.3% of starting PBMCs. These experiments were performed numerous times. To ensure operator error was not having a significant role, different individuals performed isolations using similar PBMCs. Given the low yield and suboptimal purity of these isolation experiments, a different isolation kit was then tested (CD4+ CD25+CD127dim/-Regulatory T Cell Isolation Kit II, human Miltenyi).

### 3.2.2 CD4+ CD25+CD127dim/-Regulatory T Cell Isolation Kit II (Miltenyi)

This isolation kit utilises magnetic column technology, rather than the static magnet that is applied in the kit from StemCell (Figure 2.3A). The cell solution is prepared with the antibody complexes and magnetic beads, this is then added to the top of a plastic column with a narrow necked column underneath, which sits within a magnet (Figure 2.3B). Therefore, the cell solution runs through the column and the magnetically bound cells adhere to the side of the plastic column. The non-magnetically bound cell fraction drips out the bottom of the column into a test tube (‘flow through fraction) (Figure 2.3C). The cell fraction that was adherent to the side of the column can be reclaimed by taking it out of the magnet, and therefore removing the force adhering the cells. The column is then filled with buffer and a syringe plunger is used to express the remaining cells (‘eluted fraction’) (Figure 2.3D).

This approach also utilises a two step approach to obtain $CD4^+$, $CD25^+$, CD127low Tregs. However, in contrast to the previous approach, the first step is negative selection and the second is positive selection (Figure 2.2). The first step (negative selection) is intended to remove the non-$CD4^+$ and $CD127^{high}$ (and therefore non-Treg) fraction of cells from PBMCs. This is achieved by the binding of biotin antibodies to specific cell surface markers (CD8, CD18, CD123, CD127), then incubating these cell bound antibodies to magnetic microbeads that are conjugated with antibiotin antibodies. Therefore, this non-$CD4^+$ fraction is meant to

adhere to the magnetic column and the $CD4^+$ fraction flows through the column to the tube underneath.

The second step in this isolation protocol involves positive selection of the $CD25^+$ fraction in the remaining cell solution. This is achieved by incubation of the cell solution with anti-CD25 antibodies that are conjugated to magnetic microbeads. Therefore, the $CD25^+$ fraction of the supposedly $CD4^+$, $CD127^{low}$ cell solution adheres to the magnetic column (positive selection). To obtain this cell fraction the column is removed from the magnetic stand and eluted with a plunger. The manufacturer of this preprepared product recommends this step (positive selection) be repeated twice to achieve the greatest purity. The yield of six isolation experiments is demonstrated in figure 4.3.

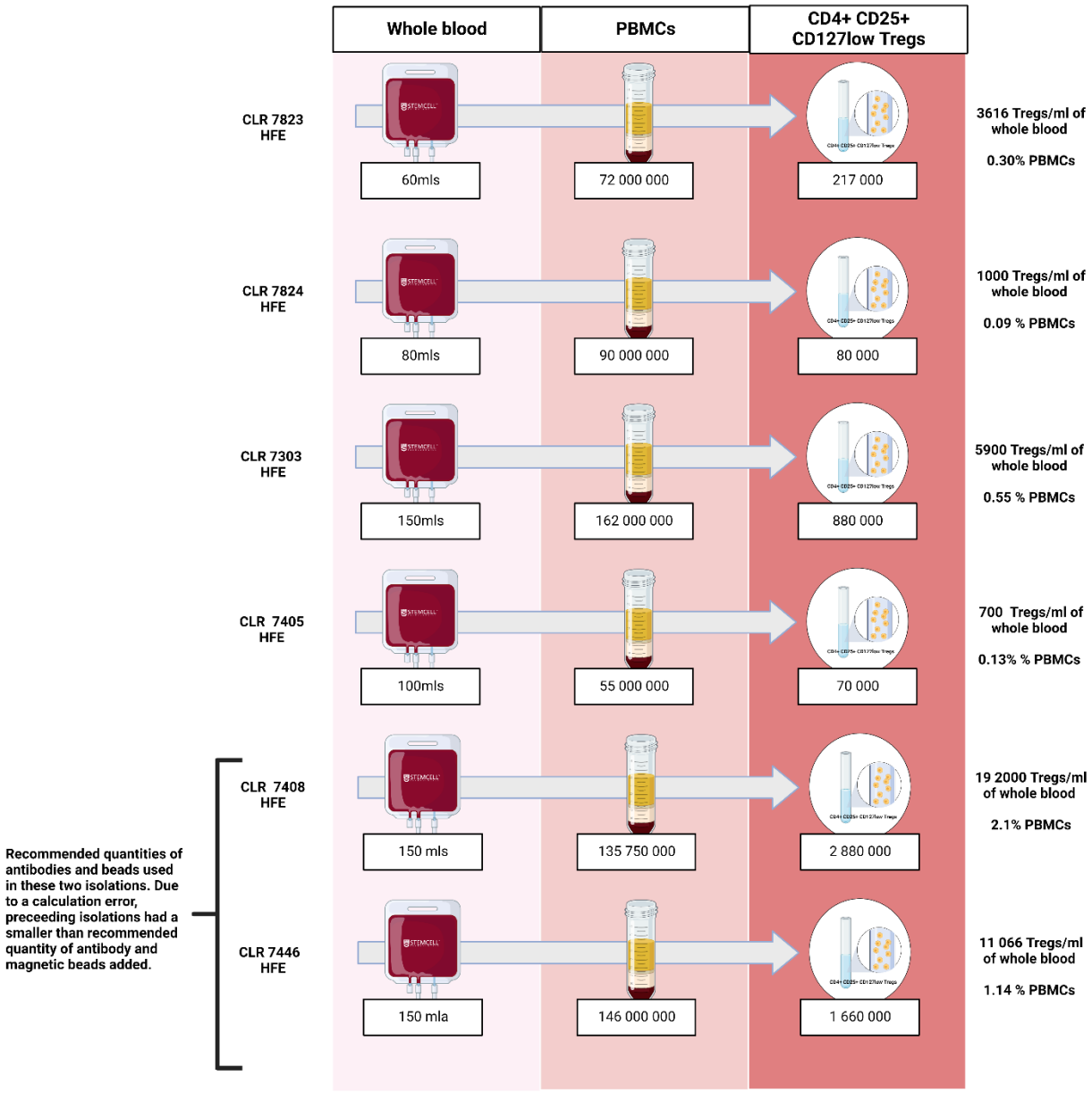


**Figure 4.3.** Yield of Treg isolation experiments using the Miltenyi Kit**.** The results of six isolations using the Miltenyi isolation kit are demonstrated. Due a calculation error, the first 4 isolations had a lower than recommended dose of magnetic beads and antibodies by a factor of 10. The yield was greater with the correct dose of antibodies but remained to be 1-2% of the PBMCs.

The yield of Tregs, when the recommended dose of antibodies and beads are used, was between 1-2% of starting PBMCs. In contrast to the StemCell isolation Kit, the columns are limited by the number of magnetically labelled cells. In the first step (Figure 2.2 - negative selection), a maximum of 100 000 000 cells can be magnetically labelled (and therefore removed) from a maximum of 500 000 000 cells to start. In the second step (Figure 2.2-

positive selection), a maximum of 10 000 000 cells (Tregs) can be labelled from a maximum of 100 000 00 cells that can be added to the column.

The purity of Tregs isolated via this method is demonstrated in Figures 4.4-4.7. The cell fractions at different steps in the process were stained with an antibody panel that included markers for live-dead status (ef780), CD4 (PercP), CD8 (Texas red or BV605), CD25 (BV421) and CD127 (BV711). These cells were then subject to flow cytometry. In figures 4.4-4.7, gating was based on size (to capture lymphocytes), then ef780 negativity (live cells), then $CD4^+$, $CD8^-$, then $CD25^+$ and $CD127^{low}$. As demonstrated in figure 4.4B, the eluted fraction from step 1 contains the greatest proportion of monocytes as indicated by a higher FSC- A and SSC-A in comparison to the encircled (and gated) lymphocyte population. Figure 4.4 demonstrates that the fraction of cells that progresses to the second step (positive selection) still contains a significant proportion of non-lymphocyte cells. Step 1 appears effective in removing the $CD8^+$ lymphocytes, as demonstrated in figure 4.4. It appears that the majority of non-lymphocyte cells are removed in step 2 of the isolation, this is clearly demonstrated in figures 4.5-4.7 row when row A is compared to the final isolate in row C. The later cell fraction has undergone enrichment for $CD4^+$ and $CD25^+$, with both these markers only being present on T-lymphocytes.

The final isolate that can be achieved via this isolation process is rich in lymphocytes (up to 87% of events), and the majority of these are $CD4^+$, $CD8^-$. As demonstrated in Figure 4.7, $CD4^+$, $CD8^-$ comprise up to 85% of the isolated lymphocytes. This $CD4^+$, $CD8^-$ population is predominantly $CD127^{low}$. Despite the majority of cells in the final isolate demonstrating to consist of a single defined $CD127^{low}$ population, CD25 expression was consistently low throughout the isolation experiments. This is not the expected finding as these cells should be Tregs, which are $CD25^+$. Reasons for this finding could be under staining of the CD25 bound fluorochrome during the staining process, or voltage settings for this marker being too low

durin flow cytometry analysis. Flow cytometry results of Tregs isolated and expanded are demonstrated in a later section within this chapter. In summary, the results of this isolation process were better in regard to both yield and purity in comparison to the StemCell but it remained inconsistent. Therefore, isolation via FACSaria cell sorting was undertaken.

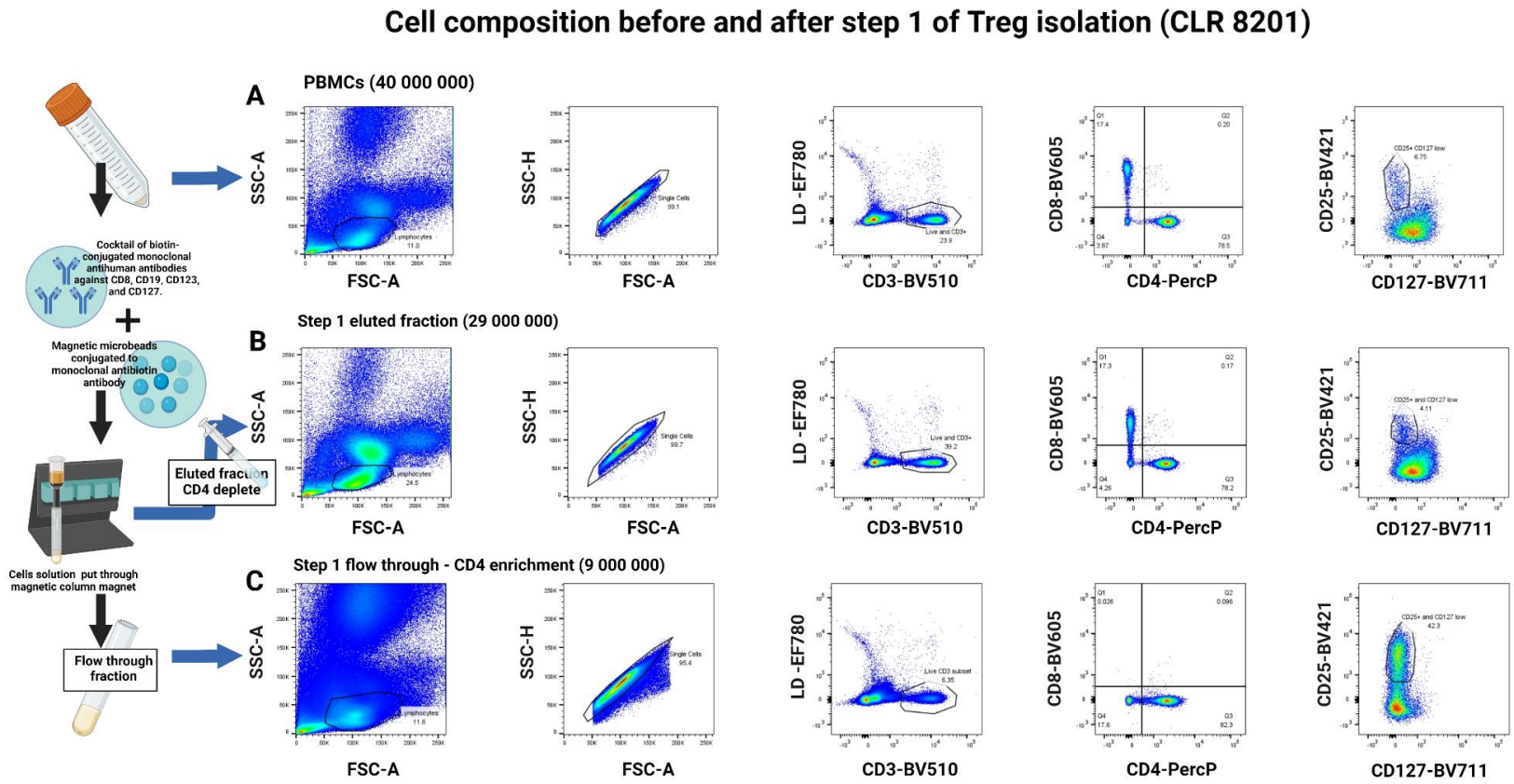


**Figure 4.4. Flow cytometry results of PBMCs, and both the eluted and flow through fraction after step 1 of the isolation (Miltenyi isolation kit).** The above demonstrates the phenotype of the starting PBMCs (A), the eluted fraction after step 1 (B) and the flow through fraction after step 1 (C). The final Treg isolate is not demonstrated as all cells were put into culture for expansion. As demonstrated in panel A, the Treg population in human peripheral blood is between 5-10% of $CD4^+$ cells. The flow cytometry results demonstrated in row B and C show that the majority of lymphocytes are lost from the isolation process during step 1, and nearly 80% of the $CD3^+$ lymphocytes are $CD4^+$. A significant portion of this eluted fraction could be Tregs and likely accounts for the low yield. Although the flow through fraction has a high percentage of $CD4^+$ lymphocytes, the actual number of $CD3^+$ lymphocytes is relatively low (11.8%). However the $CD4^+$ flow through fraction does appear to be predominantly $CD127^{low}$ and therefore has a higher proportion of Tregs.

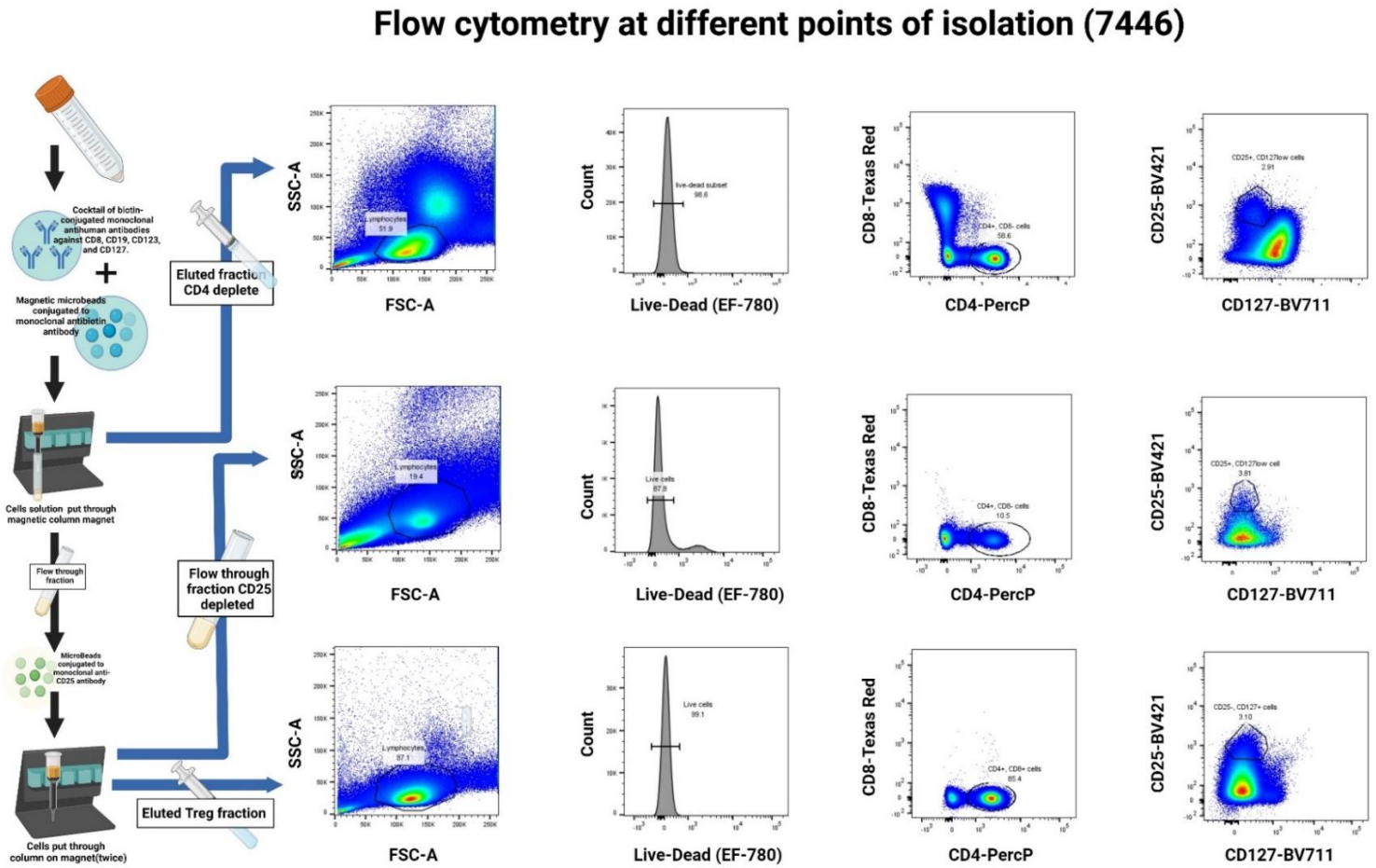


**Figure 4.5. Purity of isolation at different steps for single sample of PBMCs (Miltenyi**). The above demonstrates the phenotype of the eluted fraction after step 1 (Top row) and step 2 ( middle row) and the final Treg isolate (bottom row). The step 1 of the isolation removed a large proportion of the PBMCs that were not lymphocytes, as demonstrated by the dense cloud of cells with a higher FSC-A and SSC-A than the encircled lymphocytes. The $CD8^+$ fraction (top row) was also removed. The flow through fraction (non-tregs) from step 2 had a much lower frequency of lymphocytes than the eluted (Treg) fraction. The $CD4^+$ fraction was much higher in the final eluted (Treg) fraction in comparison to the flow through fraction (85% vs 10.5%), with a similar percentage of these $CD4^+$ being $CD25^+$ and $CD127^{low}$

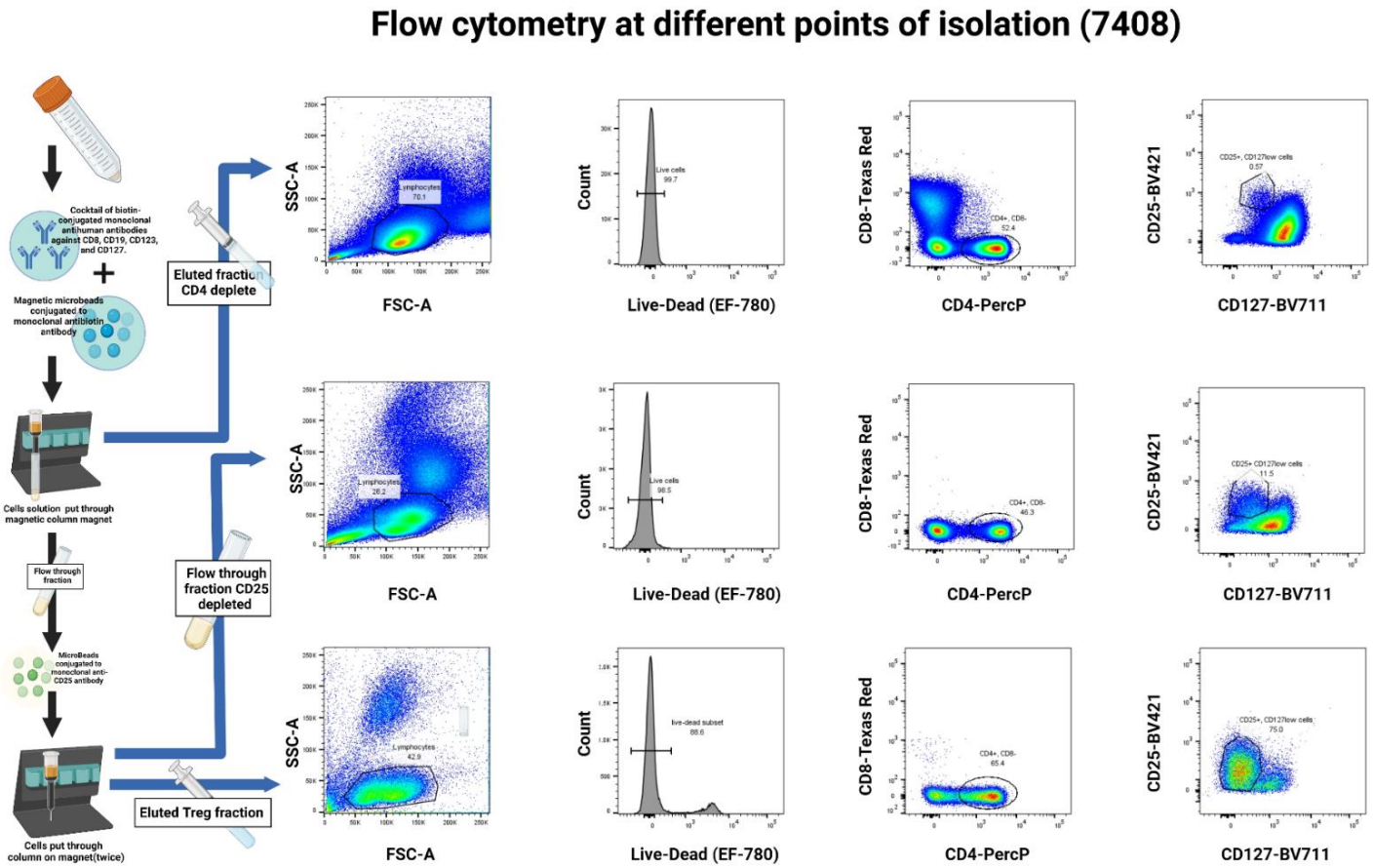


**Figure 4.6. Purity of isolation at different steps for single sample of PBMCs (Miltenyi).** The above demonstrates the phenotype of the eluted fraction after step 1 (Top row) and step 2 ( middle row) and the final Treg isolate (bottom row). This experiment appears to have isolated a $CD4^{+}$ cell population that has a higher proportion of Tregs (Approx 75%). The far right graph of the bottom row demonstrates a large and homogenous cell population that is $CD127^{low}$. The reason that this population is low on the CD25 axis could relate to either understaining with the antibody of a voltage setting for that fluorochrome (BV421) that was too low.

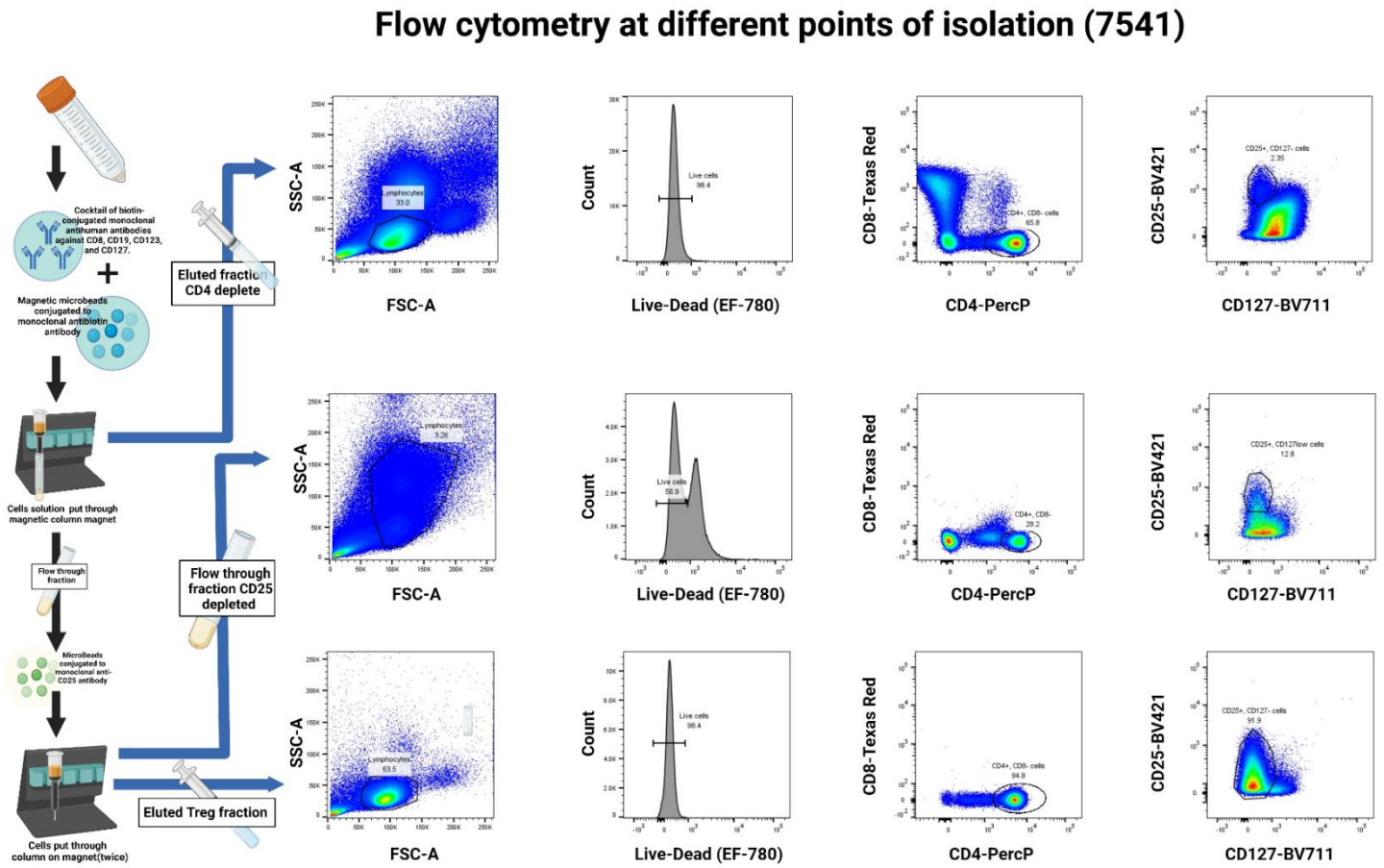


**Figure 4.7. Purity of isolation at different steps for single sample of PBMCs (Miltenyi).** The above demonstrates the phenotype of the eluted fraction after step 1 (Top row) and step 2 ( middle row) and the final Treg isolate (bottom row). Step 1 of this isolation was effection at removing a large proportion of the non-lymphocte PBMCs, as depicted in the graph on the far left of the top row, The eluted fraction after step 2 had minimal lymphocytes remaining as evidenced by the lack of a dense cloud of the appropriate FSCA-A and SCC-A for lymphocytes. The final isolate was predominantly lymphocytes, of which 94 % were $CD4^+$. If the $CD4^+$ population of this final isolate are plotted against CD25 and CD127, a predominantly homogenous population exists low on the CD127 axis. It is likely that this population is also $CD25^+$ but the voltage is too low.

### 4.3 Treg sorting via flouresence activated cell sorting (FACS)

In order to maximise time efficiency on the FACSaria machine, we first performed pre-enrichment via an immunomagnetic approach to obtain the $CD4^+$ cell population. The yield and purity of three different antibody cocktails were compared (Figure 4.8).

The three different antibody cocktails are below

1. Naive CD4 T Cell Isolation Kit II, human (Miltenyi product # 130-094-131)

2. Step 1 (negative selection) of $CD4^+$ $CD25^+$ $CD127^{dim/-}$ Regulatory T Cell Isolation Kit II, human (Miltenyi product # 130-094-775)

3. $CD4^+$ T cell isolation kit, human (Miltenyi product # 130-096-533

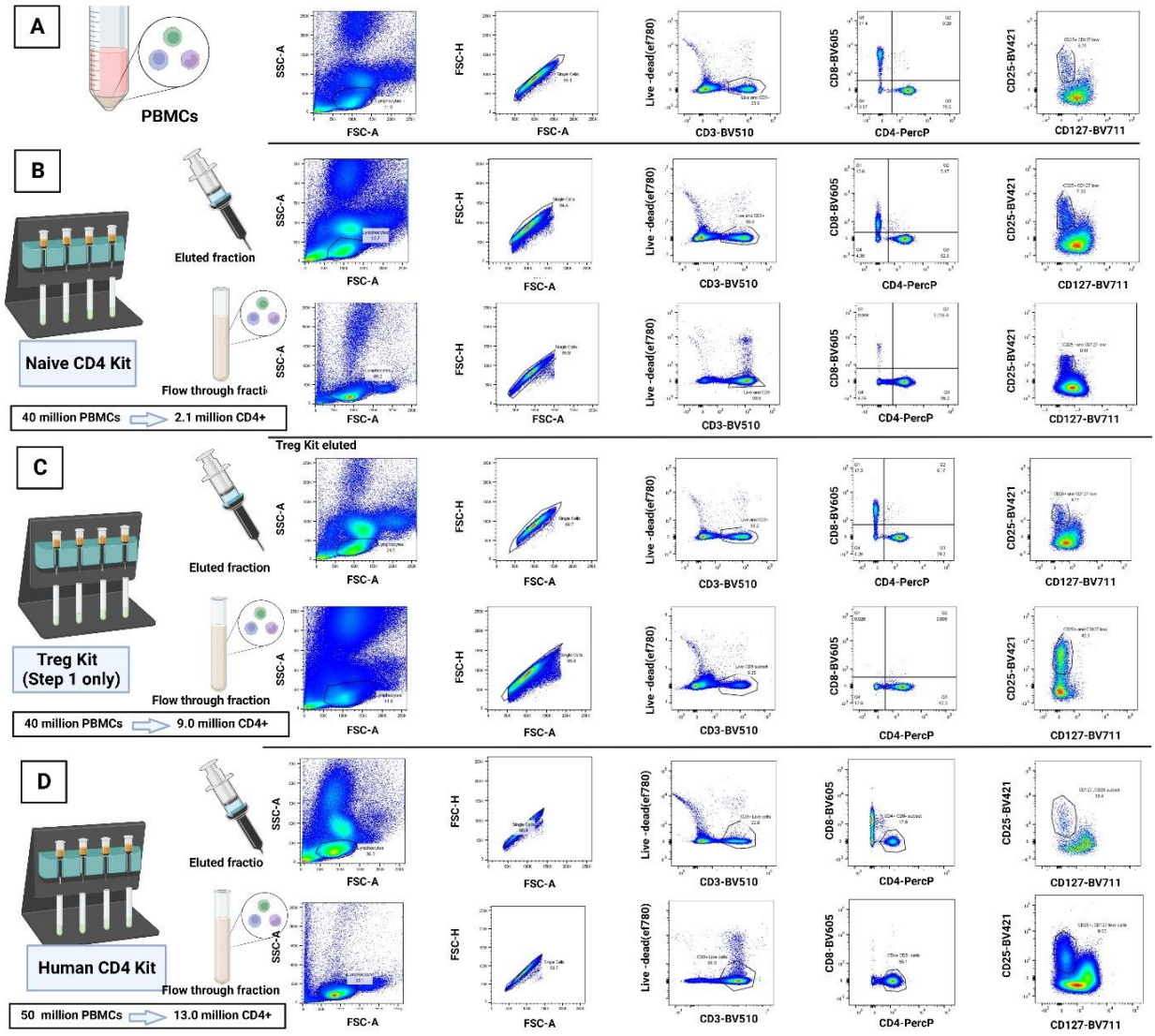


**Figure 4.8.** Comparison of different CD4 immunomagnetic isolation strategies as pre-enrichment**.** The above figure depicts the phenotype of PBMCs (A), and three different pre-enrichment antibody cocktails. B) The naïve CD4 kit had a low yoield with only 2.1 million cells being obtained from 40 million PBMCs. However 89% of these cells were lynmphocytes and 93% of these were T-lymphocytes. Furthermore, more than 90% were $CD4^+$. The main draw back of this enrichment cocktail was the overall yield, many cells that were likely Tregs were in the eluted fraction. C) The yield of the Treg Kit (step 1) was greater than that in A, with 9 million cells being obtained from 40 million PBMCs. However, a significant fraction of the lymphocytes obtained in the flow through fraction were not T-cells ($CD3^+$). A high proportion of the T-cells in the flow through fraction were $CD4^+$ (82%) but the overall percentage of $CD3^+$T cells was low (6% of lymphocytes). D)The human $CD4^+$isolation kit had the highest yield and the largest proportion of $CD4^+$ cells (purity). The majority of lymphocytes in the flow through fraction were $CD3^+$ T-cells (95% of lymphocytes) that were $CD4^+$ (96% of $CD3^+$). This isolation antibody kit was determined to be the optimal pre-enrichment process for FACS treg isolation.

As demonstrated in figure 4.8, the purity of the human $CD4^+$ kit was the highest, with more than 90% of the final isolate being lymphocytes and more than 90% of these were $CD3^+$ T cells. There was minimal remaining $CD8^+$ cells in the final flow through fraction isolated, in comparison to a high number in the eluted fraction. Furthermore, the yield was the greatest for the human $CD4^+$ kit returning 26%, as opposed to 22.5% and 5.2% the Treg Kit (step 1) and Naïve $CD4^+$ kit respectively.

To isolate Tregs using FACS, peripheral blood from both healthy volunteers and venesected blood from patients undergoing venesection due to hemochromatosis was used. This blood underwent density gradient centrifugation to obtain the PBMCs, and these subsequently underwent CD4 enrichment via negative selection. The $CD4^+$ enriched cell sample was stained with the following antibodies to allow the desired gating strategy on the FACSaria.

Antibody and fluorochrome panel

- Live dead (eF780) [1/100]
- CD3 (BV510) [1/100]
- CD4 (PerCP-Cy5.5 [1/200]
- CD8 (BV605) [1/400]
- CD25 (BV421) [1/200]
- CD127 (BV711) [1/100]

The gating strategy for 5 FACS isolation experiments are demonstrated in figure 4.9-4.13. The isolation shown in figure 4.9 & 4.12 shows steps from PBMCs, and both the eluted and flow through fractions after pre-enrichment with the human $CD4^+$ kit. The Treg activation and expansion process is further described in the next section. In summary, FACS cell sorting after pre-enrichment resulted in a Treg high purity of the final population. The consistency of results was also improved in comparison to the immunomagnetic strategies. However, the yield was similar and the FACS method consumes far greater resources.

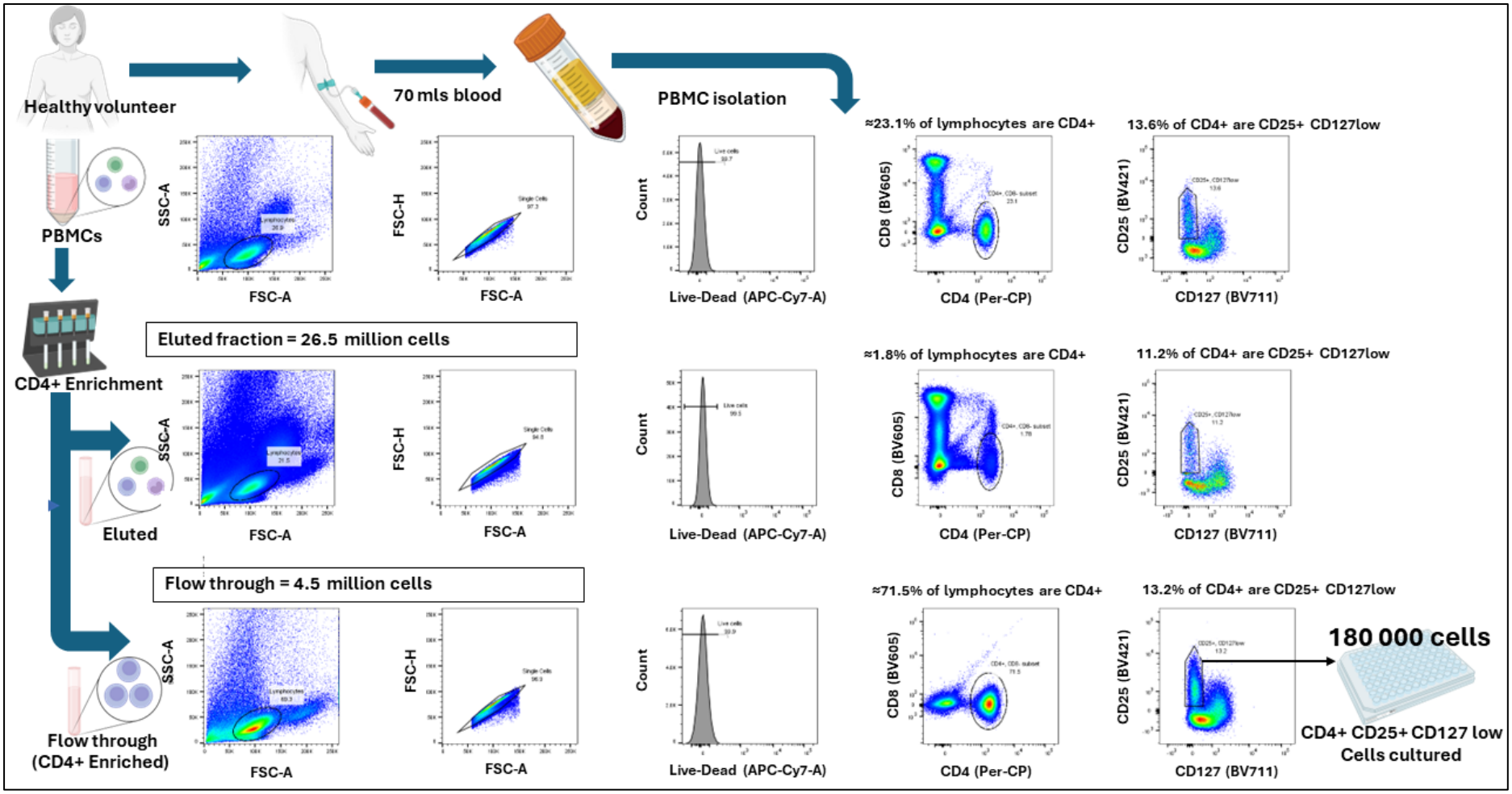


**Figure 4.9. Gating strategy for FACS sorting (Sort 1- Pre-enrichment with human CD4$^{+}$).** Gating strategy for cell sort 1. Pre-enrichment was with Human CD4 isolation kit. Gating strategy was based on lymphocytes > single cells > live cells > CD4 positive > CD25$^{+}$ and CD127$^{low}$. At the end of FACS, 180 000 cells were isolated from 45 million CD4 enriched lymphocytes.

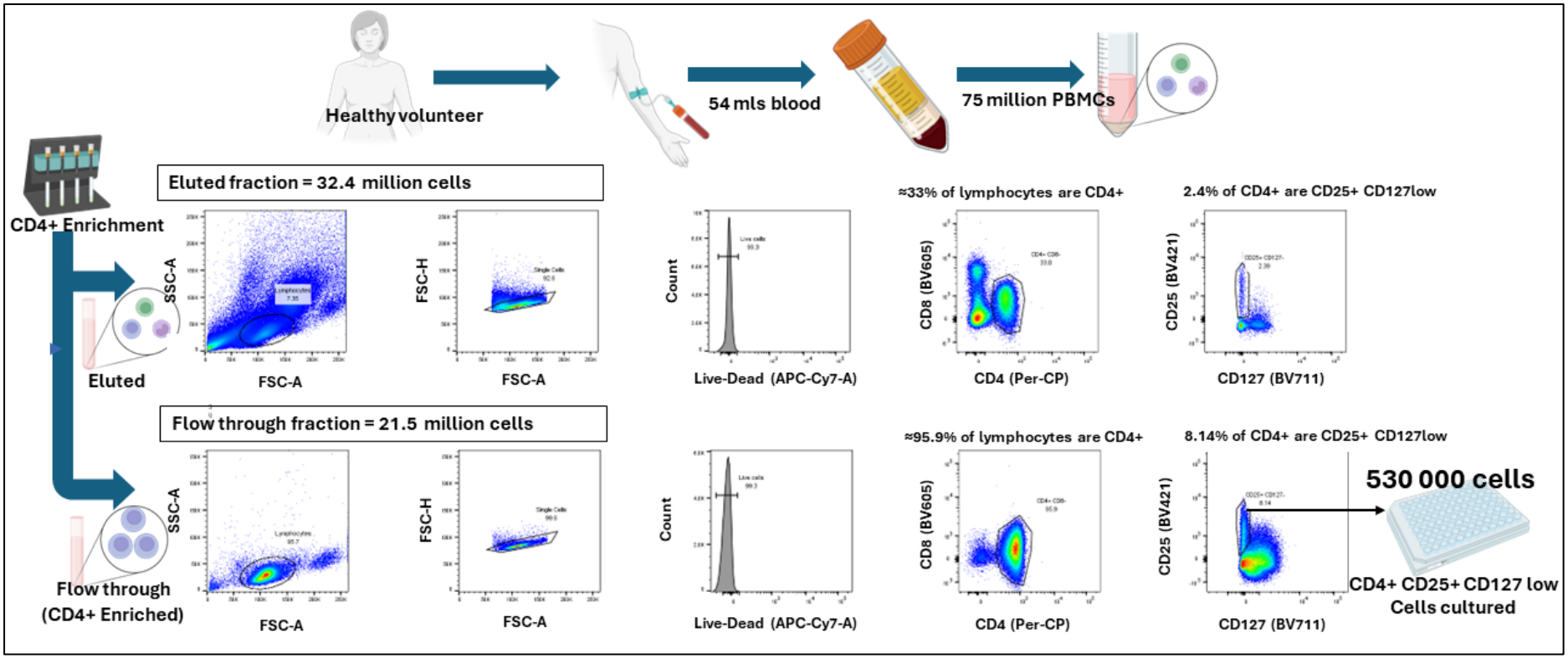


**Figure 4.10. Gating strategy for FACS sorting (Sort 2- Pre-enrichment with human CD4$^{+}$).** Gating strategy for cell sort 1. Pre-enrichment was with Human CD4 isolation kit. Gating strategy was based on lymphocytes > single cells > live cells > CD4 positive > CD25$^{+}$ and CD127$^{low}$. At the end of FACS, 530 000 cells were isolated from 21.5 million CD4 enriched lymphocytes.

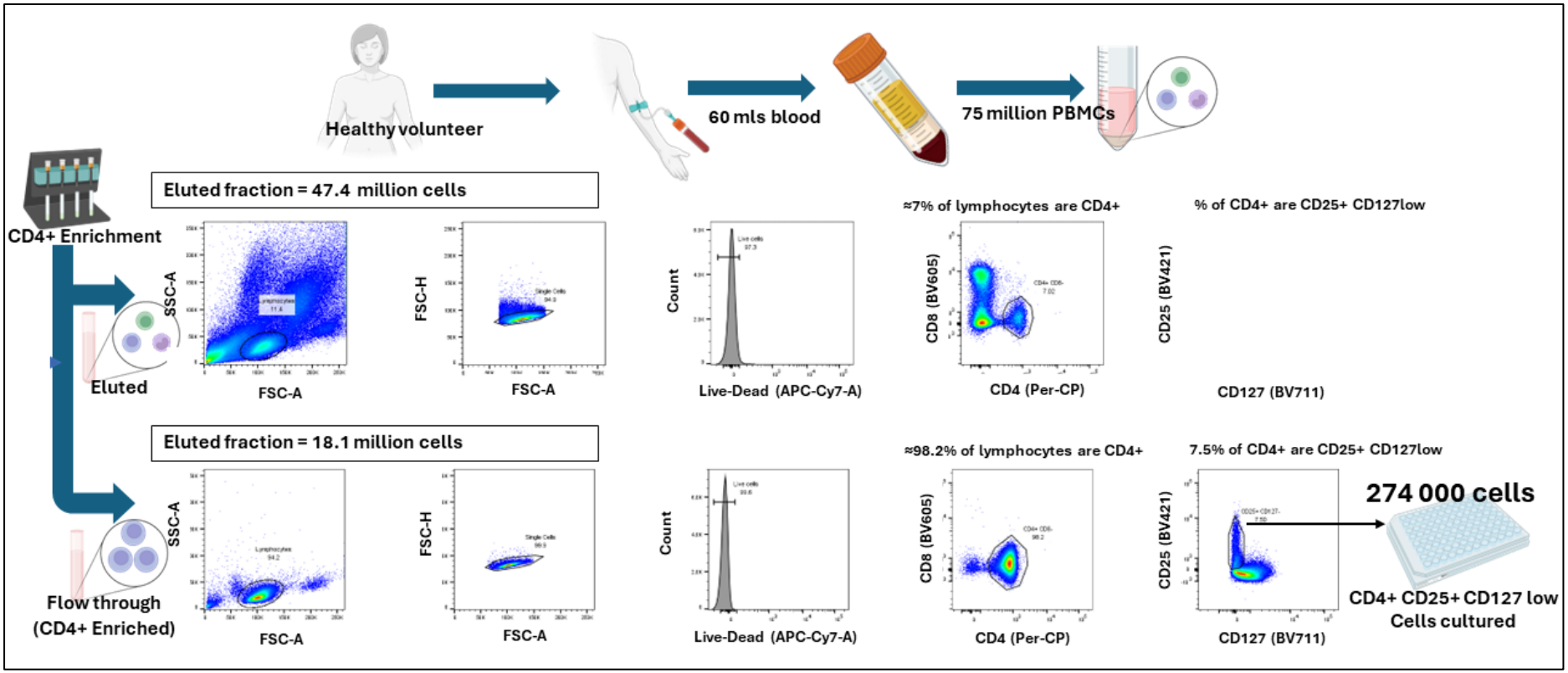


**Figure 4.11. Gating strategy for FACS sorting (Sort 3- Pre-enrichment with human CD4$^{+}$).** Gating strategy for cell sort 1. Pre-enrichment was with Human CD4 isolation kit. Gating strategy was based on lymphocytes > single cells > live cells > CD4 positive > CD25$^{+}$ and CD127$^{low}$. At the end of FACS, 274 000 cells were isolated from 18.1 million CD4 enriched lymphocytes.

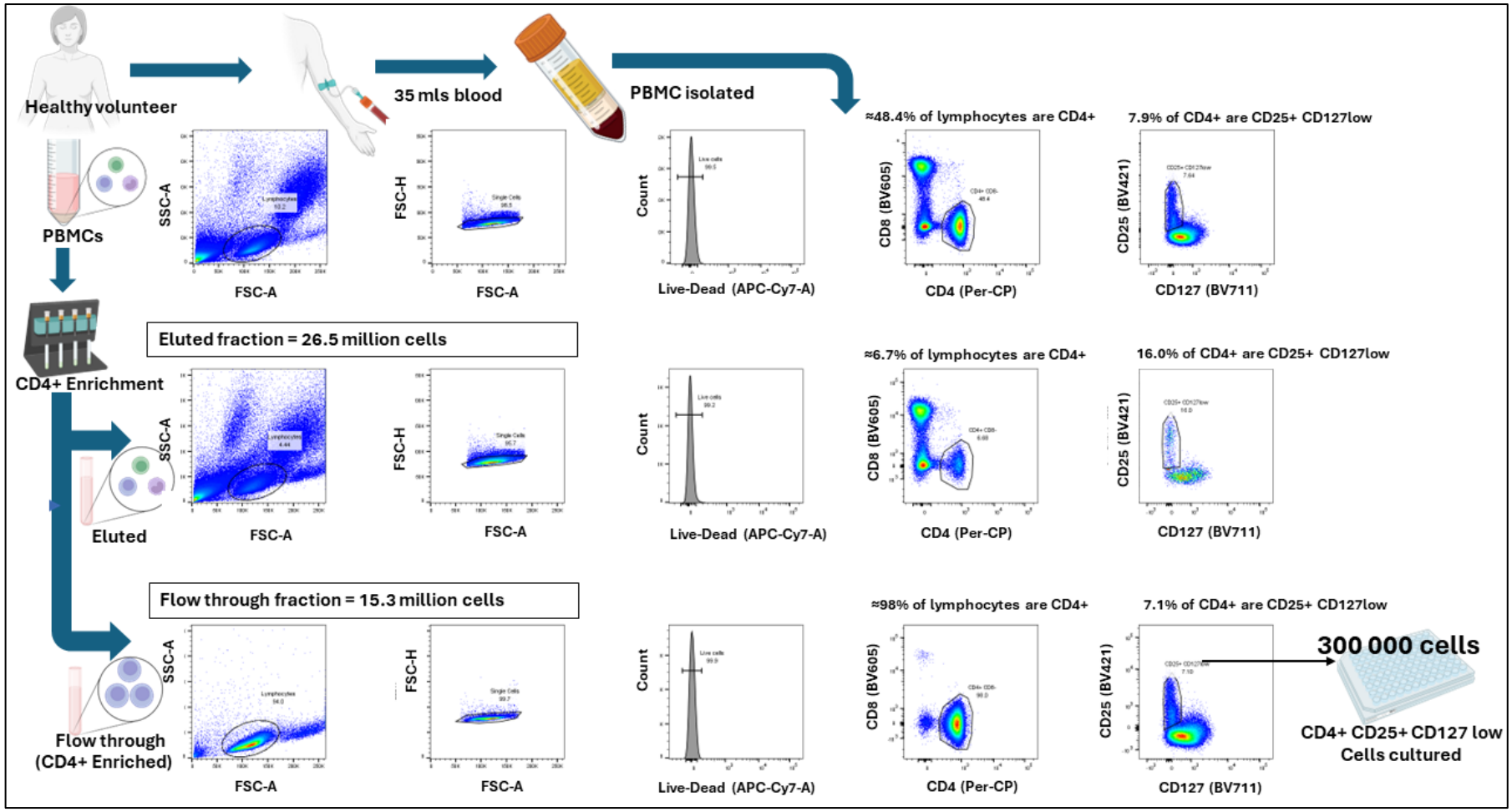


**Figure 4.12. Gating strategy for FACS sorting (Sort 4- Pre-enrichment with human CD4⁺).** Gating strategy for cell sort 4. Pre-enrichment was with Human CD4 isolation kit. Gating strategy was based on lymphocytes > single cells > live cells > CD4 positive > $CD25^{+}$ and $CD127^{low}$. At the end of FACS, 300 000 cells were isolated from 15.3 million CD4 enriched lymphocytes.

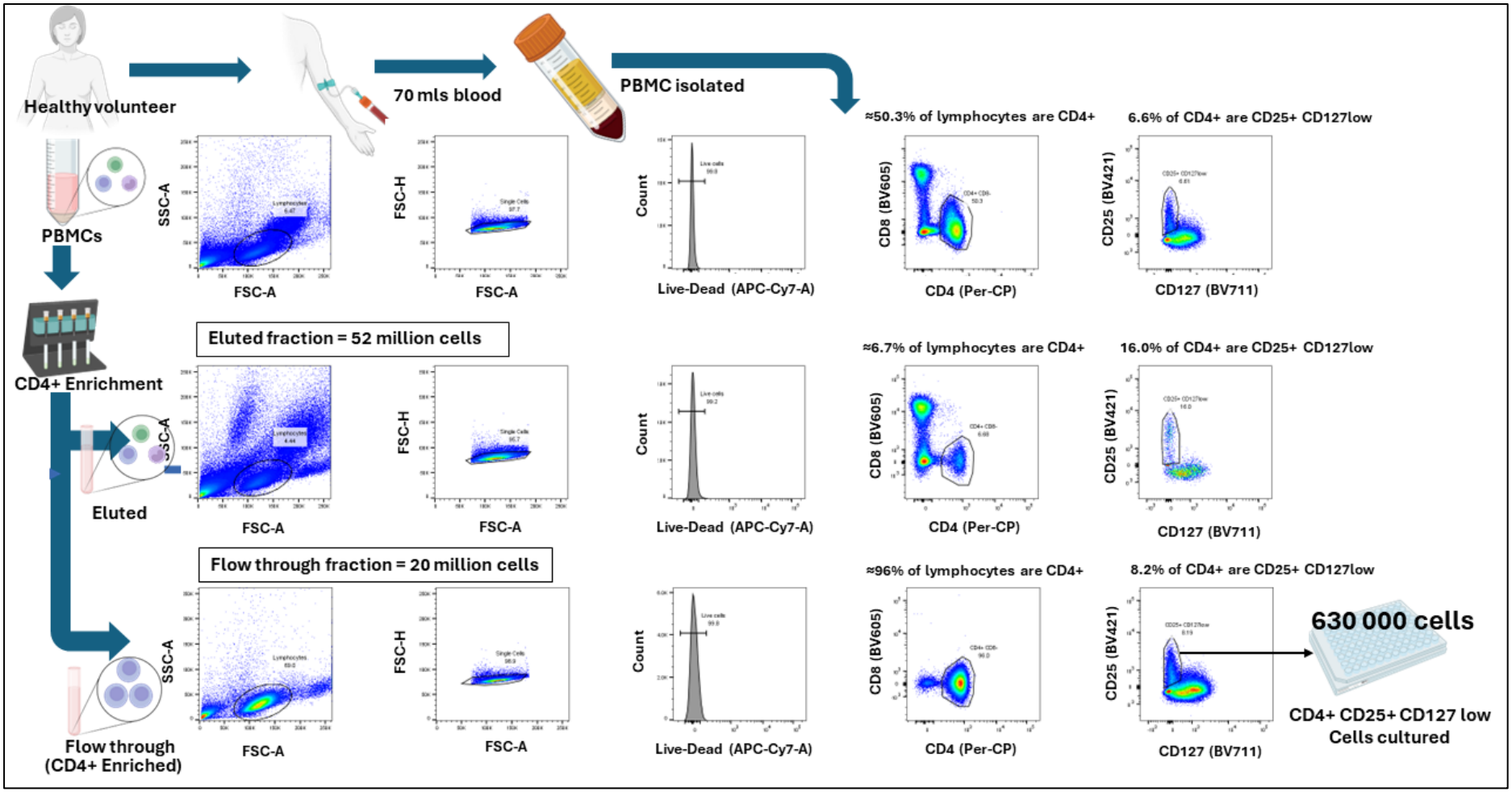


**Figure 4.13. Gating strategy for FACS sorting (Sort 5- Pre-enrichment with human CD4⁺).** Gating strategy for cell sort 5. Pre-enrichment was with Human CD4 isolation kit. Gating strategy was based on lymphocytes > single cells > live cells > CD4 positive > $CD25^{+}$ and $CD127^{low}$. At the end of FACS, 630 000 cells were isolated from 20 million CD4 enriched lymphocytes.

### 4.4 Treg activation and expansion

In this project, an initial series of expansion experiments were performed with Tregs isolated via the immunomagnetic approach. This was to learn basic cell culture techniques on the cells isolated via the less resource intensive method. The Tregs were cultured in 96 well plates as our previous laboratory experience, and supporting literature, suggests that better results are obtained with culture at a high density[168]. Activation was performed with CD3/CD28 beads (Treg expansion Kit, human. Miltenyi # 130095395) at the commencement of culture and after 14 days. The bead to cell ratio used was that recommended by the manufacturer of 4:1, however it is acknowledged that other ratios have been tested and described[169]. During the initial experiments, at the 14 day restimulation, the previously added beads were removed via magnetic extraction. Due to the identification that significant cell loss was occurring via this process, this was no performed and the initial activation beads remained in place. An attempt to phenotype the cells via flow cytometry before and after expansion was made if the cell volume permitted this. The components of the Treg media and their concentrations are listed in the methods section.

The TexMACs, human AB serum and rapamycin is combined to make up a 50ml aliquot of media, however the IL-2 is kept separate and added directly to the culture well based on this being a volume of 250 µL.

The protocol used for expansion after immunomagnetic isolation and FACS isolation is demonstrated in Figure 2.4 and 2.5 respectively. The regime outlined is a template used to guide the culture, but the decision regarding the splitting of cells and changing the media is also influenced by visual inspection and microscopy of the culture wells. This is demonstrated in Figure 4.14.

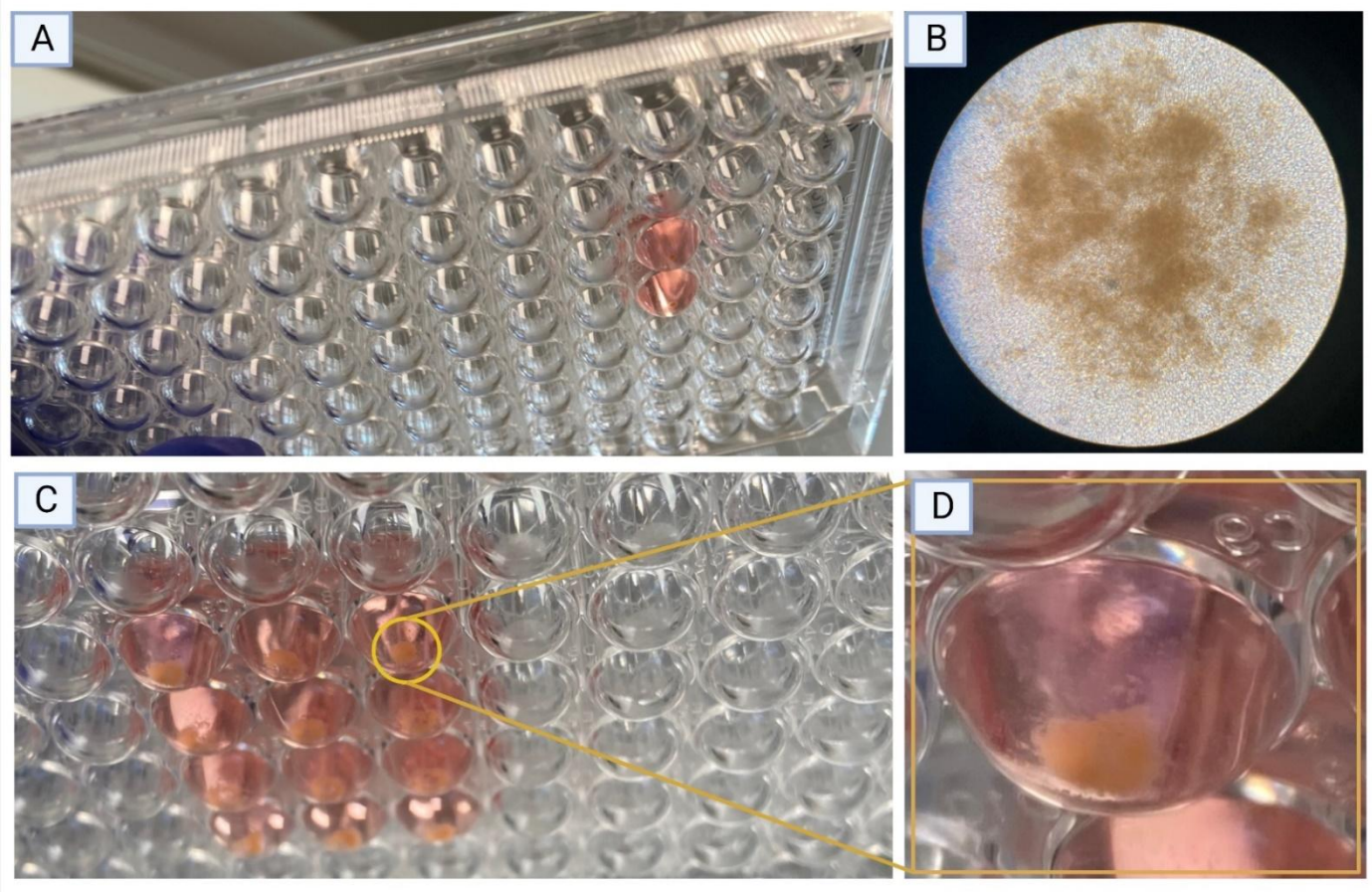


**Figure 4.14.** Cell culture images**.** Images demonstrating how cell expansion was assessed . A) Image demonstrating the cells in two 96 well plates at beginning of expansion. B) Microscope assessment of single well, dark brown in centre of image represents the activation beads. C) As expansion progressed and cell pellet enlarged, cells split and more wells filled. D) Close up image of cell pellet.

The results of the expansion of Tregs isolated via the immunomagnetic approach are demonstrated in Figure 4.15. The bead removal process involves a brief incubation of the cells within a strong magnet and this makes the activation beads adhere to the side of the tube. The cell solution is then removed, leaving the adhered beads within the original tube. Ideally, the beads are removed before flow cytometry but are reported to not exhibit any fluorescence and therefore can be analysed on this platform without removal if necessary. However, due to the fact these expanded cells are intended for a therapeutic application, bead removal at the end of expansion is required. However, a large proportion of cells can also be lost during the bead removal process. The flow cytometry profile of these post expanded samples (excluding CLR 7855) are displayed in Figure 4.16.

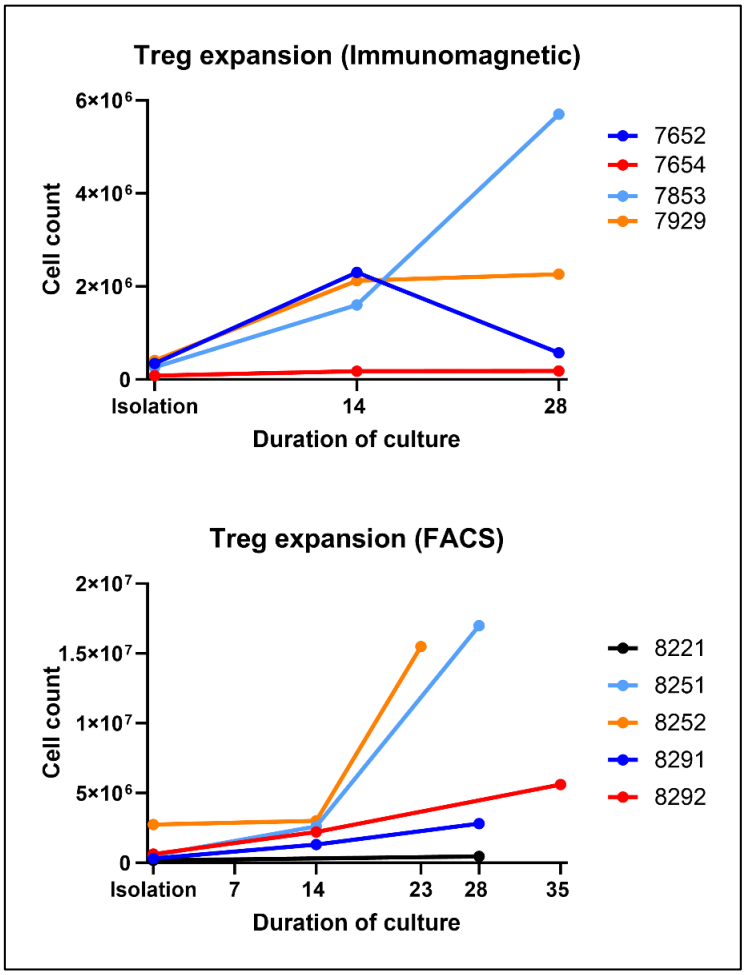


**Figure 4.15.** Expansion of Tregs isolated via different techniques**.** Line graph demonstrating the expansion of isolated Tregs after a 28 day period. The consistency of expansion was greater for the FACS isolated cells. The numbers depicted represent the cell count before bead removal.

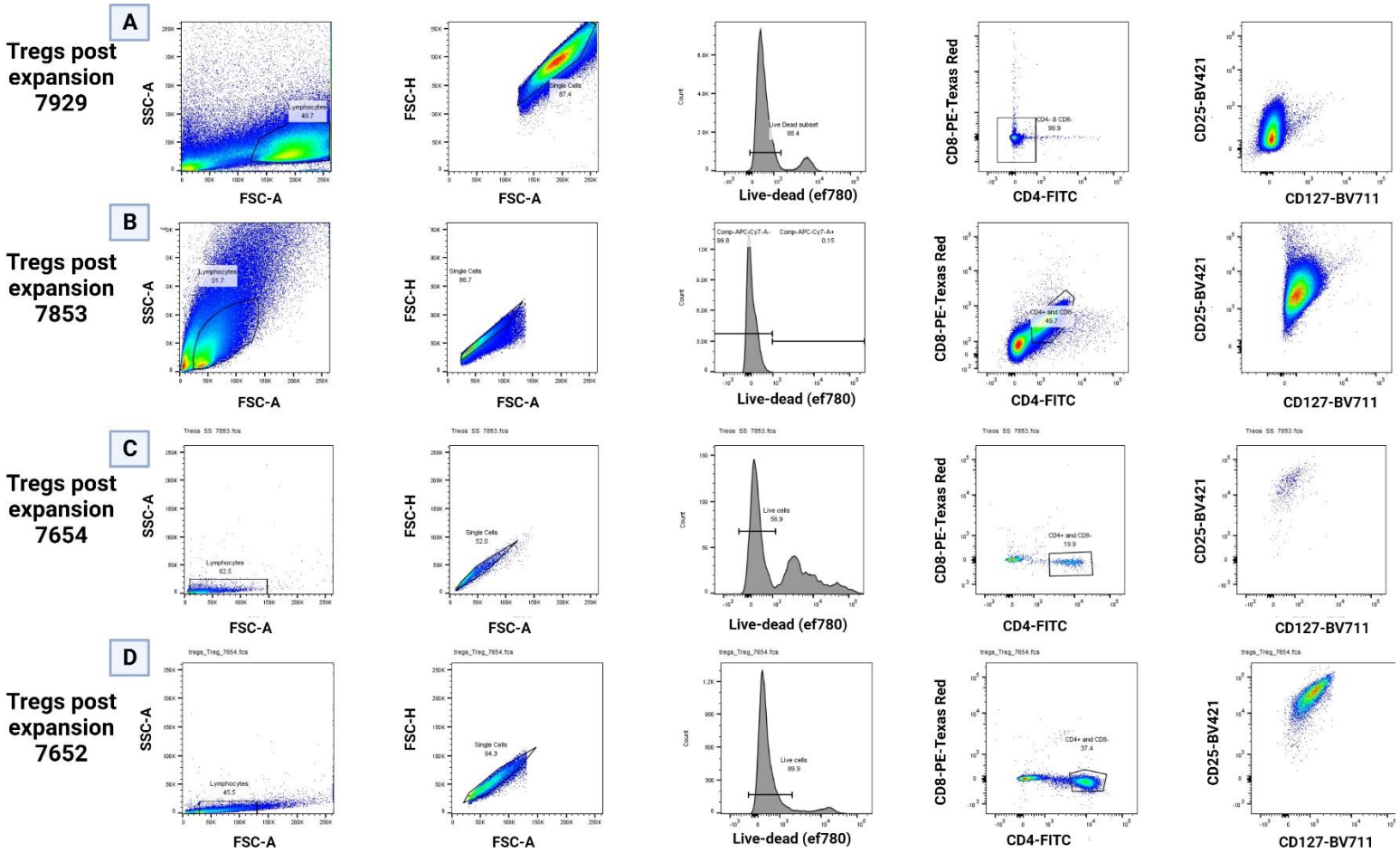


**Figure 4.16. Flow cytometry results of post expanded Tregs following immunomagnetic isolation.** Flow cytometry results of four expansions after immunomagnetic isolations. During this period, skills in flow cytometry were still developing. Much was learnt during this process. A) Tregs at end of expansion. FSC-A settin to high and SSC-A setting to low. CD4-FITC staining did not work, as evidenced by the entire live cell population being $CD4^-$. The CD25 proportion of cells is likely understained due to homogenous population that is low on the CD25 axis. B) Suboptimal FSC-A and SSC-A setting. C) SSC-A and FSC-A setting to low. D) SSC-A setting to low. Improved CD25 staining from previous.

The cells isolated via FACS were also cultured in 96 well plates using a similar protocol. Due to the loss of cells observed during bead removal at the mid point of expansion, this step was eliminated but the additional beads were still added. Figure 4.15 depicts the successful expansion of the FACS isolated Tregs by approximately 500 fold. The flow cytometry results are limited by the fact that staining for intracellular FoxP3 has not been demonstrated. Multiple attempts have been made to achieve this but consistent results are yet to be achieved.

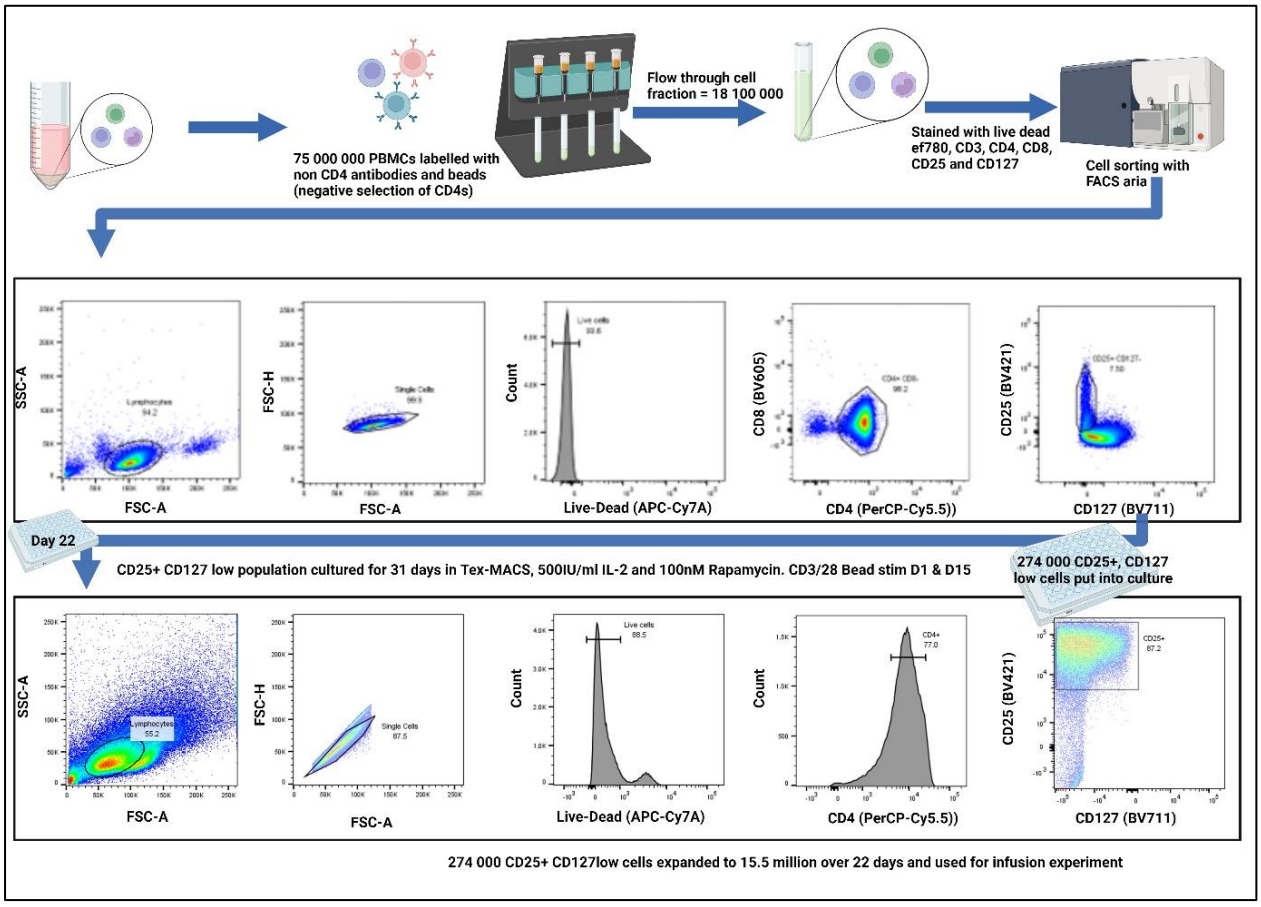


**Figure 4.17. Flow cytometry results of FACS isolated Tregs.** This figure demonstrates the FACS sorted Tregs (top row row) and the post expansion Tregs (bottom row). Prior to sorting, these cells underwent were pre-enichment with human CD4 isolation kit. The Treg population expanded from 274 000 cells to 15 100 000 over 22 days.

The expansion of the FACS isolated Tregs was far greater than that achieved with the Tregs obtained by immunomagnetic isolation techniques. However, expansion of FACS isolated Tregs failed on two occasions and possible explanation for this was an error in the reconstitution of the IL-2 powder on one occasion, and allowing the wells to dry out on another.

### 4.5 Chapter summary

Isolating Tregs is possible via a number of different techniques, only some of which have been described in this chapter. The benefits of the immunomagnetic approach are that numerous isolations can be done at a relatively low cost, it does not require advanced equipment, and does not require advanced training of the scientist undertaking the isolation. The downside of this approach is that the purity of the isolated cells is inferior to FACS Tregs isolations. The need for a high purity FACS isolations needs to weighed up against the additional expense, access to advanced machinery and the necessary training of staff that is required to undertake this form of isolation. Expansion of human Tregs that continue to be $CD25^{+}$ and CD127low is possible with the protocol described. Further phenotyping of this expanded cell population with both intracellular FoxP3 and Treg functional markers such as CTLA4 is further required. These markers will be included on flow cytometry panel used on the planned Treg liver infusion experiments.

A limitation of the data presented is the low number of experiments and the inability to achieve a high level of consistency with the Treg expansion. The number of experiments performed was limited by the resources available. An accurate assessment of the suppressive ability through either measurement of Treg specific demethylated region (TSDR) or suppression assays, was not undertaken. These methods would have given a more accurate assessment of the Tregs suppressive potency and avoided the reliance on cell markers as a surrogate. Hypomethylation of the TSDR indicates Treg lineage

commitment and stable FoxP3 expression[170]. Measurement of TSDR methylation status is possible with molecular techniques and would have served as a good marker for lineage stability. However, this was not possible due to the small amount of Treg numbers achieved at the end of expansion, and the even lower numbers reclaimed after infusion (described in chapter 5). The assessment of suppressive ability via suppression assays was also not possible due to the low total numbers of Tregs. Isolating and expanding Tregs that are of the standard accepted for administering to humans is expensive at present, and to justify the cost the benefit must be great. It may well be that the upfront healthcare cost of therapeutic Tregs would be offset by a prolonged period without immunosuppression and its associated complications. As advances in Treg isolation and expansion techniques occur, it is likely that the overall cost of this novel therapy will fall.

# Chapter 5 – Ex-vivo Regulatory T-cell infusion

## 5.1 Background

The overall aim of investigating the localisation and phenotypic stability of Tregs administered ex-vivo required investigation in an experimental model that has comparability to clinical practice. To the author, and the wider team's knowledge, this had not been performed in a human model before.

To assess the localisation of ex-vivo administered Tregs, the donor livers vasculature must be accessed to deliver the cells and therefore any experimental model must allow for this. In addition, re-isolating the cells after infusion from the liver tissue must be achievable in a pragmatic manner. Furthermore, both of these aims had to be achieved using a model that was economical and could be implemented with the available financial resources. Therefore, we utilised two different models to investigate our aims. The first was a non-clinical custom built liver wedge perfusion model (Methods section 2.15). The second was a whole liver NMP device currently used in clinical practice (Methods section 2.16), which allowed us to compare if our findings from the wedge perfusion model were clinically translatable.

This chapter outlines the results obtained during:

1. Optimisation on the wedge perfusion model
2. Treg wedge perfusion experiment results
3. Optimisation of the Whole liver (Liver Assist, XVIVO) perfusion model
3. Whole liver (Liver Assist, XVIVO) perfusion experiment results

## 5.2 Optimisation on the wedge perfusion model

The wedge perfusion model utilised in these experiments was adapted to that described by Wiggens et al (2017). This wedge perfusion model was modified to include two separate

perfusion circuits working in parallel. This allowed both a control and experimental lobe to be connected and perfused.

To optimise the cell labelling process, perfusion circuit, flow cytometry and immunofluorescence staining panels we required a cell type that was easily obtainable. We therefore used human $CD4^+$ or $CD3^+$ T-cells obtained through immunomagnetic isolation of human PBMCs. The characteristics of the five optimisation experiments are demonstrated in table 5.1.

**Table 5.1. Details of liver wedge model optimisation experiments**

| Optimisation Experiment | Graft type | Weight of liver wedge | | Duration (hours) | Cell type† | Number infused | Changes implemented |
|---|---|---|---|---|---|---|---|
| | | Experiment | Control | | | | |
| 1 | DBD | ≈50g | - | 1hr | $CD4^+$ | $25x10^6$ | Not applicable (First attempt) |
| 2 | DCD | - | - | 15hrs | $CD3^+$ | $55x10^6$ | 1. Incorporation of second wedge (control lobe)<br>2. Longer perfusion time<br>3. Larger number of cells infused |
| 3 | DCD | 39g | 29g | 14hrs | $CD3^+$ | $12x10^6$ | 1. Flow cytometry performed on wedge at end of experiment<br>2. Volume of cells comparable to what can be achieved with expanded Tregs |
| 4 | DBD | 120g | 130g | 13hrs | $CD4^+$ | $15x10^6$ | 1. Attempted experiment with larger wedge of liver tissue |
| 5 | DCD | 41g | 40g | 18hrs | $CD4^+$ | $7.8x10^6$ | 1. Utilised non-steatotic donor liver<br>2. Reverted to smaller wedge of liver tissue |

†5 optimisation experiments performed using an abundant an easily obtainable cell type (CD3+ or CD4+) that was isolated via immunomagnetic methods

### 5.2.1 Wedge optimisation experiment 1

This experiment was performed to ensure all the perfusion equipment (pump, tubing, adapters and cannulae) were compatible, the cell labelling process worked adequately, and that the cells would be visible on confocal microscopy after immunofluorescence staining. To achieve this, only a single circuit perfusion model was required. The equipment set up in this initial experiment is displayed in Figure 5.2. Given the short perfusion time, and the desire to test whether the immunofluorescent cell labelling worked, we infused a large number of cells (25 million). The design is demonstrated in Table 5.1.

The cell labelling with CMTPX was effective and the immunofluorescent microscopy panel was tested with acceptable results. The panel involved primary antibody staining for E-cadherin and CD31, with secondary fluorescent staining as per Table 2.3 (methods chapter). The tissues were also labelled with DAPI. It was noted that a large amount of autofluorescence was present in the liver microscopy, likely from lipofuscin within the hepatocytes. This made true identification of the CMTPX labelled cells challenging. Figure 5.3A demonstrates a CMTPX labelled cell and the inset (B) shows that it was within the sinusoids which are evident by CD31 staining. Determining areas of autofluorescence was possible as these areas appear bright on all channels individually (including the CMTPX channel) (Figure 5.3C-F).

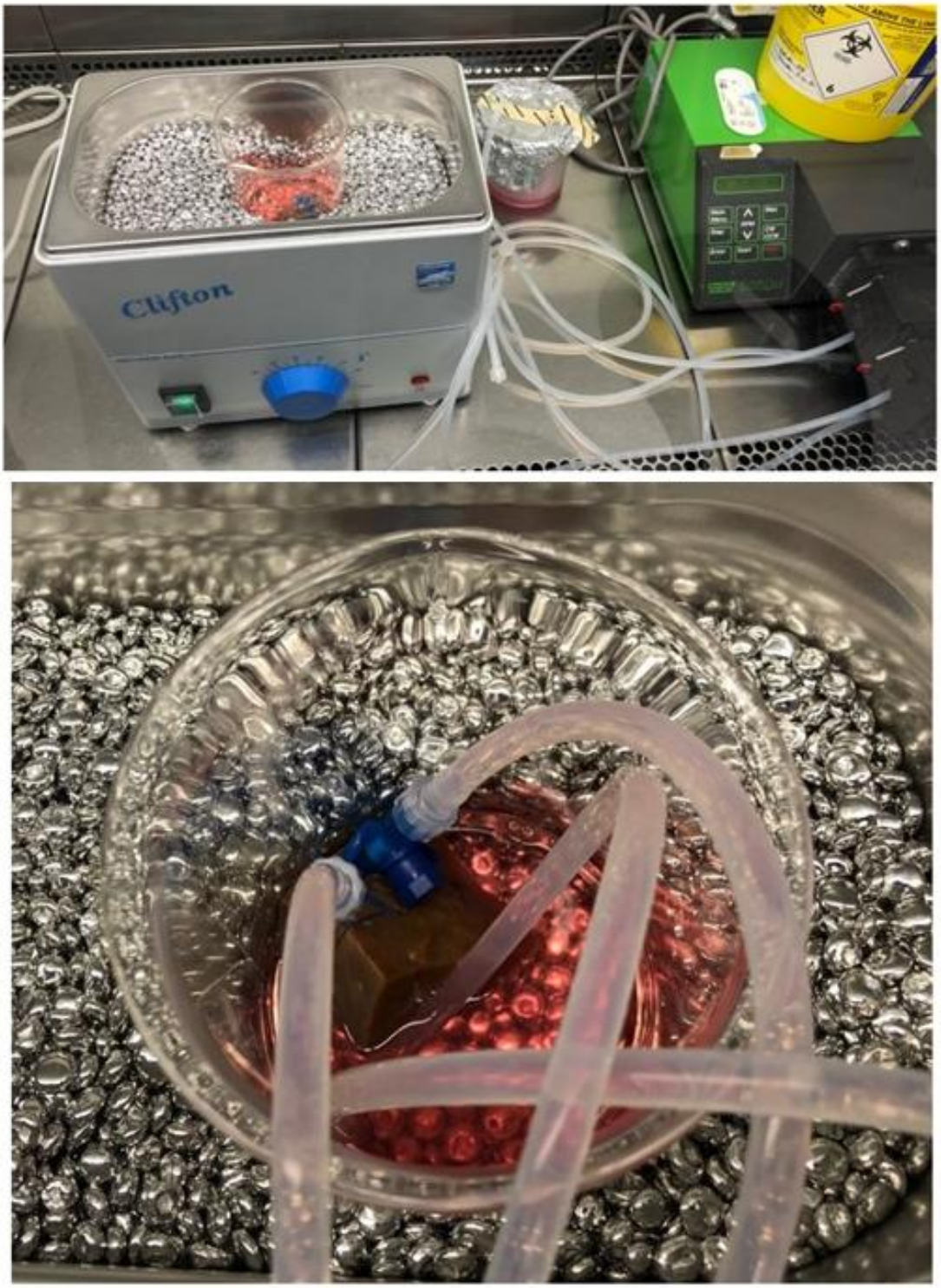


**Figure 5.2.** Image demonstrating the setup of the wedge perfusion circuit with only a single wedge of liver connected. Perstaltic pump (Watson-Marlow 505S) can be seen in top picture.

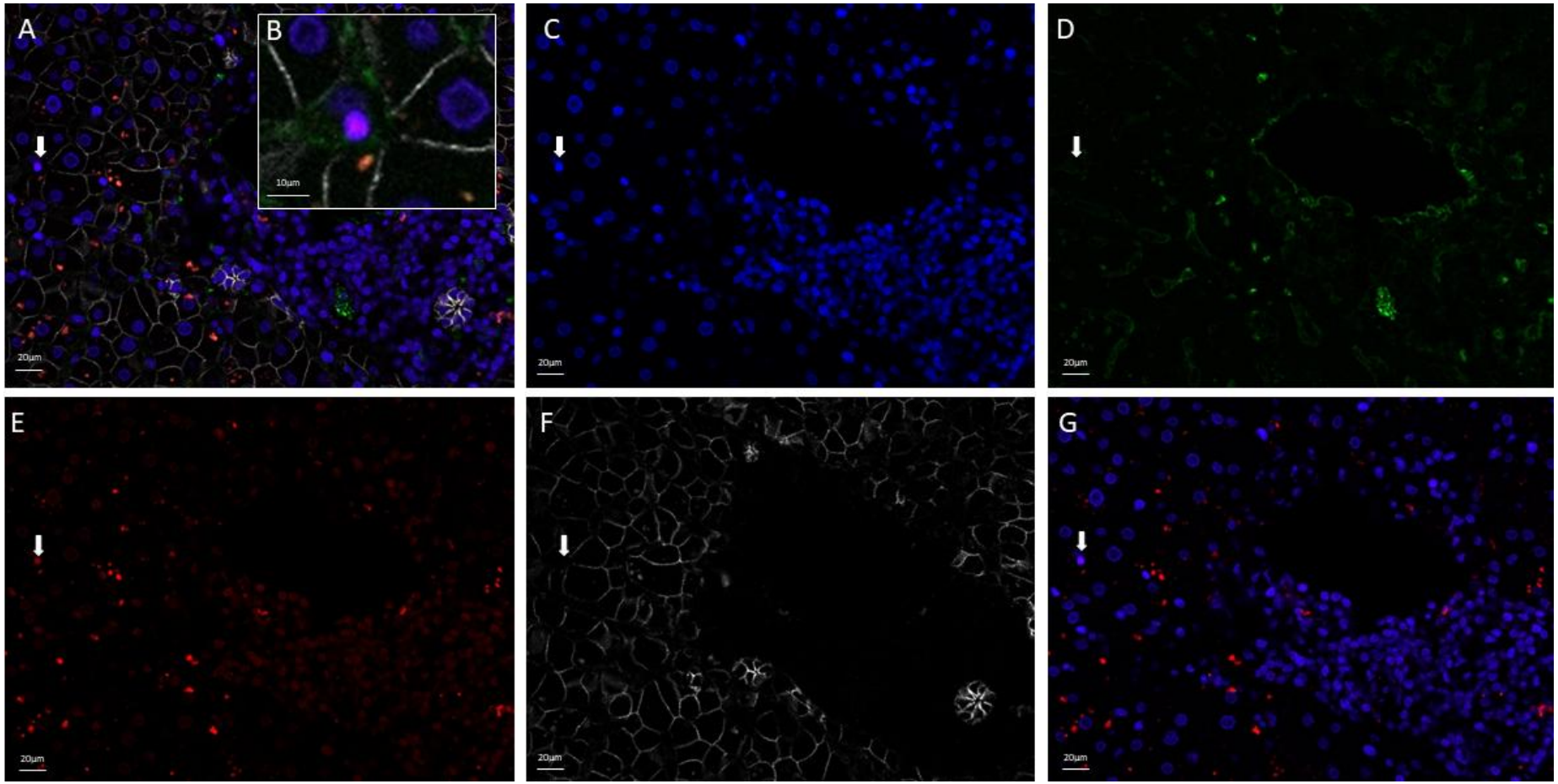


**Figure 5.3. Optimisation wedge perfusion experiment 1.** Biopsy of stained liver tissue after infusion with CMTPX labelled $CD4^{+}$. Same image location for A-G. A) This demonstrates an image with all channels [E-cadherin(white), CD31 (Green), DAPI (Blue), CMTPX (Red)] and a close up of the labelled cell is shown in inset B. The cell (white arrow) is between hepatocytes and within a CD31 stained (green) sinusoid. C) DAPI channel open only. Cell (white arrow) evident. D) CD31 channel open only and cell not evident. E) CMTPX channel open only, and cell evident. F) E-Cadherin channel open only and cell not evident. G) Both CMTPX (red) and DAPI (Blue) channel open giving cell the pink appearance.

### 5.2.2 Wedge optimisation experiment 2

**Amendments from previous experiment:**

- Incorporation of second wedge into perfusion circuit
- Longer duration of perfusion to assess for transendothelial migration
- Larger number of cells infused

After the successful utilisation of a single wedge perfusion circuit in the first optimisation experiment, a model that had two liver wedges was attempted. The benefit of this experiment set up was that one wedge could serve as a control lobe for both flow cytometry and microscopy analysis. The perfusion model was also required to be stable enough so it could be left overnight without staff supervision. This would allow more time for cell migration into the parenchyma and more reflective of clinical practice in which NMP time often exceeds 12 hours (Figure 3.5). The set up of the two wedge perfusion circuit used in this and all subsequent experiments is shown in Figure 2.6, and a schematic showing how cells were administered is shown in figure 2.7. A large number ($55x10^6$) of $CD3^+$ cells were labelled with CMTPX and infused as row 2 B in table 5.1.

### 5.2.3 Wedge optimisation experiment 3

**Amendments from previous experiment:**

- Flow cytometry performed on cells pre infusion, and both perfusate and LDLs post-perfusion
- Lower number of cells infused, closer to number that can be achieved following Treg expansion.

This experiment tested whether the CMTPX labelled cells were present in the perfusate, and LDLs at the end of the perfusion period. It is possible that a portion of the infused cells may not stay within the liver, and rather transit through the vasculature and stay in the perfusate.

Therefore, prior to infusing the cells they were stained with a simple flow cytometry antibody panel [Live-Dead (APC-Cy7a), CD3 (BV421)] and this was repeated on cells isolated from the perfusate and LDLs at the end of the experiment. The CMTPX is fluorescent and has an emission spectrum that corresponds to the PE-Texas red spectra and can be captured on this channel.

As demonstrated in figure 5.4, live CMTPX positive cells could be identified on flow cytometry in the experimental perfusate and LDLs. These were not evident in the control perfusate or LDLs. Being able to identify the CMTPX positive cells will be required for the gating strategy when Treg cells are infused. Being able to gate on CMTPX positivity will allow further assessment of suppressive function.

An interesting finding of this experiment is that there was a clear CMTPX- CD3+ population in both perfusates. This signifies that a liver resident lymphocyte population must come out of the liver wedge during the perfusion period. Despite a lower number of cells being infused, the CMTPX+ cells were still visible on microscopy.

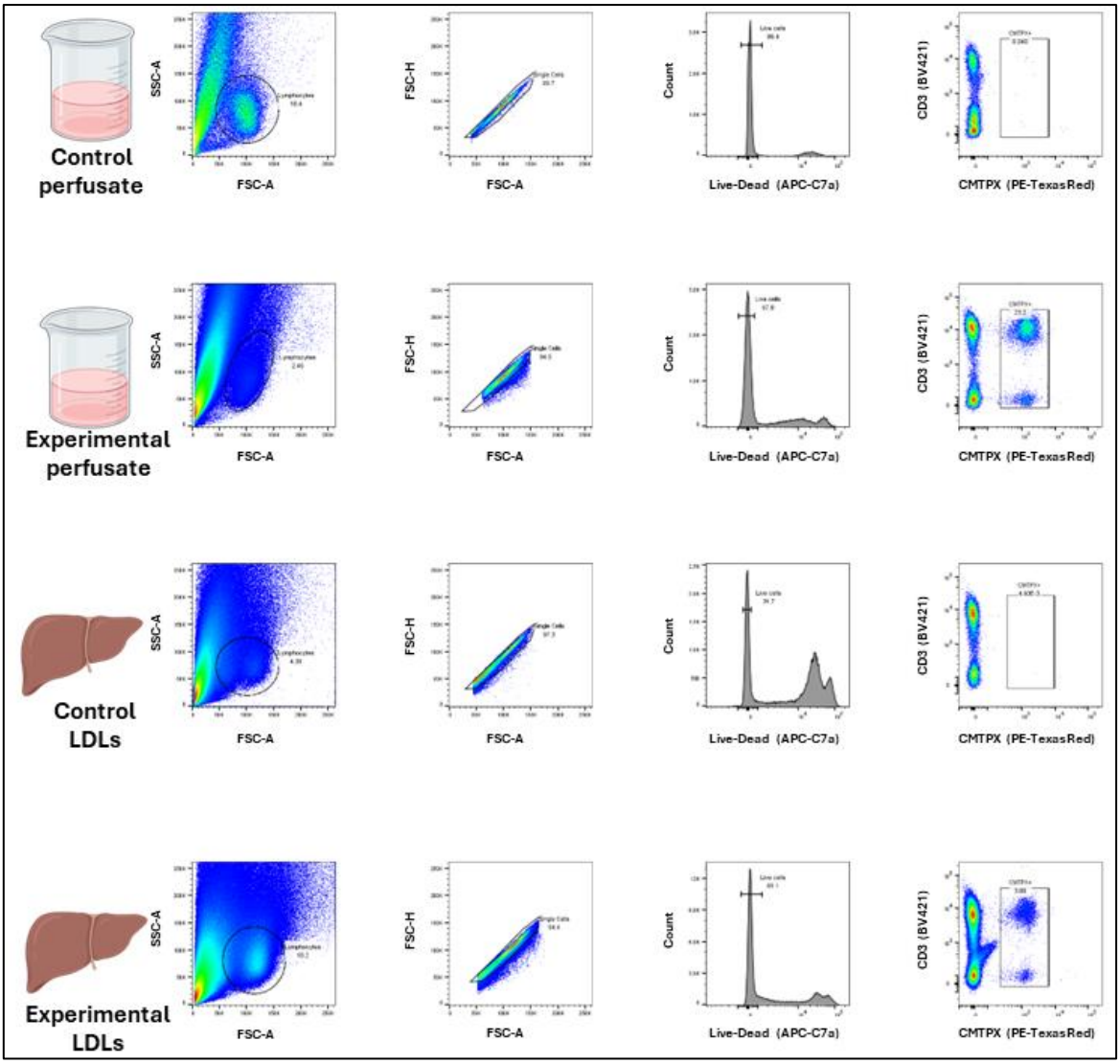


**Figure 5.4**. **Flow cytometry results from both perfusate and liver tissue after CMTPX labelled wedge perfusion (Optimisation experiment).** Both the control and experimental control perfusate underwent repeated centrifugation to obtain a cell pellet, and the liver wedges underwent LDL isolation as per methods 2.3. Gating was based on lymphocytes, single cells and then live cells. The scatter plots in the far right column show that CMTPX+ CD3+ cells were isolated from both the experimental perfusate and LDLs, but not the control samples. Therefore, these are the infused cells and gating on the CMTPX+ population will be required to perform further phenotyping of Tregs.

### 5.2.4 Wedge optimisation experiment 4

**Amendments from previous experiment:**

- Larger wedge of donor liver used to determine if more LDLs isolated

In this experiment, we used larger wedges of liver from the donor liver. This was in an effort to see if more of the infused cells remained in the liver tissue. Results from optimisation experiment 3 (figure 5.4) indicated that a portion of CMTPX positive cells remained in the perfusate. This was to explore the possibility that migration of the infused Tregs reaches a saturation point. The wedges of liver were 120-130 grams in weight. The perfusion and cell quantity were similar, however in this experiment we used $CD4^+$ enriched cells rather than $CD3^+$.

The flow cytometry and microscopy results are shown in figure 5.5 and 5.6 respectively. Despite the infused cells being pre-enriched for CD4 positivity, the majority were $CD4^-$ according to figure 5.5. An alternative is that the CD4 FITC staining did not work. It is clear that the CMTPX was very efficient in labelling the cells in solution, with all cells being positive for CMTPX. The perfusate of both the control and experimental lobes underwent repeated centrifugation and staining. A small CMTPX+ cell population was identified in the experimental perfusate. After LDL isolation and staining, a CMTPX+ cell population could not be identified. The wedges of liver that were subjected to LDL isolation were larger than the previous experiment and the donor liver was macroscopically steatotic. At the end of isolation, the pellet contained a large amount of debri, and this proved problematic. The extent of macrovesicular steatosis is evident in figure 5.7, and this likely contributed to the low yield of lymphocytes at the end of isolation.

The confocal microscopic assessment demonstrated that CMTPX positive cells were present within the liver tissue, and the cells had migrated out of the sinusoids and into the

parenchyma. Figure 5.6 demonstrates a CMTPX positive cell that has travelled out of the periportal area, and is likely between hepatocytes. The CMTPX positive cell (white arrow) can be differentiated from autofluorescence (red arrow) due to its colour, shape and the fact it is not visible on the Ecadherin (white) channel.

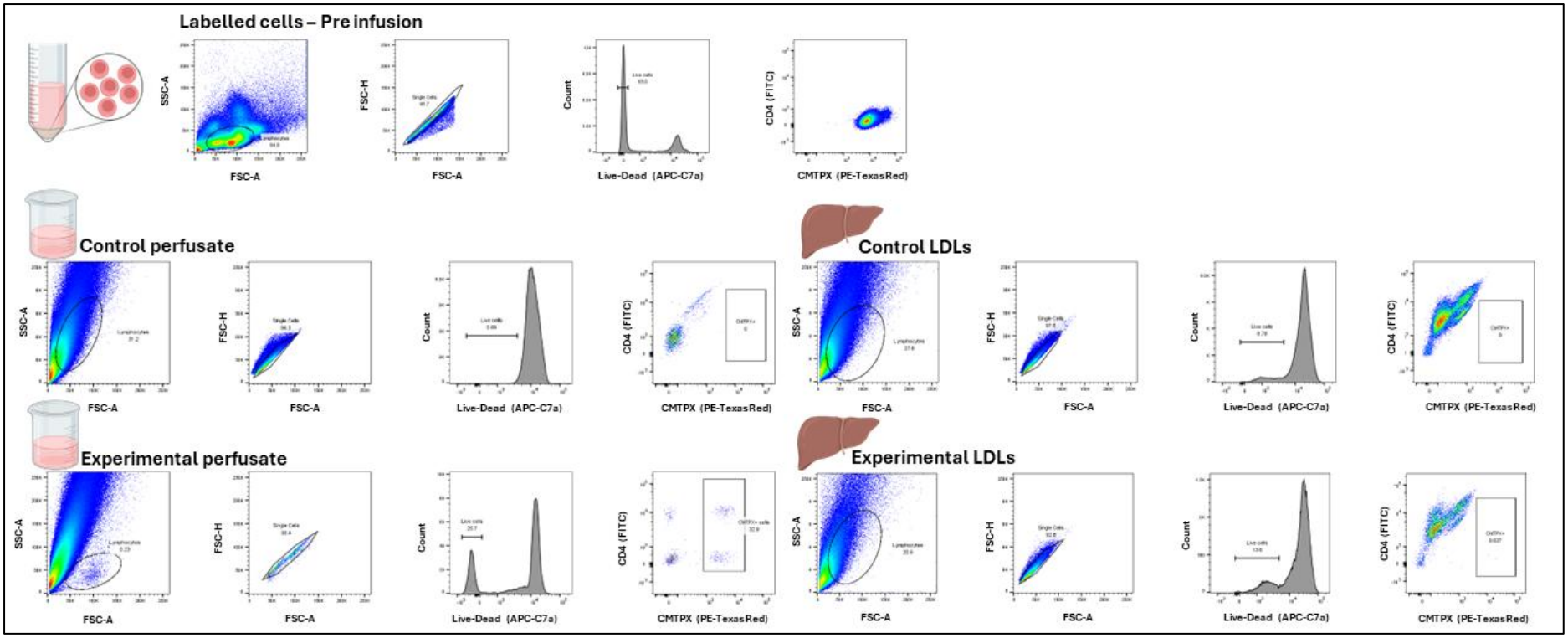


**Figure 5.5**. **Flow cytometry results of wedge perfusion optimisation experiment 4**. Flow cytometry results of labelled cells pre-infusion and both perfusate and LDLs post infusion in top panel. The CMTPX labelling process is very efficient, with nearly 100% of the cell sample taking up this fluorescent label. This was consistent across all experiments. CD4+ CMTPX + cells were identified in the experimental perfusate, and not the control perfusate. The CMTPX positive cell population could not be identified in the LDLs in either wedge. There was a large amount of debri, and a low proportion of live cells at the end of LDL isolation as evident on the live-dead histograms for both the experimental and control LDLs. As a consequence, there was a large amount of autofluorescence on the CD4 vs CMTPX scatter plots.

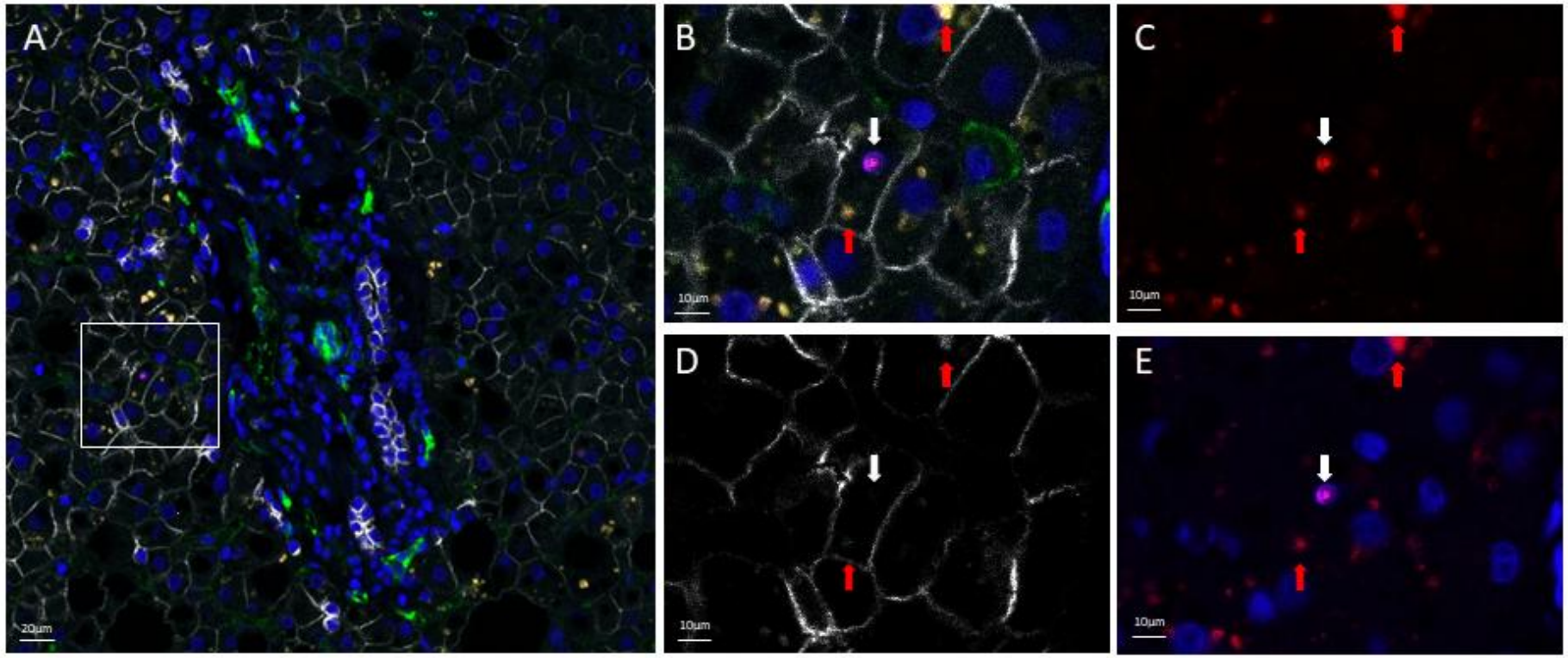


**Figure 5.6**. **Confocal microscopy of optimisation wedge perfusion experiment 4**. Image of experimental wedge liver biopsy at the end of perfusion period. A) Zoomed out image with all channels [E-Cadherin (white), CD31 (Green), DAPI (Blue), CMTPX (Red) showing location of cell in relation to portal tract. White box area of slide is demonstrated in B-E. B) Close up image of cell (white arrow). Autofluorescence displayed by red arrows. C) CMTPX channel only showing cell and and areas of autofluorescence (red arrows). D) E-cadherin channel only. E) DAPI and CMTPX channel open showing pink cell and areas of red autofluorescence.

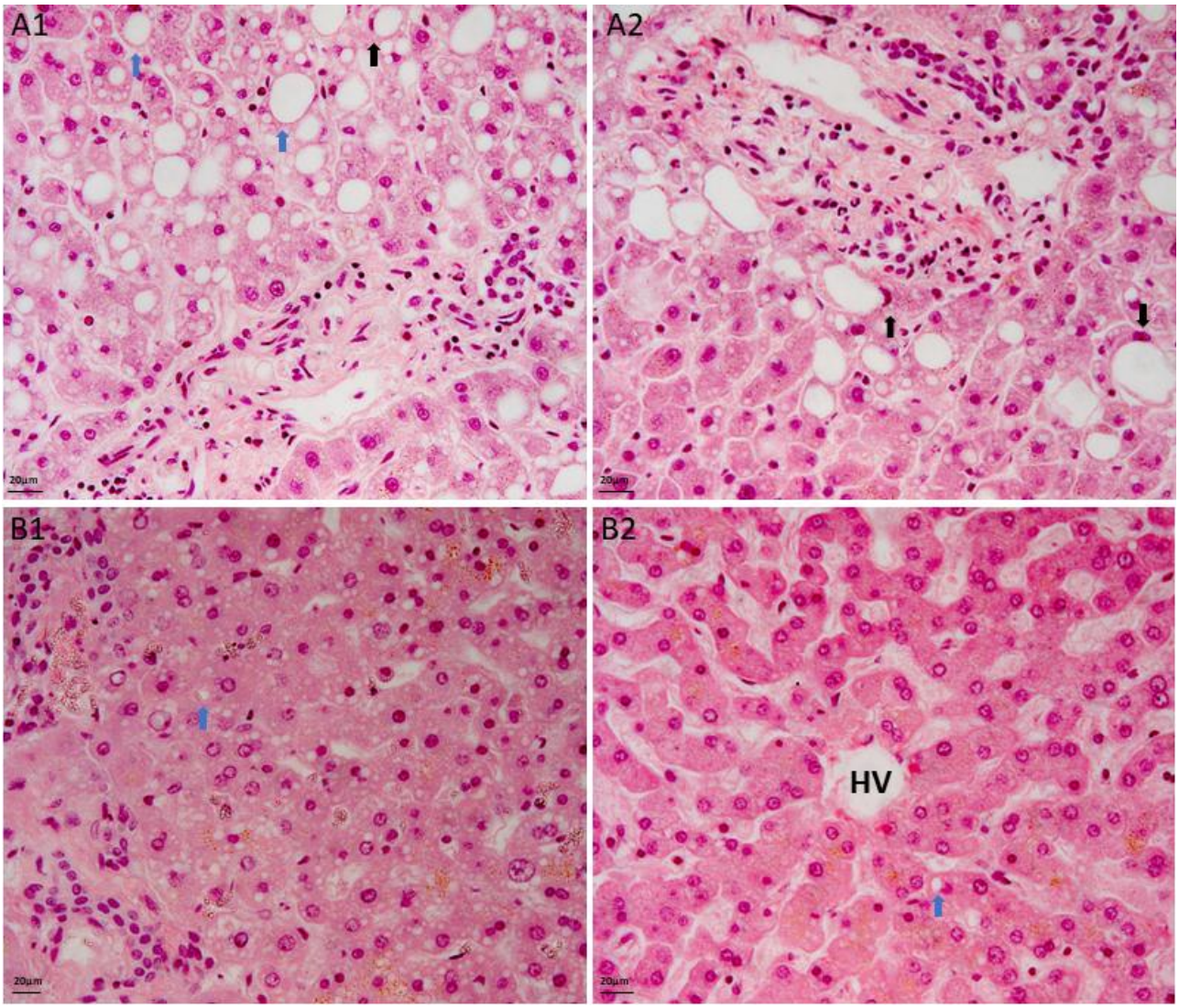


**Figure 5.7. Comparison of steatosis.** Haematoxylin and eosin staining of wedge perfusion optimisation experiment 4 (A1, A2) and 5 (B1 and B2). A1 is an image of a steatotic liver (optimisation 4) pre-infusion and A2 is post infusion of CMTPX labelled cells. Large droplet macrovesicular steotosis is evident (blue arrows). These large fat droplets displace the hepatocyte nucleus. B1 & B2 are from a non-steatotic donor liver with only small areas of microvesicular steatosis (Blue arrows). These droplets do not displace the cell nucleus.

### 5.2.5 Wedge optimisation experiment 5

**Amendments from previous experiment:**

- Utilised non-steatotic donor organs
- Reverted back to smaller wedge of liver (30-40 grams)

Following the last experiment, it was decided that optimal analysis of the LDLs at the end of perfusion would require a non-steatotic donor organ. Therefore, we were more selective in the donor organ selected. Approximately 8 million $CD4^+$ enriched T-cells were infused into the experimental lobe. Carwas taken with the LDL isolation to eliminate as much debri as possible during the process.

The flow cytometry and confocal microscopy results are demonstrated in figure 5.8 and 5.9 respectively. The CMTPX labelling showed high efficiency and avidity for the cells, with all of the cells staining positive. Although the infused cells had been through a $CD4^+$ enrichment process, the majority were $CD4^-$. The lower amount of macrovesicular steatosis resulted in less debri at the end of the isolation process, and a higher density of lymphocytes. This is evident on the SSC-A vs FSC-A scatter plots in figure 66, as based on size and granularity there are clear lymphocyte clouds in all samples except the control perfusate. In this experiment, live CMTPX labelled cells were isolated from both the perfusate and LDLs at the end of the experiment (Figure 5.8). Confocal microscopy demonstrated the CMTPX positive cells within the liver parenchyma (Figure 5.9)

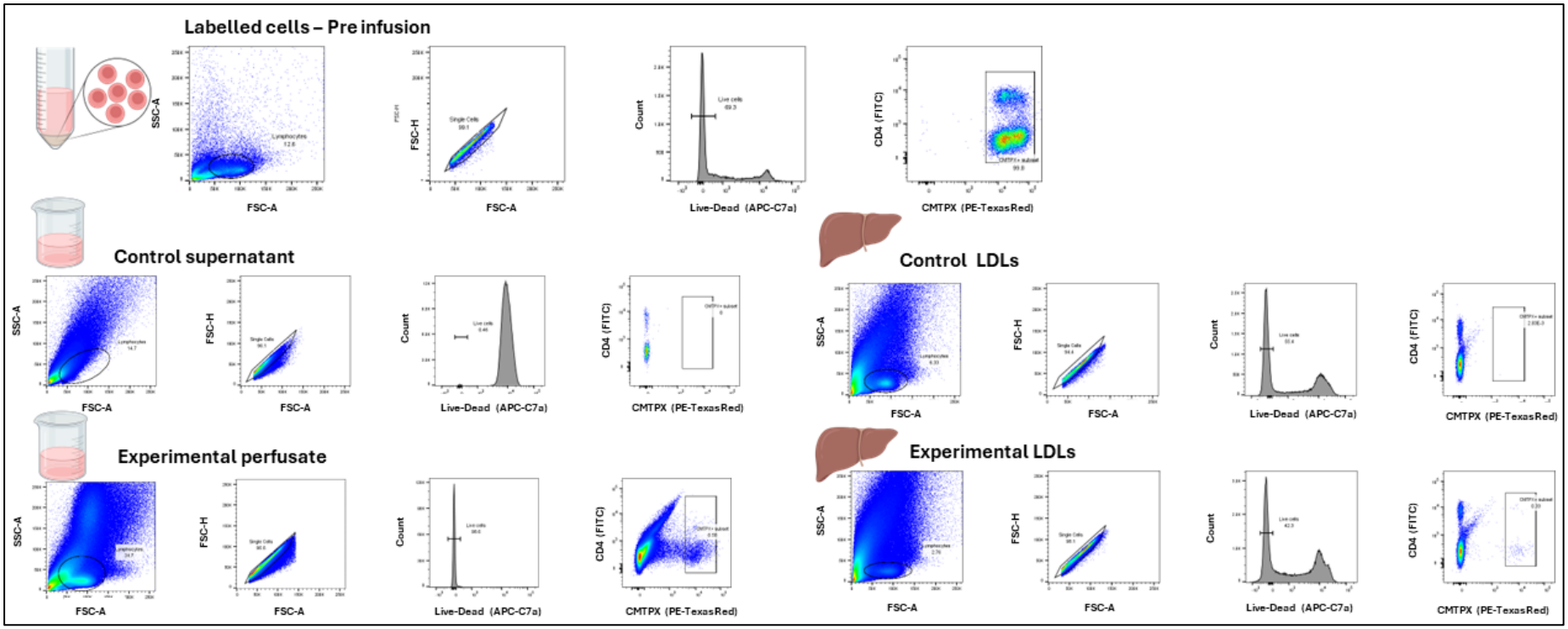


**Figure 5.8**. Wedge perfusion **optimisation experiment 5 flow cytometry result.** Flow cytometry results of optimisation experiment 5. Pre-infusion cells were stained after they were labelled with CMTPX (Top panel). A lymphocyte cloud evident in the experimental perfusate, control and experimental LDLs which appears separate from the fluorescent debri. The control supernatant demonstrates minimal cells, as evidenced by absence of a clear lymphocyte cloud and minimal live cells. The live-dead histogram of the control supernatant shows that the majority of the pellet obtained is dead debri (stained positive for the viability dye). A CMTPX positive cell subset is evident in both the experimental perfusate and the experimental LDLs.

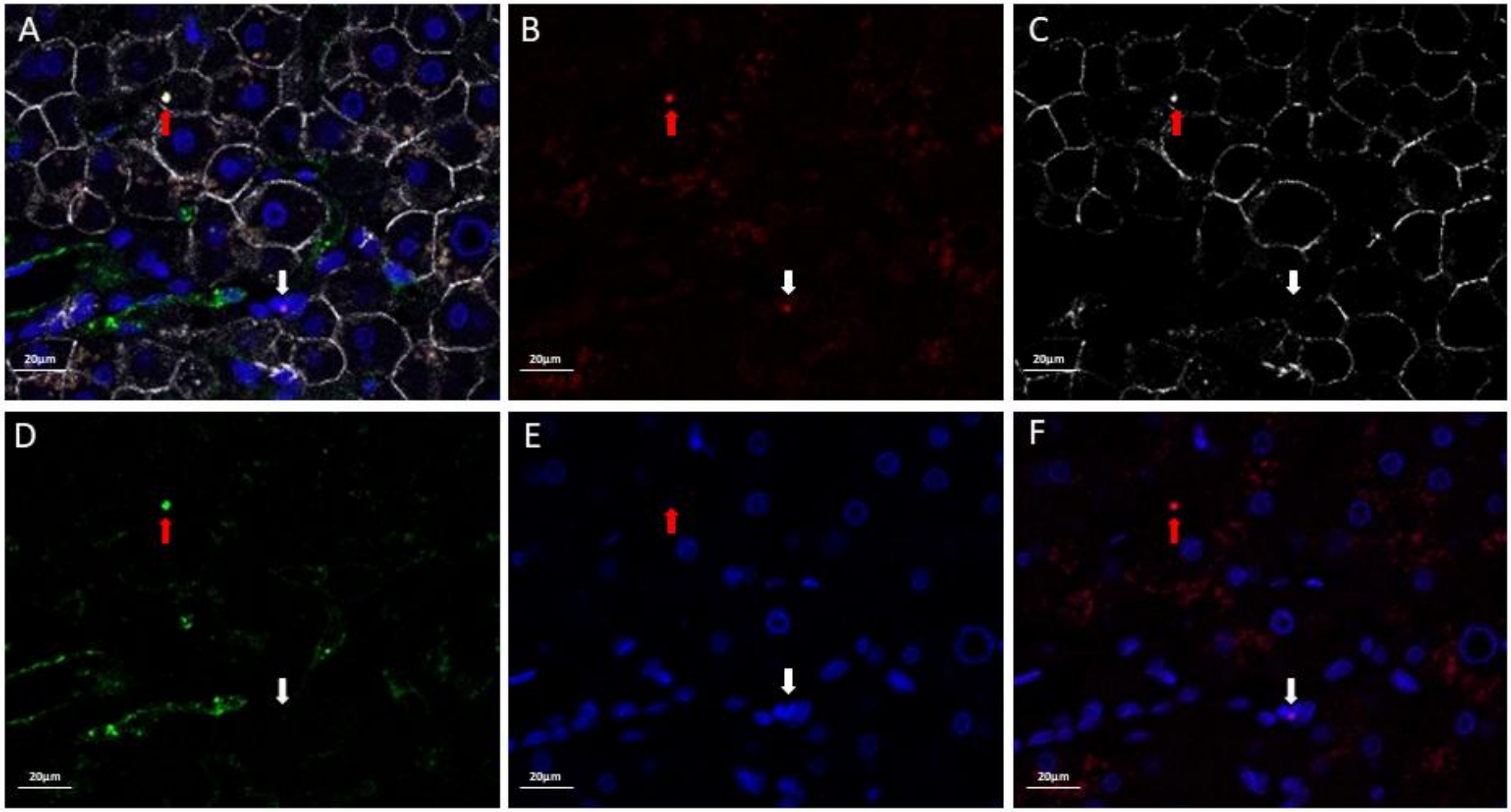


**Figure 5.9. Confocal microscopy from wedge perfusion optimisation experiment 5.** Image of experimental lobe showing a CMTPX positive cell (white arrow). A) All channels [E-cadherin (white), CD31 (green), DAPI (Blue), CMTPX (Red)] open showing cell (white arrow) and autofluorescence (Red arrows). B) CMTPX channel only C) E-cadherin channel only D) CD31 channel only E) DAPI channel only F) DAPI and CMTPX channels both open.

### 5.3 Ex-vivo wedge perfusion experiment results

Following the experience and knowledge gained during the optimisation experiments, we proceeded to perform experiments using expanded Tregs. Numerous logistical challenges were faced obtaining suitable donor livers at the 28 day point of Treg expansion, so some Tregs remained in culture for slightly shorter or longer periods. In a similar manner, the final volume of cells available at the end of culture was variable. The results are summarised in Table 5.2 below.

Table 5.2 Summary of results from wedge and whole liver experiments

| Wedge perfusion experiments | | | | | | | |
|---|---|---|---|---|---|---|---|
| Number | Duration | Cell volume | Flow cytometry identification of CMTPX+ Cells | | | | Confocal Microscope ID of CMTPX+ Cells |
| | | | Control LDL | Control Perfusate | Exp LDL | Exp Perfusate | |
| 1 | 22 hours | 3.5 million | No | No | No | No | Yes |
| 2 | 15 hours | 9.5 million | No | No | No | Yes | Yes |
| 3 | 16 hours | 15.5 million | No | No | No | Yes | Yes |
| 4 | 18 hours | 3.0 million | Not applicable | | | | Yes |
| 5 | 15 hours | 9.7 million | No | No | Yes | Yes | Yes |
| Whole liver perfusion experiments | | | | | | | |
| 1 | 4 hours | 75 million | Not applicable | | No | No | Yes |
| 2 | 4 hours | 45 million | | | Yes | No | Yes |

#### 5.3.1 Treg wedge perfusion experiment 1

During this experiment, 3.5 million expanded Tregs were infused into a 50 gram experimental wedge of liver and the control wedge was of comparable size (Figure 5.10). Cells were labelled with CMTPX as previously described in methods 2.6. The experimental wedge was perfused with TexMACS media for 4 hours whilst the cells were taken from culture, and stained with CMTPX. A small volume of cells was taken for flow cytometry

staining both before and after CMTPX labelling. After the cells were administered, the perfusion continued for 18 hours. The intracellular Treg marker, FoxP3, along with functional markers CD39, CTLA4 and TIGIT were included in the flow cytometry panel.

Figure 5.11 demonstrates the flow cytometry results of the post expanded Tregs both before and after CMTPX labelling. As demonstrated in both the labelled and unlabelled samples live-dead histograms, the majority was alive but there was a small dead population. The entire labelled sample was positive for CMTPX, and both had strong CD25 positivity. The FoxP3 expression of the CD25+ population was 42.2% (Figure 69).

The flow cytometry results of the perfusate and LDLs did not demonstrate any CD3+ CMTPX+ labelled cells in either the live or dead cell populations (Figure 5.12). The reason for this may have been due to the low number infused, or a sample processing error. Therefore phenotyping of the cells post infusion was not possible.

The confocal microscopy results are shown in figure 5.13. CMTPX positive cells were identified in the experimental lobe on the biopsy performed at the end of the perfusion period. The identified cells did not stain positive for FoxP3. Given the low proportion of FoxP3 positive Tregs in the infused sample, this is not surprising.

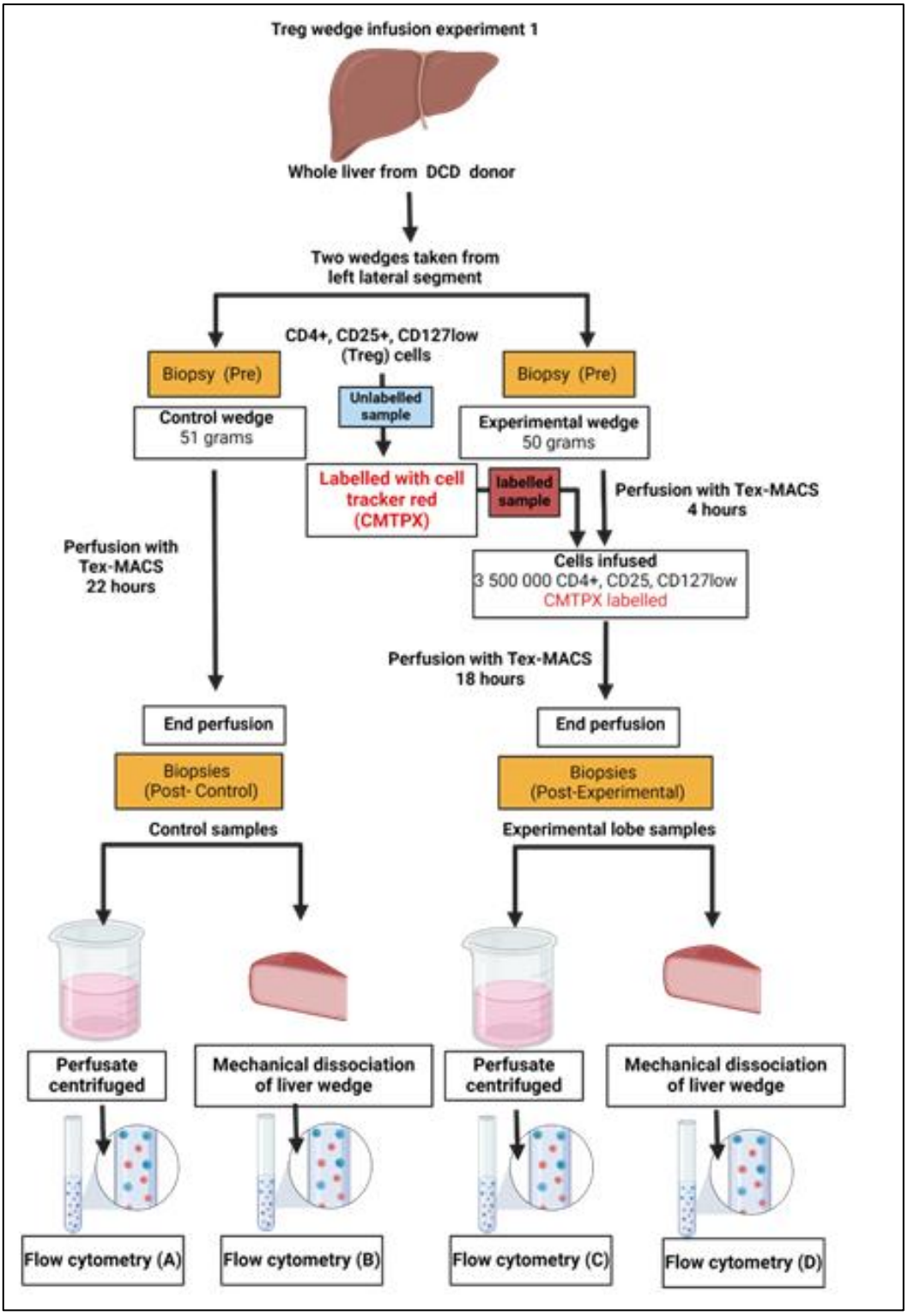


**Figure 5.10. Schematic of Treg wedge infusion experiment 1**. Diagram showing the cell quantity, weight of liver wedges and the duration of perfusion. Biopsies taken at two time points as per yellow boxes.

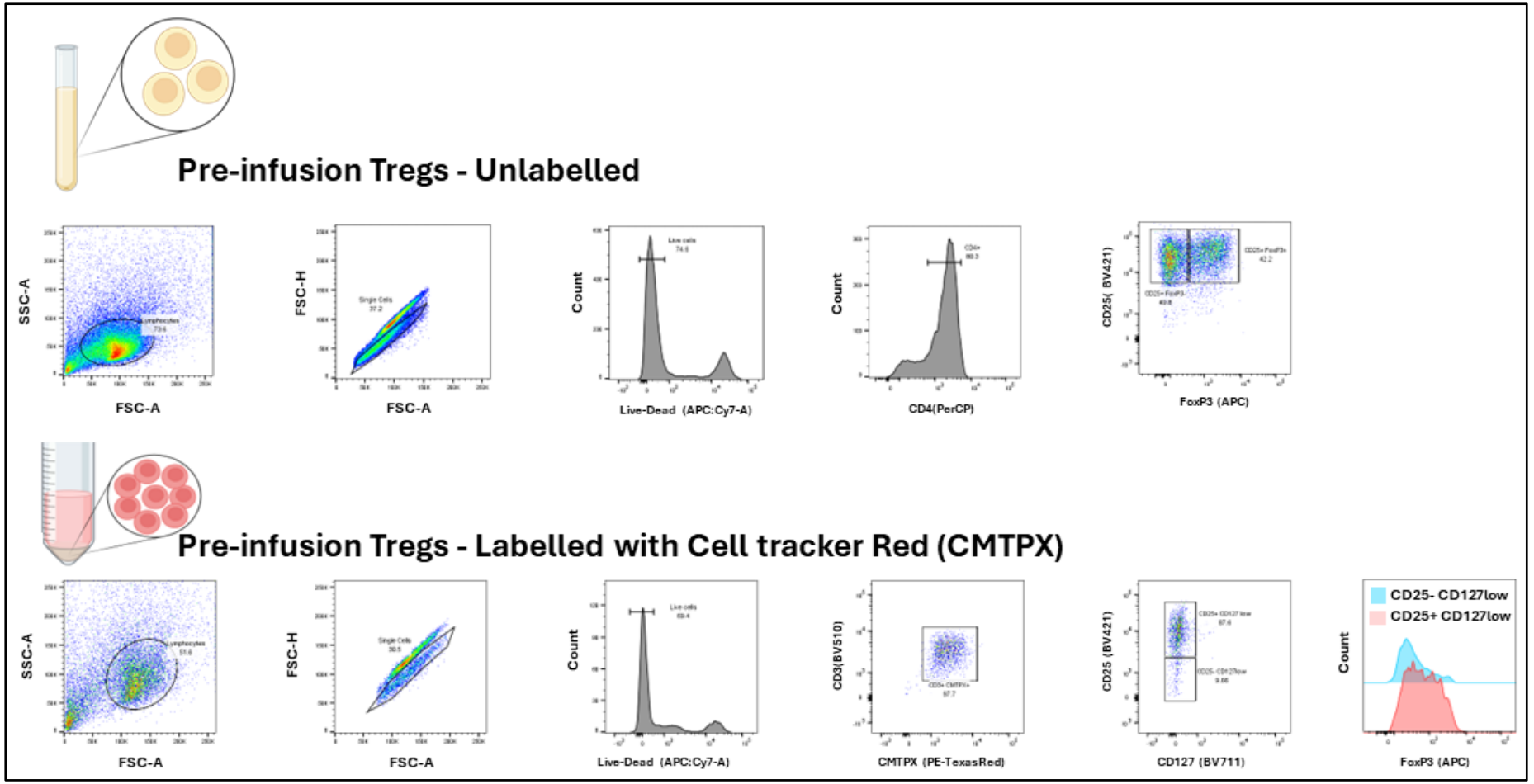


**Figure 5.11. Tregs used in wedge infusion experiment 1**. Flow cytometry results of the unlabelled and labelled Tregs used in wedge infusion experiment 1.

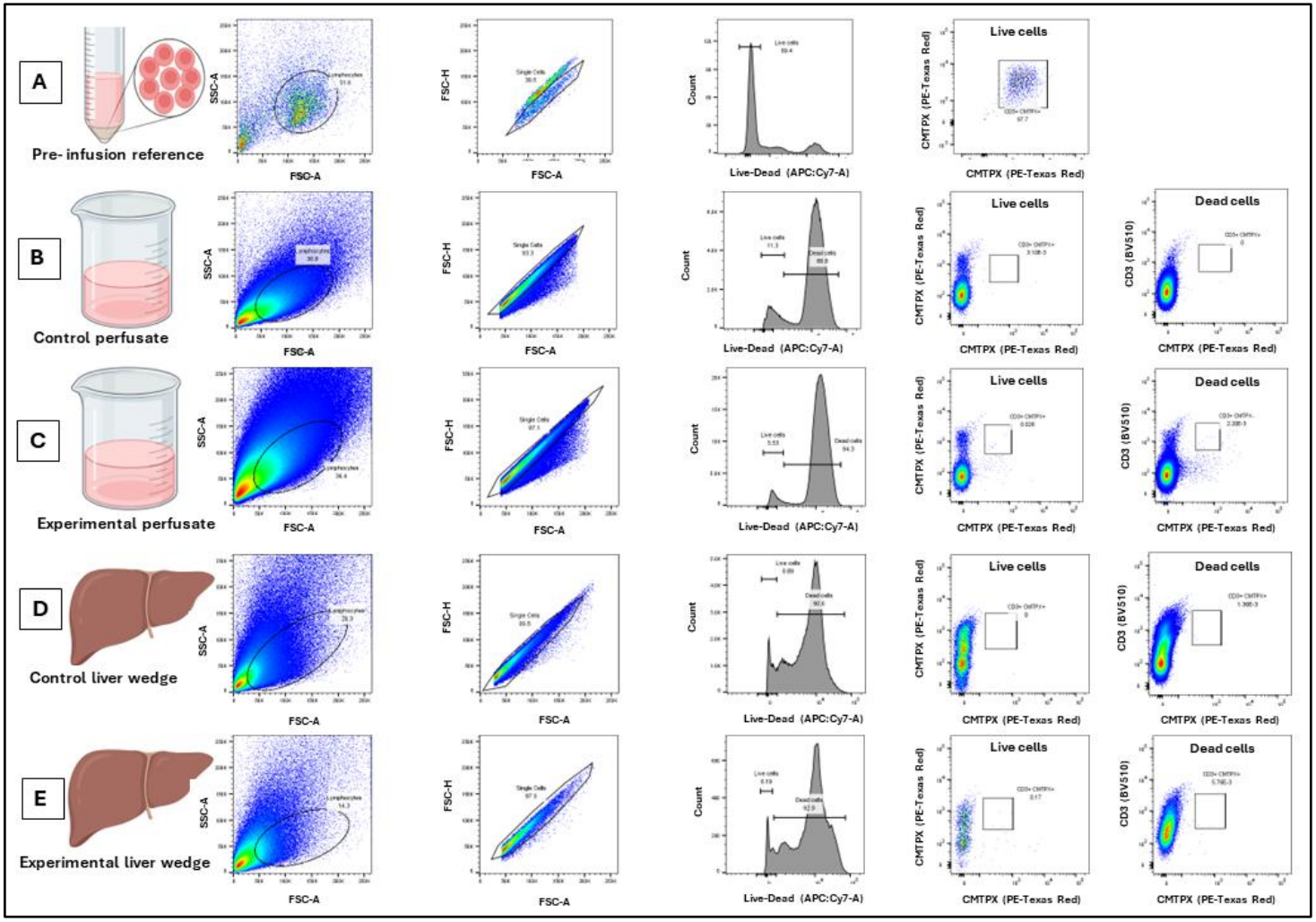


**Figure 5.12. Flow cytometry results of wedge infusion experiment 1**. Flow cytometry results of CMTPX labelled cells pre infusion (A), post infusion perfusate (B&C), post infusion LDLs (D&E). No $CD3^+$ $CMTPX^+$ cells isolated in either the live or dead cell populations in the perfusate or LDLs. $CMTPX^+$ cells were not identified in either of the experimental perfusate or liver tissue.

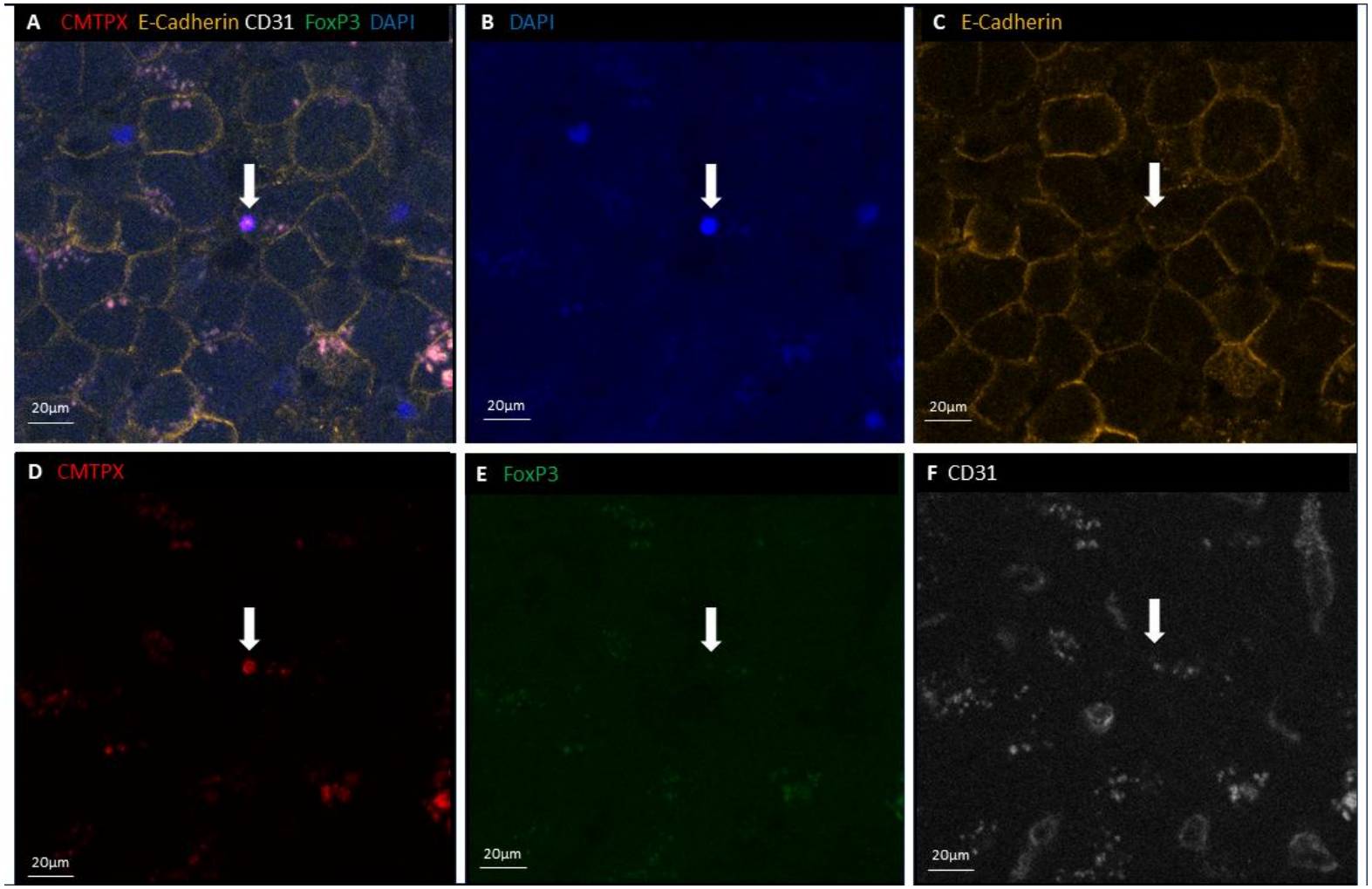


**Figure 5.13. Confocal microscopy results from Treg wedge infusion experiment 1**. Multicolour confocal images of experimental lobe liver biopsy at the end of infusion showing an ex-vivo infused CMTPX labelled cell. A) Cell evident as florescent pink and round structure when all channels activated. B) Cell seen as blue on DAPI staining due to DNA material within lymphocyte. C) Minimal florescence of cell E-cadherin channel in isolation. D) Red cell seen when CMTPX channel on by itself. E) No staining of cell for FoxP3 suggesting the labelled and infused cell was FoxP3$^{-}$. F) Image displaying CD31 staining.

### 5.3.2 Treg wedge perfusion experiment 2

In this experiment, 9.5 million expanded Tregs were infused into a 38 gram experimental wedge of liver and the control wedge was of comparable size (Figure 5.14). After administration of the CMTPX labelled Tregs, the perfusion was continued for 14 hours. The intracellular Treg marker, FoxP3, along with functional markers CD39, CTLA4 and TIGIT were included in the flow cytometry panel.

The phenotype of the cells pre infusion in both their labelled and unlabelled state are demonstrated in figure 5.15 and 5.16 respectively. The FoxP3 positivity of the CD25+ CD127 low population was approximately 80% in both samples. The expression of CD39, CTLA4 and TIGIT are shown in histograms with the FoxP3 positive and negative population overlaid.

Following infusion, $CD3^+$ and $CMTPX^+$ cells were isolated from the experimental lobes perfusate, but not the control lobe (Figure 5.17 B&C). A $CD3^+$ $CMTPX^+$ population was not identified in either of the experimental or control lobes LDLs. The phenotype of the $CD3^+$ and $CMTPX^+$ cells were compared to that of the $CD3^+$ and $CMTPX^+$ population of the labelled pre infusion sample (Figure 5.17, F). The FoxP3 positivity had reduced significantly, as indicated by the shape of the overlaid histograms. The expression of the other functional markers was similar when the pre and post samples were compared.

Confocal microscopy results of the experimental lobe are demonstrated in Figure 5.18. CMTPX positive cells were identified (Figure 5.18A) and these also had FoxP3 positivity on immunofluorescence staining (Figure 5.18E). After utilising three dimensional rendering, the cells appear to have migrated across the sinusoidal epithelium (Figure 5.18 I-J) and left the vascular compartment.

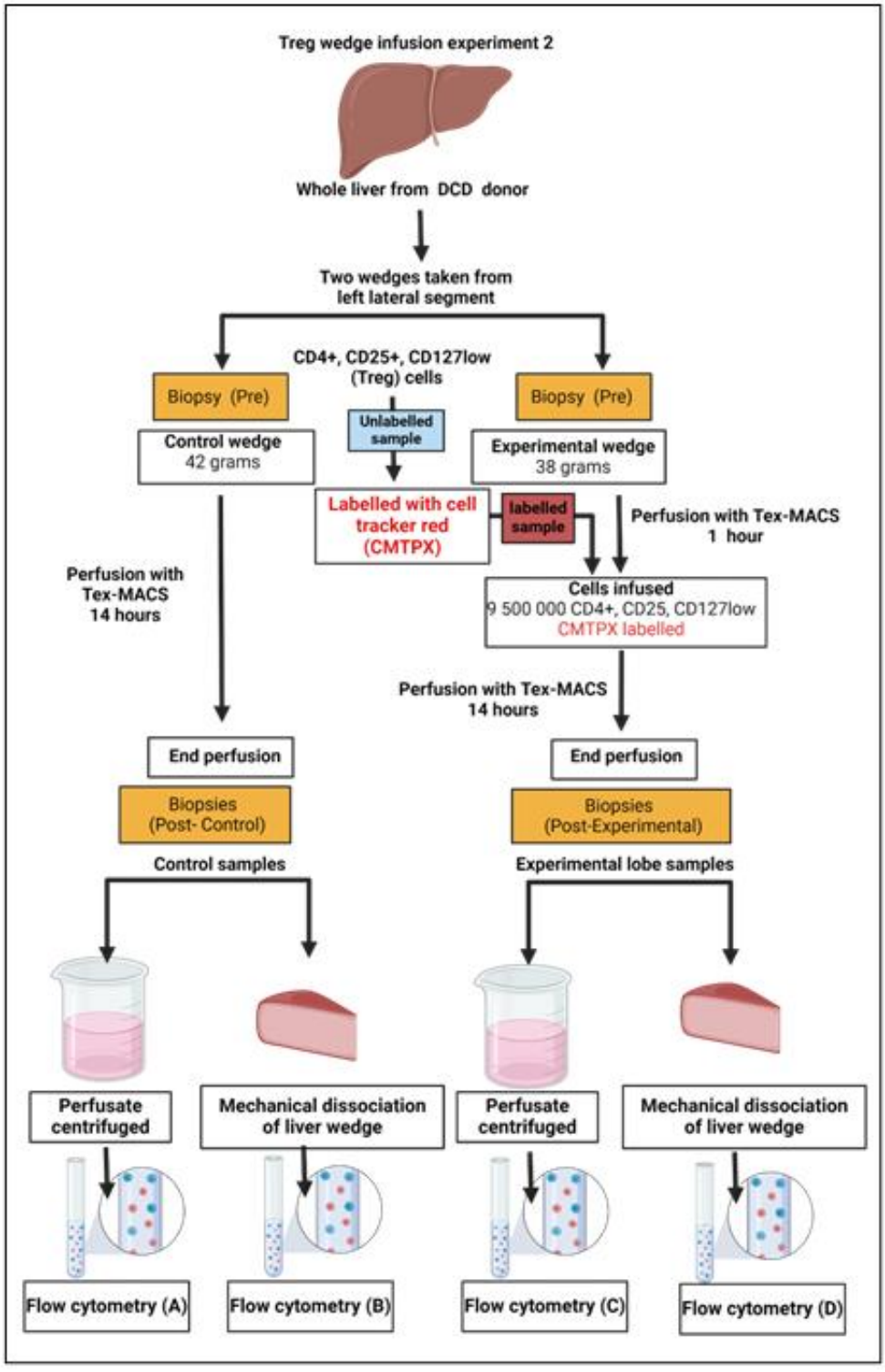


**Figure 5.14. Schematic of Treg wedge infusion experiment 2**. Diagram showing the cell quantity, weight of liver wedges and the duration of perfusion. Biopsies taken at two time points as per yellow boxes.

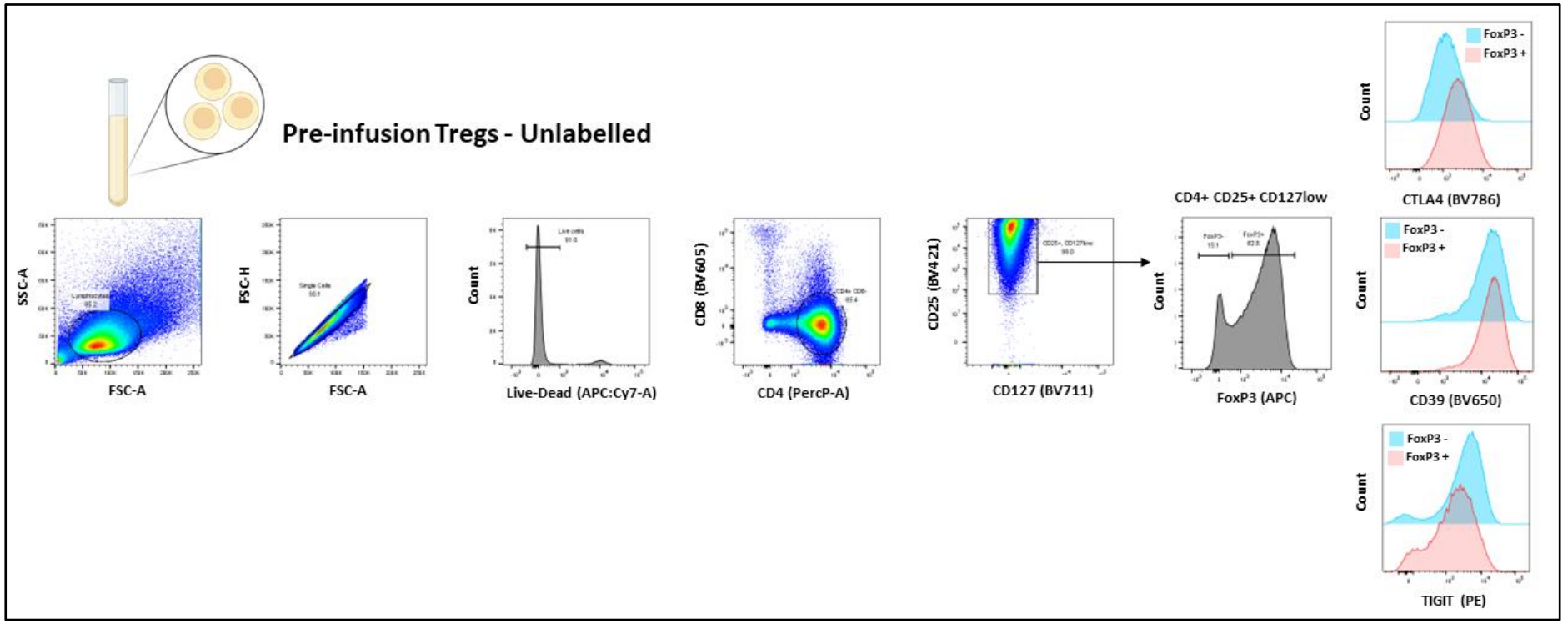


**Figure 5.15. Flow cytometry results of infused cells prior to labelling with cell tracker red (CMTPX) used in the wedge perfusion experiment 2.** Cell phenotype of Tregs prior to labelling. The FoxP3$^{+}$ and FoxP3$^{-}$ populations are compared on the histograms on the right.

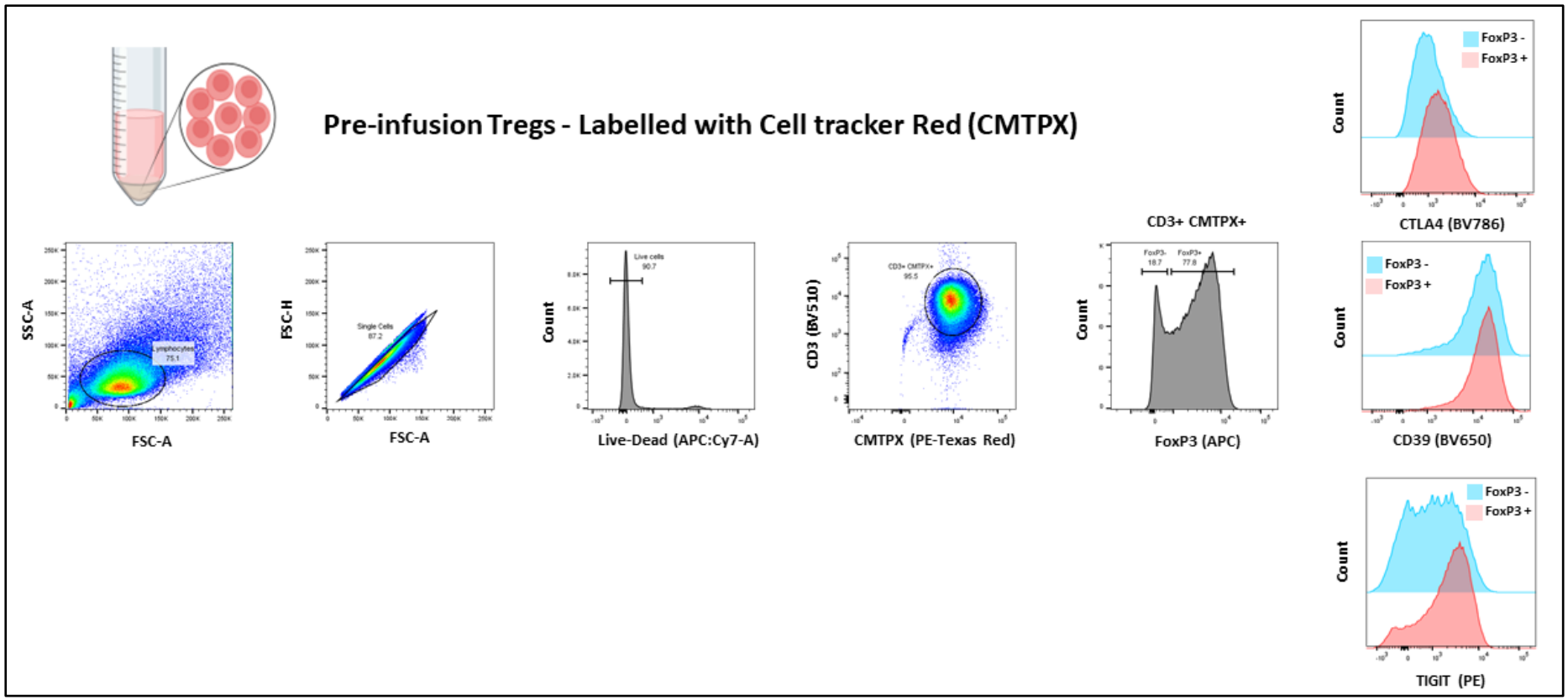


**Figure 5.16. Flow cytometry results of infused cells after labelling with cell tracker red (CMTPX) used in wedge infusion experiment 2.** Cell phenotype of Tregs after labelling. The FoxP3$^{+}$ and FoxP3$^{-}$ populations are compared on the histograms on the right.

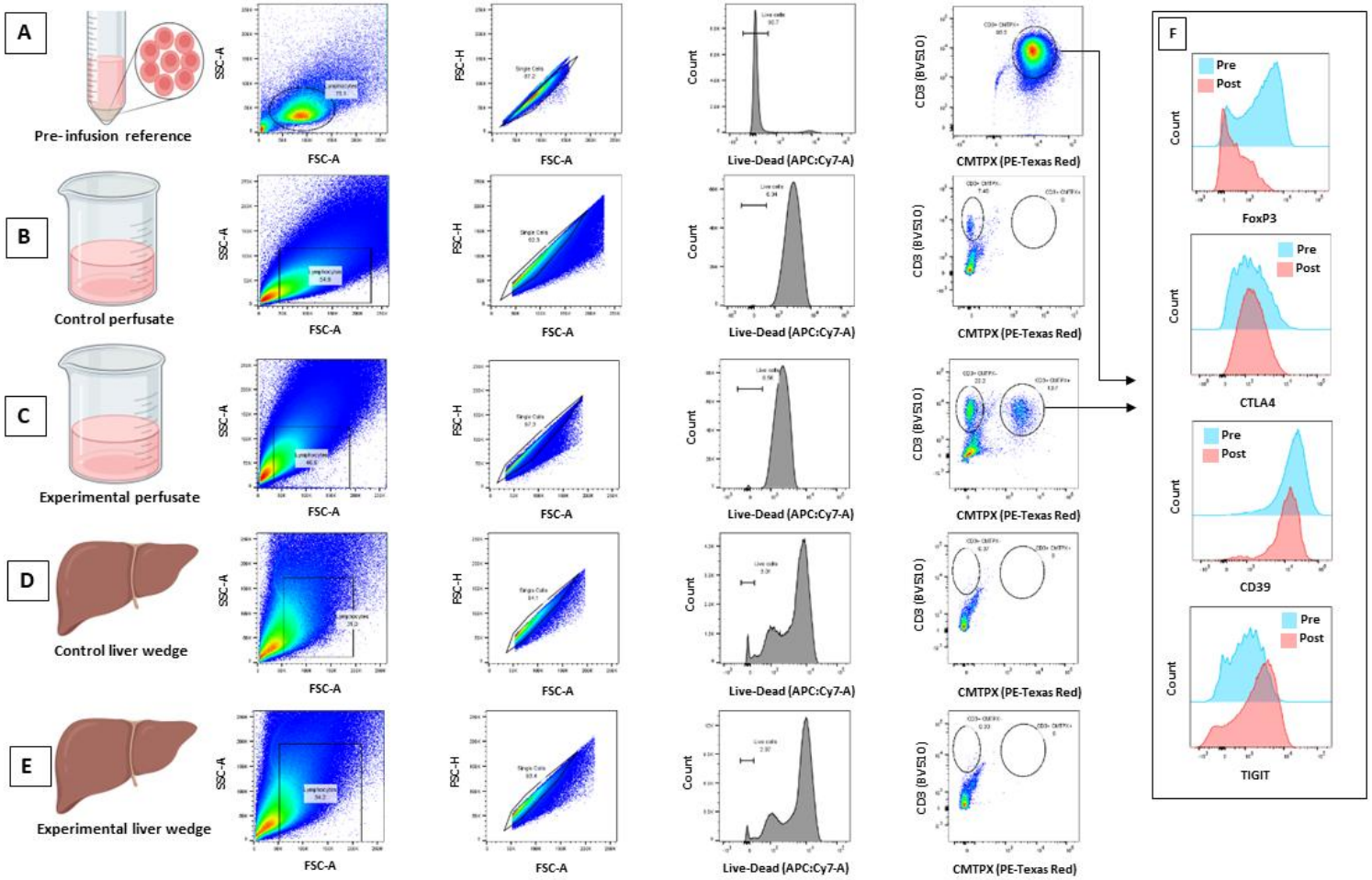


**Figure 5.17. Flow cytometry results of perfusate and liver tissue after infusion.** Flow cytometry results of Treg wedge infusion experiment 2. A) Shows the phenotype of labelled cells B) The perfusate from the control lobe which does not have any CMTPX labelled cells C) The perfusate from the experimental lobe has a $CD3^+$ $CMTPX^+$ population. D & E) Neither the control or the experimental lobe LDLs had $CMTPX^+$ cells. F) The expression of functional markers in the pre infusion sample and the experimental perfusate are demonstrated in F.

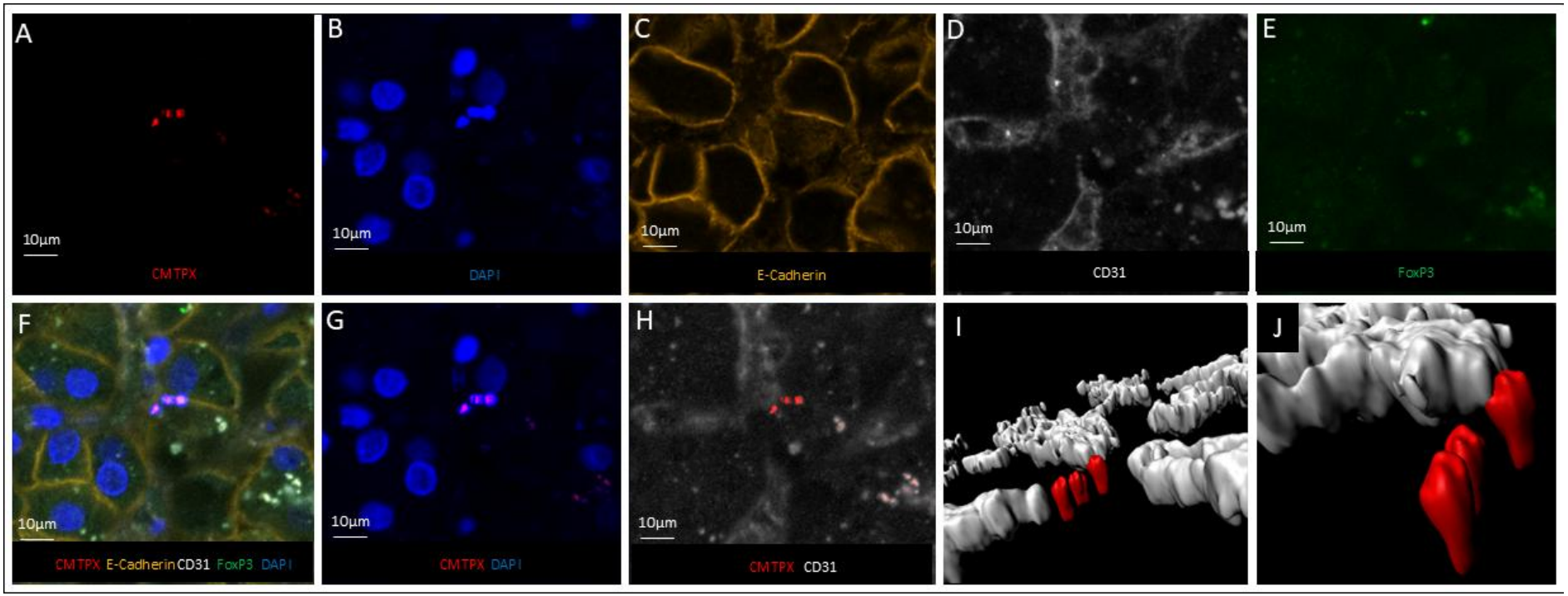


**Figure 5.18. Confocal microscopy results of Treg wedge perfusion 2.** Image from experimental wedge with different combinations of light channels activated. A-E) Single channels showing cells can be seen on CMTPX, DAPI and FoxP3 channels. They cannot be seen on the E-cadherin or CD31 channels. F) All channels showing cells G) DAPI and CMTPX channels on and cells stain positive for both H) CMTPX and CD31 channels showing red cells outside of the white vascular structures. I&J) 3D rendered images showing red cells location.

### 5.3.3 Treg wedge perfusion experiment 3

In this experiment, 15.5 million Tregs were infused into a 41 gram wedge of human liver. The control wedge was of comparable size at 40 grams. The perfusion continued for 14 hours after the cells were infused (Figure 5.19).

The flow cytometry results of the pre infusion sample are demonstrated in figure 5.20. Phenotyping was only possible on the labelled sample, which did not demonstrate clear positive and negative populations of FoxP3 or the suppressive markers.

Figure 5.21 demonstrates the results of the post infusion flow cytometry. In this experiment, both live and dead $CD3^+$ $CMTPX^+$ cells were isolated from the experimental lobes perfusate only. No $CMTPX^+$ cells were obtained from the control perfusate, experimental or control LDLs. Figure 5.21 demonstrates comparative histograms of FoxP3 and the suppressive markers for the labelled pre infusion cells and the labelled perfusate cells. The FoxP3 expression appears to be lower in the post infusion sample, with the other markers staying relatively stable as indicated by the shape of their hisogram.

Figure 5.22 shows confocal microscopy pictures demonstrating a close up of a CMTPX labelled cell. This cell was not FoxP3 positive on immunofluorescent staining.

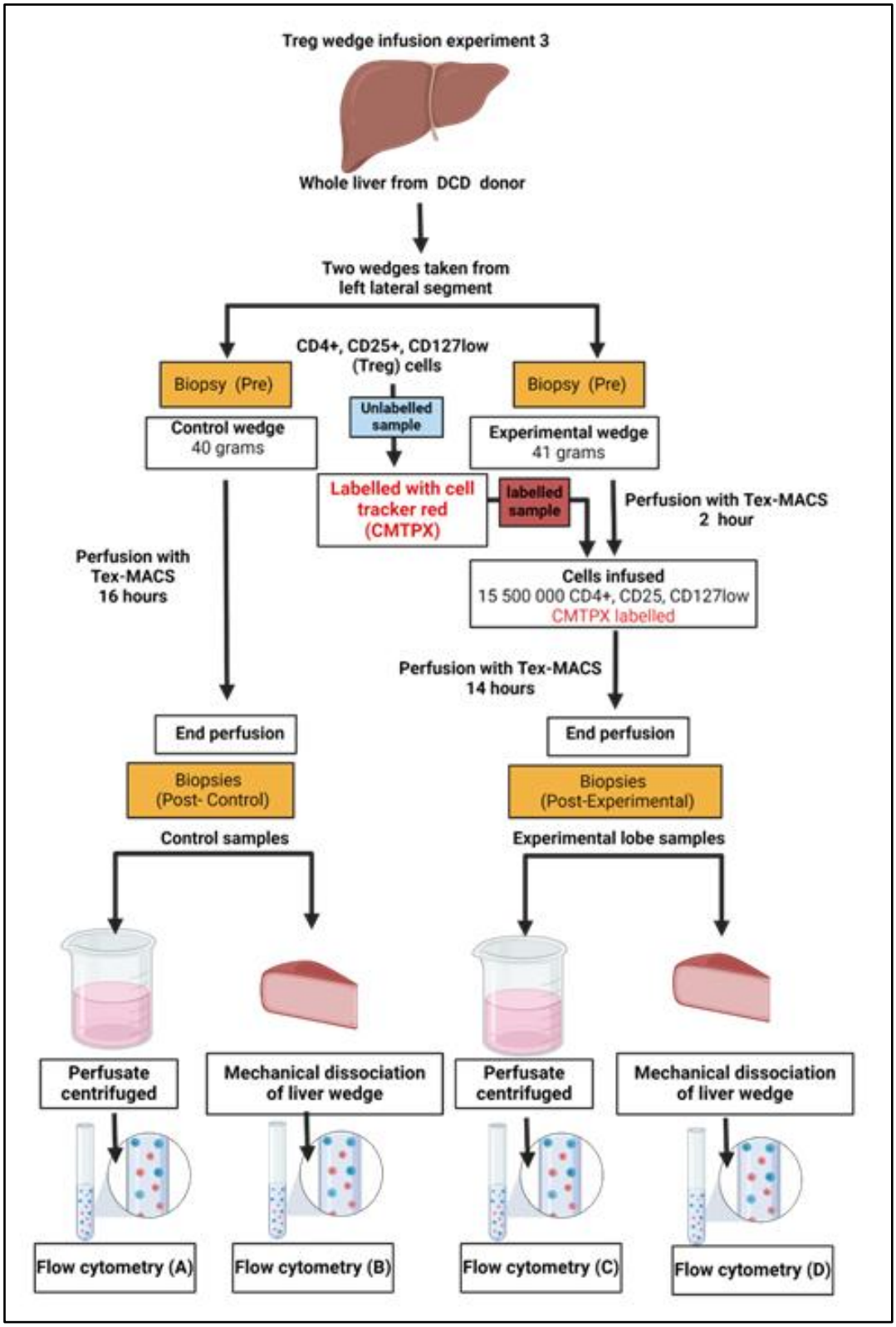


**Figure 5.19**. Schematic of Treg wedge infusion experiment 3. Diagram showing the cell quantity, weight of liver wedges and the duration of perfusion. Biopsies taken at two time points as per yellow boxes.

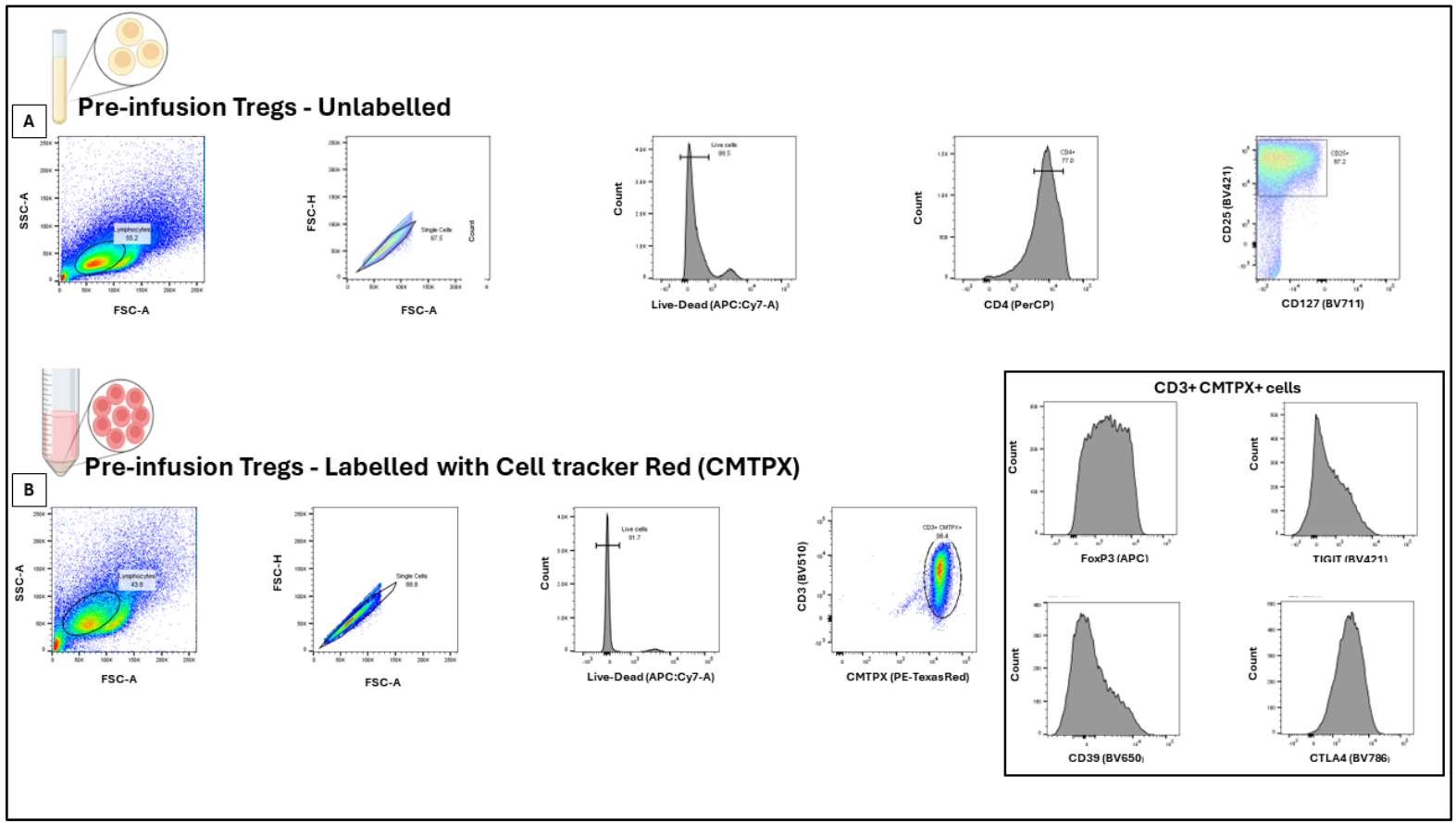


**Figure 5.20**. **Phenotype of Tregs prior to infusion for wedge infusion experiment 3.** A) Flow cytometry results prior to labelling with CMTPX B) Results and expression of functional markers after CMTPX labelling.

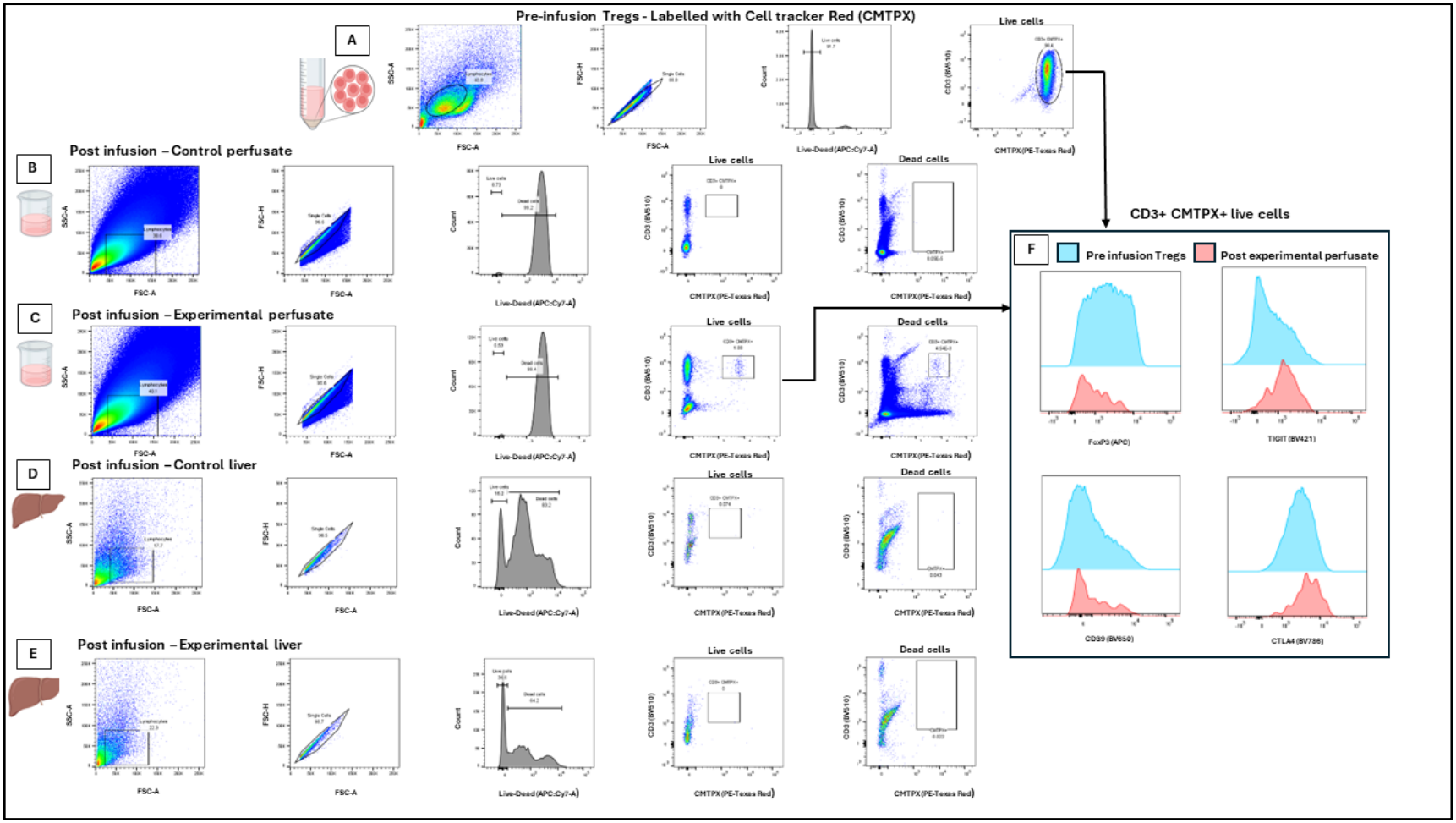


**Figure 5.21. Flow cytometry results of wedge perfusion 3.** Flow cytometry results showing the phenotype of the pre-infusion cells (A) and the samples after infusion from the control perfusate (B), experimental perfusate (C), control liver wedge (D) and experimental liver wedge (E). Live and dead CMTPX$^{+}$ cells were isolated from the experimental perfusate only. A comparison of the functional markers is shown in the histograms of inset F.

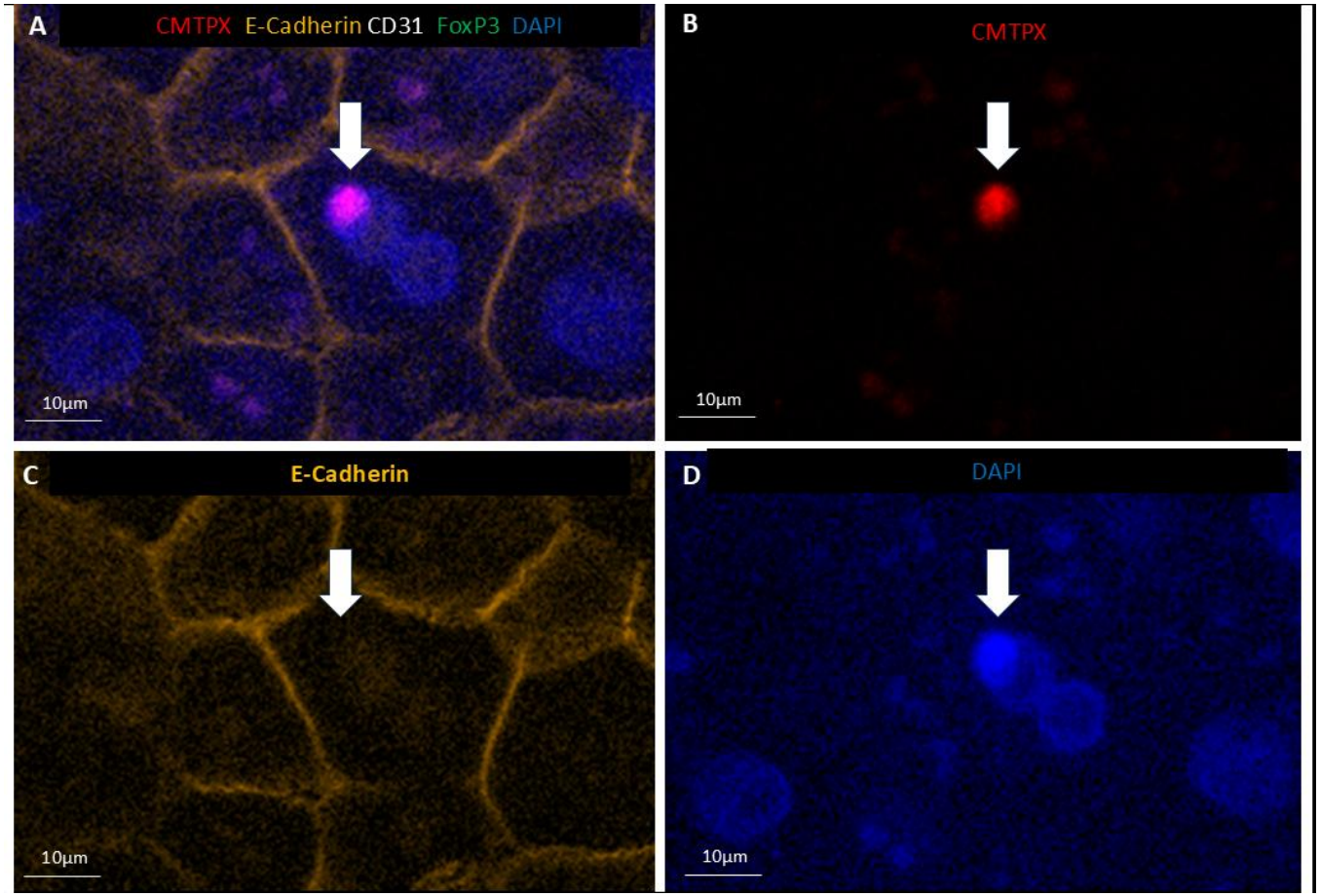


**Figure 5.22. Close up image of CMTPX labelled Treg from Treg wedge perfusion experiment 3**. Close up image of CMTPX labelled Treg in the liver tissue of the experimental lobe. The cell has exited the vasculature and appears to be either inside, above or below a hepatocytes. A) Florescent pink CMTPX labelled cell in close proximity to a binucleate hepatocyte. B) Bright red CMTPX labelled cell. The brightness and shape of the cell distinguish it from the background autofluorescence. C) Cell not evident with E-Cadherin only image. D) Dense Nuclear material in Treg distinguishes it from the hepatocyte nucleus.

### 5.3.4 Treg wedge perfusion experiment 4

During this experiment, 3 million labelled Tregs were infused into 31 grams of human liver tissue (Figure 5.23). After the administration of the Tregs, the perfusion continued for 12 hours. Unfortunately, due to voltage error on the flow cytometer, the labelled Tregs could not be phenotyped fully both before and after infusion.

The confocal microscopy results were similar to previous experiments, and could be seen in the parenchyma of the liver post infusion. Even with the low number of infused cells, the labelled Tregs were visible with confocal microscopy.

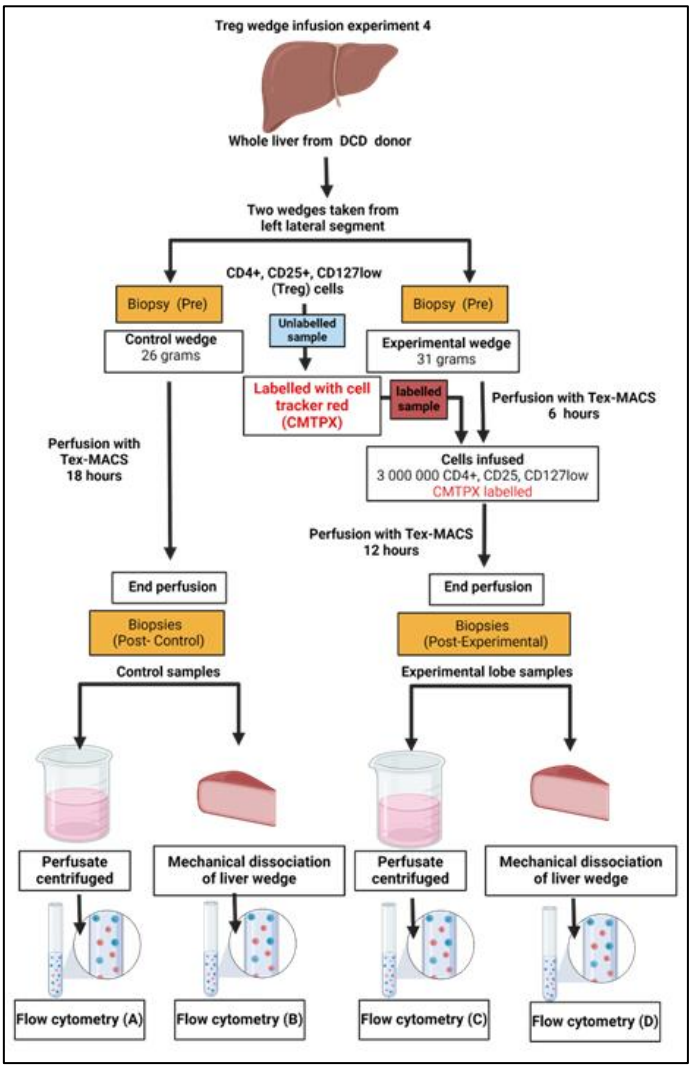


**Figure 5.23. Schematic of Treg wedge infusion experiment 4**. Diagram showing the cell quantity, weight of liver wedges and the duration of perfusion. Biopsies taken at two time points as per yellow boxes.

### 5.3.5 Treg wedge perfusion experiment 5

In this final wedge infusion experiment, 9.7 million Tregs were infused into 44 grams of human liver tissue, and the perfusion continued for 12 hours (Figure 5.24). The flow cytometry result of the preinfusion labelled and unlabelled Tregs are demonstrated in figure 5.25 and 5.26 respectively.

$CD3^+$ and $CMTPX^+$ cells were isolated from both the experimental perfusate and LDLs (Figure 5.27). They were not isolated from the control perfusate and LDLs. Both Live and dead $CD3^+$ CMTPX positive cells were identified in the perfusate and LDLs, and the phenotype of the live fraction compared with the phenotype of the pre infusion cells (Figure 5.27). The cells isolated from the perfusate appeared to have a reduced expression of TIGIT, CTLA 4 and CD39. The shape of the FoxP3 histogram remained constant in shape, without a clear positive and negative population. In the live $CD3^+$ $CMTPX^+$ cell fraction isolated from the LDLs, the shape of the histograms remained consistent but a lower amplitude. The cause of the latter is likely due to the low number of events.

Identification of CMTPX positive cells was also achieved with confocal microscopy, and appearances were consistent with similar experiments. Periodic acid Schiff staining was performed on this wedge of liver, and compared to that of a whole liver perfusion experiment (Figure 5.28). This was done to assess for hepatocyte necrosis and the glycogen status. The appearance of the liver tissue from the wedge perfusion experiment indicated that it was well glycogenated, with minimal loss of nuclei.

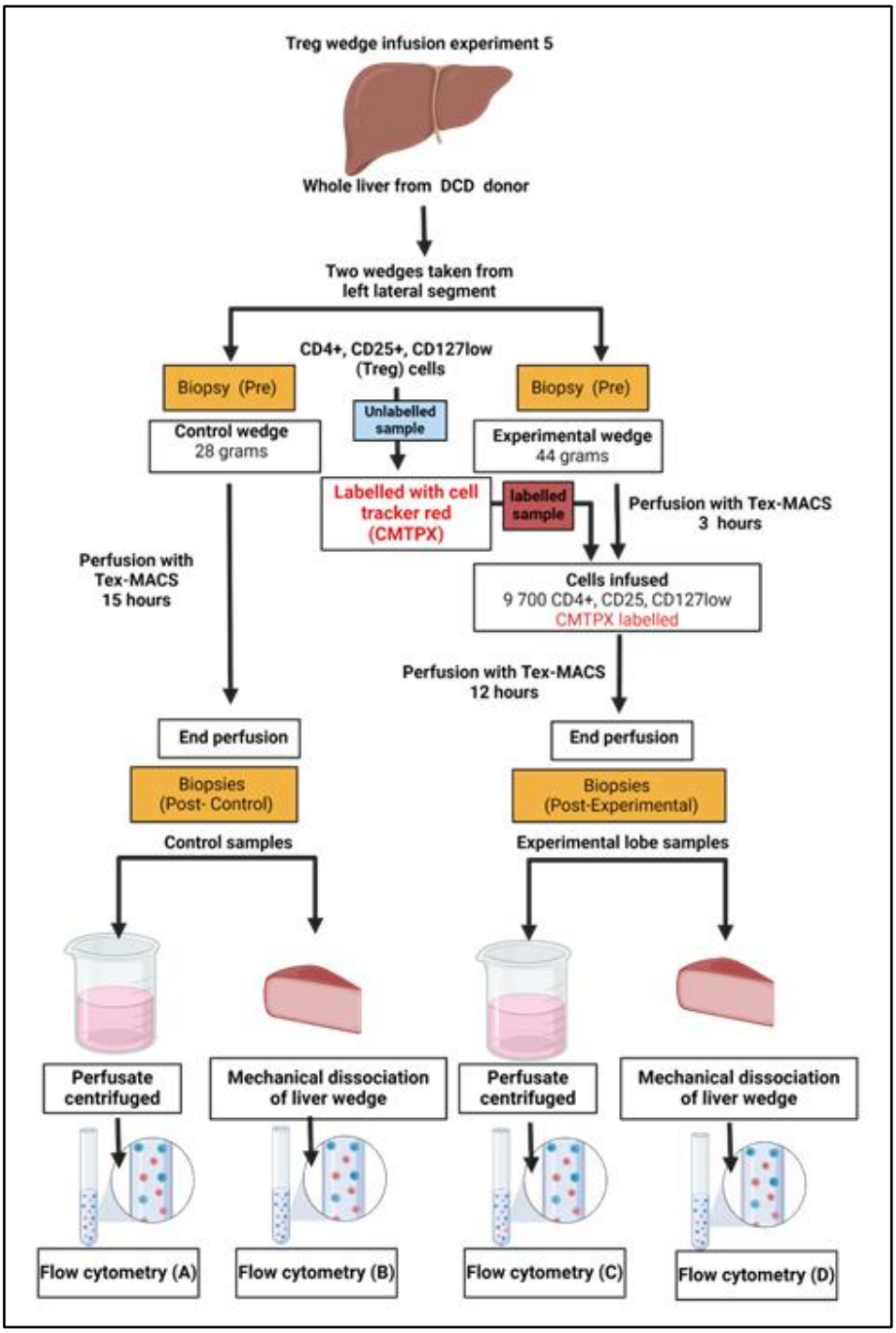


**Figure 5.24. Schematic of Treg wedge infusion experiment 5.** Diagram showing the cell quantity, weight of liver wedges and the duration of perfusion. Biopsies taken at two time points as per yellow boxes.

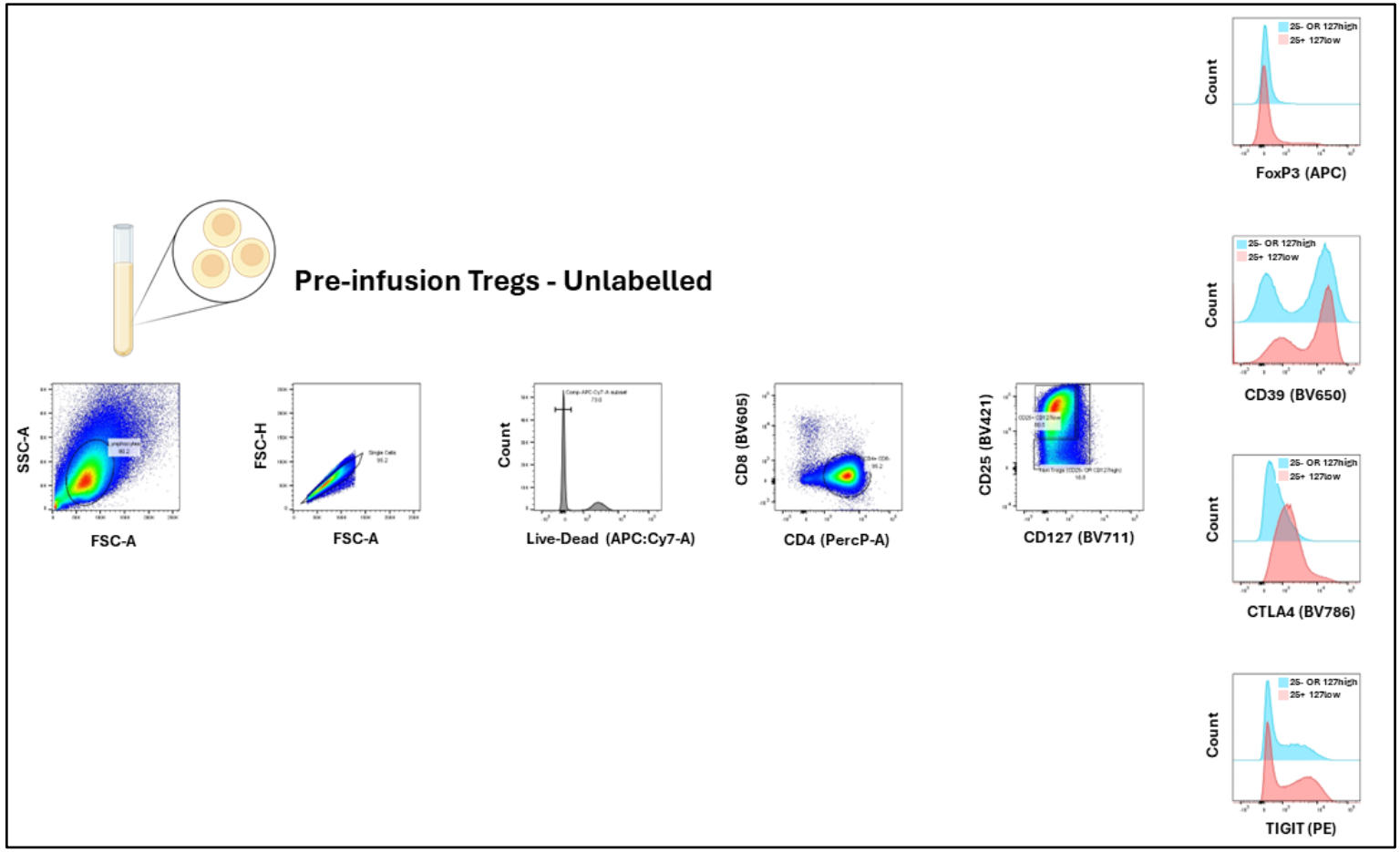


**Figure 5.25. Flow cytometry results of cells prior to infusion for wedge infusion experiment 5.** Flow cytometry results of post expanded Tregs. Histograms on right compare the expression of functional markers of $CD25^{high}$ with the $CD25^{low}$ populations.

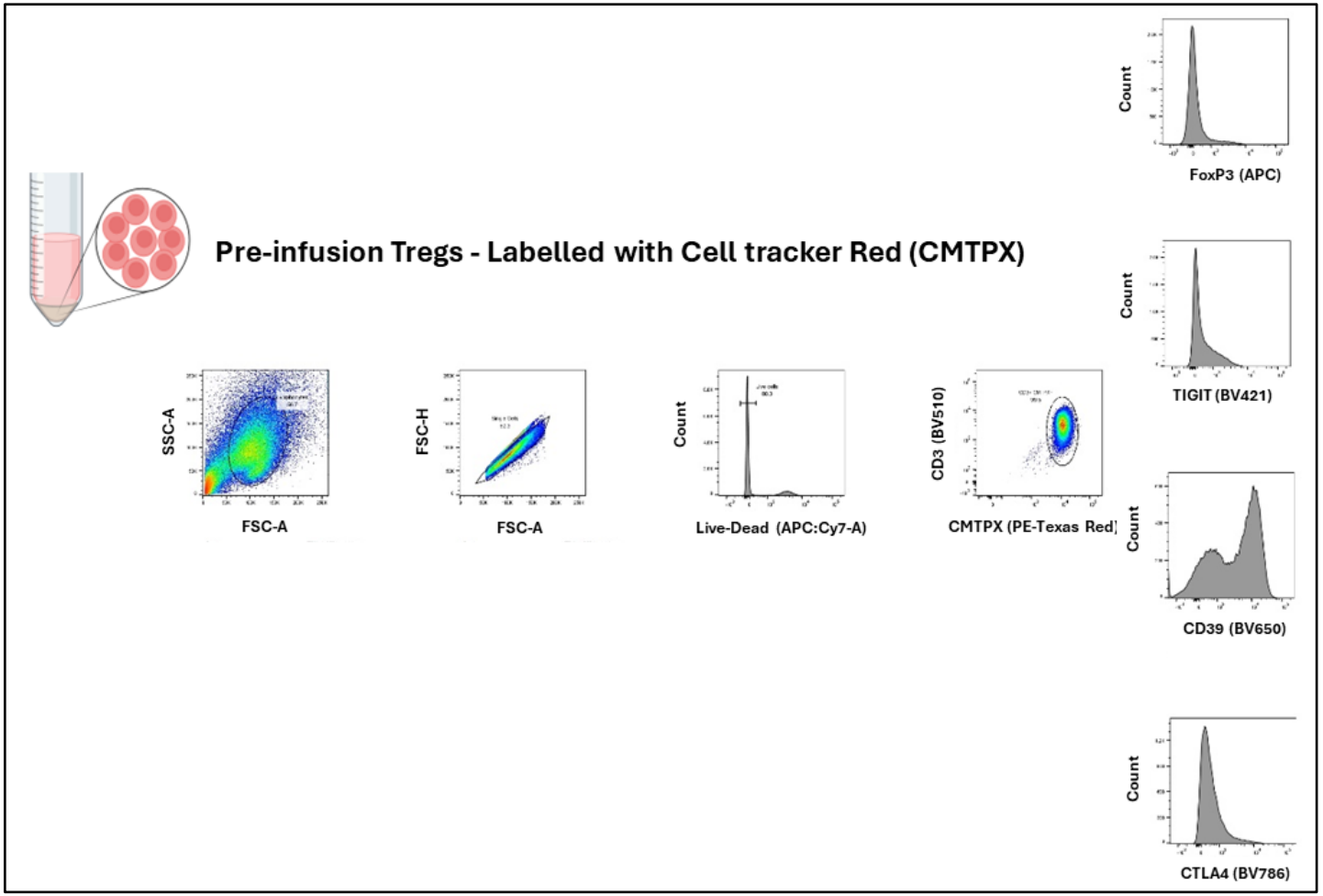


**Figure 5.26. Flow cytometry results of the cells after labelling with CMTPX**. Flow cytometry results of post expanded Tregs after CMTPX labelling. All cells stained positive for CMTPX, and the expression of FoxP3 and functional markers are shown on histograms on the right.

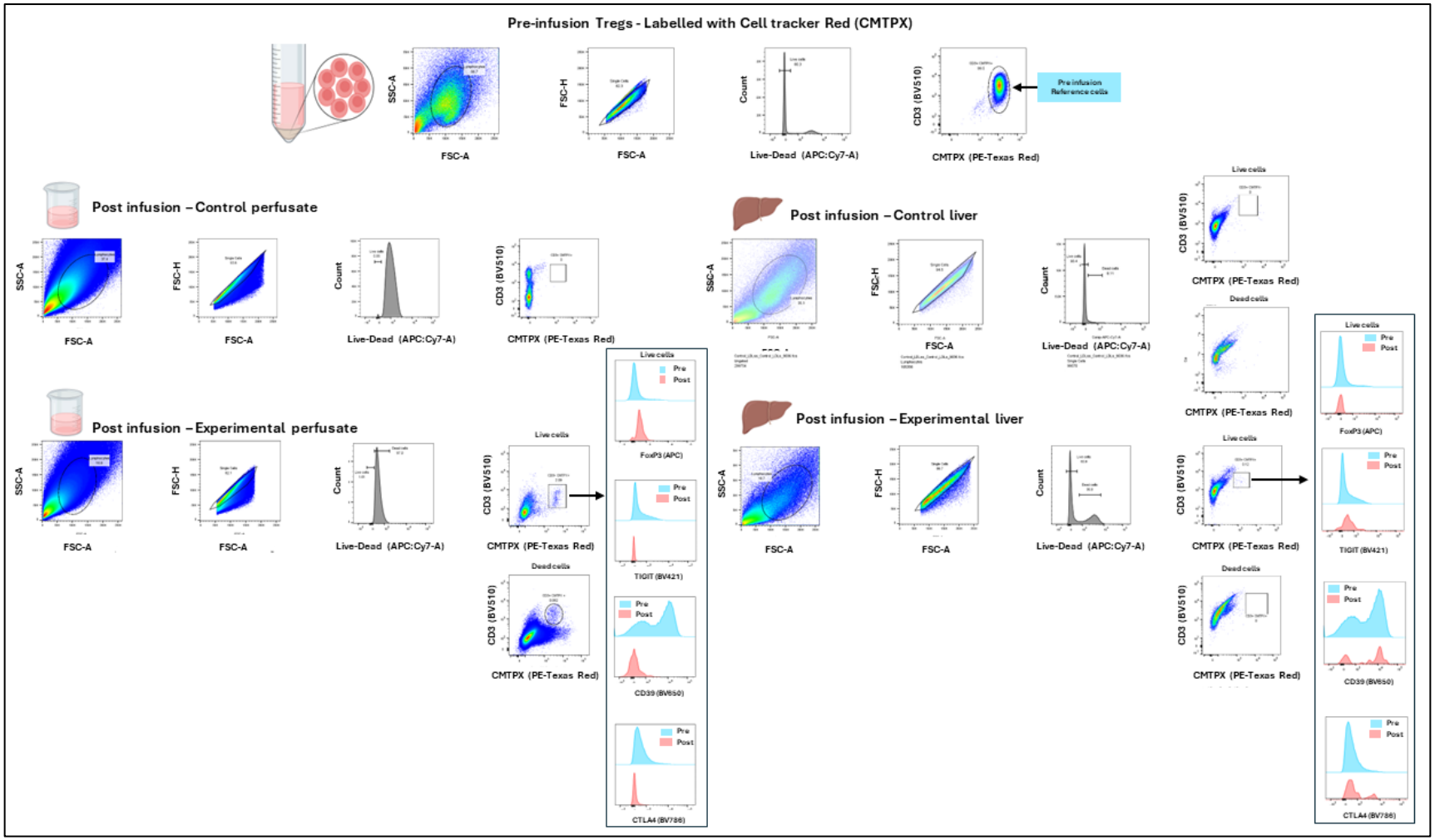


**Figure 5.27. Flow cytometry results of wedge infusion experiment 5**. Flow cytometry results. CMTPX$^{+}$ cells were isolated from both the experimental perfusate and the experimental LDLs. The cells isolated from the experimental perfusate demonstrated a fall in CD39 and CTLA 4 expression. The expression of functional markers in the experimental LDLs was similar to that of the pre-infusion sample.

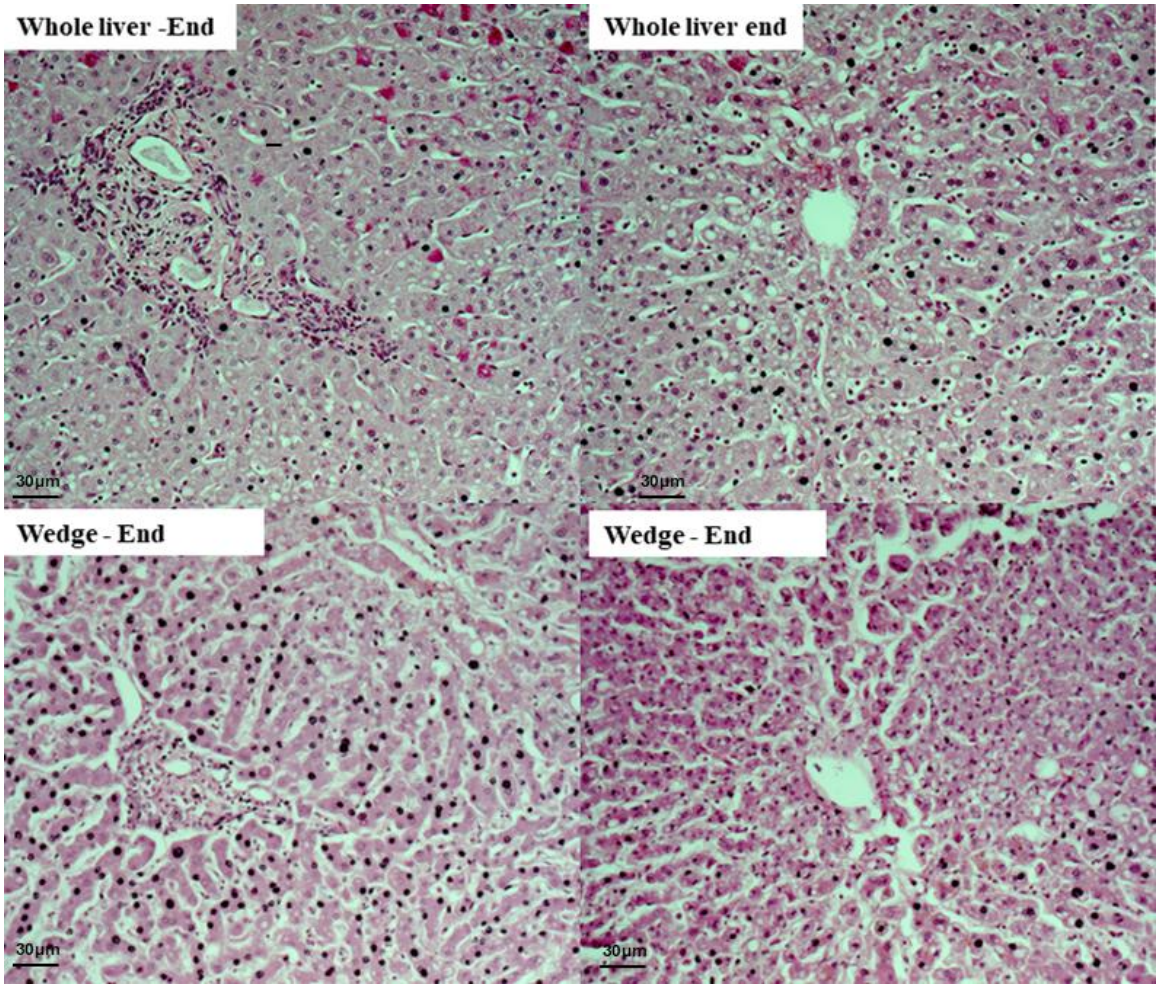


**Figure 5.28. Periodic acid Schiff (PAS) staining of liver from Treg infusion experiment 5 and Whole liver experiment 2.** PAS staining of liver after perfusion with the whole liver model (top) and the wedge model (bottom). Left images show portal tracts and right shows central veins. Minimal loss of nuclei and good cytoplasmic staining of wedge perfusion model, indicating hepatocytes do not undergo significant necrosis during perfusion period.

### 5.4.1 Whole liver optimisation experiment 1

This experiment aimed to assess wether the results from the wedge perfusion model were transferable to the NMP circuits used in clinical practice. Due to the high costs associated with this model, we did not have the resources to perform them in the same number as the wedge perfusion model. Therefore, we performed one optimisation experiment with $CD4^+$ cells and two with Tregs (Described later). All the whole liver experiments were combined with another researcher groups experiments which were investigating the effect of a defatting cocktail administered at the start of NMP.

This commercially available NMP circuit (Liver Assist, XVIVO) provides oxygenated blood at human body temperature (37°C). This is delivered via both a cannula in the hepatic artery and portal vein. The blood returns to the oxygenator by draining our the hepatic veins, and IVC into the collection bowl. Due to the fact that the hepatic artery provides the dominant supply to the bile ducts within the liver[171], the cells were delivered via the arterial circuit. The cells were injected through a port on the tubing between the oxygenator and the graft. Biopsies were performed prior to infusion, after 2 hours and after 4 hours. Assessment of cell localisation within 4 hours is important as this is the minimum duration of time that NMP is used for in clinical practice.

The confocal microscopy results are demonstrated in Figure 5.29. Our findings during this optimisation experiment confirmed the CMTPX labelled cells can be identified using a whole NMP model, and that the cells have exited the sinusoids within 4 hours. This is demonstrated in R3 & L3 of figure 5.29.

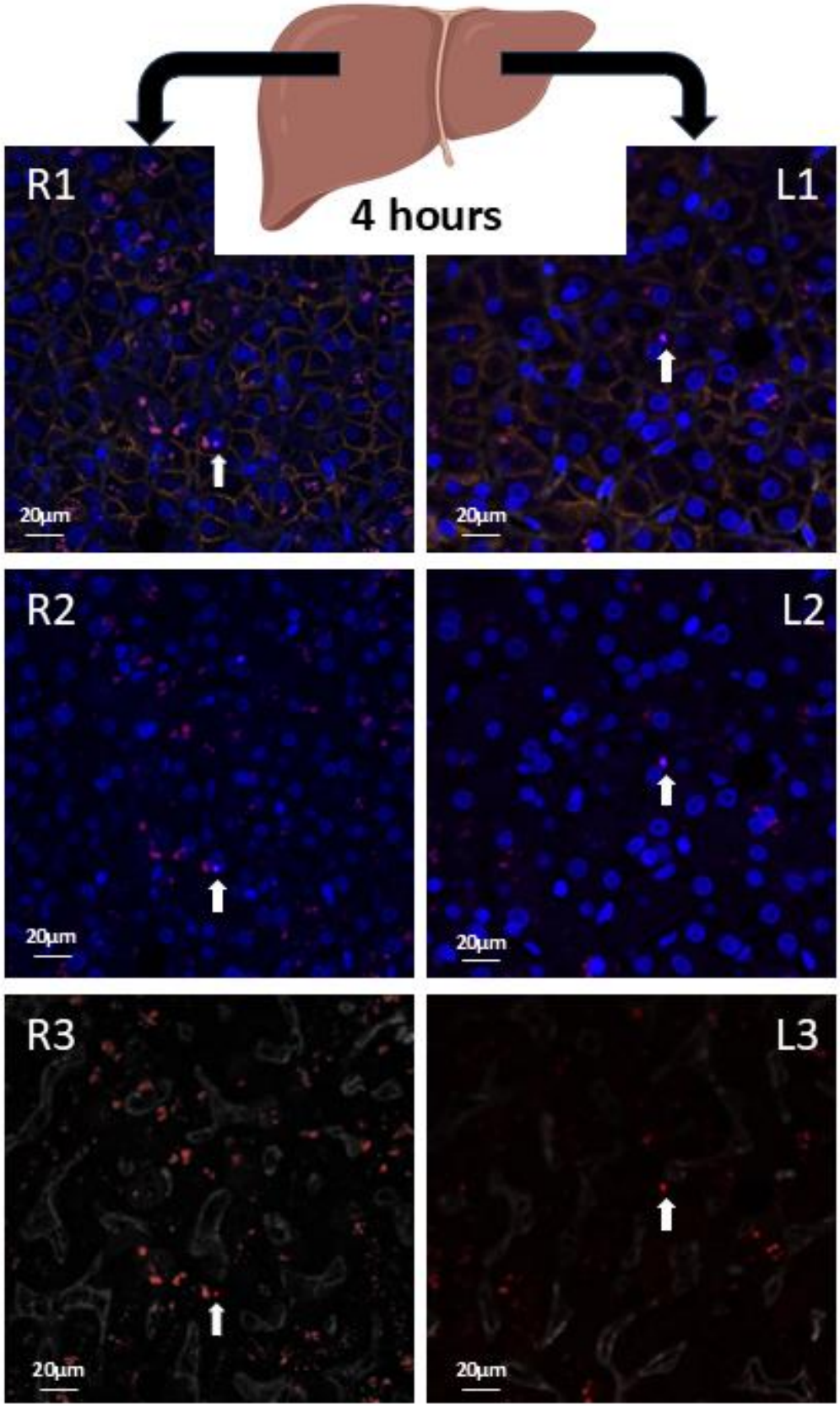


**Figure 5.29. Confocal microscopy of left and right lobe biopsies.** Confocal microscopy images of right and left lobe liver biopsies taken at 4 hours after infusion. R1 & L1) CMTPX, DAPI, E-cad. R2 & L2) CMTPX, DAPI. R3 & L3) CMTPX and CD31 channels activated

### 5.3.1 Whole liver Treg perfusion experiment 1

In this experiment, a whole DBD liver deemed not suitable for clinical transplantation was connected to the Liver Assist (XVIVO®) device. The perfusion was run for 72 hours before the Tregs were infused. At the 72 hour mark, 75 million Tregs were administered via the hepatic artery (Figure 5.30). The phenotype of these cells are demonstrated in figure 5.31. Following LDL isolation of slices of both the left and right lobes, no CMTPX positive cells were isolated (Figure 5.32). Biopsies of both the left and right lobes were taken after 2 hours and 4 hours. The infused CMTX labelled tregs were visualised in the left lobe on the biopsies at 2 hours post infusion (Figure 5.33 L2 & L3). The labelled cells were seen in the right lobe after 4 hours (Figure 5.33, R2 & R3) which appeared to be outside the hepatic sinusoids.

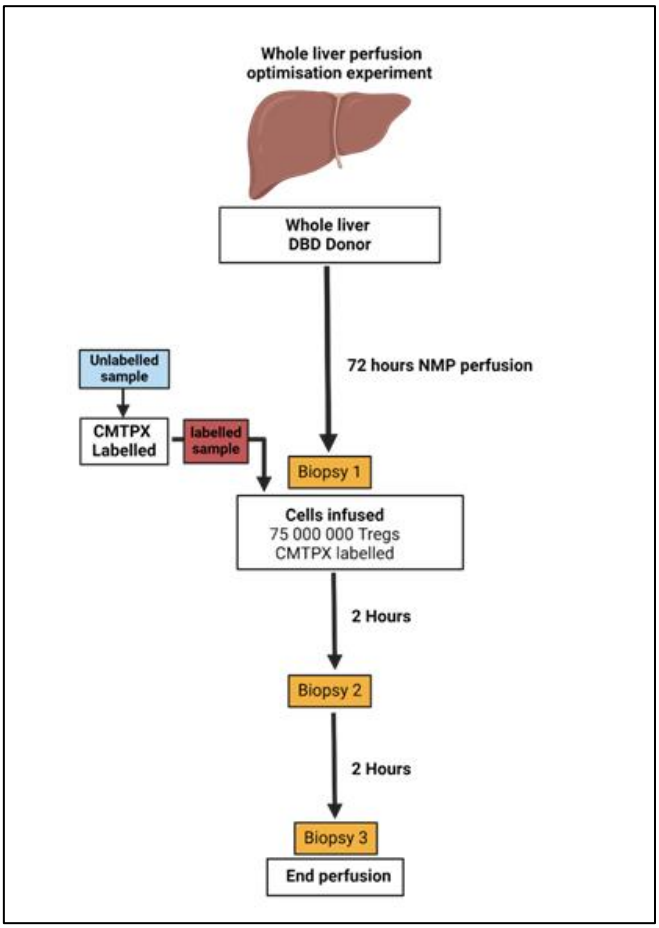


**Figure 5.30. Diagram of whole liver perfusion experiment 1**. Diagram showing the cell quantity and the duration of perfusion. Biopsies taken at three time points as per yellow boxes.

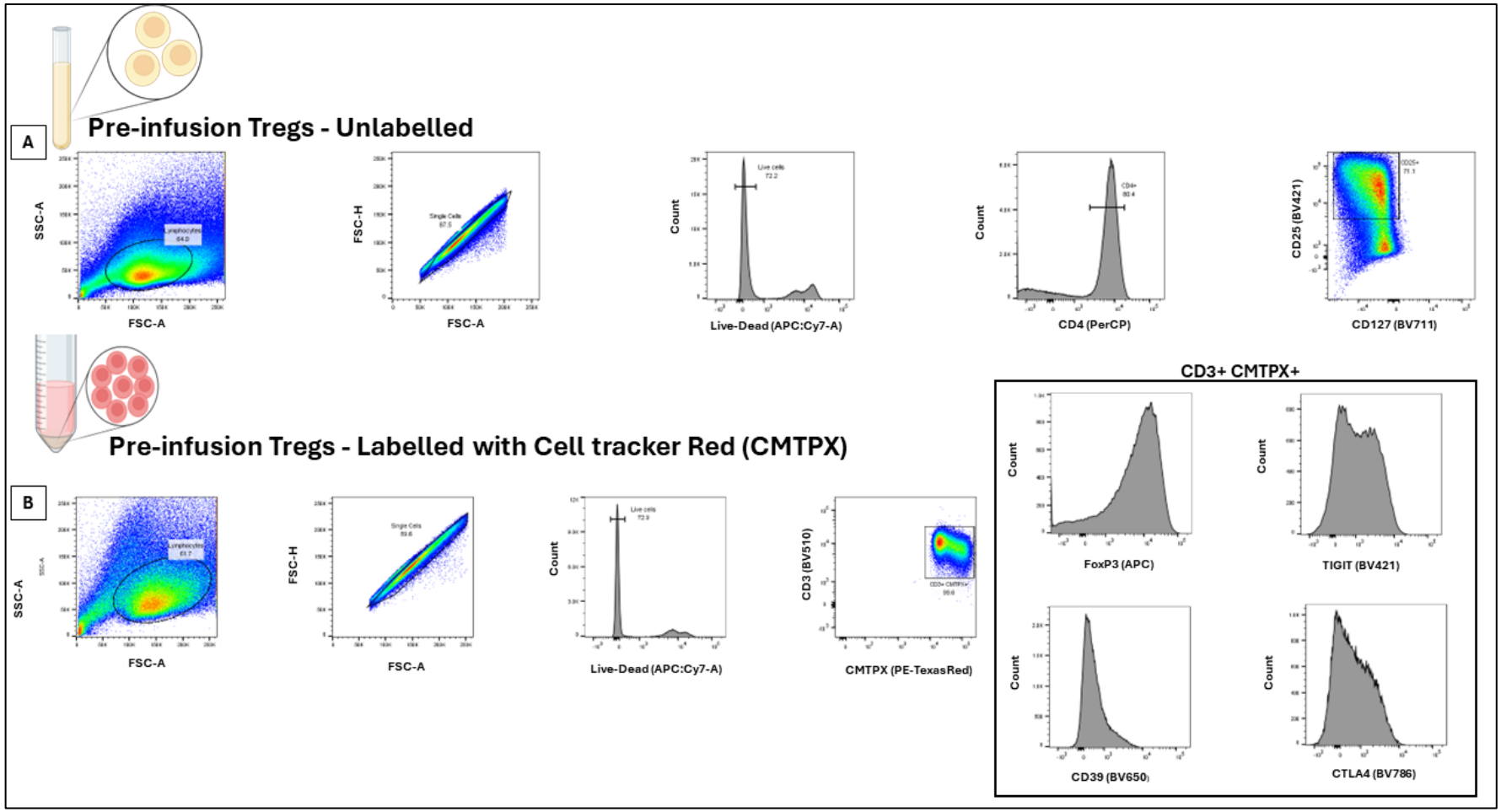


**Figure 5.31. Flow cytometry results of cells prior to infusion used in whole liver perfusion experiment 1**. A) Flow cytometry results of cells prior to labelling. B) Cells after labelling with expression of functional markers demonstrated in inset.

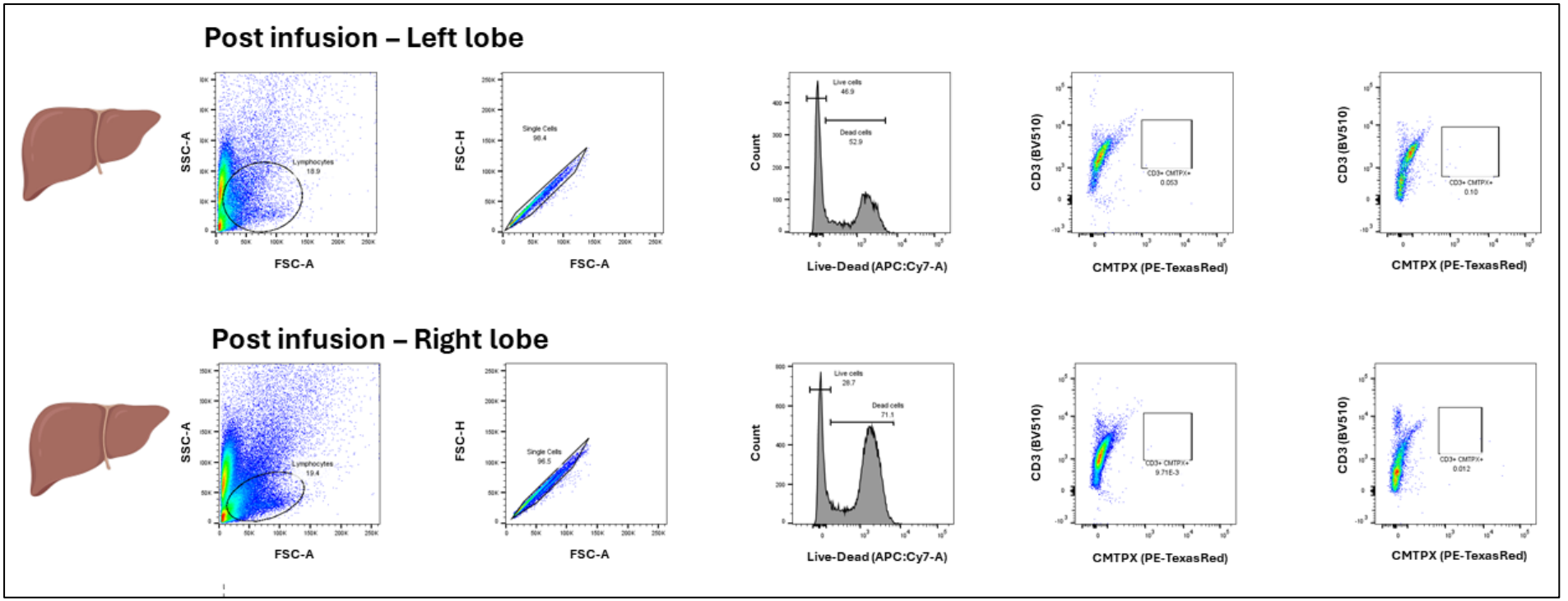


**Figure 5.32. Flow cytometry results of liver derived lymphocytes after infusion for whole liver perfusion experiment 1.** Flow cytometry results of LDLS obtained from both the left and right lobes. Neither live or dead CMTPX$^{+}$ cells were isolated during this experiment as evidenced by the empty CD3+/CMTPX+ box in right most scatter plots in both rows

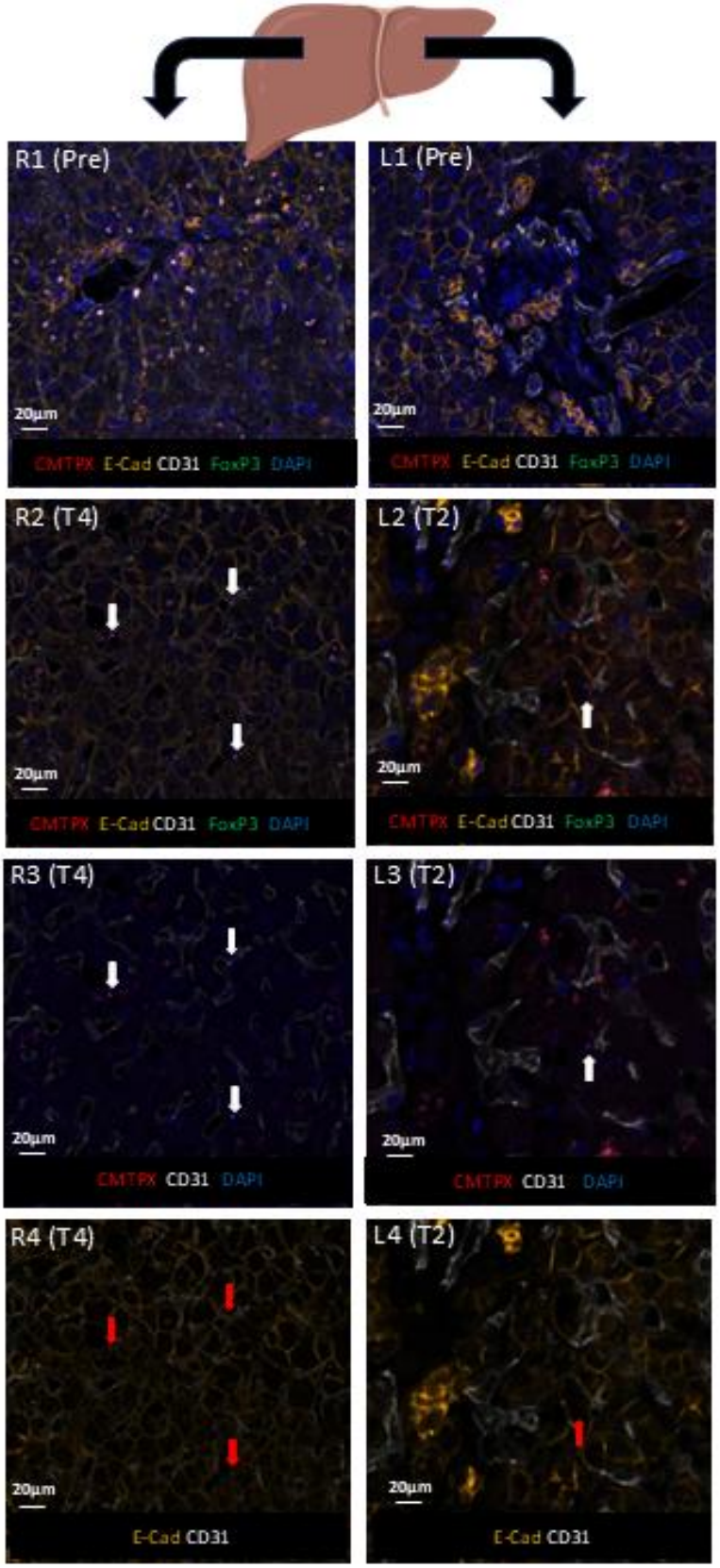


**Figure 5.33**. **Confocal microscopy results of whole liver perfusion experiment 1**. Biopsies from prior to infusion, after 2 hours on left (L2-4) and 4 hours on right (R2-4). $CMTPX^{+}$ cells indicated by white arrows. Cells not visible when CMTPX and DAPI channels are off (R4 & L4). Cells visible in biopsies from left lobe at 2 hours, and right lobe at 4 hours

### 5.3.2 Whole liver Treg perfusion experiment 2

In this experiment, 45 million Tregs were infused into a whole DBD liver declined for clinical transplantation. Similar to previous, the Tregs were administered through the hepatic artery after 72 hours of machine perfusion (Figure 5.34). The phenotype of the Tregs before and after labelling is shown in figure 5.35 & 5.36 respectively. Following infusion of Tregs, the CMTPX labelled tregs were isolated from the LDLs, but not the perfusate (Figure 5.37). The number of cells isolated from the liver tissue was too low to phenotype accurately. The confocal microscopy results are demonstrated in figure 5.38. This shows a CMTPX labelled cell in the right lobe after 4 hours which is outside the sinusoid.

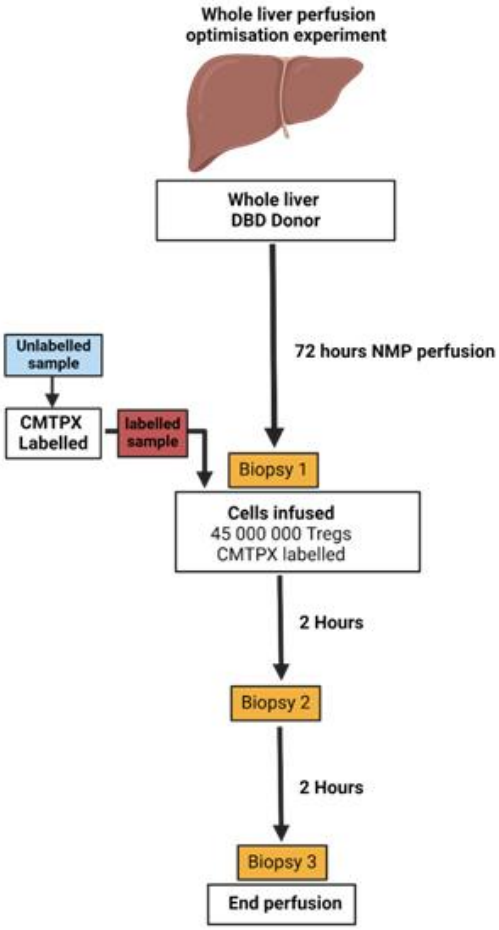


**Figure 5.34. Diagram of whole liver perfusion experiment 2**. Diagram showing the cell quantity and the duration of perfusion. Biopsies taken at three time points as per yellow boxes.

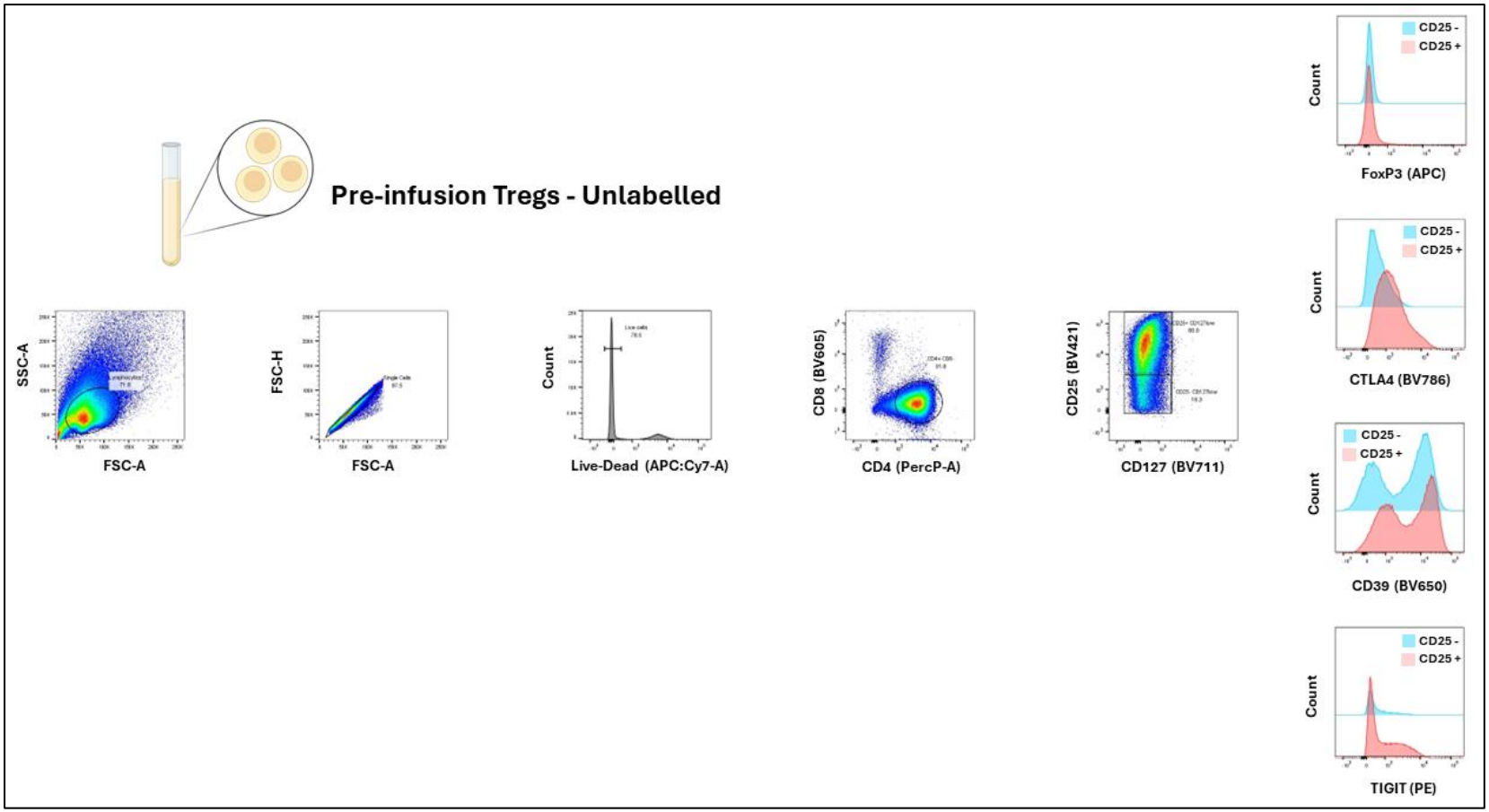


**Figure 5.35. Flow cytometry results of unlabelled cells used in whole liver experiment 2**. Cell phenotype of Tregs prior to labelling. The $CD25^{high}$ and $CD25^{low}$ populations are compared on the histograms on the right.

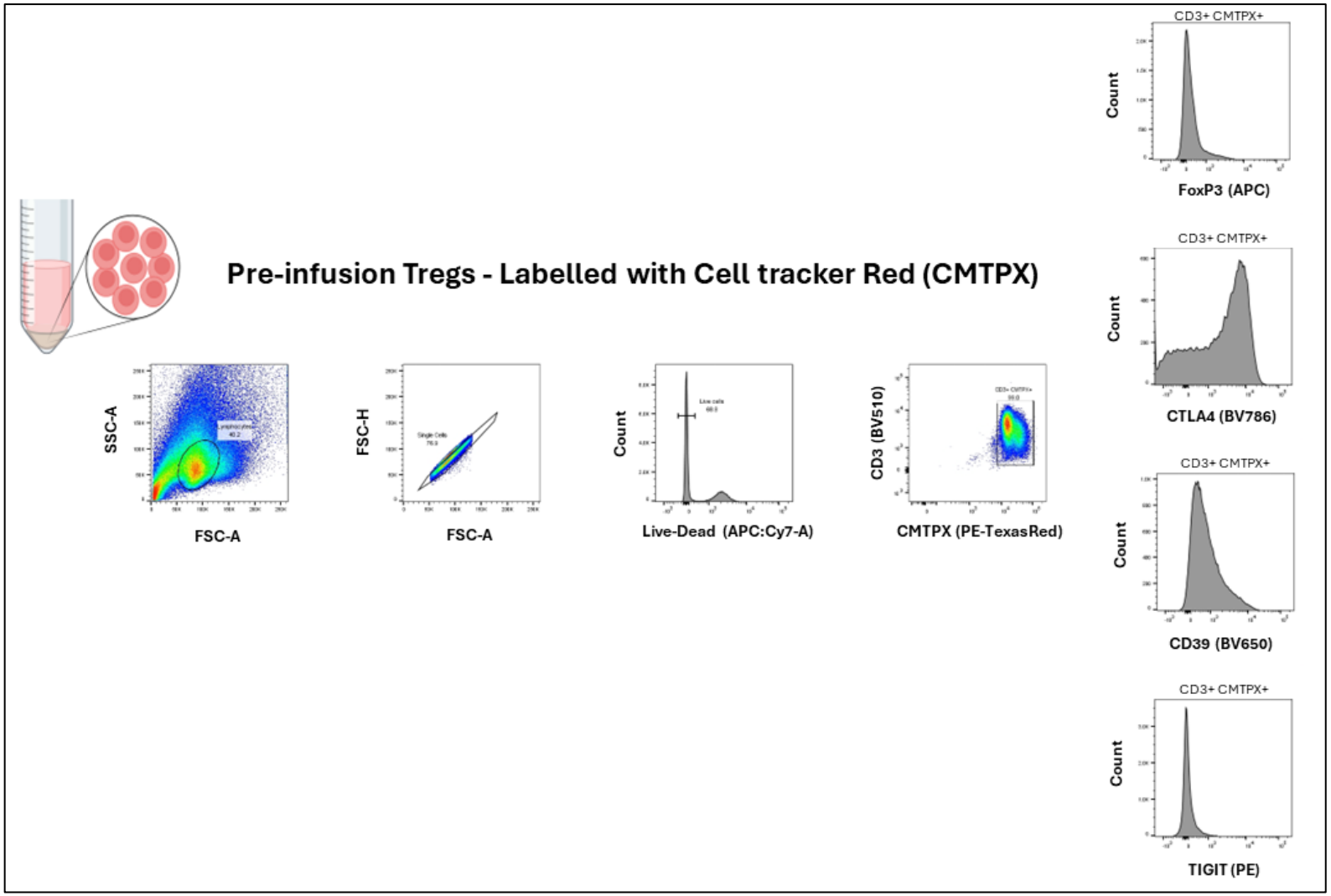


**Figure 5.36. Flow cytometry results of labelled cells used in whole liver perfusion experiment 2.Cell phenotype of Tregs after labelling**

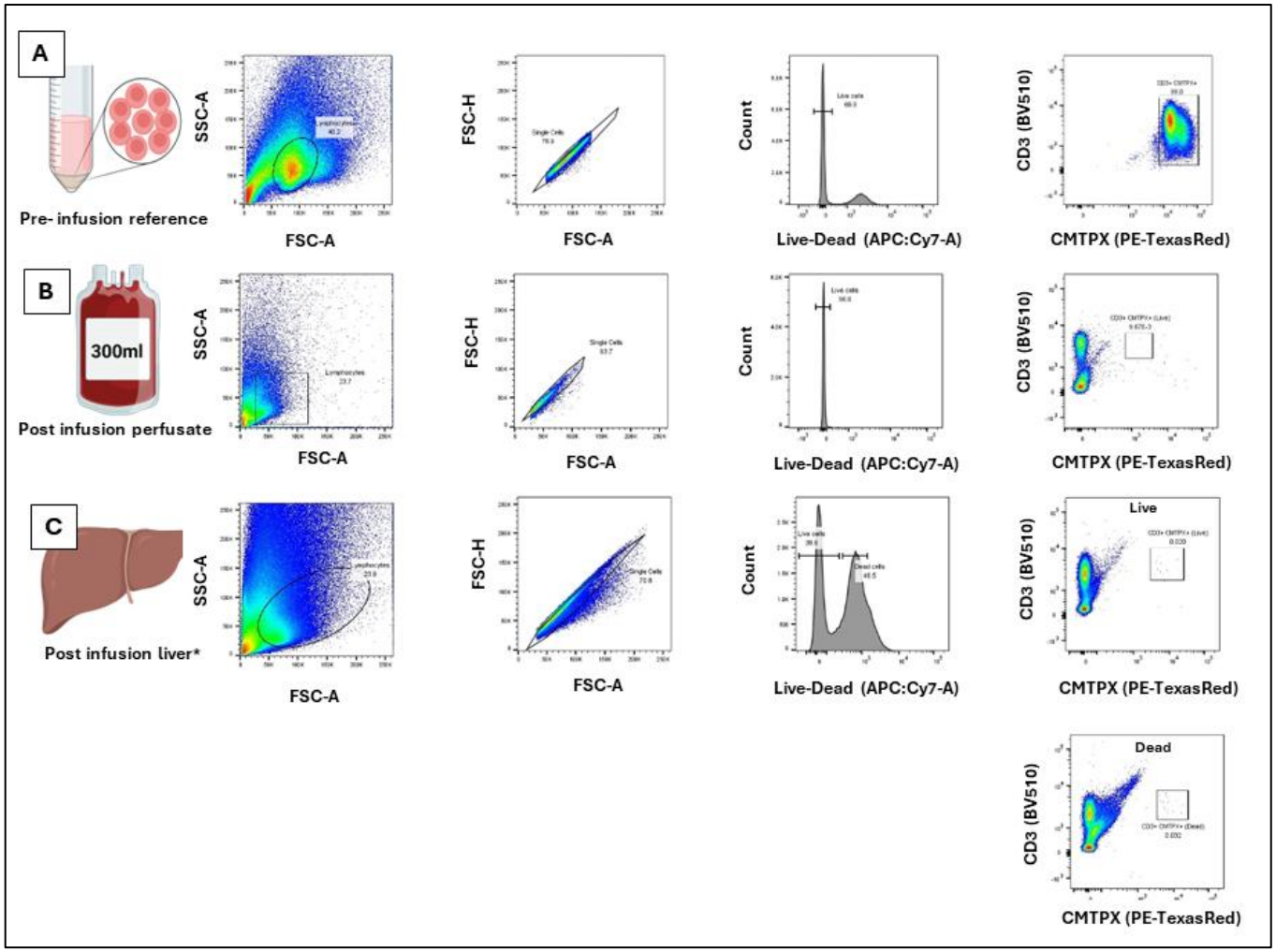


**Figure 5.37. Flow cytometry results of whole liver infusion experiment 2**. The pre-infusion phenotype of the infused cells are shown in A, and the results of the perfusate and LDLs in B & C respectively. A small number of $CMTPX^{+}$ cells were isolated from the LDLs but not enough to phenotype and compare to the preinfusion sample.

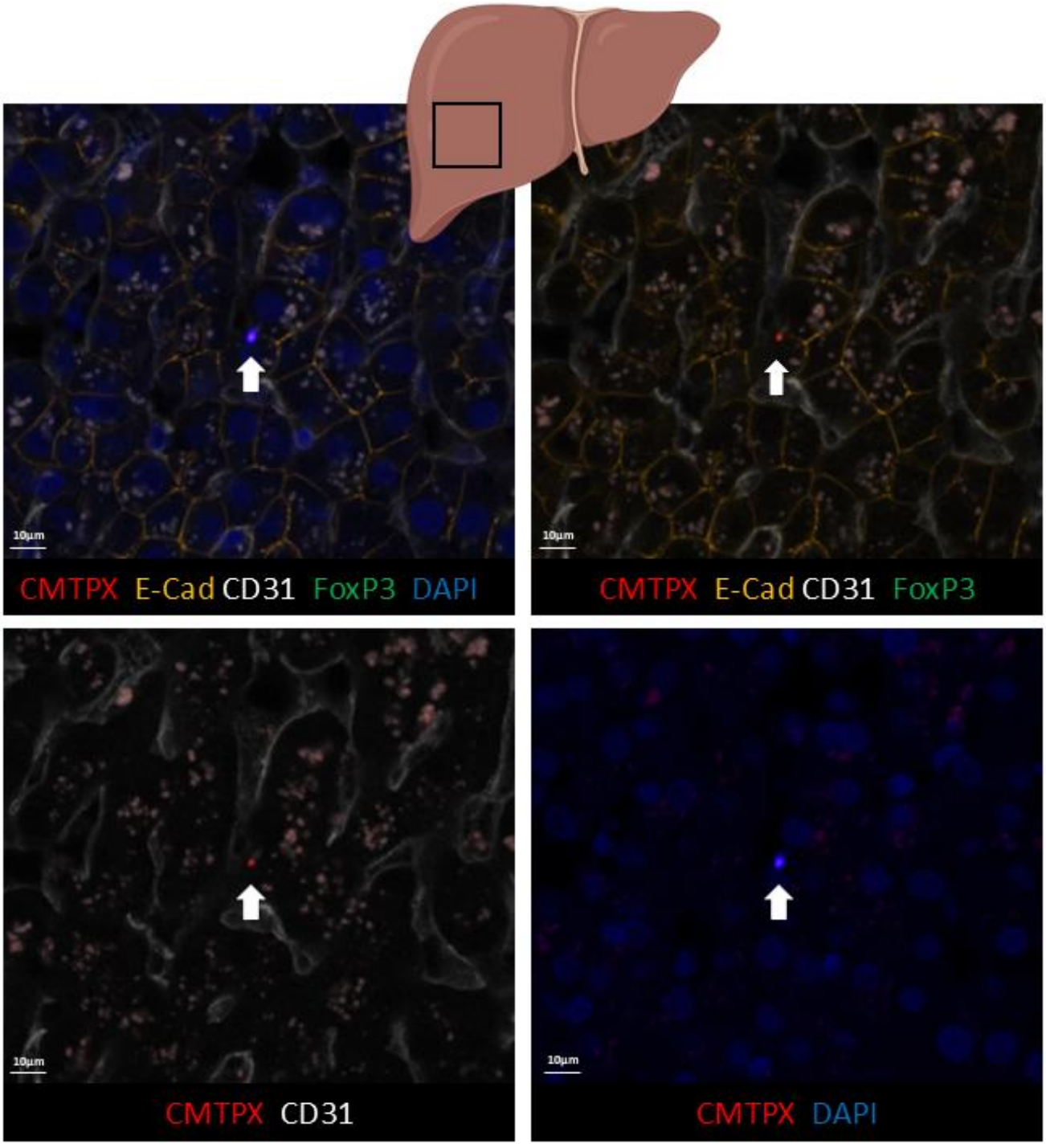


**Figure 5.38. Confocal microscopy results of whole liver experiment 2.** Confocal image of a right lobe biopsy taken 4 hours after cells were infused, with different channels activated. The CMTPX positive cell is indicated by the white arrows. In the bottom left image the cell can be seen outside the white structure (hepatic sinusoids).

## 5.4 Chapter Summary

The findings of this research have shown that Tregs infused via two different models engraft within the parenchyma. In addition to demonstrating the localisation of the infused cells, the results also demonstrate the cells remain alive once they are in the parenchyma. This confirms that the cells survive the perfusion process and to our knowledge, we are the first to demonstrate this. The cells appear to exit the hepatic sinusoids and remain adjacent to the hepatocytes. Results from the whole liver model experiments demonstrate that this occurs within 4 hours of administration. Unfortunately, it was not possible to quantify the amount of cells that stay within the liver using our methodology and this should be a focus of further research. The flow cytometry results that aimed to delineate phenotypic changes of the infused Tregs was more limited. Based on one experiment in which a small sample of the infused Tregs were isolated from the LDLs after infusion, the expression of the functional markers appeared stable. However, in two experiments labelled Tregs remained in the perfusate and the expression of functional markers reduced. This could be a real observation, or the result of differences in staining. The wedge perfusion model worked well to investigate our hypothesis as the quantity of cells in relation to the volume of liver tissue was high. Benefit would likely be gained from infusing a larger quantity of cells into the whole liver model, as we were unsuccessful in isolating an adequate sample of cells for phenotyping after these experiments.

# 6.0 - Thesis Conclusion

Liver transplantation has made great strides since it was first attempted more than 60 years ago. The early transplant clinicians and scientists, despite limited technology, made important observations and investigated these through innovative experimental models. The gains that are being made today, even with advanced technology, are small in comparison to those individuals that took liver transplantation from an experimental procedure to the standard of care within a few decades. At an international level, early outcomes following primary liver transplant now result in a 92% one year patient survival[172]. This suggests that great improvements have been made in graft selection, preservation, operative technique and early post operative care. Efforts now need to focus on strategies to improve long term graft survival by prevent allograft injury and avoidance of harmful sequalae of prolonged pharmacological immunosuppression. The administration of Treg therapy to transplant recipients is now a reality, with numerous clinical trials reported and ongoing. Furthermore, ex-vivo preservation is also now becoming commonplace in many centres and the opportunity to deliver graft directed therapy is great. This thesis represents an initial investigation into the concept isolating, expanding and delivering Tregs to the liver ex-vivo, whilst also reporting immune related changes that occur during NMP. To our knowledge, we are the first to demonstrate that the ex-vivo administered Tregs remain alive and functional once they are within the graft.

Immunosuppression regimes post liver transplantation vary significantly, and are influenced by age, native liver disease, co-morbidities and tolerability. Although there is growing recognition that immunosuppression minimisation is the best strategy, concern regarding occult and irreversible graft damage prevents this for many patients. Unfortunately, long term effects of pharmacological immunosuppression such as renal disease, infection and malignancy can all lead to premature death. Tolerance inducing therapies would be of great benefit, and should be a focus of future translational research. Investigating the effectiveness

of ex-vivo administered tolerance inducing strategies in a living animal model will require longer term follow up and cessation of immunosuppression, something that is beyond the scope of our research project.

The findings of this doctoral thesis can be summarised into 5 key points below.

**1. The immune cell compartment within the liver remain active during NMP**

Data from clinical NMP samples demonstrated numerous cytokines are elaborated from cells within the graft and these continue to increase during NMP. Although hepatocytes and cholangiocytes are capable of secreting several cytokines, the majority of production will have come from the leukocyte compartment. Given the red blood cells used in the perfusate solution are leukocyte depleted, they must be of liver donor origin. The cytokine profile appears to favour a Th1 profile, with elevated IL-17. This inflammatory cytokine profile may influence Treg phenotype, however this was not investigated rigourosly in this thesis.

**2. Retransplant recipients experience more early BPAR with NMP grafts than CS**

This clinical observation that NMP appeared to result in frequent and severe rejection was a major factor that instigated this research. Further investigation using clinical data from our large transplant centre demonstrated that there was no difference in primary transplant recipients, but there was for retransplant recipients despite having similar immunosuppressive regimes. This suggests that there is both graft and recipient factors contributing. Patients that have undergone previous organ transplant are known to display chimerism, with donor cells remaining in their circulation. This makes for a more complex interaction on exposure to foreign antigens. Further research should investigate how the immune cell profile of the recipient changes with each successive transplant.

**3. Isolating human Tregs is possible, maintaining high FoxP3 expression is challenging**

This research project involved trials at isolating human Tregs via various different methods. Different types of immunomagnetic isolation was performed, but overall the yield of Tregs was low compared to FACS. Due to the fact we were using small blood samples from human blood (as would be required in the clinical setting) the overall starting number of Tregs was to low to perform FoxP3 assessment prior to expansion. Despite using a similar conditions for expansion, the results varied significantly. Assessment of FoxP3 requires intracellular staining and achieving we failed to achieve consistent results. If ex-vivo Treg therapy was to be trialled in a clinical setting, ensuring maintenance of FoxP3 expression would be very important.

**4. Tregs administered ex-vivo move out of the vascular space and engraft into the organ**

The Tregs were labelled with CMTPX to allow their location to be identified within the liver parenchyma. In both the wedge perfusion model and the whole liver perfusion model, confocal microscopy has demonstrated the Tregs to be outside the vascular space. This was further confirmed with Z-stack images and 3D reconstruction software. This is an important finding as cell therapy is different from small molecule pharmacological therapy, and is reliant on cell migration and survival. The experiments with the whole liver model demonstrate that this occurs within 4 hours of infusion. Due to our experimental methodology, it is impossible to comment on what proportion of the infused cells engraft. This would be valuable to know so it can be considered when calculating the dose of cell therapy required.

**5. It is possible to reclaim the infused cells and test the phenotype**

This doctoral thesis required further development of an experimental model that would allow infusion experiments at low cost. The wedge perfusion experimental model utilised allowed small scale infusion experiments with the numbers of Tregs achieved post isolation and expansion. The small piece of liver was then able to undergo mechanical dissociation and LDL isolation, which included the infused cells. Using the autofluorescent properties of CMTPX, the infused cell population could be gated for using flow cytometry. We demonstrated that it was possible to do this for the labelled population within the liver parenchyma (LDLs) and perfusate at the end of the perfusion. A limitation of using this method is that CMTPX is very bright, and interferes with many other fluorochromes. This limits the options for the antibody staining panel. Using the same strategy in the whole liver model allowed us to identify our labelled population, however the event number was to low to allow thorough phenotyping. Further research would benefit from infusing a larger number of cells (to improve cell density) or subject the entire liver to mechanical dissociation in an effort to re-isolate a larger quantity of the infused cells.

The ex-vivo administration of Tregs to the liver graft would provide challenging, but not unsurpassable logistical challenges. Patients awaiting liver transplantation on the national deceased donor waitlist would be required to undergo leukapheresis to obtain their Tregs for expansion prior to transplantation, and subsequently expanded. The expanded cell population would need to be cryopreserved until the transplant is scheduled to occur.

To determine the effect the infused Tregs have on the hepatic microenviroment, further research is required. Due to the fact that the tolerance inducing effects of the infused Tregs will not be apparent in the short term, a large animal model would be required so longer-term assessment could be made. Given the large amount of safety data available following

intravenous administration of Tregs in humans, with adequate regulatory oversight, many would consider it ethically acceptable to trial this intervention in human liver transplant recipients. Analysis of gene expression changes within the graft following the receipt of the therapeutic Tregs would be informative, as gene expression within both the liver resident immune cells and parenchyma could prove to be the most sensitive platform to demonstrate the Tregs effects. Although this intervention and research would come with considerable upfront costs, the longer-term healthcare savings if chronic rejection, life threatening infections and the metabolic sequalae of immunosuppression can be avoided would be considerable.

## 7.0 References


1. Starzl TE, Fung JJ. Themes of liver transplantation. *Hepatology*. Jun 2010;51(6):1869-84. doi:10.1002/hep.23595
2. Penn I, Halgrimson CG, Starzl TE. LIVER TRANSPLANTATION IN MAN. *Ann N Y Acad Sci*. Jul 1970;170:251-258. doi:10.1111/j.1749-6632.1970.tb37018.x
3. Starzl TE, Marchioro TL, Vonkaulla KN, Hermann G, Brittain RS, Waddell WR. HOMOTRANSPLANTATION OF THE LIVER IN HUMANS. *Surg Gynecol Obstet*. Dec 1963;117:659-76.
4. National Institutes of Health Consensus Development Conference Statement: liver transplantation--June 20-23, 1983. *Hepatology*. Jan-Feb 1984;4(1 Suppl):107s-110s.
5. Sharma S, Saner FH, Bezinover D. A brief history of liver transplantation and transplant anesthesia. *BMC Anesthesiol*. Nov 26 2022;22(1):363. doi:10.1186/s12871-022-01904-1
6. Bellini MI, Yiu J, Nozdrin M, Papalois V. The Effect of Preservation Temperature on Liver, Kidney, and Pancreas Tissue ATP in Animal and Preclinical Human Models. *Journal of clinical medicine*. Sep 9 2019;8(9)doi:10.3390/jcm8091421
7. Fondevila C, Busuttil RW, Kupiec-Weglinski JW. Hepatic ischemia/reperfusion injury--a fresh look. *Experimental and molecular pathology*. Apr 2003;74(2):86-93. doi:10.1016/s0014-4800(03)00008-x
8. Boteon YL, Afford SC. Machine perfusion of the liver: Which is the best technique to mitigate ischaemia-reperfusion injury? *World J Transplant*. Jan 16 2019;9(1):14-20. doi:10.5500/wjt.v9.i1.14
9. Peralta C, Jimenez-Castro MB, Gracia-Sancho J. Hepatic ischemia and reperfusion injury: effects on the liver sinusoidal milieu. *Journal of hepatology*. Nov 2013;59(5):1094-106. doi:10.1016/j.jhep.2013.06.017
10. Jayant K, Reccia I, Shapiro AMJ. Normothermic ex-vivo liver perfusion: where do we stand and where to reach? *Expert review of gastroenterology & hepatology*. Oct 2018;12(10):1045-1058. doi:10.1080/17474124.2018.1505499
11. Martins PN, Chandraker A, Tullius SG. Modifying graft immunogenicity and immune response prior to transplantation: potential clinical applications of donor and graft treatment. *Transplant international : official journal of the European Society for Organ Transplantation*. May 2006;19(5):351-9. doi:10.1111/j.1432-2277.2006.00301.x
12. Dar WA, Sullivan E, Bynon JS, Eltzschig H, Ju C. Ischaemia reperfusion injury in liver transplantation: Cellular and molecular mechanisms. *Liver international : official journal of the International Association for the Study of the Liver*. May 2019;39(5):788-801. doi:10.1111/liv.14091
13. Hartog H, Hann A, Perera M. Primary Nonfunction of the Liver Allograft. *Transplantation*. Jan 1 2022;106(1):117-128. doi:10.1097/tp.0000000000003682
14. D'Aragon F, Belley-Cote E, Agarwal A, et al. Effect of corticosteroid administration on neurologically deceased organ donors and transplant recipients: a systematic review and meta-analysis. *BMJ Open*. Jun 30 2017;7(6):e014436. doi:10.1136/bmjopen-2016-014436
15. Choudhary NS, Saigal S, Bansal RK, Saraf N, Gautam D, Soin AS. Acute and Chronic Rejection After Liver Transplantation: What A Clinician Needs to Know. *Journal of clinical and experimental hepatology*. Dec 2017;7(4):358-366. doi:10.1016/j.jceh.2017.10.003
16. Gokmen MR, Lombardi G, Lechler RI. The importance of the indirect pathway of allorecognition in clinical transplantation. *Current opinion in immunology*. Oct 2008;20(5):568-74. doi:10.1016/j.coi.2008.06.009
17. Joly E, Hudrisier D. What is trogocytosis and what is its purpose? *Nature immunology*. Sep 2003;4(9):815. doi:10.1038/ni0903-815
18. Taner T. Liver transplantation: Rejection and tolerance. *Liver transplantation : official publication of the American Association for the Study of Liver Diseases and the International Liver Transplantation Society*. Oct 2017;23(S1):S85-s88. doi:10.1002/lt.24840

19. Banff schema for grading liver allograft rejection: an international consensus document. *Hepatology*. Mar 1997;25(3):658-63. doi:10.1002/hep.510250328
20. Demetris AJ, Bellamy C, Hubscher SG, et al. 2016 Comprehensive Update of the Banff Working Group on Liver Allograft Pathology: Introduction of Antibody-Mediated Rejection. *American journal of transplantation : official journal of the American Society of Transplantation and the American Society of Transplant Surgeons*. Oct 2016;16(10):2816-2835. doi:10.1111/ajt.13909
21. Jadlowiec CC, Morgan PE, Nehra AK, et al. Not All Cellular Rejections Are the Same: Differences in Early and Late Hepatic Allograft Rejection. *Liver transplantation : official publication of the American Association for the Study of Liver Diseases and the International Liver Transplantation Society*. Mar 2019;25(3):425-435. doi:10.1002/lt.25411
22. Klintmalm GB, Nery JR, Husberg BS, Gonwa TA, Tillery GW. Rejection in liver transplantation. *Hepatology*. Dec 1989;10(6):978-85. doi:10.1002/hep.1840100615
23. Demetris AJ, Adeyi O, Bellamy CO, et al. Liver biopsy interpretation for causes of late liver allograft dysfunction. *Hepatology*. Aug 2006;44(2):489-501. doi:10.1002/hep.21280
24. Demetris A, Adams D, Bellamy C, et al. Update of the International Banff Schema for Liver Allograft Rejection: working recommendations for the histopathologic staging and reporting of chronic rejection. An International Panel. *Hepatology*. Mar 2000;31(3):792-9. doi:10.1002/hep.510310337
25. Wozniak LJ, Venick RS. Donor-specific antibodies following liver and intestinal transplantation: Clinical significance, pathogenesis and recommendations. *International reviews of immunology*. 2019;38(3):106-117. doi:10.1080/08830185.2019.1630404
26. Aguilera I, Sousa JM, Nunez-Roldan A. Clinical relevance of GSTT1 mismatch in solid organ and hematopoietic stem cell transplantation. *Human immunology*. Nov 2013;74(11):1470-3. doi:10.1016/j.humimm.2013.06.004
27. Demetris AJ, Bellamy CO, Gandhi CR, Prost S, Nakanuma Y, Stolz DB. Functional Immune Anatomy of the Liver-As an Allograft. *American journal of transplantation : official journal of the American Society of Transplantation and the American Society of Transplant Surgeons*. Jun 2016;16(6):1653-80. doi:10.1111/ajt.13749
28. O'Leary JG, Michelle Shiller S, Bellamy C, et al. Acute liver allograft antibody-mediated rejection: an inter-institutional study of significant histopathological features. *Liver transplantation : official publication of the American Association for the Study of Liver Diseases and the International Liver Transplantation Society*. Oct 2014;20(10):1244-55. doi:10.1002/lt.23948
29. Davies HS, Pollard SG, Calne RY. Soluble HLA antigens in the circulation of liver graft recipients. *Transplantation*. Mar 1989;47(3):524-7. doi:10.1097/00007890-198903000-00025
30. Abrol N, Jadlowiec CC, Taner T. Revisiting the liver's role in transplant alloimmunity. *World J Gastroenterol*. Jul 7 2019;25(25):3123-3135. doi:10.3748/wjg.v25.i25.3123
31. Zhang R. Donor-Specific Antibodies in Kidney Transplant Recipients. *Clinical journal of the American Society of Nephrology : CJASN*. Jan 6 2018;13(1):182-192. doi:10.2215/cjn.00700117
32. Del Bello A, Congy-Jolivet N, Muscari F, et al. Prevalence, incidence and risk factors for donor-specific anti-HLA antibodies in maintenance liver transplant patients. *American journal of transplantation : official journal of the American Society of Transplantation and the American Society of Transplant Surgeons*. Apr 2014;14(4):867-75. doi:10.1111/ajt.12651
33. Kaneku H, O'Leary JG, Banuelos N, et al. De novo donor-specific HLA antibodies decrease patient and graft survival in liver transplant recipients. *American journal of transplantation : official journal of the American Society of Transplantation and the American Society of Transplant Surgeons*. Jun 2013;13(6):1541-8. doi:10.1111/ajt.12212

10.1002/ajt.12212
34. Iacob S, Cicinnati VR, Dechene A, et al. Genetic, immunological and clinical risk factors for biliary strictures following liver transplantation. *Liver international : official journal of the International Association for the Study of the Liver*. Sep 2012;32(8):1253-61. doi:10.1111/j.1478-3231.2012.02810.x

35. Demetris AJ, Ruppert K, Dvorchik I, et al. Real-time monitoring of acute liver-allograft rejection using the Banff schema. *Transplantation*. Nov 15 2002;74(9):1290-6. doi:10.1097/00007890-200211150-00016
36. Atif M, Conti F, Gorochov G, Oo YH, Miyara M. Regulatory T cells in solid organ transplantation. *Clin Transl Immunology*. 2020;9(2):e01099. doi:10.1002/cti2.1099
37. Feng S, Bucuvalas JC, Mazariegos GV, et al. Efficacy and Safety of Immunosuppression Withdrawal in Pediatric Liver Transplant Recipients: Moving Towards Personalized Management. *Hepatology (Baltimore, Md)*. Aug 12 2020;doi:10.1002/hep.31520
38. Rickert CG, Markmann JF. Current state of organ transplant tolerance. *Current opinion in organ transplantation*. Aug 2019;24(4):441-450. doi:10.1097/mot.0000000000000670
39. Whitehouse GP, Hope A, Sanchez-Fueyo A. Regulatory T-cell therapy in liver transplantation. *Transplant international : official journal of the European Society for Organ Transplantation*. Aug 2017;30(8):776-784. doi:10.1111/tri.12998
40. Benitez C, Londono MC, Miquel R, et al. Prospective multicenter clinical trial of immunosuppressive drug withdrawal in stable adult liver transplant recipients. *Hepatology*. Nov 2013;58(5):1824-35. doi:10.1002/hep.26426
41. Feng S, Ekong UD, Lobritto SJ, et al. Complete immunosuppression withdrawal and subsequent allograft function among pediatric recipients of parental living donor liver transplants. *Jama*. Jan 18 2012;307(3):283-93. doi:10.1001/jama.2011.2014
42. Feng S, Bucuvalas JC, Mazariegos GV, et al. Efficacy and Safety of Immunosuppression Withdrawal in Pediatric Liver Transplant Recipients: Moving Toward Personalized Management. *Hepatology*. May 2021;73(5):1985-2004. doi:10.1002/hep.31520
43. Baroja-Mazo A, Revilla-Nuin B, Parrilla P, Martinez-Alarcon L, Ramirez P, Pons JA. Tolerance in liver transplantation: Biomarkers and clinical relevance. *World journal of gastroenterology*. Sep 14 2016;22(34):7676-91. doi:10.3748/wjg.v22.i34.7676
44. de la Garza RG, Sarobe P, Merino J, et al. Trial of complete weaning from immunosuppression for liver transplant recipients: factors predictive of tolerance. *Liver Transpl*. Sep 2013;19(9):937-44. doi:10.1002/lt.23686
45. Appenzeller-Herzog C, Rosat A, Mathes T, et al. Time since liver transplant and immunosuppression withdrawal outcomes: Systematic review and individual patient data meta-analysis. *Liver Int*. Jan 2024;44(1):250-262. doi:10.1111/liv.15764
46. Cvetkovski F, Hexham JM, Berglund E. Strategies for Liver Transplantation Tolerance. *Int J Mol Sci*. Feb 24 2021;22(5)doi:10.3390/ijms22052253
47. Starzl TE, Murase N, Abu-Elmagd K, et al. Tolerogenic immunosuppression for organ transplantation. *Lancet*. May 3 2003;361(9368):1502-10. doi:10.1016/s0140-6736(03)13175-3
48. Benítez CE, Puig-Pey I, López M, et al. ATG-Fresenius treatment and low-dose tacrolimus: results of a randomized controlled trial in liver transplantation. *Am J Transplant*. Oct 2010;10(10):2296-304. doi:10.1111/j.1600-6143.2010.03164.x
49. Levitsky J, Thudi K, Ison MG, Wang E, Abecassis M. Alemtuzumab induction in non-hepatitis C positive liver transplant recipients. *Liver Transpl*. Jan 2011;17(1):32-7. doi:10.1002/lt.22180
50. Ellias SD, Larson EL, Taner T, Nyberg SL. Cell-Mediated Therapies to Facilitate Operational Tolerance in Liver Transplantation. *Int J Mol Sci*. Apr 13 2021;22(8)doi:10.3390/ijms22084016
51. Macedo C, Tran LM, Zahorchak AF, et al. Donor-derived regulatory dendritic cell infusion results in host cell cross-dressing and T cell subset changes in prospective living donor liver transplant recipients. *Am J Transplant*. Jul 2021;21(7):2372-2386. doi:10.1111/ajt.16393
52. Detry O, Vandermeulen M, Delbouille MH, et al. Infusion of mesenchymal stromal cells after deceased liver transplantation: A phase I-II, open-label, clinical study. *J Hepatol*. Jul 2017;67(1):47-55. doi:10.1016/j.jhep.2017.03.001
53. Nishizuka Y, Sakakura T. Thymus and reproduction: sex-linked dysgenesia of the gonad after neonatal thymectomy in mice. *Science (New York, NY)*. Nov 7 1969;166(3906):753-5. doi:10.1126/science.166.3906.753

54. Gershon RK, Kondo K. Infectious immunological tolerance. *Immunology*. Dec 1971;21(6):903-14.
55. Shevach EM. The resurrection of T cell-mediated suppression. *J Immunol*. Apr 1 2011;186(7):3805-7. doi:10.4049/jimmunol.1100364
56. Sakaguchi S, Sakaguchi N, Asano M, Itoh M, Toda M. Immunologic self-tolerance maintained by activated T cells expressing IL-2 receptor alpha-chains (CD25). Breakdown of a single mechanism of self-tolerance causes various autoimmune diseases. *J Immunol*. Aug 1 1995;155(3):1151-64.
57. Jeffery HC, Braitch MK, Brown S, Oo YH. Clinical Potential of Regulatory T Cell Therapy in Liver Diseases: An Overview and Current Perspectives. *Front Immunol*. 2016;7:334. doi:10.3389/fimmu.2016.00334
58. Shevach EM. Mechanisms of foxp3+ T regulatory cell-mediated suppression. *Immunity*. May 2009;30(5):636-45. doi:10.1016/j.immuni.2009.04.010
59. Wang D, Zhang H, Liang J, et al. CD4+ CD25+ but not CD4+ Foxp3+ T cells as a regulatory subset in primary biliary cirrhosis. *Cell Mol Immunol*. Nov 2010;7(6):485-90. doi:10.1038/cmi.2010.40
60. Zhang S, Goswami S, Ma J, et al. CD4(+)T Cell Subset Profiling in Biliary Atresia Reveals ICOS(-) Regulatory T Cells as a Favorable Prognostic Factor. *Front Pediatr*. 2019;7:279. doi:10.3389/fped.2019.00279
61. Sakaguchi S, Sakaguchi N, Shimizu J, et al. Immunologic tolerance maintained by CD25+ CD4+ regulatory T cells: their common role in controlling autoimmunity, tumor immunity, and transplantation tolerance. *Immunological reviews*. Aug 2001;182:18-32. doi:10.1034/j.1600-065x.2001.1820102.x
62. Romano M, Fanelli G, Albany CJ, Giganti G, Lombardi G. Past, Present, and Future of Regulatory T Cell Therapy in Transplantation and Autoimmunity. *Frontiers in immunology*. 2019;10:43. doi:10.3389/fimmu.2019.00043
63. Vitale S, Russo V, Dettori B, et al. Type I interferons induce peripheral T regulatory cell differentiation under tolerogenic conditions. *Int Immunol*. Aug 25 2020;doi:10.1093/intimm/dxaa058
64. Tai X, Cowan M, Feigenbaum L, Singer A. CD28 costimulation of developing thymocytes induces Foxp3 expression and regulatory T cell differentiation independently of interleukin 2. *Nature immunology*. Feb 2005;6(2):152-62. doi:10.1038/ni1160
65. Kretschmer K, Apostolou I, Hawiger D, Khazaie K, Nussenzweig MC, von Boehmer H. Inducing and expanding regulatory T cell populations by foreign antigen. *Nature immunology*. Dec 2005;6(12):1219-27. doi:10.1038/ni1265
66. Gregori S, Roncarolo MG. Engineered T Regulatory Type 1 Cells for Clinical Application. *Front Immunol*. 2018;9:233. doi:10.3389/fimmu.2018.00233
67. Richardson N, Ng STH, Wraith DC. Antigen-Specific Immunotherapy for Treatment of Autoimmune Liver Diseases. *Front Immunol*. 2020;11:1586. doi:10.3389/fimmu.2020.01586
68. Miyara M, Yoshioka Y, Kitoh A, et al. Functional delineation and differentiation dynamics of human CD4+ T cells expressing the FoxP3 transcription factor. *Immunity*. Jun 19 2009;30(6):899-911. doi:10.1016/j.immuni.2009.03.019
69. Wang K, Song ZL, Wu B, Zhou CL, Liu W, Gao W. Different phenotypes of CD4(+)CD25(+)Foxp3(+) regulatory T cells in recipients post liver transplantation. *Int Immunopharmacol*. Apr 2019;69:194-201. doi:10.1016/j.intimp.2019.01.048
70. Li L, Boussiotis VA. The role of IL-17-producing Foxp3+ CD4+ T cells in inflammatory bowel disease and colon cancer. *Clin Immunol*. Aug 2013;148(2):246-53. doi:10.1016/j.clim.2013.05.003
71. Whitehouse G, Gray E, Mastoridis S, et al. IL-2 therapy restores regulatory T-cell dysfunction induced by calcineurin inhibitors. *Proc Natl Acad Sci U S A*. Jul 3 2017;114(27):7083-7088. doi:10.1073/pnas.1620835114

72. Nafady-Hego H, Li Y, Ohe H, et al. The generation of donor-specific CD4+CD25++CD45RA+ naive regulatory T cells in operationally tolerant patients after pediatric living-donor liver transplantation. *Transplantation*. Dec 27 2010;90(12):1547-55. doi:10.1097/TP.0b013e3181f9960d
73. Kim HJ, Barnitz RA, Kreslavsky T, et al. Stable inhibitory activity of regulatory T cells requires the transcription factor Helios. *Science (New York, NY)*. Oct 16 2015;350(6258):334-9. doi:10.1126/science.aad0616
74. Josefowicz SZ, Lu LF, Rudensky AY. Regulatory T cells: mechanisms of differentiation and function. *Annual review of immunology*. 2012;30:531-64. doi:10.1146/annurev.immunol.25.022106.141623
75. Rubtsov YP, Rasmussen JP, Chi EY, et al. Regulatory T cell-derived interleukin-10 limits inflammation at environmental interfaces. *Immunity*. Apr 2008;28(4):546-58. doi:10.1016/j.immuni.2008.02.017
76. Qureshi OS, Zheng Y, Nakamura K, et al. Trans-endocytosis of CD80 and CD86: a molecular basis for the cell-extrinsic function of CTLA-4. *Science*. Apr 29 2011;332(6029):600-3. doi:10.1126/science.1202947
77. Wang X, Sun L, Zhang L, Jiang Z. Effect of Adoptive Transfer or Depletion of Regulatory T Cells on Triptolide-induced Liver Injury. *Frontiers in pharmacology*. 2016;7:99. doi:10.3389/fphar.2016.00099
78. Erhardt A, Biburger M, Papadopoulos T, Tiegs G. IL-10, regulatory T cells, and Kupffer cells mediate tolerance in concanavalin A-induced liver injury in mice. *Hepatology (Baltimore, Md)*. Feb 2007;45(2):475-85. doi:10.1002/hep.21498
79. Starzl TE, Iwatsuki S, Van Thiel DH, et al. Evolution of liver transplantation. *Hepatology (Baltimore, Md)*. Sep-Oct 1982;2(5):614-36. doi:10.1002/hep.1840020516
80. Fujiki M, Esquivel CO, Martinez OM, Strober S, Uemoto S, Krams SM. Induced tolerance to rat liver allografts involves the apoptosis of intragraft T cells and the generation of CD4(+)CD25(+)FoxP3(+) T regulatory cells. *Liver transplantation : official publication of the American Association for the Study of Liver Diseases and the International Liver Transplantation Society*. Feb 2010;16(2):147-54. doi:10.1002/lt.21963
81. Bashuda H, Kimikawa M, Seino K, et al. Renal allograft rejection is prevented by adoptive transfer of anergic T cells in nonhuman primates. *The Journal of clinical investigation*. Jul 2005;115(7):1896-902. doi:10.1172/jci23743
82. Li Y, Zhao X, Cheng D, et al. The presence of Foxp3 expressing T cells within grafts of tolerant human liver transplant recipients. *Transplantation*. Dec 27 2008;86(12):1837-43. doi:10.1097/TP.0b013e31818febc4
83. Hann A, Osei-Bordom DC, Neil DAH, Ronca V, Warner S, Perera M. The Human Immune Response to Cadaveric and Living Donor Liver Allografts. *Front Immunol*. 2020;11:1227. doi:10.3389/fimmu.2020.01227
84. Ronca V, Wootton G, Milani C, Cain O. The Immunological Basis of Liver Allograft Rejection. *Frontiers in immunology*. 2020;11:2155. doi:10.3389/fimmu.2020.02155
85. Howard TK, Klintmalm GB, Cofer JB, Husberg BS, Goldstein RM, Gonwa TA. The influence of preservation injury on rejection in the hepatic transplant recipient. *Transplantation*. Jan 1990;49(1):103-7. doi:10.1097/00007890-199001000-00023
86. Yu J, Liu Z, Li C, et al. Regulatory T Cell Therapy Following Liver Transplantation. *Liver transplantation : official publication of the American Association for the Study of Liver Diseases and the International Liver Transplantation Society*. Nov 22 2020;doi:10.1002/lt.25948
87. Todo S, Yamashita K, Goto R, et al. A pilot study of operational tolerance with a regulatory T-cell-based cell therapy in living donor liver transplantation. *Hepatology (Baltimore, Md)*. Aug 2016;64(2):632-43. doi:10.1002/hep.28459
88. Sánchez-Fueyo A, Whitehouse G, Grageda N, et al. Applicability, safety, and biological activity of regulatory T cell therapy in liver transplantation. *American journal of transplantation :*

*official journal of the American Society of Transplantation and the American Society of Transplant Surgeons*. Apr 2020;20(4):1125-1136. doi:10.1111/ajt.15700
89. Sawitzki B, Harden PN, Reinke P, et al. Regulatory cell therapy in kidney transplantation (The ONE Study): a harmonised design and analysis of seven non-randomised, single-arm, phase 1/2A trials. *Lancet (London, England)*. May 23 2020;395(10237):1627-1639. doi:10.1016/s0140-6736(20)30167-7
90. Todo S, Yamashita K. Anti-donor regulatory T cell therapy in liver transplantation. *Human immunology*. May 2018;79(5):288-293. doi:10.1016/j.humimm.2017.12.010
91. Safinia N, Vaikunthanathan T, Fraser H, et al. Successful expansion of functional and stable regulatory T cells for immunotherapy in liver transplantation. *Oncotarget*. Feb 16 2016;7(7):7563-77. doi:10.18632/oncotarget.6927
92. Li L, Kim J, Boussiotis VA. IL-1β-mediated signals preferentially drive conversion of regulatory T cells but not conventional T cells into IL-17-producing cells. *J Immunol*. Oct 1 2010;185(7):4148-53. doi:10.4049/jimmunol.1001536
93. Koenen HJ, Smeets RL, Vink PM, van Rijssen E, Boots AM, Joosten I. Human CD25highFoxp3pos regulatory T cells differentiate into IL-17-producing cells. *Blood*. Sep 15 2008;112(6):2340-52. doi:10.1182/blood-2008-01-133967
94. Kopf H, de la Rosa GM, Howard OM, Chen X. Rapamycin inhibits differentiation of Th17 cells and promotes generation of FoxP3+ T regulatory cells. *Int Immunopharmacol*. Dec 15 2007;7(13):1819-24. doi:10.1016/j.intimp.2007.08.027
95. Oo YH, Ackrill S, Cole R, et al. Liver homing of clinical grade Tregs after therapeutic infusion in patients with autoimmune hepatitis. *JHEP Rep*. Oct 2019;1(4):286-296. doi:10.1016/j.jhepr.2019.08.001
96. Oo YH, Weston CJ, Lalor PF, et al. Distinct roles for CCR4 and CXCR3 in the recruitment and positioning of regulatory T cells in the inflamed human liver. *Journal of immunology (Baltimore, Md : 1950)*. Mar 15 2010;184(6):2886-98. doi:10.4049/jimmunol.0901216
97. Wawman RE, Bartlett H, Oo YH. Regulatory T Cell Metabolism in the Hepatic Microenvironment. *Frontiers in immunology*. 2017;8:1889. doi:10.3389/fimmu.2017.01889
98. Han JW, Joo DJ, Kim JH, et al. Early reduction of regulatory T cells is associated with acute rejection in liver transplantation under tacrolimus-based immunosuppression with basiliximab induction. *American journal of transplantation : official journal of the American Society of Transplantation and the American Society of Transplant Surgeons*. Aug 2020;20(8):2058-2069. doi:10.1111/ajt.15789
99. Demirkiran A, Kok A, Kwekkeboom J, et al. Low circulating regulatory T-cell levels after acute rejection in liver transplantation. *Liver transplantation : official publication of the American Association for the Study of Liver Diseases and the International Liver Transplantation Society*. Feb 2006;12(2):277-84. doi:10.1002/lt.20612
100. Wang K, Song ZL, Wu B, Zhou CL, Liu W, Gao W. The T-helper cells 17 instead of Tregs play the key role in acute rejection after pediatric liver transplantation. *Pediatric transplantation*. May 2019;23(3):e13363. doi:10.1111/petr.13363
101. Ozeki M, Salah A, Aini W, Tamaki K, Haga H, Miyagawa-Hayashino A. Abnormal Localization of STK17A in Bile Canaliculi in Liver Allografts: An Early Sign of Chronic Rejection. *PloS one*. 2015;10(8):e0136381. doi:10.1371/journal.pone.0136381
102. Wan R, Tang L, Shan R, Zeng L, Chen H, Gao L. Humoral immunity-mediated chronic rejection in liver transplantation is associated with predominant IL-10 expression. *Frontiers in bioscience (Elite edition)*. Jan 1 2012;4:2121-30. doi:10.2741/529
103. Demetris AJ, Bellamy C, Hübscher SG, et al. 2016 Comprehensive Update of the Banff Working Group on Liver Allograft Pathology: Introduction of Antibody-Mediated Rejection. *American journal of transplantation : official journal of the American Society of Transplantation and the American Society of Transplant Surgeons*. Oct 2016;16(10):2816-2835. doi:10.1111/ajt.13909

104. Louis S, Braudeau C, Giral M, et al. Contrasting CD25hiCD4+T cells/FOXP3 patterns in chronic rejection and operational drug-free tolerance. *Transplantation*. Feb 15 2006;81(3):398-407. doi:10.1097/01.tp.0000203166.44968.86
105. Raigani S, De Vries RJ, Uygun K, Yeh H. Pumping new life into old ideas: Preservation and rehabilitation of the liver using ex situ machine perfusion. *Artif Organs*. Feb 2020;44(2):123-128. doi:10.1111/aor.13579
106. Slapak M, Wigmore RA, MacLean LD. Twenty-four hour liver preservation by the use of continuous pulsatile perfusion and hyperbaric oxygen. *Transplantation*. Jul 1967;5(4):Suppl:1154-8. doi:10.1097/00007890-196707001-00052
107. van Rijn R, Schurink IJ, de Vries Y, et al. Hypothermic Machine Perfusion in Liver Transplantation - A Randomized Trial. *N Engl J Med*. Apr 15 2021;384(15):1391-1401. doi:10.1056/NEJMoa2031532
108. Nasralla D, Coussios CC, Mergental H, et al. A randomized trial of normothermic preservation in liver transplantation. *Nature*. May 2018;557(7703):50-56. doi:10.1038/s41586-018-0047-9
109. Durán M, Calleja R, Hann A, et al. Machine perfusion and the prevention of ischemic type biliary lesions following liver transplant: What is the evidence? *World J Gastroenterol*. May 28 2023;29(20):3066-3083. doi:10.3748/wjg.v29.i20.3066
110. Melandro F, Basta G, Torri F, et al. Normothermic regional perfusion in liver transplantation from donation after cardiocirculatory death: Technical, biochemical, and regulatory aspects and review of literature. *Artif Organs*. Sep 2022;46(9):1727-1740. doi:10.1111/aor.14330
111. Gaurav R, Butler AJ, Kosmoliaptsis V, et al. Liver Transplantation Outcomes From Controlled Circulatory Death Donors: SCS vs in situ NRP vs ex situ NMP. *Ann Surg*. Jun 1 2022;275(6):1156-1164. doi:10.1097/sla.0000000000005428
112. Ceresa CDL, Nasralla D, Coussios CC, Friend PJ. The case for normothermic machine perfusion in liver transplantation. *Liver transplantation : official publication of the American Association for the Study of Liver Diseases and the International Liver Transplantation Society*. Feb 2018;24(2):269-275. doi:10.1002/lt.25000
113. Ravikumar R, Jassem W, Mergental H, et al. Liver Transplantation After Ex Vivo Normothermic Machine Preservation: A Phase 1 (First-in-Man) Clinical Trial. *American journal of transplantation : official journal of the American Society of Transplantation and the American Society of Transplant Surgeons*. Jun 2016;16(6):1779-87. doi:10.1111/ajt.13708
114. Selzner M, Goldaracena N, Echeverri J, et al. Normothermic ex vivo liver perfusion using steen solution as perfusate for human liver transplantation: First North American results. *Liver transplantation : official publication of the American Association for the Study of Liver Diseases and the International Liver Transplantation Society*. Nov 2016;22(11):1501-1508. doi:10.1002/lt.24499
115. Bral M, Gala-Lopez B, Bigam D, et al. Preliminary Single-Center Canadian Experience of Human Normothermic Ex Vivo Liver Perfusion: Results of a Clinical Trial. *Am J Transplant*. Apr 2017;17(4):1071-1080. doi:10.1111/ajt.14049
116. Reiling J, Butler N, Simpson A, et al. Assessment and Transplantation of Orphan Donor Livers: A Back-to-Base Approach to Normothermic Machine Perfusion. *Liver Transpl*. Dec 2020;26(12):1618-1628. doi:10.1002/lt.25850
117. Mergental H, Perera MT, Laing RW, et al. Transplantation of Declined Liver Allografts Following Normothermic Ex-Situ Evaluation. *American journal of transplantation : official journal of the American Society of Transplantation and the American Society of Transplant Surgeons*. Nov 2016;16(11):3235-3245. doi:10.1111/ajt.13875
118. Watson CJ, Kosmoliaptsis V, Randle LV, et al. Preimplant Normothermic Liver Perfusion of a Suboptimal Liver Donated After Circulatory Death. *Am J Transplant*. Jan 2016;16(1):353-7. doi:10.1111/ajt.13448
119. Mergental H, Laing RW, Kirkham AJ, et al. Transplantation of discarded livers following viability testing with normothermic machine perfusion. *Nat Commun*. Jun 16 2020;11(1):2939. doi:10.1038/s41467-020-16251-3

120. Perera T, Mergental H, Stephenson B, et al. First human liver transplantation using a marginal allograft resuscitated by normothermic machine perfusion. *Liver Transpl*. Jan 2016;22(1):120-4. doi:10.1002/lt.24369
121. Stimmeder S, Leber B, Sucher R, Stiegler P. Genetic Modulation: Future Trends Toward Graft Optimization During Machine Perfusion. *Transplantation*. Mar 1 2024;108(3):614-624. doi:10.1097/tp.0000000000004738
122. Sampaziotis F, Muraro D, Tysoe OC, et al. Cholangiocyte organoids can repair bile ducts after transplantation in the human liver. *Science*. Feb 19 2021;371(6531):839-846. doi:10.1126/science.aaz6964
123. Sousa Da Silva RX, Bautista Borrego L, Lenggenhager D, et al. Defatting of Human Livers During Long-Term e x situ Normothermic Perfusion: Novel Strategy to Rescue Discarded Organs for Transplantation. *Ann Surg*. Nov 1 2023;278(5):669-675. doi:10.1097/sla.0000000000006047
124. Dengu F, Abbas SH, Ebeling G, Nasralla D. Normothermic Machine Perfusion (NMP) of the Liver as a Platform for Therapeutic Interventions during Ex-Vivo Liver Preservation: A Review. *J Clin Med*. Apr 7 2020;9(4)doi:10.3390/jcm9041046
125. Laing RW, Stubblefield S, Wallace L, et al. The Delivery of Multipotent Adult Progenitor Cells to Extended Criteria Human Donor Livers Using Normothermic Machine Perfusion. *Front Immunol*. 2020;11:1226. doi:10.3389/fimmu.2020.01226
126. NHSBT. DeFat. Accessed December, 2023. https://www.nhsbt.nhs.uk/clinical-trials-unit/current-trials-and-studies/defat/
127. McKinnon KM. Flow Cytometry: An Overview. *Curr Protoc Immunol*. Feb 21 2018;120:5.1.1-5.1.11. doi:10.1002/cpim.40
128. Staunstrup NH, Petersen CC, Fuglsang T, et al. Comparison of electrostatic and mechanical cell sorting with limited starting material. *Cytometry A*. Apr 2022;101(4):298-310. doi:10.1002/cyto.a.24523
129. Milward K, Hester J, Wood KJ. Isolation of Human Regulatory T Lymphocytes by Fluorescence-Activated Cell Sorting. *Methods Mol Biol*. 2019;1899:43-54. doi:10.1007/978-1-4939-8938-6_4
130. Battaglia M, Stabilini A, Roncarolo MG. Rapamycin selectively expands CD4+CD25+FoxP3+ regulatory T cells. *Blood*. Jun 15 2005;105(12):4743-8. doi:10.1182/blood-2004-10-3932
131. Markmann JF, Abouljoud MS, Ghobrial RM, et al. Impact of Portable Normothermic Blood-Based Machine Perfusion on Outcomes of Liver Transplant: The OCS Liver PROTECT Randomized Clinical Trial. *JAMA Surg*. Mar 1 2022;157(3):189-198. doi:10.1001/jamasurg.2021.6781
132. Chapman WC, Barbas AS, D'Alessandro AM, et al. Normothermic Machine Perfusion of Donor Livers for Transplantation in the United States: A Randomized Controlled Trial. *Ann Surg*. Nov 1 2023;278(5):e912-e921. doi:10.1097/sla.0000000000005934
133. Hann A, Lembach H, Nutu A, et al. Assessment of Deceased Brain Dead Donor Liver Grafts via Normothermic Machine Perfusion: Lactate Clearance Time Threshold Can Be Safely Extended to 6 Hours. *Liver Transpl*. Mar 2022;28(3):493-496. doi:10.1002/lt.26317
134. Olthoff KM, Kulik L, Samstein B, et al. Validation of a current definition of early allograft dysfunction in liver transplant recipients and analysis of risk factors. *Liver Transpl*. Aug 2010;16(8):943-9. doi:10.1002/lt.22091
135. Lee ACH, Edobor A, Lysandrou M, et al. The Effect of Normothermic Machine Perfusion on the Immune Profile of Donor Liver. *Front Immunol*. 2022;13:788935. doi:10.3389/fimmu.2022.788935
136. Hautz T, Salcher S, Fodor M, et al. Immune cell dynamics deconvoluted by single-cell RNA sequencing in normothermic machine perfusion of the liver. *Nat Commun*. Apr 21 2023;14(1):2285. doi:10.1038/s41467-023-37674-8
137. Kany S, Vollrath JT, Relja B. Cytokines in Inflammatory Disease. *Int J Mol Sci*. Nov 28 2019;20(23)doi:10.3390/ijms20236008

138. Spolski R, Li P, Leonard WJ. Biology and regulation of IL-2: from molecular mechanisms to human therapy. *Nat Rev Immunol*. Oct 2018;18(10):648-659. doi:10.1038/s41577-018-0046-y
139. Mills KHG. IL-17 and IL-17-producing cells in protection versus pathology. *Nat Rev Immunol*. Jan 2023;23(1):38-54. doi:10.1038/s41577-022-00746-9
140. He Y, Hwang S, Ahmed YA, et al. Immunopathobiology and therapeutic targets related to cytokines in liver diseases. *Cell Mol Immunol*. Jan 2021;18(1):18-37. doi:10.1038/s41423-020-00580-w
141. Taniguchi T, Takaoka A. A weak signal for strong responses: interferon-alpha/beta revisited. *Nat Rev Mol Cell Biol*. May 2001;2(5):378-86. doi:10.1038/35073080
142. Upadhyay V, Fu YX. Lymphotoxin signalling in immune homeostasis and the control of microorganisms. *Nat Rev Immunol*. Apr 2013;13(4):270-9. doi:10.1038/nri3406
143. Hunter CA, Jones SA. IL-6 as a keystone cytokine in health and disease. *Nat Immunol*. May 2015;16(5):448-57. doi:10.1038/ni.3153
144. Mathis S, Weissenbacher A, Putzer G, et al. Interleukin-6 Levels During Normothermic Machine Perfusion Impact Postreperfusion Hemodynamics of Liver Graft Recipients: A Prospective Single-center Observational Study. *Transplantation*. Oct 30 2023;doi:10.1097/tp.0000000000004852
145. Ghanei Z, Mehri N, Jamshidizad A, Joupari MD, Shamsara M. Immunization against leukemia inhibitory factor and its receptor suppresses tumor formation of breast cancer initiating cells in BALB/c mouse. *Sci Rep*. Jul 10 2020;10(1):11465. doi:10.1038/s41598-020-68158-0
146. Jones SA, Jenkins BJ. Recent insights into targeting the IL-6 cytokine family in inflammatory diseases and cancer. *Nat Rev Immunol*. Dec 2018;18(12):773-789. doi:10.1038/s41577-018-0066-7
147. Hamilton JA. Colony-stimulating factors in inflammation and autoimmunity. *Nat Rev Immunol*. Jul 2008;8(7):533-44. doi:10.1038/nri2356
148. Kimura M, Moteki H, Ogihara M. Role of Hepatocyte Growth Regulators in Liver Regeneration. *Cells*. Jan 4 2023;12(2)doi:10.3390/cells12020208
149. Berger A. Th1 and Th2 responses: what are they? *BMJ*. 2000;321:424. doi:doi:10.1136/bmj.321.7258.424
150. Lee HL, Jang JW, Lee SW, et al. Inflammatory cytokines and change of Th1/Th2 balance as prognostic indicators for hepatocellular carcinoma in patients treated with transarterial chemoembolization. *Sci Rep*. Mar 1 2019;9(1):3260. doi:10.1038/s41598-019-40078-8
151. Chen S, Saeed A, Liu Q, et al. Macrophages in immunoregulation and therapeutics. *Signal Transduct Target Ther*. May 22 2023;8(1):207. doi:10.1038/s41392-023-01452-1
152. Faitot F, Besch C, Battini S, et al. Impact of real-time metabolomics in liver transplantation: Graft evaluation and donor-recipient matching. *J Hepatol*. Apr 2018;68(4):699-706. doi:10.1016/j.jhep.2017.11.022
153. Cortes M, Pareja E, García-Cañaveras JC, et al. Metabolomics discloses donor liver biomarkers associated with early allograft dysfunction. *J Hepatol*. Sep 2014;61(3):564-74. doi:10.1016/j.jhep.2014.04.023
154. Hrydziuszko O, Perera MT, Laing R, et al. Mass Spectrometry Based Metabolomics Comparison of Liver Grafts from Donors after Circulatory Death (DCD) and Donors after Brain Death (DBD) Used in Human Orthotopic Liver Transplantation. *PLoS One*. 2016;11(11):e0165884. doi:10.1371/journal.pone.0165884
155. Lonati C, Dondossola D, Zizmare L, et al. Quantitative Metabolomics of Tissue, Perfusate, and Bile from Rat Livers Subjected to Normothermic Machine Perfusion. *Biomedicines*. Feb 24 2022;10(3)doi:10.3390/biomedicines10030538
156. Zhang A, Carroll C, Raigani S, et al. Tryptophan Metabolism via the Kynurenine Pathway: Implications for Graft Optimization during Machine Perfusion. *J Clin Med*. Jun 15 2020;9(6)doi:10.3390/jcm9061864
157. Karimian N, Raigani S, Huang V, et al. Subnormothermic Machine Perfusion of Steatotic Livers Results in Increased Energy Charge at the Cost of Anti-Oxidant Capacity Compared to Normothermic Perfusion. *Metabolites*. Oct 24 2019;9(11)doi:10.3390/metabo9110246

158. Bruinsma BG, Sridharan GV, Weeder PD, et al. Metabolic profiling during ex vivo machine perfusion of the human liver. *Sci Rep*. Mar 3 2016;6:22415. doi:10.1038/srep22415
159. Frediani JK, Beyh YS, Gupta N, et al. Metabolomics profiling in acute liver transplant rejection in a pediatric population. *Sci Rep*. Nov 4 2022;12(1):18663. doi:10.1038/s41598-022-18957-4
160. Pareja E, Cortes M, Hervás D, et al. A score model for the continuous grading of early allograft dysfunction severity. *Liver Transpl*. Jan 2015;21(1):38-46. doi:10.1002/lt.23990
161. Peschel G, Krautbauer S, Weigand K, et al. Rising Lysophosphatidylcholine Levels Post-Hepatitis C Clearance. *Int J Mol Sci*. Jan 18 2024;25(2)doi:10.3390/ijms25021198
162. Law SH, Chan ML, Marathe GK, Parveen F, Chen CH, Ke LY. An Updated Review of Lysophosphatidylcholine Metabolism in Human Diseases. *Int J Mol Sci*. Mar 6 2019;20(5)doi:10.3390/ijms20051149
163. Jassem W, Xystrakis E, Ghnewa YG, et al. Normothermic Machine Perfusion (NMP) Inhibits Proinflammatory Responses in the Liver and Promotes Regeneration. *Hepatology*. Aug 2019;70(2):682-695. doi:10.1002/hep.30475
164. Kabata H, Motomura Y, Kiniwa T, Kobayashi T, Moro K. ILCs and Allergy. *Adv Exp Med Biol*. 2022;1365:75-95. doi:10.1007/978-981-16-8387-9_6
165. Fung JJ. Tolerance and chimerism in liver transplantation. *Transplant Proc*. Nov 1997;29(7):2817-8. doi:10.1016/s0041-1345(97)00690-8
166. Sesti F, Puliani G, Feola T, et al. Characterization of circulating immune cells and correlation with Tie2/Angiopoietins level in well differentiated neuroendocrine gastroenteropancreatic tumors: a cross-sectional analysis. *Endocrine*. Dec 12 2022;doi:10.1007/s12020-022-03257-8
167. Romano M, Sen M, Scottà C, et al. Isolation and expansion of thymus-derived regulatory T cells for use in pediatric heart transplant patients. *Eur J Immunol*. Aug 2021;51(8):2086-2092. doi:10.1002/eji.202048949
168. MacDonald KN, Hall MG, Ivison S, et al. Consequences of adjusting cell density and feed frequency on serum-free expansion of thymic regulatory T cells. *Cytotherapy*. Nov 2022;24(11):1121-1135. doi:10.1016/j.jcyt.2022.06.006
169. Kim J, Hope CM, Perkins GB, et al. Rapamycin and abundant TCR stimulation are required for the generation of stable human induced regulatory T cells. *Clin Transl Immunology*. 2020;9(12):e1223. doi:10.1002/cti2.1223
170. Alvarez Salazar EK, Cortés-Hernández A, Alemán-Muench GR, et al. Methylation of FOXP3 TSDR Underlies the Impaired Suppressive Function of Tregs from Long-term Belatacept-Treated Kidney Transplant Patients. *Front Immunol*. 2017;8:219. doi:10.3389/fimmu.2017.00219
171. Hann A, Oo YH, Perera M. Regulatory T-Cell Therapy in Liver Transplantation and Chronic Liver Disease. *Front Immunol*. 2021;12:719954. doi:10.3389/fimmu.2021.719954
172. Muller X, Marcon F, Sapisochin G, et al. Defining Benchmarks in Liver Transplantation: A Multicenter Outcome Analysis Determining Best Achievable Results. *Ann Surg*. Mar 2018;267(3):419-425. doi:10.1097/sla.0000000000002477

# 8.0 Appendix

## 8.1 Publications relating to thesis

Clarke G, Mergental H, **Hann A,** Perera MTPR, Afford SC, Mirza DF. How Machine Perfusion Ameliorates Hepatic Ischaemia Reperfusion Injury. *Int J Mol Sci*. 2021 Jul 14;22(14):7523.

**Hann A,** Osei-Bordom DC, Neil DAH, Ronca V, Warner S, Perera MTPR. The Human Immune Response to Cadaveric and Living Donor Liver Allografts. *Front Immunol*. 2020 Jun 22;11:1227

**Hann A**, Oo YH, Perera MTPR. Regulatory T-Cell Therapy in Liver Transplantation and Chronic Liver Disease. *Front Immunol*. 2021 Oct 14;12:719954

**Hann A,** Nutu A, Clarke G, Patel I, Sneiders D, Oo YH, Hartog H, Perera MTPR. Normothermic Machine Perfusion-Improving the Supply of Transplantable Livers for High-Risk Recipients. *Transpl Int*. 2022 May 31;35:10460

Halle-Smith JM, Hall LA**, Hann A**,Hartog H, Perera MTPR and Neil DAH(2022) Seventh Day Syndrome Revisited: Early Recognition of theClinical Syndrome and an Evolving Understanding of Its Etiology.Front. Transplant.

**Hann A**, Lembach H, Nutu A, Dassanayake B, Tillakaratne S, McKay SC, Boteon APCS, Boteon YL, Mergental H, Murphy N, Bangash MN, Neil DAH, Isaac JL, Javed N, Faulkner T, Bennet D, Moore R, Vasanth S, Subash G, Cuell J, Rao R, Cilliers H, Russel S, Haydon G, Mutimer D, Roberts KJ, Mirza DF, Ferguson J, Bartlett D, Isaac JR, Rajoriya N, Armstrong MJ, Hartog H, Perera MTPR. Outcomes of normothermic machine perfusion of liver grafts in repeat liver transplantation (NAPLES initiative). *Br J Surg*. 2022 Mar 15;109(4):372-380.

**Hann A,** Lembach H, Nutu A, Mergental H, Isaac JL, Isaac JR, Oo YH, Armstrong MJ, Rajoriya N, Afford S, Bartlett D, Mirza DF, Hartog H, Perera MTPR. Assessment of Deceased Brain Dead Donor Liver Grafts via Normothermic Machine Perfusion: Lactate Clearance Time Threshold Can Be Safely Extended to 6 Hours. Liver Transpl. 2022 Mar;28(3):493-496.

Hartog H, **Hann A,** Perera MTPR. Primary Nonfunction of the Liver Allograft. Transplantation. 2022 Jan 1;106(1):117-128.

Halle-Smith JM, **Hann A,** Cain OL, Perera MTPR, Neil DAH. Lactic Acidosis, Hypoglycemia, and Eosinophilia: Novel Markers of Antibody-Mediated Rejection Causing Graft Ischemia. Liver Transpl. 2021 Dec;27(12):1857-1860.

**Hann A,** Lembach H, Alzoubi M, McKay SC, Hartog H, Neil DAH, Mirza DF, Perera MTPR. Hepatocyte necrosis on liver allograft biopsy: Normothermic machine perfusion is the ideal platform for using these grafts in high-risk recipients. Clin Transplant. 2021 Jul;35(7):e14380.

Halle-Smith JM, Hall L, **Hann A,** Arshad A, Armstrong MJ, Bangash MN, Murphy N, Cuell J, Isaac JL, Ferguson J, Roberts KJ, Mirza DF, Perera MTPR. Low C-reactive Protein and Urea Distinguish Primary Nonfunction From Early Allograft Dysfunction Within 48 Hours of Liver Transplantation. Transplant Direct. 2023 May 24;9(6):e1484.

Halle-Smith JM, Hall LA, **Hann A,** Isaac JL, Murphy N, Roberts KJ, Rajoriya N, Perera MTPR. Emergency retransplant for primary non-function of liver allograft. Br J Surg. 2023 Sep 6;110(10):1267-1270.

## 8.2 Scholarships and awards

Catherine Marie Enright Kelly Memorial Research Scholarship  fromRoyal Australasian College of Surgeons.

- This scholarship provided $66 000 AUD in funding and was pivotal in allowing this research degree to be completed. The research team are incredibly grateful for this opportunity

The Calne-Williams Medal from the British Transplant Society

- The award is for the best oral paper presented by trainees who are members of the Society at the ‘Calne-Williams Medal paper session’ during the British Transplantation Society Annual Congress.
- This award was given for a presentation delivered at the 2023 British Transplant Society Meeting in Edinburg titled “Normothermic machine preservation of large DBD liver grafts is associated with early allograft dysfunction”

The Roy Calne Award from the British Transplant Society

- The British Transplantation Society Roy Calne Award recognises “a most outstanding contribution published in a peer review journal, as a single paper, in the broad field of transplantation” by a member aged under 40 years.
- This award was received for the publication “**Hann A**, Lembach H, Nutu A, Dassanayake B, Tillakaratne S, McKay SC, Boteon APCS, Boteon YL, Mergental H, Murphy N, Bangash MN, Neil DAH, Isaac JL, Javed N, Faulkner T, Bennet D, Moore R, Vasanth S, Subash G, Cuell J, Rao R, Cilliers H, Russel S, Haydon G, Mutimer D, Roberts KJ, Mirza DF, Ferguson J, Bartlett D, Isaac JR, Rajoriya N, Armstrong MJ, Hartog H, Perera MTPR. Outcomes of normothermic machine perfusion of liver grafts in repeat liver transplantation (NAPLES initiative). *Br J Surg*. 2022 Mar 15;109(4):372-380.